

BIOMARKER INVESTIGATION OF THE HEALTH EFFECTS OF CT X-RAY EXPOSURE IN CHILDREN

A PLEA TO "IMAGE GENTLY"

CHARLOT VANDEVOORDE

Promotor: Prof. Dr. H. Thierens
Co-promotor: Prof. Dr. Ir. K. Bacher

Thesis submitted in fulfilment of the requirements for the
degree of Doctor in Health Sciences

Department of Basic Medical Sciences
Faculty of Medicine and Health Sciences

2015





Universiteit Gent
Faculteit Geneeskunde en
Gezondheidswetenschappen
Vakgroep Medische Basiswetenschappen
Onderzoeksgroep Straling en DNA repair

Supervisors

Prof. Dr. H. Thierens (promotor)
Prof. Dr. Ir. K. Bacher (co-promotor)

Examination Board

Chairman: Prof. Dr. Ir. C. De Wagter¹
Prof. Dr. R. Cornelissen¹
Prof. Dr. M. van Eijkeren¹
Prof. Dr. T. Kerre¹
Prof. Dr. K. Verstraete¹
Prof. Dr. J. Slabbert²
Prof. Dr. K. Rothkamm³

¹ Ghent University, Ghent, Belgium

²iThemba Labs, Cape Town, South Africa

³University Medical Center Hamburg – Eppendorf, Hamburg, Germany

Research institute:

Ghent University
Faculty of Medicine and Health Sciences
Department of Basic Medical Sciences
De Pintelaan 185 B3
B-9000 Ghent, Belgium
Tel.: +32-9-264 65 19

Dankwoord

*It always seems impossible
Untill it's done*

— Nelson Mandela

Het schrijven van een doctoraat is als een lange reis, vol avonturen, met hoge toppen en diepe dalen. Het was wellicht de boeiendste reis van mijn leven, maar toch komt het einde nu in zicht. Dat einde gaat gepaard met gemengde gevoelens. Enerzijds ben ik blij en opgelucht dat ik het gehaald heb, anderzijds betekent het ook afscheid nemen van een fantastische periode. Toen ik aan dit doctoraat begon, had ik nooit durven denken dat ik hier vandaag in de Italiaanse zon dit laatste stukje van mijn thesis zou schrijven. Het leek altijd iets onmogelijk veraf. Daarom ben ik toch een beetje trots en vooral gelukkig dat ik het tot een goed einde gebracht heb. Wanneer ik vandaag terugblik, kan ik met een gerust hart vaststellen dat het een mooie tijd geweest is en kan ik met een tevreden gevoel een nieuwe start nemen. Dat was niet mogelijk geweest zonder de hulp en steun van een heleboel mensen, die ik hiervoor wil bedanken. Ik probeer het kort te houden, maar je weet hoe dat gaat bij mij...

Mijn grootste dank gaat uit naar mijn promotor, *professor Thierens*, de beste gids die ik me tijdens mijn doctoraatsreis kon voorstellen. Uw deur stond altijd open voor vragen, problemen, vondsten, bedenkingen... en dat werkte ook andersom. Ik kan de uren en dagen niet tellen die we in elkaars bureau doorbrachten, gebogen over moeilijke vraagstukken met naast ons een tas koffie, die vaak al eens koud werd. Ons afscheid valt samen en we zullen beiden nieuwe wegen inslaan, maar ik ben er zeker van dat de verbondenheid blijft. U was mijn promotor en zoveel meer. Hetgeen ik van u geleerd heb, zal ik de rest

van mijn carrière verder proberen uitbouwen en als een mooie herinnering meenemen. Bedankt voor het vertrouwen, de leuke werksfeer, uw uitgebreide kennis, ervaring en de niet te onderschatten input in dit doctoraat!

Ook mijn co-promotor, professor Bacher, moet hier zeker bedankt worden. ‘Als we nu Charlot eens vragen of ze geïnteresseerd zou zijn in een doctoraat?’ Die vraag moet in het voorjaar van 2010 in het hoofd van *Klaus* zijn opgekomen. Intussen zijn we vijf jaar verder en is Klaus (meer dan verdiend) professor Bacher geworden. Hoewel het onderwerp van mijn doctoraat door omstandigheden sterk gedeveerd is, zal ik toch nooit vergeten dat je me als prille doctoraatsstudent inwijdde in de wereld van congressen, Europese meetings en me meenam naar het Weense hoofdkwartier van het IAEA. Schitterende ervaringen die me een zekere maturiteit gaven voor het vervolgverhaal van mijn doctoraat (en van Wenen mijn lievelingsstad in Europa maakten).

Onderzoek doe je nooit alleen, een belangrijke les die ik tijdens mijn doctoraat leerde. Dit doctoraat was nooit gelukt zonder een paar zeer waardevolle samenwerkingen, waarvoor ik een heleboel mensen moet bedanken die me altijd met raad en daad bijgestaan hebben...

Hier wil ik in de eerste plaats professor Vral bedanken. *Anne*, jouw deur stond altijd voor mij open, ook 's avonds laat wanneer de werkvloer al lang leeggelopen was. Jouw toewijding voor mijn onderzoek en waardevol advies betekenden een grote meerwaarde voor deze thesis. Ik wil je ook bedanken om me mee te nemen als ‘foci-verantwoordelijke’ naar de RENEB meetings. Ook al maakt biologische dosimetrie geen deel uit van dit doctoraat, ik heb er veel van opgestoken en ik heb ervaring opgedaan waar ik in mijn verdere carrière nog vaak op zal terugvallen. Een meer dan welgemeende bedankt voor de mogelijkheden die je me hebt gegeven en om er steeds voor mij te zijn! Naast Anne wens ik ook het volledige *team van 6B3* te bedanken. Op het einde van mijn doctoraat heb veel tijd bij jullie in het labo doorgebracht. Naast het INW, kon ik me hier ook ‘thuis’ voelen en het was steeds een plezier bij jullie te mogen vertoeven. Bedankt om me steeds met open armen te ontvangen, om me wegwijs te maken in jullie in labo's en voor de vele PBS voorraden die aan mij werden opgeofferd. En ik kan deze passage niet laten passeren zonder mijn ‘radiobiologische maatjes’ *Julie en Annelot* in het bijzonder te bedanken. Jullie maakten vaak het verschil tussen ‘weekend’ of ‘geen weekend’! Ik kon altijd op jullie rekenen wanneer mijn labo agenda weer even niet haalbaar was om alleen te bolwerken. Een grote dankjewel daarvoor! De kers op de taart van dit doctoraat was toch wel ons congres in Japan, een onvergetelijke ervaring die ik samen met jullie kon beleven. Ook al zit ik aan de andere kant van de wereld, mijn deur staat altijd open en ik hoop jullie daar te zien!

Wie deze thesis helemaal leest (maar ik ben er me van bewust dat veel mensen na dit stukje zullen afhaken), zal de link met het Europees EPI-CT project al snel ontdekken. In the framework of this project, I wish to thank

my Biology colleagues for the wonderful meetings and the good atmosphere amongst us. *Maria, Ute, Janet, Marie, Siamak, Carita* and *Eileen*, it was great to be part of the team! *Ausra* and *Daniel*, thank you very much for your valuable input for my first paper. A special thank you to *Sarah* and *Hussein*, our collaboration goes further than EPI-CT and I wish to thank you for all the nice moments we shared together. Hussein, it was always a pleasure to work with you and good to have you by my side during the meetings. It meant a lot to me! Sarah, thank you for your professionalism, enthusiasm, the interesting discussions and involving me in the project.

Het is absoluut niet gemakkelijk om iedereen in een paar zinnen te bedanken die aan deze thesis heeft meegeholpen en dat geldt zeker voor het tweede artikel in dit doctoraat. Eerst en vooral wil ik de ouders en kindjes bedanken die meegewerkt hebben aan deze studie en die de bloedstalen wilden afstaan die onmisbaar en noodzakelijk waren voor dit onderzoek. Deze boodschap geldt trouwens voor alle vrijwilligers die bloed doneerden voor deze thesis. Zonder jullie was het allemaal niet mogelijk geweest!

Bij het includeren van patiënten voor deze studie kreeg ik ondersteuning vanuit meerdere diensten. In Leuven gaat mijn dank eerst en vooral uit naar *Dr. Luc Breysem* die alle ouders persoonlijk opbelde om hen op de hoogte te brengen van de studie. Een ongeziene inspanning, die van deze studie een succesverhaal maakte in UZ Leuven. Daarnaast wens ik ook *Hilde* en *Ilse* bedanken om alles in goede te banen te leiden wanneer ik in Leuven arriveerde, ook *Walter* en *Herman* voor het branden van de beelden. In UZ Brussel gaat mijn bewondering en dank uit naar *Dr. Caroline Ernst*. Caroline, bedankt voor je onophoudelijk enthousiasme bij je werk en je inzet voor deze studie. In AZ Sint-Jan gaat mijn dank uit naar twee artsen, enerzijds radioloog *Dr. Kris Van De Moortele* voor de inspanning om deze studie op te zetten in Brugge en anderzijds neonatoloog en pediatriesch cardioloog *Dr. Wim Decaluwe* en zijn nooit aflatende strijd voor elk druppeltje bloed en de toegewijde zorg voor elk patiëntje. In UZ Gent gaat mijn dank uit naar *Dr. Peter Smeets* en *Dr. Nele Herregods*, die ondanks het lage aantal pediatrische CT patiëntjes in UZ Gent steeds een inspanning leverden om rekrutering mogelijk te maken. Als laatste wens ik in AZ Sint-Lucas *Dr. Adelard De Backer* te bedanken. Uw interesse en motivatie maakten deze studie mogelijk in uw ziekenhuis. Mijn oprechte dank voor alle inspanningen en de tijd die u in deze studie investeerde.

Het laatste jaar nam dit doctoraat een interessante wending naar de immunologie, wat de basis vormde voor mijn derde artikel. Een insteek die ik te danken heb aan *professor Jan Philippé*. Het was een plezier om met u samen te werken! Een meer dan welgemeende dankuwel voor de vrijheid die u mij gaf in uw labo, uw interesse in mijn werk en de hulp bij de analyses. Mijn dank gaat hierbij ook uit naar Sofie en de rest van uw team, die me zoveel keren hun flow cytometer in beslag lieten nemen en steeds hielpen bij al mijn vra-

gen. En in dit immunologisch rijtje wens ik ook *professor Bart Vandekerckhove* uitdrukkelijk te bedanken, zonder hem was het hematopoïetische stamcelverhaal niet mogelijk geweest. Bedankt om uw ervaring en kennis met ons te delen! Hierbij wil ik ook graag *Greet, Stijn, Yasmine, Katia* en in het bijzonder *Sophie* bedanken.

Een belangrijk deel van dit onderzoek gebeurde in samenwerking met mijn thesisstudenten. Ook zij hebben een belangrijke rol gespeeld voor mij en mogen hier dus zeker niet vergeten worden. *Delphine, An, Veerle DP, Charlotte, Jeroen, Jan, Veerle T* en *Greet*, jullie hebben prima werk geleverd en het was bijzonder aangenaam om elk van jullie te begeleiden tijdens jullie thesisjaren!

Plezier hebben in je werk is in grote mate afhankelijk van je werkomgeving. Een goede sfeer op een afdeling is essentieel en ik kan zeggen dat die sfeer fantastisch is op ons INW! Ik denk dat ik het jullie niet hoeft te vertellen, maar ik zal met pijn in het hart vertrekken. ‘What happens in the salon, stays in the salon’ maar er zijn gelukkig nog heel wat zaken waarover ik wél kan schrijven in dit dankwoord.

Gebouw N7 van het INW herbergt naast de medische fysica, ook de fysische controle, die in deze biotoop gezellig samenleven. Straling vormt ons raakvlak en ondanks het feit dat we niet rechtstreeks samenwerkten, had ik er de allerbeste collega's. *Myriam*, bedankt voor de aangename babbels, het delen van jouw ervaring, ons geweldig congres in Manchester en de leuke zwempauzes. *Levi*, bedankt om me terug aan te zetten tot frisbeeën (ook al was het van korte duur) en om ons vrouwenteam menigmaal als enige man te vervoegen! *Lothar*, je bent toegekomen tijdens de drukste periode van mijn doctoraat, maar ik had de kans je te leren kennen als een behulpzame en enthousiaste collega, die meteen leek te passen in ons team. *Nancy*, bedankt voor het geduld met mijn dosimeters, jouw grapjes en het feit dat je mijn naam nooit vergat! Als laatste fyco-lid wil ik zeker en vast *Isabelle* bedanken; voor het organiseren van de verjaardagslunchen, de cadeautjes en zoveel meer. Bovenal wil ik jou bedanken voor het luisteren, jouw dagelijks enthousiasme, reiservaringen en de hulp bij alles waar nodig!

Bij de medische fysica, wil ik beginnen bij de lieve *Virginie* waar geen enkele doctoraatsstudent in ons labo omheen kan. Ik weet niet hoe ik je kan bedanken voor alles wat je tijdens mijn doctoraat voor mij betekend hebt. Je hebt me zo vaak uit de nood geholpen, leefde met alle gebeurtenissen mee en ik kon voor alles bij jou terecht. Ik kan alleen maar zeggen dat ik heel blij ben dat jij er bent! *Liesbeth* en *An*, ik ben de laatste in ons rijtje van 2015 om mijn doctoraat af te ronden. Ontzettend bedankt om me door deze periode heen te helpen. Maar ook los van thesisraad, wil ik jullie vooral bedanken voor de goeie babbels, die lang niet altijd over het werk moesten gaan. *Liesbeth* ook voor de rust in de soms alomtegenwoordige chaos, en *An* voor de liften

naar Aalter en de band die ons geboortedorp toch wel tussen ons schiep. *An DH*, alhoewel we nooit rechtstreeks moesten samenwerken, zat je nooit veraf. Bedankt voor de grappige momenten en je creatieve inbreng bij elk origineel cadeau! *Kim*, al zat jij dan wat verder weg, je hebt mijn middagpauzes vanaf mijn eerste dag op het INW weten op te fleuren. Bedankt om mijn studenten op te vangen wanneer nodig, voor jouw ervaring en voor de vele goede bab-bels. *Dimi* en *Chamberlain*, bedankt om het testosterongehalte terug op pijl te brengen onder de doctoraatsstudenten en voor jullie enthousiaste bijdrage tijdens elke salonparty. *Régine*, ook al ‘woon’ je officieel niet bij ons in N7, ik heb jou altijd als een van ons beschouwd. Bedankt voor alle wijze raad en hulp tijdens mijn kort assistent-intermezzo. Ook de collega’s waarmee ik maar kort kon samenwerken, verdienen een welgemeende dankjewel. *Joke* en *Laurence*, bedankt om voor mij het ‘foci-pad’ te effenen! En *Nele* voor het ter hulp springen bij elk computerprobleem. En dan is het de beurt aan mijn ‘Duinrell-besties’! Bedankt voor alle leuke momenten die we samen beleefden! Mijn bureaugenootje *Lore*, jouw optimisme heeft menige dagen gered. Ik wil je bedanken voor al je steunende woorden, het vele luisteren en jouw uitmuntend talent als binnenbureau-architect. Ik wens je veel succes met alles wat in de toekomst komen zal, maar ik weet dat je het fantastisch goed gaat doen. We waren een goed team! *Caro*, ondanks de soms vreemde robotachtige (en andere) interesses, zeker een ingenieur met laag ‘nerd-gehalte’. Bedankt om altijd precies die grapjes of opmerkingen te maken die mijn dag opfleurd. En *Sofie*, al even bij ons weg, maar nooit vergeten! Bedankt om niet alleen mijn biologiemaatje te zijn, maar ook mijn wijze raadgever op de juiste momenten. Je wordt nog steeds gemist op het INW. And I would like to end this paragraph with a special thank you to my dear colleague and friend *Nati*. I still regret the fact that I couldn’t spend more time with you during my most tough PhD months. I can’t thank you enough for your optimism, the patience to read and correct my thesis, your support in the lab and so much more!

Het doctoraat was vaak zeven dagen op zeven werken, maar toch slaagden een aantal mensen er in om mijn drukke dagen op te fleuren. Familie en vrienden mogen daarom in dit dankwoord niet ontbreken.

Mijn biomedische en ‘kanker-straling’ maatjes, sommigen van jullie zitten er ook midden in en weten als geen ander hoe het leven tijdens een doctoraat kan zijn. Bedankt voor het luisteren en het begrip! Ik bijt de spits af en ben er zeker van dat jullie het allemaal nog zoveel beter zullen doen! De boog moest gelukkig niet altijd gespannen staan en daar zorgden de kerstfeestjes, etentjes en wandelingen voor. Ook de niet-doctorandi mogen zeker niet vergeten worden, een grote dankjewel om ons ‘gezaag’ te aanhoren en ons ook in te wijden in jullie minstens even interessante leef- en werkwereld. En hier verdient *Iris* toch een extra woord van dank. We hadden het geluk om in de eerste jaren van mijn doctoraat onze vriendschap zowel tijdens als buiten de werkuren

te beleven. Dat leek soms te mooi om waar te zijn en op een dag heb je de moeilijke knoop moeten doorhakken om toch voor jouw onderwijsdroom te kiezen. Ik heb je altijd bewonderd in die keuze en ben blij jou vandaag en de voorbije jaren zo gelukkig te zien. Daarnaast heb je mij onrechtstreeks de kans gegeven om ook mijn juiste weg in te slaan, deze van de radiobiologie, waarvoor ik ontzettend dankbaar ben. Ik wens je heel veel succes met alles wat komen zal en ben zo fier op jouw twee kleine meisjes!

De ‘Supporters van de Liefde’ die een paar jaar geleden als een toevallig samenraapsel van vrienden ontstonden, maar vandaag niet weg te denken zijn uit mijn Gentse leven. Merci voor alle leuke momenten, toffe feestjes en de vriendschap! *Jonas* (of Jones of Chippie) voor jou een bijzondere dankjewel om de uitdaging aan te gaan om van dit doctoraat een mooi boekje te maken! Dat was me zelf nooit gelukt!

De ‘Mestfest club’, een vrolijke bende die me drie jaar geleden meteen als een van hen beschouwde. De onvergetelijke Mallorca reis, babyborrels, trouwfeesten en urenlange babbels na (of tijdens) de basketmatchen, vormden welgekomen pauzes tijdens mijn doctoraat.

En dan mijn lieve vriendinnen, er is helaas geen plaats om voor elk van jullie een paragraaf te schrijven. Ik wil jullie ontzettend bedanken voor alle steun de voorbije jaren. De zalige vakanties, de pauzes in Londen, de leuke trouwfeesten, de ontspannende etentjes, wandelingen, sportintermezzo’s en de vele peptalks... het lijstje is eindeloos. Jullie zijn stuk voor stuk fantastisch! Toch verdient er eentje een speciale vermelding in dit dankwoord. Mijn liefste *Hanna*, er zullen nooit genoeg woorden zijn om uit te drukken hoe ik jou bewonder. Als het donker genoeg is, worden échte sterren zichtbaar. Je bent voor elk van ons een inspiratie om ervoor te gaan in ons leven, onze dromen na te jagen, maar ook op tijd stil te staan en te genieten. Daar moet ik nog elke dag aan werken, maar jij hebt me zoveel geleerd. En die herinnering is, zoals Lene en ik met een glimlach en in koor zouden zeggen, voor altijd!

Na de vrienden, komt de familie die er op hun beurt voor zorgden dat ik de stress van het doctoraat even kon afwerpen en me de kans gaven om in een rustige, ontspannen omgeving te vertoeven.

Eerst en vooral mijn ouders. Ik denk dat ik in alle eerlijkheid kan zeggen dat dit proefschrift er niet had gelegen als jullie er niet waren geweest. *Papa*, jij weet als geen ander hoe je me moet stimuleren om datgene te doen wat gedaan moet worden en mijn gedachten te ordenen in tijden van chaos, hoe hard ik me er ook soms tegen verzet! Bedankt voor alle wijze raad en het feit dat ik altijd op jou kon steunen (wat soms leunen was). *Mama*, jou wil ik bedanken voor jouw onvoorwaardelijke toewijding, de zorgende hand die meermaals nodig was en de opvang in tijden van crisis. Altijd vol liefde en vertrouwen. Een moederhart zoals er geen ander in de wereld bestaat!

Mijn drie knappe *broers* en mijn fantastische *zus*. Wanneer ik over jullie spreek, begin ik meteen te glimlachen. Als wij samen zijn, is het altijd plezier! Bedankt om mij altijd op te beuren, te luisteren en er gewoon te zijn. Ik ben een trotse grote zus!

Ook mijn grootouders mogen niet ontbreken. *Opa*, jouw wijsheid en kennis ondervinden geen leeftijdsgrenzen. Ik hoop dat ik jouw leergierigheid en interesses even lang mag meedragen. En in dit rijtje mag mijn lieve *oma Roza* zeker niet ontbreken. Je bent er altijd voor ons en koestert ons als échte schatten. Bedankt voor alle bemoedigende, lieve oma-knuffels en de honderden kaarsjes die je tijdens mijn unief periode hebt moeten branden. Ze hebben hun werk goed gedaan!

En dan had ik het geluk om tijdens deze doctoraatsperiode één iemand te leren kennen, die intussen zoveel meer is dan een vriend of familielid. Het leukste aan elke dag is 's avonds thuiskomen, bij mijn *Thomas*. Hij gelooft in mij en zie hier, het is me gelukt! Zonder enig bezwaar werd je mee ondergedompeld in de wereld van de straling, leerde je leven met mijn onvoorspelbaar werkschema, luisterde je 's avonds laat nog uren naar mijn hersenspinsels en daagde je me uit voor een spelletje Carcassonne als het me even teveel werd. In dit dankwoord verdienen ook jouw ouders, *Ann* en *Frank*, zeker en vast een plekje. Jullie Italiaanse gastvrijheid kent geen grenzen en zorgde meermaals voor een welgekomen adempauze. Thomas, nadat de voorbije jaren vooral in het teken stonden van mijn doctoraat, ben ik vandaag vooral blij dat we eindelijk meer tijd zullen hebben om te genieten. En aan ons avontuur in Zuid-Afrika te beginnen!

Charlot

September 2015

Summary / Samenvatting

Computed Tomography (CT) is the examination with the largest contribution in dose to the medical diagnostic dose burden in Belgium (55.72%), while only 11% of the 16.4 million radiological procedures each year are CT scans (1). Furthermore, the annual frequency of medical examinations per caput in Belgium is relatively high compared with neighbouring countries. Belgian inhabitants receive more than 3 times the average medical radiation dose per caput compared to the Netherlands (2). Without any doubt the introduction of CT has tremendously improved diagnostic imaging. However, the high x-ray doses have raised serious health concerns, especially for the radiosensitive paediatric patient population. It is generally anticipated that children have a higher radiation sensitivity compared to adults regarding ionizing radiation (IR) induced malignancies and the associated risk for exposure induced death (3). The subject of this PhD dissertation is to assess the health effects of IR exposure in children by using biomarkers of exposure. Within this PhD thesis, special attention is paid to the induction of deoxyribonucleic acid double-strand breaks (DNA DSBs) by CT x-rays in children since these lesions have a proven relevance for radiation-induced health effects.

The first part of this PhD dissertation outlines why children are the most important target group in medical radiation protection. The susceptibility of children to the effects of IR has been a focus of interest for over half a century. Compared to adults tissues and organs of children are growing and developing, which makes them more sensitive to radiation effects since they contain a larger proportion of stem cells and growing cells. Furthermore, children have a longer life expectancy compared to adults, in which the potential oncogenic effects associated with IR exposure can appear. **Chapter 1** gives an overview of the current epidemiological data to illustrate the age dependency of radiation sensitivity. Special attention is given to Annex B of the recent United Nations Scientific Committee on the Effects of Atomic Radiation (UNSCEAR) 2013 report 'Effects of radiation exposure of children' (3). Since several epidemiological studies show a strongly increased risk in both incidence and mortality of leukaemia after IR exposure in childhood, this chapter also describes the functional hierarchy of haematopoiesis and haematopoietic stem and progenitor cells (HSPCs) as potential target cells for radiation-induced leukaemogenesis. In **chapter 2**, we describe the medical radiation burden in Belgium and the issues related to CT imaging in children. Furthermore, an overview is given of epidemiological studies dealing with leukaemia and cancer risks related to CT x-ray exposure of children. However, the characterization of health effects of IR at low dose levels, as used in CT imaging, remains a challenge due to the statistical uncertainties associated with the small excess number of cases at low doses. Special emphasis is given to the ongoing European FP7 project, EPI-CT, which will offer opportunities to better address the current limitations. In this project it is also anticipated that significant insights

will emerge from radiation biomarker studies, which will shed new light on the cellular and molecular responses at low doses. The latter approach was used in this PhD dissertation and **chapter 3** gives an overview of the cellular and molecular mechanisms involved in the DNA damage response. Several biomarkers of exposure are discussed, which are available at a certain time point after IR exposure and can be used to validate a correlation between exposure and biological response. For this PhD research, the phosphorylated histone subtype H2A isoform X (γ -H2AX) foci assay was used as a sensitive biomarker for radiation-induced DNA DSBs, and the micronucleus (MN) assay to determine the mutagenic effects of IR exposure. The first part ends with the aim (**chapter 4**) and outline (**chapter 5**) of the PhD research.

The second part of the PhD thesis consists of the original research, presented in three scientific papers. **Chapter 6** presents a paper in the framework of the EPI-CT project. We performed a series of *in vitro* feasibility experiments to optimise the γ -H2AX foci assay to use it as an exposure biomarker in a prospective multicentre paediatric radiology setting. This comprised the critical evaluation of a number of ethical and technical hurdles related to biological sample collection in a paediatric radiology setting (small blood sample volume), processing and storing of blood samples (effect of storing blood at 4°C), the reliability of foci scoring for low-doses by using merge γ -H2AX/p53 binding protein 1 (53BP1) scoring), as well as the impact of contrast agent administration as potential confounding factor. In order to evaluate the feasibility of pooling the γ -H2AX data when different centres are involved in an international multicentre study, two intercomparison studies in the low-dose range (10-500 mGy) were performed. The results demonstrate that it is feasible to apply the γ -H2AX foci assay as a cellular biomarker of exposure in an international multicentre prospective study of paediatric CT imaging after validation in an *in vivo* pilot study. The second paper, presented in **chapter 7**, shows the results of a prospective multicentre study in Belgium in which we used the optimised γ -H2AX foci assay to determine the number of x-ray induced DNA DSBs in children undergoing a chest or abdomen CT examination. In order to estimate the lifetime attributable risk (LAR) of cancer incidence and mortality associated with the paediatric CT examinations, the Biological Effects of Ionizing Radiation (BEIR) VII risk model was used. To this end patient specific blood doses and organs doses were calculated based on the individual patient CT images by using ImpactMC simulation software 1.3.1. Plotting of the *in vivo* induced γ -H2AX foci versus the calculated blood dose indicated a low-dose hypersensitivity, which was supported by an *in vitro* dose response study on umbilical cord blood. Furthermore, differences in patient dose levels between radiology centres were reflected in differences in DNA damage. The latter observations emphasize the importance of dose reduction techniques and should encourage medical practitioners to maximize the benefit-to-risk ratio

of paediatric CT imaging. The study indicated also a diminishing trend of the foci-to-dose ratio versus age, however, this age dependency was not statistical significant. In a third paper, presented in **chapter 8**, we investigated further the age dependency in radiosensitivity of children compared to adults. To this end we compared the residual γ -H2AX/53BP1 foci numbers and chromosomal radiosensitivity at cellular level in T-lymphocytes of newborns (umbilical cord blood) and adult volunteers. Newborn T-lymphocytes showed significantly higher residual foci yields 24 h post-irradiation and a higher number of radiation-induced MN. T-lymphocytes of newborns are practically all phenotypically immature. Since these cells are characterised by a closed chromatin structure, this could be an underlying mechanism of the observed higher radiosensitivity of newborns compared to adults. This was confirmed by a comparative study of radiation-induced residual foci and MN in isolated naive (CD45RA⁺) and memory (CD45RO⁺) T-lymphocytes of adults. The results of paper 3 suggest that the observed differences in radiosensitivity between newborn and adult T-lymphocytes can be explained by the immunophenotypic change of T-lymphocytes with age. Since radiation-induced leukaemia is one of the most prominent malignancies with an apparent higher excess risk among those exposed at young ages, studies of the DNA damage response and outcome of HSPCs after IR exposure are warranted. In our third paper, we could show that a significantly lower number of residual foci was observed in newborn Cluster of Differentiation (CD)34⁺ HSPCs compared to newborn T-lymphocytes. Together with the high number of radiation-induced MN, these results could suggest that HSPC quiescence promotes mutagenesis after IR exposure.

The third part presents a general discussion of the results of this PhD dissertation. **Chapter 9** addresses the *in vitro* and *in vivo* low dose hypersensitivity observed in the γ -H2AX foci study on paediatric patients undergoing a CT examination (paper 2). The results of the current study are compared with a previous study of our research group on paediatric patients undergoing a cardiac catheterisation (4) and other biomarker studies in paediatric diagnostic radiology. The *in vivo* biomarker data illustrate the necessity of reduction of the CT related x-ray dose for paediatric patients. In this framework the plea to “Image Gently” is further explained. The bystander effect, a possible underlying mechanism of the observed dose response behaviour, is also discussed in this chapter. The high radiosensitivity of HSPCs and the potential trigger to develop radiation-induced leukaemia are discussed in **chapter 10**. This chapter elucidates that the comparison of murine and human data is not that straightforward and several issues need to be addressed as e.g. the impact of the niche before we can extrapolate the *in vitro* results to an *in vivo* situation. In **chapter 11**, we discuss the observed difference in radiosensitivity between newborns and adults. The observed differences in chromosomal radio-

sensitivity and residual DNA damage in naive and memory T-lymphocytes indicate that the immunophenotypic profile of the lymphocytes can explain the higher radiosensitivity of newborn compared to adult. In view of these findings we discuss differences in chromatin condensation as a hallmark for age dependency in radiation effects. The final conclusions of this PhD dissertation are presented in **chapter 12**, which should encourage the medical field to reduce the radiation burden of paediatric patients and create awareness to “Image Gently”. The results of this PhD dissertation allow a better understanding of the health consequences of low dose exposure in children, as used in medical diagnostic applications. Some future perspectives resulting from the scientific work performed are described in **chapter 13**. Further research is needed 1) to have a better understanding of the low dose hypersensitivity observed in the paediatric CT study; 2) to elucidate differences in radiosensitivity between primitive HSCs and lineage-committed progenitors; and 3) to study the chromatin structure of naive and memory lymphocytes in order to gain more insight in the role of chromatin condensation on the observed age dependency in radiosensitivity.

References

1. *Personal communication with Federal Agency of Nuclear Control (FANC) Belgium - Thanks to Petra Willems. 2015.*
2. *DDM2. DDM2 Project Report Part 1: European Population Dose. 2014.*
3. *UNSCEAR. Sources, Effects and Risks of ionizing radiation. New York: United Nations Scientific Committee on the Effects of Atomic Radiation, 2013.*
4. *Beels L, Bacher K, De Wolf D, Werbrouck J, Thierens H. gamma-H2AX Foci as a Biomarker for Patient X-Ray Exposure in Pediatric Cardiac Catheterization Are We Underestimating Radiation Risks? Circulation. 2009;120(19):1903-9.*

Ondanks het feit dat CT onderzoeken slechts 11% uitmaken van de 16,4 miljoen radiologische onderzoeken die jaarlijks plaatsvinden in België, vormen ze toch de belangrijkste bijdrage in stralingsbelasting door medische diagnostiek (55,72%) (1). Daarenboven is het aantal medisch diagnostische onderzoeken per inwoner in België relatief hoog in vergelijking met onze buurlanden. De gemiddelde medische stralingsbelasting per inwoner is 3 keer hoger in België dan in Nederland (2). Desondanks de hoge stralingsbelasting, bestaat er geen twijfel dat de introductie van CT de diagnostische beeldvorming enorm verbeterd heeft. Het wordt algemeen aangenomen dat kinderen gevoeliger zijn voor de negatieve effecten van ioniserende straling (IS), met name kankerinductie en mortaliteit, in vergelijking met volwassenen (3). Net daarom vormen zij een groep die vanuit stralingsbeschermingsoogpunt extra aandacht verdient. Het doel van dit doctoraatsonderzoek was dan ook om met behulp van biomerkers de gezondheidsrisico's voor kinderen, veroorzaakt door blootstelling aan IS, te kwantificeren op DNA niveau. In dit doctoraat werd specifiek aandacht geschonken aan de inductie van DNA dubbelstrengbreuken (DSB) door CT x-stralen blootstelling bij kinderen aangezien deze lesies zeer relevant zijn in het kader van stralingsgeïnduceerde gezondheidsrisico's.

In het eerste deel van dit proefschrift wordt toegelicht waarom kinderen zo'n belangrijke groep vormen in de medische stralingsbescherming. De hoge stralingsgevoeligheid van kinderen vormt al ettelijke decennia een belangrijke focus voor onderzoek. Vergeleken met volwassenen zijn de weefsels en organen van kinderen volop in groei en ontwikkeling, waardoor ze een grotere fractie aan stamcellen en delende cellen bevatten, wat ze gevoeliger maakt voor stralingseffecten. Daarnaast hebben kinderen een langere levensverwachting in vergelijking met volwassenen, wat resulteert in een langere tijdspanne waarin de potentieel oncogene effecten ten gevolge van stralingsblootstelling tot uiting kunnen komen. **Hoofdstuk 1** geeft een overzicht van de huidige epidemiologische data om de leeftijdsafhankelijkheid in stralingsgevoeligheid te illustreren. Er wordt hierbij extra aandacht gegeven aan Annex B van het recente UNSCEAR 2013 rapport *'Effects of radiation exposure of children'* (3). Omdat verscheidene epidemiologische studies een sterke stijging tonen in het risico op leukemie ten gevolge van een stralingsblootstelling als kind, voor zowel incidentie als mortaliteit, werd in dit hoofdstuk ook de functionele hiërarchie van hematopoïese beschreven en de hematopoïetische stam- en progenitorcellen (HSPC) als potentiële targetcellen voor stralingsgeïnduceerde leukemogenese. In **hoofdstuk 2** wordt de medische stralingsbelasting in België besproken en de problematiek rond CT beeldvorming voor kinderen. Daarnaast wordt er een overzicht gegeven van de recente epidemiologische studies op leukemie en kankerrisico's door CT x-stralen blootstelling bij kinderen. Toch blijven dergelijke studies moeilijk door de grote statistische

onzekerheid op het aantal gevallen bij lage dosis blootstelling. In dit hoofdstuk wordt extra aandacht gegeven aan het Europees FP7 project, EPI-CT, dat waarschijnlijk nieuwe opportuniteiten zal bieden om de huidige beperkingen bij epidemiologische studies op kinderen die een CT onderzoek ondergaan te reduceren. Er wordt verwacht dat ook biomerker studies waardevolle informatie zullen opleveren over de cellulaire en moleculaire effecten van lage dosis blootstellingen. Deze manier van werken werd dan ook toegepast in dit doctoraatsonderzoek en **hoofdstuk 3** geeft een overzicht van de cellulaire en moleculaire mechanismen die betrokken zijn in de DNA schade respons. Verschillende biomerkers worden besproken die kunnen gebruikt worden om stralingsblootstelling te detecteren en meer informatie te verschaffen over de dosis-effect relatie. In dit doctoraatsonderzoek werd gebruikt gemaakt van de gevoelige γ -H2AX foci techniek voor de detectie van DNA DSB na stralingsblootstelling en de micronucleus (MN) assay om de mutagene effecten van IS blootstelling te bepalen. Het eerste deel van dit proefschrift wordt afgesloten met de doelstelling en de uitwerking van dit doctoraatsonderzoek, in **hoofdstuk 4** en **5** respectievelijk.

Het tweede deel van deze thesis bestaat uit drie wetenschappelijke artikels resulterend uit het doctoraatsonderzoek. **Hoofdstuk 6** stelt een studie voor die uitgevoerd werd in het kader van het Europees EPI-CT project. Er werden een aantal *in vitro* experimenten uitgevoerd om de γ -H2AX foci techniek te optimaliseren voor gebruik als biemerker bij lage dosis blootstelling in een prospectieve multicenter studie in pediatrie radiologie. Dit deel omvat een kritische evaluatie van een aantal ethische en technische moeilijkheden gekoppeld aan onder meer bloedafname in een pediatrie setting (kleiner volume van de bloedstalen), het verwerken en bewaren van de bloedstalen (effect van bewaring op 4°C), de betrouwbaarheid van foci scoring voor lage dosis blootstellingen (dubbele γ -H2AX/53BP1 immunokleuring), alsook de impact van de contrastvloeistof op γ -H2AX foci inductie. Om na te gaan of het mogelijk zou zijn om de γ -H2AX foci data van verschillende onderzoeksinstellingen samen te voegen in een internationale multicenter studie werden er twee vergelijkende studies uitgevoerd in het lage dosis gebied (10-500 mGy). De resultaten van deze *in vitro* studie tonen aan dat het mogelijk is om de γ -H2AX foci techniek te gebruiken als een lage dosis biemerker in een internationale multicenter studie, na validatie in een *in vivo* pilootstudie. Een tweede artikel in **hoofdstuk 7**, stelt de resultaten voor van een prospectieve multicenter studie in België. Hierbij werd de geoptimaliseerde γ -H2AX foci techniek gebruikt om het aantal x-stralen geïnduceerde DNA DSB te bepalen in lymfocyten van kinderen die een CT thorax of abdomen onderzoek ondergingen in één van de deelnemende centra. Het BEIR VII risicomodel werd gebruikt om het *lifetime attributable risk* (LAR) op kanker incidentie en mortaliteit te bepalen voor de pediatrie patiënten die opgenomen werden

in de studie. Hiervoor werden patiënt specifieke bloed- en orgaandosisen berekend op basis van de CT beelden van de individuele patiënt met behulp van de ImpactMC simulatie software 1.3.1. Wanneer de *in vivo* γ -H2AX foci resultaten uitgezet werden ten opzichte van de berekende bloeddosiswaarden werd een lage dosis hypersensitiviteit waargenomen. Deze hypersensitiviteit werd bevestigd door een *in vitro* dosis respons studie op navelstrengbloed. De onderlinge verschillen in patiëntdosisniveaus tussen de deelnemende ziekenhuizen waren ook te zien in de overeenkomstige DNA schade. Deze bevindingen benadrukken het belang van dosisreductie technieken en moeten artsen en medisch personeel aansporen tot justificatie en optimalisatie van CT scans voor kinderen. De studie wees ook op een daling van de foci-versus-dosis verhouding met de leeftijd van de patiënten. Helaas was deze trend in leeftijdsafhankelijkheid niet statistisch significant. In een derde artikel dat voorgesteld wordt in **hoofdstuk 8**, gaat het onderzoek dieper in op de leeftijdsafhankelijkheid in radiosensitiviteit van kinderen in vergelijking tot volwassenen. Hiervoor werden het aantal residuele γ -H2AX/53BP1 foci 24 u na blootstelling bepaald alsook de chromosomale gevoeligheid met behulp van de MN assay in T-lymfocyten afkomstig van pasgeborenen (navelstrengbloed) en volwassenen. De T-lymfocyten van de pasgeborenen vertoonden een significant hoger aantal residuele foci en stralingsgeïnduceerde MN. De T-lymfocyten van pasgeborenen zijn bijna allemaal fenotypisch immatuur. Deze status wordt gekenmerkt door een gesloten chromatine structuur, wat een onderliggende oorzaak zou kunnen zijn voor de waargenomen hogere stralingsgevoeligheid van pasgeborenen in vergelijking met volwassenen. Dit werd bevestigd in een vergelijkende studie naar de stralingsgevoeligheid van geïsoleerde naïeve (CD45RA⁺) en memory (CD45RO⁺) T-lymfocyten afkomstig van volwassenen, waar opnieuw een hoger aantal residuele foci en MN werden waargenomen in naïeve T-lymfocyten. De resultaten van dit derde artikel suggereren dat het waargenomen verschil in stralingsgevoeligheid van T-lymfocyten tussen pasgeborenen en volwassenen zou kunnen verklaard worden door de immunofenotypische veranderingen van T-lymfocyten met de leeftijd. Aangezien stralingsgeïnduceerde leukemie één van de meeste prominente maligniteiten is met een duidelijke leeftijdsafhankelijkheid in radiosensitiviteit, werden er in dit doctoraatsonderzoek ook *in vitro* studies uitgevoerd naar de respons op DNA schade en de uitkomst na stralingsgeïnduceerde DNA schade in HSPC. De resultaten worden voorgesteld in het derde artikel, waar een significant lager aantal residuele foci werd waargenomen in de CD34⁺ cellen in vergelijking met de T-lymfocyten van pasgeborenen. Daarnaast werd er ook voor CD34⁺ cellen een hoog aantal stralingsgeïnduceerde MN teruggevonden. Deze resultaten suggereren dat de 'quiescence' van HSPC mogelijk mutagenese kan promoten na stralingsblootstelling.

Het derde deel van de doctoraatsproefschrift omvat een algemene discussie. In **hoofdstuk 9** lichten we de *in vitro* en *in vivo* lage dosis hypersensitiviteit verder toe, die geobserveerd werd in de γ -H2AX foci studie op pediatrische patiënten die een CT onderzoek ondergingen. De resultaten van de huidige studie worden vergeleken met een voorgaande studie van onze onderzoeksgroep waar deze hypersensitiviteit ook geobserveerd werd bij kinderen die een hartkatheterisatie ondergingen (4). De *in vivo* biomerker resultaten illustreren het belang van CT dosisreductie voor pediatrische patiënten. Daarom wordt in de hoofdstuk de “*Image Gently*” campagne toegelicht. Het bystander effect wordt gezien als een mogelijk onderliggend mechanisme voor de geobserveerde hypersensitiviteit en wordt in dit hoofdstuk ook verder toegelicht. De hoge radiosensitiviteit van HSPC, wat een potentiële trigger kan zijn voor het ontstaan van stralingsgeïnduceerde leukemie, wordt besproken in **hoofdstuk 10**. Verder komt in dit hoofdstuk ook naar voor dat de vergelijking tussen resultaten bekomen met HSPC van muizen en mensen niet altijd zo eenvoudig is en dat de projectie van *in vitro* naar *in vivo* situaties met o.a. de impact van de “*niche*” nog verder onderzoek vereist. In **hoofdstuk 11** wordt het verschil in stralingsgevoeligheid tussen pasgeborenen en volwassenen verder besproken. Het verschil in chromosomale stralingsgevoeligheid en residuele DNA schade op cellulair niveau tussen naïeve en memory T-lymfocyten wijst erop dat het immunofenotypisch profiel van de lymfocyten een rol speelt in het waargenomen verschil in stralingsgevoeligheid tussen pasgeborenen en volwassenen. Daarom gaat dit hoofdstuk verder in op het verschil in chromatine condensatie als mogelijke verklaring voor de leeftijdsafhankelijkheid van stralingseffecten. De finale conclusies van dit doctoraatsproefschrift worden voorgesteld in **hoofdstuk 12**. De resultaten bekomen in dit proefschrift voor lage dosis blootstelling van kinderen moeten de medische wereld aansporen om de stralingsbelasting van kinderen verder te reduceren en de “*Image Gently*” principes in acht te nemen. Een aantal mogelijke toekomstperspectieven die voortvloeien uit dit onderzoek worden aangehaald in **hoofdstuk 13**. Verder onderzoek is nodig om 1) de lage dosis hypersensitiviteit beter in kaart te brengen en te begrijpen; 2) het verschil in stralingsgevoeligheid tussen de primitieve HSC en de progenitorcellen te ontrafelen; en 3) de chromatine structuur van naïve en memory lymfocyten beter te kennen zodat we meer inzicht krijgen in de rol van de chromatine structuur in de leeftijdsafhankelijke stralingsgevoeligheid.

Referenties

1. *Personal communication with Federal Agency of Nuclear Control (FANC) Belgium - Thanks to Petra Willems. 2015.*
2. *DDM2. DDM2 Project Report Part 1: European Population Dose. 2014.*
3. *UNSCEAR. Sources, Effects and Risks of ionizing radiation. New York: United Nations Scientific Committee on the Effects of Atomic Radiation, 2013.*
4. *Beels L, Bacher K, De Wolf D, Werbrouck J, Thierens H. gamma-H2AX Foci as a Biomarker for Patient X-Ray Exposure in Pediatric Cardiac Catheterization Are We Underestimating Radiation Risks? Circulation. 2009;120(19):1903-9.*

Contents

Dankwoord	I
Summary	IX
Samenvatting	XII
Contents	XIX
List of Acronyms	XXIII

PART I: Introduction

Children are the most important target group in medical radiation protection

1 Radiosensitivity of children to radiation-induced malignancies with special emphasis on leukaemia.....	3
1.1 Ionizing radiation and cancer risks in children: what have we learned from epidemiology?.....	4
1.1.1 The use of epidemiology data for paediatric risk assessment.....	4
1.1.2 UNSCEAR 2013: Are children more sensitive to radiation than adults?.....	9
1.1.2.1 Leukaemia	11
1.1.2.2 Thyroid cancer.....	14
1.1.2.3 Breast cancer.....	17
1.1.2.4 Brain and central nervous system (CNS) tumours	20
1.2 Origin of radiation-induced leukaemia: the pursuit of genomic stability of haematopoietic stem cells.....	21
1.2.1 Haematopoiesis.....	24
1.2.2 Radiation-sensitivity of HSPCs	29
1.3 References	31
2 Use of x-rays in paediatric diagnostic imaging	37
2.1 Medical radiation burden	38
2.2 Issues related to CT imaging in children	41
2.2.1 Frequency of CT imaging in children	41
2.2.2 Why are age-appropriate CT settings required for children?.....	43
2.3 Dose Reference Levels (DRLs) in paediatric CT imaging	45
2.3.1 Dose quantities in CT imaging	46
2.3.2 National DRLs	47
2.3.3 European DRLs	49
2.4 Overview of epidemiological studies on paediatric CT imaging.....	50
2.5 Estimation of radiation risk in paediatric radiology: the BEIR VII model	55
2.6 References	59

3	Biomarkers of x-ray induced DNA damage and repair	63
3.1	The DNA damage response	64
3.1.1	DNA damage sensors and transducers	66
3.1.2	DNA damage Effectors.....	69
3.1.2.1	Cell Cycle Checkpoints	69
3.1.2.2	DNA repair pathways	70
3.1.2.3	Apoptosis.....	73
3.2	Chromatin structure and DNA repair.....	75
3.3	Detection of x-ray effects at DNA level	78
3.3.1	Mutagenic effects: cytogenetic assays	78
3.3.2	The γ -H2AX foci assay to detect DNA DSB damage and repair	81
3.3.2.1	The role of γ -H2AX in the DDR	81
3.3.2.2	Technical aspects of γ -H2AX foci detection	82
3.3.2.3	Double immunostaining of 53BP1/ γ -H2AX foci	84
3.4	Ethical considerations for biomarker studies in children	86
3.5	References	88
4	Aim of the research	93
4.1	References	95
5	Outline of the research	97
5.1	References	99

PART II: Original Research

6	PAPER I.....	103
7	PAPER II.....	125
8	Paper III	143

PART III: General Discussion

9	Radiation risks in paediatric CT imaging.....	165
9.1	Biomarker studies in paediatric diagnostic radiology.....	166
9.1.1	Behaviour of the γ -H2AX dose response in diagnostic studies on children	167
9.1.2	Low dose hypersensitivity indicates a bystander effect.....	172
9.1.3	Importance of blood dose calculation in biomarker studies	175
9.1.4	Paediatric patient data point to age-dependency in DNA damage induced by CT x-rays..	177
9.2	Uncertainties in paediatric radiation risk assessment	179

9.3 In vivo biomarker data illustrates the necessity of CT dose reduction: the “Image Gently” message.....	184
9.4 References	187
10 Radiation-induced leukaemia and radiosensitivity of haematopoietic stem- and progenitor cells.....	191
10.1 A distinctive DNA damage response in HSPCs	192
10.2 Extrapolation of “in vitro” results to the “in vivo” situation: protective role of the bone marrow niche	198
10.3 The leukemic stem cell: Are HSPCs the target cells for radiation-induced leukaemia?	202
10.4 References	207
11 Age dependence in radiation sensitivity.....	211
11.1 Biological evidence regarding age-dependent radiosensitivity	212
11.2 Differences in immunophenotypic profile of newborn and adult T-lymphocytes	215
11.3 Chromatin condensation plays a critical role in radiosensitivity of naive and memory T-lymphocytesw.....	218
11.4 References	223
12 Final Conclusions	227
13 Future Perspectives	231
13.1 References	235
 PART IV: Curriculum Vitae	
14 Curriculum Vitae	239

List of Acronyms

A

Ab Antibody
ABC Transporter ATP-Binding Cassette Transporter
ALARA As Low As Reasonably Achievable
ALL Acute Lymphoid Leukaemia
AML Acute Myeloid Leukaemia
Apaf1 Apoptotic Protease Activating Factor 1
APML Acute Promyeloid Leukaemia
AT Ataxia Telangiectasia
ATB Age at Time of Bombing
AT Ataxia Telangiectasia
ATCM Automatic Tube Current Modulation
ATM Ataxia Telangiectasia Mutated
ATR ATM- and RAD3-related
ATRIP ATR Interacting Protein

B

Bak Bcl-2 homologous antagonist killer
Bax Bcl-2-associated X
Bcl-2 B-cell CLL/lymphoma 2
BEIR Biological Effects of Ionizing Radiation
BER Base-Excision Repair
BLM Bloom's syndrome helicase
BM Bone Marrow
BN Binucleated
BRCA 1/2 Breast-Cancer early onset 1/2
BRCT BRCA1 C-terminal
BSA Bovine Serum Albumin
53BP1 p53 Binding Protein 1

C

CA Chromosome Aberrations
CBMN Cytokinesis-Block Micronucleus
CBX Carboxolone
CD Cluster of Differentiation
CD45RA* naive RA isoform of the CD45 molecule
CD45RO* memory RO isoform of the CD45 molecule
CHD Congenital Heart Disease
CI Confidence Interval
CLL Chronic Lymphoid Leukaemia
CLP Common Lymphoid Progenitor
CM T Cell Central Memory T Cell
CML Chronic Myeloid Leukaemia
CMP Common Myeloid Progenitor
CNS Central Nervous System
COX-2 Cyclooxygenase-2

CSC Cancer Stem Cell
CT Computed Tomography
CtBP CtBP-interacting protein
CTDI Computed Tomography Dose Index
CTDI_{vol} Volume Weighted Computed Tomography Dose Index
CTDI_w Weighted Computed Tomography Dose Index
Cx Connexin
Cyclin-Cdk Cyclin-dependent kinase

D

DAP Dose-Area Product
DAPI 4',6-Diamidino-2-Phenylindole
DDM2 Dose DataMed 2
DDR DNA Damage Response
DDREF Dose and Dose Rate Effectiveness Factor
diAcH3 Diacetylated Histone H3
DLP Dose-Length Product
DoReMi Low Dose Research towards Multidisciplinary Integration
DNA Dioxiribonucleic Acid
DNA-PKcs DNA-dependent Protein Kinase catalytic subunit
DRL Dose Reference Level
DS Dosimetry System
DSB Double-Strand Break
DS02 Dosimetry System 2002

E

EAR Excess Absolute Risk
EM T Cell Effector Memory T Cell
EPA Environmental Protection Agency
EPI-CT Epidemiological Study to Quantify Risks for Paediatric Computerised Tomography and to Optimise Doses
ERR Excess Relative Risk
EXO1 Exonuclease 1

F

FANC Federal Agency of Nuclear Control
FCS Foetal Calf Serum
FISH Fluorescence In Situ Hybridization
FITC Fluorescein Isothiocyanate

G

- GJIC** Gap Junction-Mediated Intercellular Communication
GMP Granulocyte and Macrophage Progenitor
G-CSF Granulocyte-Colony Stimulating Factor
Gy Gray

H

- H2AX** histone subtype H2A isoform X
HDAC Histone Deacetylase
HIF-1 Hypoxia-Inducible Factor-1
HR Homologous Recombination
HSC Haematopoietic Stem Cell
HSPC Haematopoietic Stem and Progenitor Cell

I

- ICRP** International Commission on Radiological Protection
IL Interleukin
IR Ionizing Radiation
IRIF Irradiation-Induced Foci

K

- kV** KiloVoltage

L

- LAR** Lifetime Attributable Risk
LET Linear Energy Transfer
LIG4 DNA ligase 4
LNT Linear No-Threshold
LSC Leukaemic Stem Cell
LSS Life Span Study

M

- mA** milliAmpere
MDC1 Mediator of DNA damage Checkpoint 1
MEP Megakaryocyte and Erythrocyte Progenitor
MELODI Multidisciplinary European Low Dose Initiative

- MHC** Major Histocompatibility Complex
MLP Multilymphoid Progenitor
MMR Mismatch Repair
MN Micronucleus
mPB Mobilized-Peripheral Blood
MPP Multipotent Progenitors
MRN Mre11/Rad50/Nbs1 complex
MSC Mesenchymal Stem Cell
MSCT Multi-Slice Computed Tomography
MWU Mann Whitney U

N

- NBUD** Nuclear Bud
NDRL National Dose Reference Level
NER Nucleotide Excision Repair
NHEJ Non-Homologous End Joining
NK Natural Killer
NPB Nucleoplasmic Bridge
NRPB National Radiological Protection Board

P

- PACS** Picture Archiving and Communication System
PB Peripheral Blood
PF Predisposing Factor
PFA Paraformaldehyde
PFGE Pulsed-Field Gel Electrophoresis
PHA Phytohaemagglutinin
PIDRL European Diagnostic Reference Levels for Paediatric Imaging
PIKK Phosphatidylinositol 3-Kinase like Kinase
PP2A Protein Phosphatase 2
Puma p53 Up-regulated Modular of Apoptosis

R

- RBM** Red Bone Marrow
RNS Reactive Nitrogen Species
ROS Reactive Oxygen Species
RPA Replication Protein A
RX Radiography X-rays

S

- SCF** Stem Cell Factor
- SEM** Standard Error of the Mean
- SIR** Standardised Incidence Ratios
- SSB** Single-Strand Break
- ssDNA** single-stranded DNA
- Sv** Sievert

T

- TCR** T Cell Receptor
- TEM** Transmission Electron Microscopy
- TGF- β** Transforming Growth Factor β
- TNF- α** Tumour Necrosis Factor α
- TPO** Thrombopoietin
- TRITC** Tetramethyl Rhodamine Isothiocyanate
- TSA** Trichostatin A

U

- UCB** Umbilical Cord Blood
- UNSCEAR** United Nations Scientific Committee on the Effects of Atomic Radiation
- US** Ultrasound

V

- VPA** Valproic Acid

W

- w_r** Radiation Weighting Factor

X

- XLF** XRCC4-Like Factor

PAE

RTI

**Children are the most
important target
group in medical
radiation protection**

1

Radiosensitivity of children to radiation-induced malignancies with special emphasis on leukaemia

Since its discovery, x-rays have become an indispensable tool in current medical practice. However, ionizing radiation (IR) is a known carcinogen and we need to weight the benefits against the cancer risks (1). Children are recognized as a vulnerable population group, since they are considerably more sensitive compared to adults regarding radiation-induced malignancies and the associated risk for exposure induced death. There are several reasons for this difference in radiation sensitivity. First, tissues and organs of children are growing and developing and more sensitive to radiation effects than those that are fully mature and differentiated, since they contain a larger proportion of stem cells and growing cells (2). Secondly, children have a longer life expectancy compared to older adults, in which the potential oncogenic effects associated with IR exposure can appear (3). The increase in sensitivity varies with age, with the younger ages being more at risk (4). The susceptibility of children to the effects of IR has been a focus of interest for over half a century. In the following chapter we give an overview of the current epidemiological data to illustrate the age dependency in radiation sensitivity, with special emphasis on radiation-induced leukaemia.

1.1**Ionizing radiation and cancer risks in children: what have we learned from epidemiology?**

Epidemiological studies provide the primary data on the carcinogenic effects of radiation in humans. The fact that IR causes cancer in humans has been known for over a century. In 1902, the first radiation-induced cancer had been reported in an area of ulcerated skin. By 1911, there were already reports of leukaemia arising in radiation workers. Later, extensive epidemiological evidence for cancer risk from IR exposure came from the Life Span Study (LSS) of the Japanese atomic bomb survivor cohort (5, 6).

1.1.1**The use of epidemiology data for paediatric risk assessment**

Epidemiological studies of cancer following IR exposure are characterized by large population size, long-term follow-up of the cohort and well-characterized dose estimates for individuals. Certainly for children, a large population size is usually required since cancer is a rare outcome in this population. Radiation-induced leukaemia generally occurs with a minimum latency of about 2-3 years, while solid tumours only start to appear a minimum of 10 to 15 years after exposure and often do not occur until the child has reached adulthood. The major strength of epidemiological studies is that they provide direct information on health risks in humans. However, epidemiological studies are observational rather than experimental (the investigator cannot control the circumstances of exposure), which introduces a high potential for bias or confounding (7). Analysis of epidemiological data on childhood radiation exposure is difficult as it is hard to adjust for all the confounding factors which can modify the risk of cancer following radiation exposure. These factors include: gender - females are more sensitive than males for some radiation-induced cancers; age at exposure - younger children are more susceptible; attained age - cancer might not appear until the child has reached adulthood (when cancer typically occurs); time since exposure - especially important for solid tumours with a long latency period of 10 years and longer; the presence of underlying diseases; and the influence of other potential carcinogens (e.g. cigarette smoke) (8).

Radiation-induced cancer risks are generally expressed as excess relative risk (ERR) or excess absolute risk (EAR). Both risk factors represent increased cancer rates relative to an unexposed population. ERR assumes that a radiation-related risk is proportional to the baseline risk as well as the exposure, while EAR assumes that the radiation-related risk does not depend on the level of baseline risk (3). Both ERR and EAR will decrease with increasing age at exposure. The ERR decreases with increasing attained age, while the EAR increases; these differences reflect the strong increase in baseline risk with attained age (9). Furthermore, the ERR of certain cancers (e.g. thyroid cancer) after irradiation in childhood is high, but the background absolute risk is low so that the EAR is comparatively small (7). Despite the mentioned differences, both metrics are useful in comparing the impact of exposure in children versus adults.

Describing the health effects of radiation exposure during childhood or adolescence compared to those occurring during adulthood is a complex matter. Many of the large epidemiological studies and reports on the sources and effects of IR exposure have also included children as part of the study population. To date, however, there is a lack of comprehensive reports specifically addressing all aspects of radiation exposure of children and the consequent health effects and associated risks. Information is often buried in epidemiological reports on general population exposure. The current risk estimates are derived from several epidemiological studies:

- The LSS cohort of Japanese atomic bomb survivors (35 382 persons or 41% of the exposed population was 0-20 years old at exposure)
- Accidents such as Chernobyl (27% of the evacuated people were 0-17 years old)
- Populations that have been exposed to fallout from the testing of nuclear weapons (e.g. Marshall Islands, where 39% of the inhabitants were children under 10 years of age)
- Medically exposed populations: radiotherapy for childhood cancers and benign conditions or diagnostic x-rays for disease follow-up

If we want to consider the results of the medically irradiated group, they should be treated with care since the individuals suffered from a known or suspected illness and may not be representative for the whole population in their carcinogenic response to radiation. Nonetheless, medical ir-

radiation studies provide a valuable support to the findings of the Japanese survivor studies (7).

Figure 1.1 and Figure 1.2 show the ERR of respectively the incidence and mortality at 1 Sievert (Sv) of certain sites of cancer other than leukaemia for the LSS cohort presented in the United Nations Scientific Committee on the Effects of Atomic Radiation (UNSCEAR) 2000 report (7, 10). The latter committee was established by the General Assembly of the United Nations in 1955 and its mandate is to assess and report levels and effects of exposure to IR. The assembly has designated 27 countries to provide senior scientists, who publish authoritative reports which form a scientific basis for evaluating radiation risk and for establishing protective measures throughout the world (www.unscear.org). The ERR values in Fig 1.1 and 1.2 represent the average for all survivors (all ages and both sexes) over the entire period of follow-up. The figures illustrate clearly the elevated risk for both incidence and mortality of female breast cancer and thyroid cancer. Leukaemia risks are not presented in Figure 1.1 and 1.2 since the ERR is dramatically higher than for other cancers; the ERR at 1 Sv for leukaemia incidence is 4.4 (90% confidence interval (CI): 3.2-5.6) (7). Furthermore radiation-induced leukaemia has a short latency period, a different dose-response relationship and time post-exposure behaviour compared to solid tumours. Most types of leukaemia, acute myeloid leukaemia (AML), chronic myeloid leukaemia (CML) and acute lymphoid leukaemia (ALL), were in excess with the notable exception of chronic lymphoid leukaemia (CLL). The radiation-induced risk of leukaemia is especially pronounced at young ages at exposure. The ERR for the survivors exposed as young children (age at exposure < 15 y) approaches 100/Sv within the subsequent decade (8). The excess risk for leukaemia is characterized by a wave that peaks within about 10 years of exposure and then subsides. For solid tumour incidence during 1958-1987, the ERR at 1 Sv is 0.63 (95% CI: 0.52-0.74) (11), whereas mortality during 1950-1990 it is 0.40 (90% CI: 0.31-0.51) (7).

As already mentioned, the above risk estimates are an average for a population of all ages and result in a risk of radiation-induced cancer of about 10% for an acute dose of 1 Sv (1 Gy of x-rays). However, if this dose is spread out over a longer period of time at a lower dose-rate or in a series of fractions a dose and dose-rate effectiveness factor (DDREF) of 2 has to be taken into account and the risk is about 5%/Sv (2, 12). The International Commission on Radiological Protection (ICRP) deduced from these data

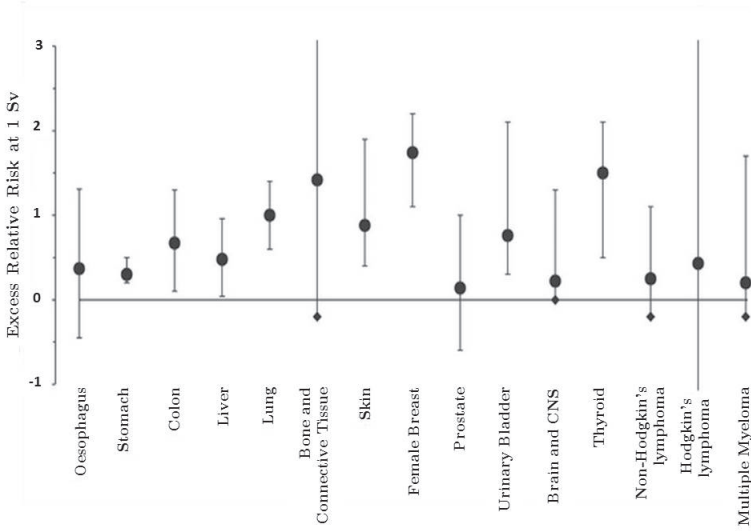


FIGURE 1.1

The ERR at 1 Sv for cancer incidence up to 1987 and corresponding 90% CI of different cancer sites among the Japanese atomic bomb survivors (UNSCEAR 2000) (♦ indicates that the lower 90% confidence limit is lower than this value). Figure from (7). The ERR represents the elevated risk of cancer incidence due to a radiation exposure of 1 Sv, proportional to the baseline cancer risk for the different organs.

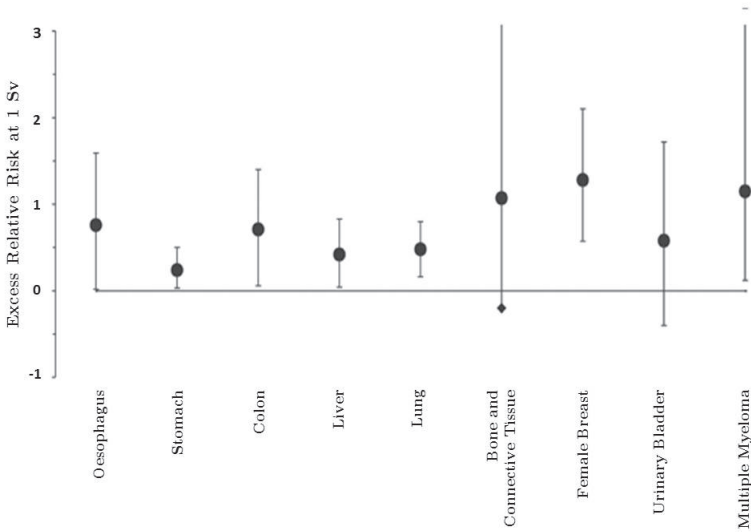


FIGURE 1.2

The ERR at 1 Sv for cancer mortality during 1950-1990 and corresponding 90% CI of different cancer sites among the Japanese atomic bomb survivors (UNSCEAR 2000) (♦ indicates that the lower 90% confidence limit is lower than this value). Figure from (7). The ERR represents the elevated risk of cancer incidence due to a radiation exposure of 1 Sv, proportional to the baseline cancer risk for the different organs.

the dependence of cancer incidence and mortality on age at exposure for both males and females, illustrated in Figure 1.3. ICRP has developed, maintained and elaborated the International System of Radiological Protection used world-wide as the common basis for radiological protection standards, legislation and guidelines. For individuals in the first decade of life, the risk is closer to 15%/Sv, while for adults exposed in late middle age, the risk drops to 1-2%/Sv (13, 14). Figure 1.3 shows also a clear gender difference, especially at early ages, which indicates that girls are more radiosensitive than boys.

PART I

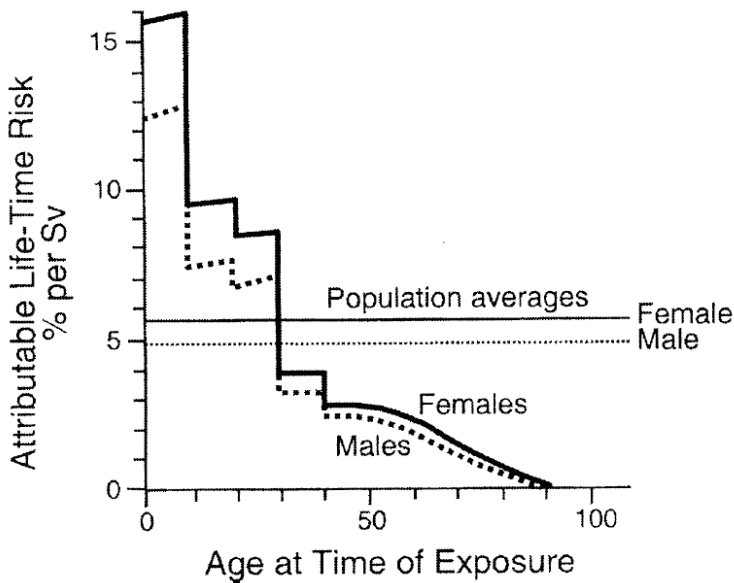


FIGURE 1.3

The attributable lifetime risk of cancer as a function of age for a single whole-body radiation dose of 1 Sv, which shows a decrease in radiosensitivity with age. These estimates are based on a multiplicative model and a DDREF of two (2).

1.1.2**UNSCEAR 2013: Are children more sensitive to radiation than adults?**

At present, there is a lack of statistically sufficient projections of lifetime risks for specific tumour sites following exposure at young ages. The current estimates do not adequately capture the known variation and additional work is needed. Therefore, UNSCEAR has dedicated an entire volume on the scientific findings on effects of radiation exposure of children in volume 2 of the 2013 Report (15). The definition of “child” is not always consistent in scientific literature, therefore, the UNSCEAR committee had defined “children” as those exposed as infants, children and adolescents (age < 20 years).

According to the latest findings of the UNSCEAR committee, the general perception that children are more vulnerable to radiation exposure than adults is not universally true. In the UNSCEAR 2006 Report, the committee stated that lifetime cancer risk estimates for those exposed as children were uncertain and might be a factor of 2-3 times higher than estimates for a population exposed at all ages. This conclusion was based upon a lifetime projection model combining all tumour types (16). In the 2013 report, the UNSCEAR committee has reviewed 23 different cancer types and reports the following scientific findings:

- For about 25% of tumour types, children are clearly more radiosensitive. These include leukaemia, as well as thyroid, skin, breast and brain cancer.
- For about 15% of tumour types (e.g. bladder cancer) children appear to have about the same radiosensitivity for tumour induction as adults.
- For about 10% of tumour types (e.g. lung cancer) children appear less sensitive to external radiation exposure than adults.
- For 20 % of tumour types (e.g. oesophagus cancer), the data are too weak to draw a conclusion regarding differences in risk with age at exposure.
- For about 30% of tumour types (including multiple myeloma, Hodgkin lymphoma, pancreas, prostate, rectum, and uterus cancer), there is only a weak or no relationship between radiation exposure and risk at any age of exposure.

Thus, the commonly held notion that children might be two-three times more sensitive to radiation than adults is true for some malignancies but certainly not for all. The UNSCEAR committee recommends to avoid generalization of the risk of childhood radiation exposure. Furthermore, the currently used estimates do not adequately capture the known variations and additional work is needed. Nevertheless, current scientific data still highlight the fact that infants and children are a target group of high concern in medical radiation protection. As shown in the last reviews of the atomic bomb survivors, both ERR and EAR for all solid cancers were and still continue to be higher for younger ages at exposure. The lifetime risk on a radiation-induced malignancy for a given dose is seriously higher in children than in adults: 2-3 times for all solid tumours (depending on the models and the compared ages) and 3-5 times for leukaemia.

One of the reasons why children are more sensitive to IR is related to aspects of developmental anatomy that affect their response to radiation. Tissues and organs of children are growing and developing, moreover, the growth period of the human body is unusually long compared to other mammalian species. In addition, there are remarkable differences in growth rate of different parts of the human body. For example, the head and the brain are proportionally much larger in young children, which could mean that the absorbed dose in specific organs is quite different at different ages and developmental stages. Figure 1.4 illustrates the difference in organ size and growth across tissue types and age. The lymphoid tissue is large at birth and grows rapidly until late childhood, and then declines in absolute mass. The neural group grows rapidly and completes >90% of the postnatal increase by the end of early childhood (17), while the musculoskeletal tissues grow primarily during childhood and early adolescence, and gonads do not mature until late adolescence (15).

In the following sections, we will discuss the tumour types for which children are clearly more sensitive than adults as presented in the UNSCEAR 2013 report. For some of these malignancies, depending upon the circumstances, the risks for children can be quite high, but it remains important to keep in mind that tumour induction in children compared to adults is quite variable and depends on tumour type, age and gender.

Due to the differences in dose quantities used in the cited publications, the risk estimates will be expressed per organ equivalent dose in Sievert (Sv) or absorbed organ dose in Gray (Gy) in the following sections. An absorbed organ dose in Gy is used when no allowance was made for the

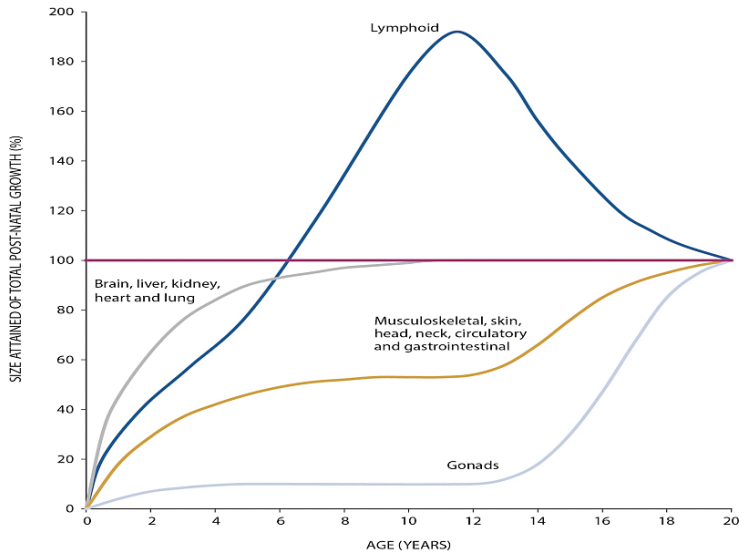


FIGURE 1.4

Growth curves of different parts and tissues of the body, showing four main patterns of growth. All the curves are attained as a percentage of the total gain from birth to maturity, and plotted so that size at 20 years of age is 100% on the vertical scale (purple line). Figure from (15), based on (17).

biologic effectiveness of different types of radiation. This is particularly important for the risk estimates derived from the LSS cohort, as a given dose of neutrons has a greater biological effectiveness than the same dose of γ - or x- rays. Allowance can be made for the different effectiveness of various types of radiation, by using a radiation weighting factor w_R , resulting in an equivalent dose expressed in Sv. The ICRP has assigned radiation weighting factors to specified radiation types (sometimes called radiation qualities) dependent on their relative biological effectiveness. The w_R for x-rays and γ -rays is typically 1, for protons 2, for high-energy neutrons 10 and for alpha particles 20. Thus for example, an absorbed dose of 1 Gy by high-energy neutrons will lead to an equivalent dose of 10 Sv.

1.1.2.1

Leukaemia

The LSS studies showed a strong increased risk in both incidence and mortality of leukaemia (18, 19). Most types of leukaemia, except CLL, can be induced by IR with a minimum latency of about two years (15). The acute

forms of leukaemia predominate and occur more rapidly after exposure than chronic leukaemia. Leukaemia risk is best described by a linear-quadratic dose response model (18) and this model has been adapted by the ICRP (14), the Biological Effects of Ionizing Radiation (BEIR) (20) and UNSCEAR (16) committees. International and national authorities rely on the work of these committees for the evaluation of the scientific information on the health effects of exposure to IR. The most substantial human data on radiation-induced leukaemia come from studies of three major population groups, which included also children: the survivors of the atomic bombing in Japan, persons exposed to high doses of pelvic radiation therapy and persons treated with x-rays for ankylosing spondylitis or other benign diseases.

By the late 1940's, physicians in Hiroshima and Nagasaki had noticed an apparent increase in leukaemia incidence among survivors (particularly children) who were near the hypocentres at the time of the atomic bombing. The first published report of an increased risk of leukaemia among the atomic bomb survivors appeared in 1952 (19). Since then, risks of leukaemia and other haematological malignancies have been the subject of several studies on the LSS cohort, showing a clear age-at-exposure effect for leukaemia (18, 19, 21, 22). Richardson *et al.* demonstrated a marked variation of ERR with age at exposure in the LSS cohort, with the risk being notably higher at younger ages at exposure, as illustrated in Figure 1.5 (21). Richardson and colleagues examined the leukaemia mortality among atomic bomb survivors during 1950-2000 using the estimated red bone marrow (RBM) dose. Adjusted RBM dose estimates were reported in this study, taking into account random errors attributable to the survivor's location and shielding. The calculated doses represent a weighted dose per Gy, which is the sum of the γ - and neutron irradiation. Figure 1.5 shows clearly the higher excess deaths in the earlier years among those exposed at young age, which is followed by a rapid decline with time. The majority of excess leukaemia deaths from radiation among those exposed as children occurred during the follow-up period before 1975 (23). For child of 10 years at the time of the bombing, the ERR/1 Gy RBM dose peaks at ~65 some 7 years after exposure and then attenuates with time since exposure, such that at 25 years after the bombings the ERR was still raised but at a level comparable with the ERR for those exposed as adults. There is, however, still evidence of a small increase in leukaemia risk among the survivors still alive and a significant linear radiation dose response for myelod-

ysplastic syndromes in A-bomb survivors 40 to 60 years after the radiation exposure (23). The latter syndromes are characterized by an increased risk of developing AML.

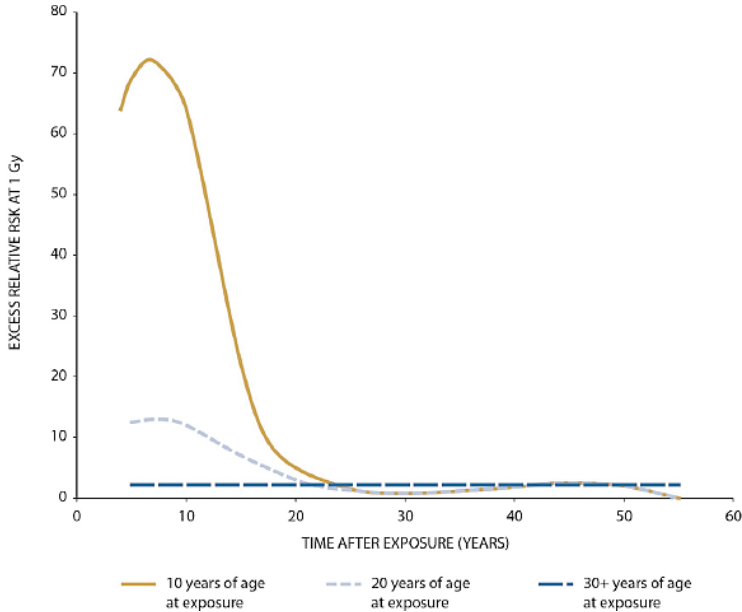


FIGURE 1.5

Estimated ERR at 1 Gy for leukaemia mortality, taking into account all types of leukaemia as a function of age at exposure and time since exposure in the LSS cohort (15, 21).

Several studies have identified an increased risk for childhood leukaemia incidence or mortality after radiotherapy for the treatment of benign disease (24-27), whereas others have not (28). Lundell and Holm did not find an association between incidence of childhood leukaemia and radiation dose for infants who were treated with radiotherapy for skin haemangiomas (28). Despite the relatively large number of infants studied, the low average dose to the bone marrow probably limited the possibility of detecting a small radiation risk. Darby *et al.* reported a 3-fold increase in leukaemia mortality in children treated with radiotherapy for ankylosing spondylitis (24). There was evidence that the risks of acute myeloid (AML),

acute lymphoid (ALL), and chronic myeloid leukaemia (CML) were all increased, but no evidence of any increase in CLL. Murray *et al.* found more leukaemia deaths than expected in children exposed to ionizing radiation for thymic enlargement (ratio of observed to expected deaths was 4.5) (26). Children treated with radiotherapy for tinea capitis (ringworm of the scalp) exhibited a subsequent excess risk of leukaemia that commenced a few years after exposure in both an Israeli cohort of almost 11 000 children (mean age at treatment, 7.1 years) (25) and a smaller cohort of just over 2000 children from New York City (mean age at treatment, 7.8 years) (27). In the group of Israeli children, the assessed individual bone marrow dose was 0.3 Gy and the ERR/Gy for leukaemia at all ages was 4.4 over the entire follow-up (on average up to 26 years).

Overall, the risk of radiation-induced leukaemia in children appears to be three- to fivefold greater than the risk to adults, based on several studies covering various types of exposure (15).

1.1.2.2

Thyroid cancer

Thyroid carcinoma is the most frequent type of endocrine tumour and accounts for about 1% of all malignancies (29). Thyroid cancer is approximately twice as common in females as in males, with an increasing incidence with age. In 1950, Duffy and Fitzgerald reported that IR appears to be an important causal factor for thyroid cancer (30). Several following studies confirmed this finding, including data from the LSS cohort, the radioiodine exposure in Chernobyl, and head and neck radiotherapy populations. Robbins *et al.* estimated that 9% of thyroid cancers in the general population may be attributable to IR (31). Especially the thyroid gland of children is highly susceptible to the carcinogenic effect of IR (32).

There are several factors that modify the risk of thyroid cancer (15):

- The *latency period* from IR exposure to the clinical development of thyroid neoplasms, which varies widely among epidemiology studies of radiation-induced thyroid cancer. On the basis of pooled analysis of seven previously published studies (five cohort and two case-control) of acute external irradiation and thyroid cancer. Ron *et al.* reported that thyroid cancer risk peaked at about 15-19 years after IR exposure, but was still elevated beyond 40 years (33).

- The *age at exposure*, since the thyroid of children and adolescents is more radiosensitive than in adults. Except for high therapeutic doses, exposure over the age of 30 years from external radiation have not been found to significantly increase the risk of thyroid cancer (15).
- *Gender* appears also to be a modifying factors, since several epidemiological studies indicate that females are more sensitive than males. The EAR for females may be 2 - 4 times higher than in males (34), while the ERR per dose unit is about the same for both sexes or only slightly higher in females, due to the higher incidence of spontaneous thyroid carcinoma in females.
- Also *ethnic background* appears to be a modifying factor. This has particularly been reported in studies of persons of Jewish ancestry (35).
- Several authors suggested that iodine deficiency may be a prompting factor in radiation-induced thyroid cancer. Iodine deficiency may induce an increasing incidence of benign thyroid conditions, but very high iodine intake also affects thyroid function and, possibly, thyroid cancer risk (36, 37). An important epidemiological study on radiation-induced thyroid cancer of Cardis *et al.* indicates that in areas of iodine deficiency, the radiation-related cancer risk may be three times higher than in areas of normal iodine levels (38). They also suggest that with iodine prophylaxis, the risk can be reduced by about a factor of three. On the other hand, the study of Brenner *et al.* on the Ukrainian cohort did not find a statistical significant modification of radiation risk in the case of either low iodine excretion levels or the use of stable iodine prophylaxis (39).

Several reports were published on the incidence of thyroid cancer among the atomic bomb survivors (40-42). The LSS mortality studies did not include thyroid cancer, because the death rate from thyroid cancer is very low compared with most other cancers. As already mentioned the incidence of thyroid cancer increases with decreasing age at exposure and attained age. In the last review of thyroid cancer incidence in the LSS cohort from 1958 through 2005 (42), both the ERR and EAR significantly and rapidly decreased with increasing age at exposure by 53% and 70% respectively, per decade increase in age at exposure. Allowing for the modifying effect of age at exposure, the ERR tended to decrease and the EAR to increase with increasing attained age (see Figure 1.6).

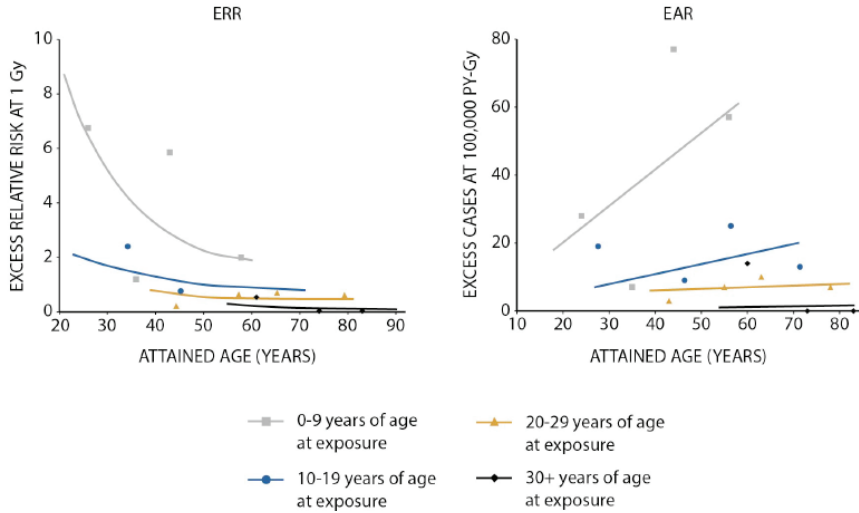


FIGURE 1.6

Fitted temporal patterns and age-at-exposure variation in the radiation-associated risk for thyroid cancer in the LSS cohort. The left panel presents the ERR at a thyroid dose of 1 Gy and the right panel the fitted EAR at 10^5 person-years-Gy⁻¹. Thyroid dose estimates from the current survivor dosimetry system (DS02) were used for the analyses. All curves and data points are gender-averaged estimates. Figure from (43).

Numerous epidemiological studies were published on radiation-induced thyroid cancer incidence for paediatric populations treated with radiotherapy for benign diseases or other types of cancer (e.g. Hodgkin's disease, neuroblastoma...). A pooled analysis (atomic bomb survivors, children treated for tinea capitis, two studies of children irradiated for enlarged tonsils, and infants irradiated for an enlarged thymus gland) was published by Ron *et al.* and gives the best estimate of risk for individuals exposed under 15 years of age to external radiation (33). The ERR at 1 Gy was estimated to be 7.7 following exposures in childhood (age less than 15 years), which is one of the highest risk estimates for any tissue.

One of the most dramatic findings after the Chernobyl incident was a large increase in thyroid cancers in children. Particularly, internal irradiation from ¹³¹I intake by the ingestion of fresh contaminated milk gave more than 80% of the total thyroid dose (15). Cardis *et al.* identified an excess risk at all thyroid doses above 0.2 Gy (38). In some locations where contamination was highest, as in the Gomel region, the incidence of thyroid cancer increased over a 100-fold.

1.1.2.3**Breast cancer**

Breast cancer is the most common cancer among women, one in ten of all new cancer diagnosed worldwide each year is a cancer of the female breast (44). The data concerning female breast cancer risk following radiation exposure come primarily from three major population groups: the LSS cohort, patients who underwent a diagnostic radiology exposure, and persons who have had radiotherapy to the breast for benign (thymic enlargement in infancy, skin haemangioma, etc.) or malignant (Hodgkin's lymphoma, Wilm's tumour, sarcomas, etc.) diseases in which the developing breast tissue was exposed to radiation (15). Several population studies have suggested a number of factors that modify radiation-induced breast cancer risk: irradiation at the time of menarche or the time of first pregnancy, nulliparity, obesity, family history of breast cancer, history of benign breast disease and genetic factors (BRCA1/BRCA2 and ataxia telangiectasia mutated (ATM) gene mutations) (15). However, these modifying factors should be interpreted cautiously. Up to now, age at exposure and the age at risk (attained age), are the only two strong modifying factors that were repeatedly observed by different investigators (45).

The excess risk of breast carcinoma among female survivors of the atomic bombs in Japan was already noticed in 1968 (46). Several updates followed since then and indicated a linear and statistically highly significant radiation dose response. Preston *et al.* (45) reported ERRs at 1 Gy for those exposed at ages 5, 25 and 45 years of 2.6, 1.8 and 1.1 respectively. The corresponding EARs were 21.1, 11.6 and 4.9 per 10^4 person years per Gy.

An analysis of 'age at exposure effects' on females breast cancer risk was performed by Land *et al.* (47) and McDougall *et al.* (48). Both studies found similar higher risk estimates for those irradiated in early childhood and around the time of puberty (before age 20) compared to individuals after age 20. Tokunaga *et al.* (49) reported that the ERR per Sv depends strongly on the age of exposure in the LSS cohort, also called age at time of bombing (ATB), which decreased by approximately 3.7% per additional year. The ERR of the age ranges 0-19, 20-39 and ≥ 40 years ATB were 2.41, 1.25 and 0.48 per Sv, respectively (see Figure 1.7 which shows more steps in age range: 0-9; 10-19; 20-29; 30-39; 40-49). Only marginally statistically significant ERR was found for the group ≥ 40 years at time of exposure. In this study risk rates were analysed by taking into account the average breast equivalent dose in Sv, assuming a w_R of 10 for neutrons. Land *et*

al. (50) evaluated if early childhood exposure may result in breast cancer at a younger age. Women who were exposed at ages 0-19 years in the LSS cohort had a corresponding high ERR of 13.5 at 1 Gy before the age of 35, which is two times higher than the ERR at 1 Gy for cancers occurring after age 35. Despite the fact that risk estimates vary between different publications, a higher risk of breast cancer for those exposed at young ages is evident from the LSS cohort.

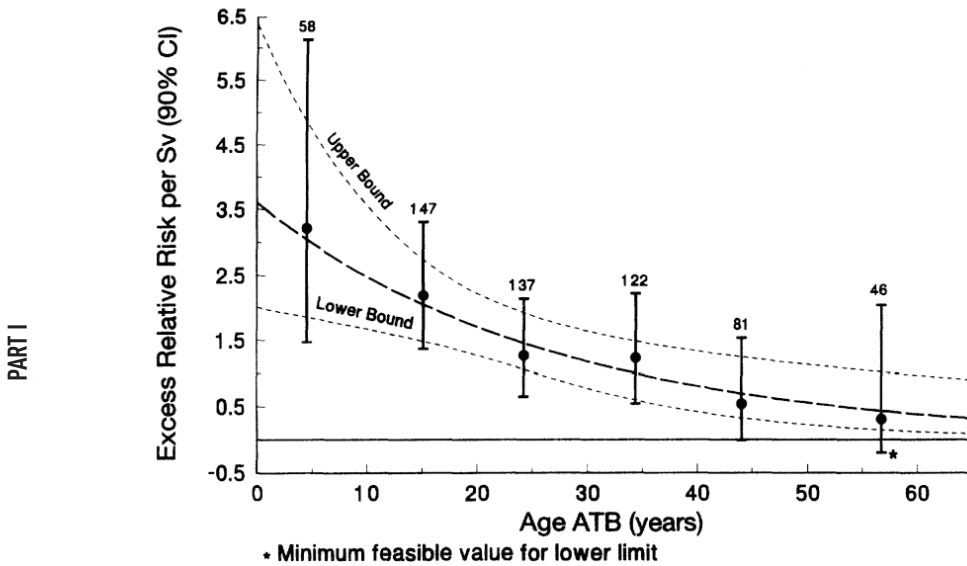


FIGURE 1.7

Estimated excess relative risk per Sv (breast equivalent dose), by interval of age at the time of bombings (ATB). Estimates and 90% confidence limits are stratified on city, ATB and attained age. The corresponding total number of cases appears above the upper confidence limit for each interval of ATB (49).

Besides the studies of the survivors of the atomic bombings in Japan, there are several studies reporting the occurrence of excess breast cancer incidence and mortality among a Canadian cohort of female patients exposed to multiple fluoroscopic examinations before 1965 for the treatment of pulmonary tuberculosis by artificial pneumothorax (51, 52). The latest report on the Canadian multiple fluoroscopic examination study, based on the mortality experience from 1950 to 1987, reported a statistically significant higher radiation risk for those exposed before the age of 10 than after

that age in the fluoroscopy study (53). This is an inconsistency with the LSS cohort, where a maximal ERR for those exposed between ages 10 and 14 years was observed, and a lower risk for those exposed before age 10. In the fluoroscopy study, however, the highest ERR is seen for those exposed between ages 0 and 9, with a substantially lower ERR for those exposed between 10 and 14 years. The authors reported estimates of ERR of breast cancer mortality for the combined Canadian fluoroscopy and atomic-bombing survivor cohorts at 1 Sv of 1.41, 0.44, 0.24, 0.05 and -0.01 after exposure at age ranges of 0-9, 10-19, 20-29, 30-39 and 40-49, respectively. Besides the Canadian cohort, other epidemiology studies were published on radiation-induced breast cancer in diagnostic medically exposed populations, including a Massachusetts tuberculosis cohort (54) and scoliosis cohort (55) monitored by radiography x-rays (RX) or fluoroscopic examinations for treatment efficacy and disease progress.

A number of studies have examined the risk of breast cancer after radiotherapy for various childhood malignancies (Hodgkin's lymphoma, Wilm's tumour, sarcomas, etc.) and benign diseases (thymic enlargement in infancy and skin haemangiomas). These reports took into account relevant variables such as the radiation dose both to breast tissue and to the ovaries (the latter related to oestrogen secretion), patient age, and genetic variations related to the primary malignancy (15, 56). The mean absorbed dose to the breast in the study of Hildreth *et al.* on the increased breast cancer risk in girls treated for presumed thymic enlargement in infancy was 0.71 Gy (about 90% of the patients was less than 6 months of age at time of exposure) (57). The dose response ERR for breast cancer was 1.10 per 1 Gy. Follow-up studies after treatment of Hodgkin's disease with mantle radiotherapy have indicated at least a fourfold increase of breast cancer risk, with doses to the breast varying from 4 to 40 Gy, depending upon the technical factors and positioning (15). Radiation-induced breast cancer has been reported to have more adverse clinicopathological features compared with breast cancer in age-matched population controls, especially the incidence of bilateral breast cancer seems to be increased in women treated with radiation exposure of the chest for paediatric or young adult cancer (58, 59).

Overall, several studies indicate the higher risk of radiation-induced breast cancer from exposure in childhood compared to adulthood. The increased risk in children appears to be about three- to fivefold (60). Epidemiological data support a linear dose response relationship for doses to the breast up to about 3 Gy (15).

1.1.2.4**Brain and central nervous system (CNS) tumours**

The most commonly described intracranial radiation-induced malignancies are meningioma, sarcoma, and glioma (61). It is often difficult to separate brain tumours into either strictly malignant or non-malignant categories, because some tumour types may be slowly growing (15). Primary malignancies of the CNS are among the most lethal of cancers. In the United States, the 5-year survival for malignant CNS tumours is approximately 30% (16). The first report of a radiation-induced tumour of the CNS was published by Mann *et al.* in 1953 (62). The LSS reports showed only a moderate degree of association between IR and tumours of the CNS, because CNS tumours are relatively rare. Preston *et al.* reported a dose dependent ERR for nervous system tumours with an ERR of 1.2 per Sv and the largest ERR of 4.5 per Sv was observed for schwannomas (63). Individual weighted brain doses were calculated as the sum of the γ -ray dose plus 10 times the neutron dose by using the DS86 system. The data suggested an age at exposure effect for nervous system tumours (except schwannoma), with a higher ERR of 1.2/Sv for individuals exposed before age 20 compared to individuals exposed after age 20 for whom the ERR was 0.2/Sv.

Brain tumours, both malignant and benign, have been reported following radiotherapy for tinea capitis and haemangioma, after exposure of the order of 1 Gy. The health effects associated with radiation therapy for childhood tinea capitis was reported by Shore *et al.* for the New York cohort (64) and by Ron *et al.* for the Israeli patients (25). The mean dose to the brain in both studies was between 1.4 and 1.5 Gy. A linear model provided the most adequate fit for malignant brain tumours and meningiomas up to a dose of 2.7 Gy. The ERR/Gy was 4.63 for benign meningiomas, while for malignant brain tumours, the ERR/Gy was 1.98. The ERR/Gy decreased with increasing age at exposure for malignant but not for benign tumours. Similar findings were reported by Sadetzki *et al.*, who did not see an age at exposure effect for benign meningiomas, but noted a significant decrease in the ERR/Gy with age at exposure for malignant brain tumours of 3.6, 2.2 and 0.5 for ages 0-4, 5-9 and 10-15 years, respectively {Sadetzki, 2005, Long-term follow-up for brain tumor development after childhood exposure to ionizing radiation for tinea capitis}(65). Among the haemangioma cohort (66), the mean absorbed intracranial dose was lower (0.07 Gy). In this cohort, the ERR was 2.7 per Gy for malignant and

benign tumours combined, and the ERR decreased with increasing age at exposure. These studies on radiotherapy for benign conditions noted a strong dose response relationship, a decreasing risk of brain tumours with increasing age at exposure, and an elevated risk at 30 and more years after exposure.

Finally, a number of studies have linked subsequent neoplasms of the CNS, mainly gliomas, to previous cranial radiation for childhood cancers, especially for ALL (67). Neglia *et al.* published a report in 2006 on subsequent primary neoplasms of the CNS occurring within a cohort of 14 361 5-year survivors of childhood cancers (Childhood Cancer Survivor Study) (68). Gliomas occurred at a median time of 9 years from original diagnosis. Radiation exposure was associated with increased risk of subsequent glioma (odds ratio of 6.78). The ERR per Gy was highest among children exposed at less than 5 years of age, which may reflect the higher susceptibility of the developing brain to radiation. The UNSCEAR report of 2006 points out that malignant tumours of the CNS are seen mostly after high doses from radiotherapy and the risk is predominantly after exposure in childhood (16).

1.2

Origin of radiation-induced leukaemia: the pursuit of genomic stability of haematopoietic stem cells

Leukaemia is the most common childhood cancer, accounting for almost 1 out of 3 cancers diagnosed in children under 15 years of age in industrialized countries (69-71). Acute leukaemia accounts for the majority of paediatric cases, with 80% ALL and approximately 20% AML (72). An advisory group of the National Radiological Protection Board (NRPB 2003) tasked with estimating the incidence of different types of cancer for the UK population reported that myeloid leukaemias made up just over a third of spontaneous leukaemias, whereas radiation-induced myeloid leukaemias (especially AML) were over-represented compared to their lymphoid counterparts (73), as illustrated in Table 1.1. As described in section 1.1.2.1, the leukaemia risk depends strongly on the age at exposure (see Figure 1.5). The age effect involves different types of leukaemias; ALL is more common among children whereas CML and AML are more com-

mon among adults (19). This was also confirmed by Bartley *et al.* in a study on diagnostic x-ray exposure and risk of childhood leukaemia, showing an increased risk of childhood ALL (specifically B-cell ALL) but not AML (74). A possible explanation for the difference between the time and age distribution for ALL risk compared with that for AML and CML, is that ALL is concentrated largely in childhood in the general population while the incidence of AML and CML generally increases progressively with attained age. It is possible that the much higher risk for ALL in childhood exposure compared to exposure at adult age reflects the population dynamics of the relevant “target” population. It is known that normal lymphoid lineage-committed progenitors are most active early in life and decline in activity thereafter (75).

TABLE 1.1

Comparison of the percentage incidence rates for spontaneous and radiation-induced leukaemia (assuming 0% radiation-induced CLL), in a population of all ages, based on (71). The term LET refers to Linear Energy Transfer.

	AML	CML	CML	CLL
Spontaneous	27%	9%	9%	55%
Low-LET radiation	53%	22%	25%	0%
Thorotrast (high-LET)	80%	15%	5%	0%

Leukaemia is a cancer of blood-forming cells, that usually begins in the bone marrow with high numbers of abnormal white blood cells. These white blood cells are not fully developed and are called ‘blasts’ or leukaemia cells. The various types of leukaemia are primarily identified by the target cell that undergoes transformation. When the cancer develops in the lymphoid lineage, it is called lymphoid leukaemia (or lymphocytic leukaemia), while cancer of the myeloid lineage (monocytes and granulocytes) is described as myeloid leukaemia. The rate of disease progression is an additional feature used in classification. In chronic leukaemias, the blasts accumulate slowly and continue to differentiate into haematopoietic cells,

therefore, the disease progression is slow. In contrast, acute leukaemias are characterized by a rapid increase of blast cells, which decreases the capacity of the bone marrow to produce healthy blood cells, resulting in a rapid disease progression.

- Chronic myeloid leukaemia: CML is a malignant, clonal myeloproliferative disorder, affecting myeloid, erythroid and megakaryocytic blood elements. It was the first identified haematological malignancy that is associated with a specific chromosomal abnormality, identified as the Philadelphia chromosome (76).
- Acute myeloid leukaemia: AML has been described as a clonal disorder in which transformation and uncontrolled proliferation of an abnormally differentiated, long-lived myeloid progenitor cell results in high circulating numbers of immature blood forms and replacement of the bone marrow by malignant cells(78). Several specific cytogenetic abnormalities are closely, and sometimes uniquely, associated with morphologically and clinically distinct subsets of AML and can help to determine disease aggressiveness, response to treatment and prognosis (78). For example, the finding of a translocation between chromosomes 15 and 17, or t(15;17), is associated with a diagnosis of acute promyelocytic leukaemia (79).
- Chronic lymphoid leukaemia: CLL represents a monoclonal expansion of lymphocytes and in a majority of cases, B-lymphocytes are involved. The neoplastic cell is characterized as a hypoproliferative, immunologically incompetent small lymphocyte, refractory to apoptosis. B-CLL's apoptosis resistance depends in part on the altered activation of various survival pathways, triggered by the microenvironment and the B-CLL cells themselves (80). The disease primarily involves the bone marrow, with secondary release of the neoplastic cells in the peripheral blood. The circulating cells further selectively infiltrate the lymph nodes, spleen and liver (77).
- Acute lymphoid leukaemia: ALL is a malignant clonal disorder of the bone marrow lymphoid precursor cells, resulting in a high number of circulating blasts that lack the potential for differentiation and maturation. The normal development of haematopoietic cells is inhibited, followed by a replacement of the normal marrow cells by malignant cells (76).

As described in the previous sections, epidemiological studies of moderately or highly exposed groups have confirmed that leukaemia is particularly sensitive to induction by IR; and especially those exposed at young ages are at high risk (15, 18). Furthermore, Brenner *et al.* and Little *et al.* reported significant excesses of leukaemia in children exposed to low-dose IR (81, 82). Together with a recent study in the United Kingdom, which reported elevated risks of leukaemia and brain tumours after CT scans in childhood and adolescence (see chapter 3), we can consider leukaemia as the most important malignancy after radiation exposure during childhood (83). Most leukaemias originate from precursor cells in the bone marrow. Therefore, red bone marrow, which harbours haematopoietic stem and progenitor cells (HSPCs), is of critical interest.

1.2.1

Haematopoiesis

The HSPC population forms the fundamental base from which all major blood lines are derived through a process called haematopoiesis (or haemopoiesis). Two major cell lineages arise from the HSPCs: myeloid (granulocytes, erythrocytes, platelets and mononuclear phagocytes) and lymphoid (lymphocytes) cell lineages (84). Haematopoiesis is driven by a rare population of haematopoietic stem cells (HSCs) that asymmetrically self-renew, a process in which the ‘parent’ stem cell forms another parent stem cell and a daughter cell. In this biological process of self-renewal the HSC with long-term differentiation capability generates progeny with the same potential to differentiate into mature blood cells, without depletion of the stem cell pool.

In mammals, haematopoiesis occurs as a sequential process that moves to different anatomic sites during embryonic and foetal development, childhood and adult life (see Figure 1.8). In the prenatal period, the sites of haematopoiesis include the yolk sac, where blood formation occurs in blood islands; the foetal liver, spleen and finally, the bone marrow. During childhood and adult life, the bone marrow is the only source of new blood cells. However, maturation, activation, and some proliferation of lymphoid cells occur in secondary lymphoid organs (spleen, thymus and lymph nodes). In infancy, all the bone marrow is haematopoietic but during childhood there is progressive replacement of red active marrow by yellow inactive adipose tissue throughout the long bones, so that in adult life active red marrow is confined to the bones of the axial skeleton (cra-

nium, sternum, ribs and vertebrae) (85). Within the bone marrow exists a tightly controlled local microenvironment, also called bone marrow niche, that regulates the quiescence, proliferation and differentiation of HSCs. Regulatory signals within the niche emanate from surrounding cells in the form of secreted molecules and also from physical signals such as oxygen tension, shear stress, contractile forces and temperature (86).

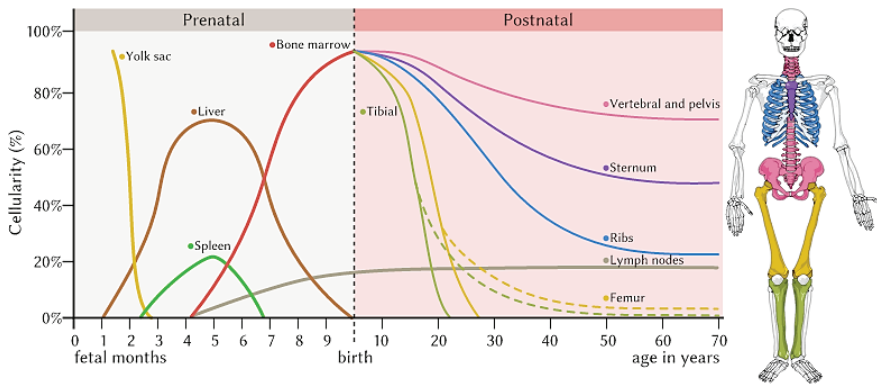


FIGURE 1.8

Illustration of the different sites of human haematopoiesis in pre- and postnatal periods. Marrow cellularity is the volume ratio of haematopoiesis and fat. The figure illustrates the age dependency of cellularity. In newborns, nearly all marrow is haematopoietic and with aging, cellularity diminishes due to the increase in the amount of fat in the long bones. Figure from (87).

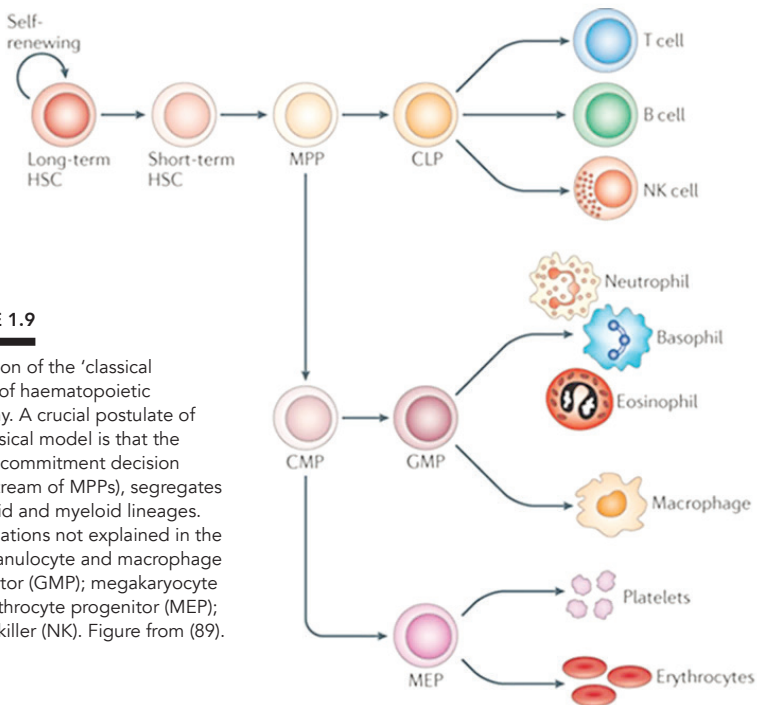
A functional hierarchy has been proposed for the haematopoietic compartment, illustrated in Figure 1.9. Haematopoiesis starts with stem cell division in which one cell replaces the stem cell (self-renewal) and the other is committed to differentiation. The early committed progenitors express low levels of transcription factors that may commit them to discrete cell lineages. Which cell lineage is selected for differentiation may depend both on chance (stochastic theory) and on the external signals received by progenitor cells (determinism theory). Several transcription factors have been isolated that regulate differentiation along the major cell lineages.

Self-renewing multipotent HSCs are at the apex of the haematopoietic hierarchy based on their ability to give rise to all cell types of the haematopoietic system (Figure 1.9). The self-renewing long-term HSCs first dif-

differentiate into short-term HSCs and multipotent progenitors (MPPs) with less self-renewal capacity. Together, these three cell types constitute the HSPC population. In this classical model, the lineage decision occurs as a stepwise bifurcation to a myeloid and lymphoid line (88). MPPs further differentiate into the two main branches of haematopoietic development that arise from the common lymphoid progenitor (CLP) and the common myeloid progenitor (CMP). All mature peripheral blood cells, shown on the right part of Figure 1.9, are derived from these progenitors.

FIGURE 1.9

Illustration of the 'classical model' of haematopoietic hierarchy. A crucial postulate of the classical model is that the earliest commitment decision (downstream of MPPs), segregates lymphoid and myeloid lineages. Abbreviations not explained in the text: granulocyte and macrophage progenitor (GMP); megakaryocyte and erythrocyte progenitor (MEP); natural killer (NK). Figure from (89).



HSC and their differentiated progenitor populations are distinguishable from other blood cells by the expression of specific cell surface lineage markers, such as Clusters of Differentiation (CD) proteins and cytokine receptors. The most important positive marker for HSPCs is the adhesion molecule CD34, which plays a central role in HSPC recognition. Table 1.2 presents the commonly expressed CD markers reported in literature for various subpopulations of HSPCs (90, 91). CD34⁺ cells can be used in the

treatment of various malignant and genetic diseases. Clinically applicable sources of CD34⁺ HSPCs are umbilical cord blood (UCB), bone marrow (BM) and mobilized peripheral blood (mPB) after administration of growth factors (e.g. granulocyte colony-stimulating factor, G-CSF) (92). The HSPC source used for an individual patient may depend on the availability of the graft, the disease, the age of the patient and the risks of complications after the transplant. The number of detectable CD34⁺ cells is very low in healthy donors, the CD34 antigen is expressed on 1-3% of BM cells and 0.1-0.4% of UCB cells (93). The characterization and isolation of HSPCs from these samples provides valuable information for clinical research and has emerged as a model system for stem cell biology. The mechanisms controlling HSPC homing to the bone marrow, self-renewal and differentiation, are thought to be influenced by a diverse set of cytokines, chemokines, receptors and intracellular signalling molecules.

TABLE 1.2

CD marker combinations of different HSPC subpopulations of the classical human haematopoiesis model.

	Cell Type	CD Marker Definition
HSC	Haematopoietic Stem Cell	CD34 ⁺ CD38 ⁻ CD90 ⁺ CD45RA ⁻ CD49f ⁺
MPP	Multipotent Progenitor	CD34 ⁺ CD38 ⁻ CD90 ⁺ CD45RA ⁻ CD49f ⁺
CLP	Common Lymphoid Progenitor	CD34 ⁺ CD10 ⁺ CD7 ⁺
CMP	Common Myeloid Progenitor	CD34 ⁺ CD38 ⁺ CD123 ^{med} CD135 ⁺ CD45RA ⁻
GMP	Granulocyte and Macrophage Progenitor	CD34 ⁺ CD38 ⁺ CD123 ^{med} CD135 ⁺ CD45RA ⁺
MEP	Granulocyte and Macrophage Progenitor	CD34 ⁺ CD38 ⁺ CD123 ⁻ CD135 ⁻ CD45RA ⁻ CD110 ⁺

Figure 1.10 shows the major classes of human HSPCs defined by cell surface phenotypes. However, this figure deviates from the classical model of haematopoiesis shown in Figure 1.9, since CLP is replaced by a multi-lymphoid progenitor (MLP). The latter cell is still a progenitor giving rise to all lymphoid lineages (B, T and NK cells), but experimental data have shown that early lymphoid progenitors in humans retain myeloid programs (94). Therefore, Doulatov *et al.* proposed a broader term – multilymphoid progenitor – to describe lymphoid progenitors that may have additional myeloid potentials (88). Hence, the MLPs presented in Figure 1.10 are not lymphoid restricted and possess myeloid potential. However, there still remain uncertainties on the precise lineage output of the lymphoid progenitors. Both Figure 1.9 and 1.10 show that genomic instability in CD34⁺ HSPCs can give rise to both myeloid and lymphoid leukaemias.

PART I

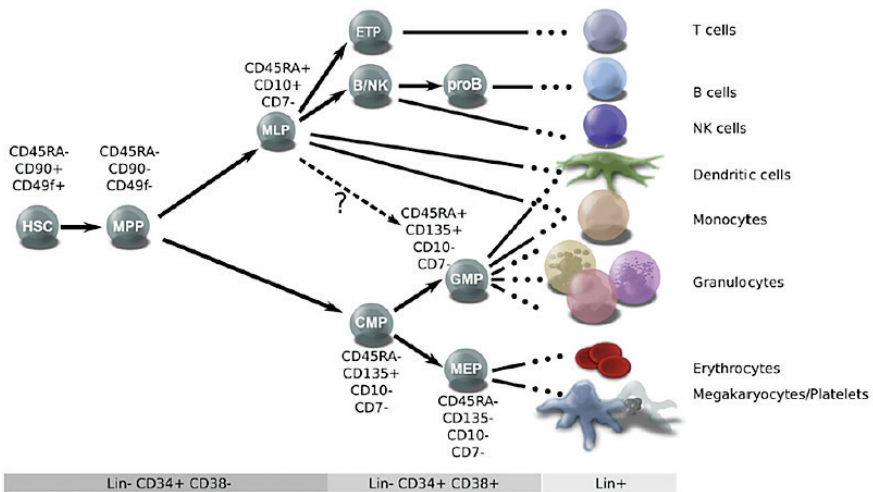


FIGURE 1.10

Model of lineage determination in human haematopoietic hierarchies, illustrating the major classes of HSPCs defined by cell surface phenotypes which are listed next to each population. Figure from (88).

1.2.2**Radiation-sensitivity of HSPCs**

A characteristic feature of HSCPs is their ability to self-renew and differentiate throughout life. Due to their long life span, accumulation of radiation damage in stem cells can compromise their genomic integrity and potentially give rise to cancer. Stem cells may thus be the major target of radiation-induced carcinogenesis (95). On the other hand, unrepaired genotoxic damage may cause cell death and stem cell pool depletion, resulting in degradation of haematopoietic cell function and failure of haematopoiesis, which is the most critical direct effect of whole body high dose radiation exposure. Proper regulation of DNA damage responses in HSPCs is crucial and appropriate regulation of the cell cycle is required for homeostasis. During the constant replenishment of blood cells, HSPCs migrate from the bone marrow into the blood stream. Therefore, HSPCs reflect the genomic integrity of the stem cell pool and are an ideal model to study the possible health risk of radiation exposure on the bone marrow. The haematopoietic system is a traceable tissue with cellular components which can be analysed or purified based on their cell-surface CD markers, and which can serve as a model system to unravel the origin radiation-induced leukaemia. However, little is known about the radiation sensitivity of human HSPCs. The suppression of haematopoiesis is a severe side effect of high dose IR exposure as used in radiotherapy for cancer patients and it is believed that haematotoxicity mainly arises from the impairment of HSPCs. Therefore, most of the studies on radiation responsiveness of HSPCs focus on self-renewal and (clonogenic) survival (92, 96-98). However, in this PhD dissertation we focus on mutagenic and consequential leukaemogenic effects of IR exposure. Therefore, we are interested in the nonlethal DNA modifications in HSPCs, that can be unrepaired or misrepaired and eventually lead to malignant disease. However, the cellular outcome of unrepaired DNA double-strand breaks (DSBs) remains unclear and will be further discussed in the Discussion section of this PhD thesis.

Radiation-induced genomic instability is a hallmark of cancer development and a possible mechanism through which radiation exposure may induce the transformation of HSPCs to leukemic cancer cells (99). Milyavsky *et al.* provided a genetic approach to gain mechanistic insight into the response of human HSPCs to DNA damage (100). Significant differences in response were observed between HSC/MPP and progenitors, with HSC/MPP undergoing higher levels of apoptosis compared to the

progenitor population. However, other publications, mostly on murine HSPCs, report that more primitive HSCs are more radioresistant to apoptosis compared to their progenitor cells, in order to ensure repopulation of the damaged bone marrow (92, 95). In the latter hypothesis, tissue maintenance is favoured in haematopoietic tissue, as the rare HSCs appear to be more resistant than their daughter progenitor cells. A possible mechanism of the relative resistance of HSCs is their increased antioxidant defence, since they contain lower levels of reactive oxygen species (ROS) compared to progenitors (101). The contradiction between human and murine studies on the radiosensitivity of HSPCs will be further discussed in the Discussion section of this PhD thesis (see chapter 10).

The haematopoietic tissue is at high risk for carcinogenesis, demonstrated by epidemiological studies, suggesting that the DNA repair may not be optimum. HSCs adopt a quiescent state within the bone marrow niche and remain largely in the G_0 and G_1 phase of the cell cycle, which is necessary for their long-term population maintenance (102). Non-dividing HSCs employ the error-prone non-homologous end joining pathway (NHEJ) to repair DNA DSBs (103), but the survival of cells with misrepaired damage can favour long-term accumulation of genetic anomalies. Evidence suggests that the quiescent stage of HSCs results in an attenuation of checkpoint control and DNA damage responses for repair and apoptosis, which is a dangerous mechanism through which potentially dangerous lesions can accumulate in the stem cell pool with age (104). The characteristic that certain types of leukaemia may be stem cell-driven, provided one the first conclusive pieces of evidence for the existence of cancer stem cells (105). A cancer stem cell is defined as a self-renewing cell within a tumour that has the capacity to regenerate the phenotypic diversity of the original tumour (106). Accumulation of radiation-induced DNA damage could trigger HSPCs to become leukemic stem cells. Tissues in which malignancies originate, such as blood, brain, breast, skin and gut, are organised as a cellular hierarchy with a small population of tissue-specific stem cells responsible for both development and maintenance of tissues over the human lifetime (106). Despite the multiple regulatory systems that prevent abnormal proliferation, mutations do occur. Most mutations are inconsequential since the abnormal cell is eventually eliminated from the pool of replicating cells, but at some low frequency these mutations may accumulate and eventually lead to cancer.

1.3

References

1. Ron E. Ionizing radiation and cancer risk: evidence from epidemiology. *Pediatric Radiology*. 2002;32(4):232-7.
2. Hall EJ. Lessons we have learned from our children: cancer risks from diagnostic radiology. *Pediatric Radiology*. 2002;32(10):700-6.
3. Brody AS, Frush DP, Huda W, Brent RL, American Academy of Pediatrics Section on Radiology. Radiation risk to children from computed tomography. *Pediatrics*. 2007;120(3):677-82.
4. Pierce DA, Shimizu Y, Preston DL, Vaeth M, Mabuchi K. Studies of the Mortality of Atomic Bomb Survivors. Report 12, Part I. Cancer: 1950-1990. *Radiation Research*. 2012;178(2):AV61-AV87.
5. Shah DJ, Sachs RK, Wilson DJ. Radiation-induced cancer: a modern view. *British Journal of Radiology*. 2012;85(1020):E1166-E73.
6. Ozasa K, Shimizu Y, Suyama A, Kasagi F, Soda M, Grant EJ, et al. Studies of the Mortality of Atomic Bomb Survivors, Report 14, 1950-2003: An Overview of Cancer and Noncancer Diseases. *Radiation Research*. 2012;177(3):229-43.
7. Wakeford R. The cancer epidemiology of radiation. *Oncogene*. 2004;23(38):6404-28.
8. UNSCEAR. Sources and Effects of ionizing radiation. New York: United Nations Scientific Committee on the Effects of Atomic Radiation, 2000.
9. Gilbert ES. Ionizing radiation and cancer risks: What have we learned from epidemiology? *International Journal of Radiation Biology*. 2009;85(6):467-82.
10. UNSCEAR 2000 Report to the General Assembly, with scientific annexes. New York: 2000.
11. Thompson DE, Mabuchi K, Ron E, Soda M, Tokunaga M, Ochikubo S, et al. Cancer incidence in atomic-bomb survivors. 2. Solid Tumors, 1958-1987. *Radiation Research*. 1994;137(2):S17-S67.
12. Valentin J. Low-dose extrapolation of radiation-related cancer risk. *Ann ICRP*. 35. England 2005. p. 1-140.
13. The 2007 Recommendations of the International Commission on Radiological Protection. ICRP publication 103. *Annals of the ICRP*. 37. England 2007. p. 1-332.
14. The 1990 Recommendations of the International Commission on Radiological Protection. ICRP publication 60. *Annals of the ICRP*. 21. England 1991. p. 1-201.
15. UNSCEAR. Sources, Effects and Risks of ionizing radiation. New York: United Nations Scientific Committee on the Effects of Atomic Radiation, 2013.
16. UNSCEAR. Effects of ionizing radiation. New York: United Nations Scientific Committee on the Effects of Atomic Radiation, 2006.
17. Valentin J. Basic anatomical and physiological data for use in radiological protection: reference values: ICRP Publication 89. *Annals of the ICRP*. 2002;32(3-4):1-277.
18. Hsu WL, Preston DL, Soda M, Sugiyama H, Funamoto S, Kodama K, et al. The Incidence of Leukemia, Lymphoma and Multiple Myeloma among Atomic Bomb Survivors: 1950-2001. *Radiation Research*. 2013;179(3):361-82.
19. Preston DL, Kusumi S, Tomonaga M, Izumi S, Ron E, Kuramoto A, et al. Cancer incidence in atomic-bomb survivors. 3. Leukemia, Lymphoma and Multiple-Myeloma, 1950-1987. *Radiation Research*. 1994;137(2):S68-S97.
20. Health Risks from Exposure to Low Levels of Ionizing Radiation: BEIR VII Phase 2: The National Academies Press; 2006.
21. Richardson D, Sugiyama H, Nishi N, Sakata R, Shimizu Y, Grant EJ, et al. Ionizing radiation and leukemia mortality among Japanese Atomic Bomb Survivors, 1950-2000. *Radiation Research*. 2009;172(3):368-82.
22. Douple EB, Mabuchi K, Cullings HM, Preston DL, Kodama K, Shimizu Y, et al. Long-term Radiation-Related Health Effects in a Unique Human Population: Lessons Learned from the Atomic Bomb Survivors of Hiroshima and Nagasaki. *Disaster medicine and public health preparedness*. 2011;5(0 1):S122-S33.
23. Pierce DA, Shimizu Y, Preston DL, Vaeth M, Mabuchi K. Studies of the mortality of atomic bomb survivors. Report 12, Part I. Cancer: 1950-1990. *Radiation Research*. 1996;146(1):1-27.
24. Darby SC, Doll R, Gill SK, Smith PG. Long term mortality after a single treatment course with X-rays in patients treated for ankylosing spondylitis. *British Journal of Cancer*. 1987;55(2):179-90.
25. Ron E, Modan B, Boice JD, Jr. Mortality after radiotherapy for ringworm of the scalp. *American Journal of Epidemiology*. 1988;127(4):713-25.
26. Murray R, Heckel P, Hempelmann LH. Leukemia in Children Exposed to Ionizing Radiation. *New England Journal of Medicine*. 1959;261(12):585-9.
27. Shore RE, Moseson M, Harley N, Pasternack BS. Tumors and other diseases following childhood X-ray treatment for ringworm of the scalp (*Tinea capitis*). *Health Physics*. 2003;85(4):404-8.

28. Lundell M, Holm LE. Mortality from leukemia after irradiation in infancy for skin hemangioma. *Radiation Research*. 1996;145(5):595-601.
29. Danese D, Gardini A, Farsetti A, Sciacchitano S, Andreoli M, Pontecorvi A. Thyroid carcinoma in children and adolescents. *European Journal Pediatrics*. 1997;156(3):190-4.
30. Duffy BJ, Jr, Fitzgerald PJ. Thyroid cancer in childhood and adolescence; a report on 28 cases. *Cancer*. 1950;3(6):1018-32.
31. Robbins J, Merino MJ, Boice JD, Jr, Ron E, Ain KB, Alexander HR, et al. Thyroid cancer: a lethal endocrine neoplasm. *Annals of Internal Medicine*. 1991;115(2):133-47.
32. Boice JD, Jr. Radiation-induced thyroid cancer--what's new? *Journal of the National Cancer Institute*. 97. United States 2005. p. 703-5.
33. Ron E, Lubin JH, Shore RE, Mabuchi K, Modan B, Pottern LM, et al. Thyroid-cancer after exposure to external radiation - A pooled analysis of 7 studies *Radiation Research*. 1995;141(3):259-77.
34. Davis FG, Boice JD, Hrubec Z, Monson RR. Cancer mortality in a radiation-exposed cohort of Massachusetts tuberculosis patients. *Cancer Research*. 1989;49(21):6130-6.
35. Shore RE. Issues and epidemiological evidence regarding radiation-induced thyroid cancer. *Radiation Research*. 1992;131(1):98-111.
36. Dal Maso L, Bosetti C, La Vecchia C, Franceschi S. Risk factors for thyroid cancer: an epidemiological review focused on nutritional factors. *Cancer Causes Control*. 2009;20(1):75-86.
37. Kolonel LN, Hankin JH, Wilkens LR, Fukunaga FH, Hinds MW. An epidemiologic study of thyroid cancer in Hawaii. *Cancer Causes Control*. 1990;1(3):223-34.
38. Cardis E, Kesminiene A, Ivanov V, Malakhova I, Shibata Y, Khrouch V, et al. Risk of thyroid cancer after exposure to (131I) in childhood. *Journal of the National Cancer Institute*. 2005;97(10):724-32.
39. Brenner AV, Tronko MD, Hatch M, Bogdanova TI, Oliynik VA, Lubin JH, et al. I-131 Dose Response for Incident Thyroid Cancers in Ukraine Related to the Chernobyl Accident. *Environmental Health Perspectives*. 2011;119(7):933-9.
40. Parker LN, Belsky JL, Yamamoto T, Kawamoto S, Keehn RJ. Thyroid Carcinoma After Exposure to Atomic Radiation A Continuing Survey of a Fixed Population, Hiroshima and Nagasaki, 1958-1971. *Annals of Internal Medicine*. 1974;80(5):600-4.
41. Preston DL, Ron E, Tokuoka S, Funamoto S, Nishi N, Soda M, et al. Solid cancer incidence in atomic bomb survivors: 1958-1998. *Radiation Research*. 2007;168(1):1-64.
42. Socolow EL, Hashizume A, Neriishi S, Niitani R. Thyroid Carcinoma in Man after Exposure to Ionizing Radiation. *New England Journal of Medicine*. 1963;268(8):406-10.
43. Furukawa K, Preston D, Funamoto S, Yonehara S, Ito M, Tokuoka S, et al. Long-term trend of thyroid cancer risk among Japanese atomic-bomb survivors: 60 years after exposure. *International Journal of Cancer*. 2013;132(5):1222-6.
44. Ferlay J, Héry C, Autier P, Sankaranarayanan R. Global Burden of Breast Cancer. In: Li C, editor. *Breast Cancer Epidemiology*: Springer New York; 2010. p. 1-19.
45. Preston DL, Mattsson A, Holmberg E, Shore R, Hildreth NG, Boice JD. Radiation effects on breast cancer risk: A pooled analysis of eight cohorts. *Radiation Research*. 2002;158(2):220-35.
46. Wanebo CK, Johnson KG, Sato K, Thorslund TW. Breast Cancer after Exposure to the Atomic Bombings of Hiroshima and Nagasaki. *New England Journal of Medicine*. 1968;279(13):667-71.
47. Land CE, Tokunaga M, Koyama K, Soda M, Preston DL, Nishimori I, et al. Incidence of Female Breast Cancer among Atomic Bomb Survivors, Hiroshima and Nagasaki, 1950-1990. *Radiation Research*. 2003;160(6):707-17.
48. McDougall JA, Sakata R, Sugiyama H, Grant E, Davis S, Nishi N, et al. Timing of Menarche and First Birth in Relation to Risk of Breast Cancer in A-Bomb Survivors. *Cancer Epidemiology Biomarkers & Prevention*. 2010;19(7):1746-54.
49. Tokunaga M, Land CE, Tokuoka S, Nishimori I, Soda M, Akiba S. Incidence of female breast cancer among atomic bomb survivors, 1950-1985. *Radiation Research*. 1994;138(2):209-23.
50. Land CE, Tokunaga M, Tokuoka S, Nakamura N. Early-onset breast cancer in A-bomb survivors. *Lancet*. 1993;342(8865):237.
51. Mackenzie I. Breast Cancer Following Multiple Fluoroscopies. *British Journal of Cancer*. 1965;19(1):1-8.
52. Miller AB, Howe GR, Sherman GJ, Lindsay JP, Yaffe MJ, Dimmer PJ, et al. Mortality from breast cancer after irradiation during fluoroscopic examinations in patients being treated for tuberculosis. *New England Journal of Medicine*. 1989;321(19):1285-9.
53. Howe GR, McLaughlin J. Breast cancer mortality between 1950 and 1987 after exposure to fractionated moderate-dose-rate ionizing radiation in the Canadian fluoroscopy cohort study and a comparison with breast cancer mortality in the atomic bomb survivors study. *Radiation Research*. 1996;145(6):694-707.

54. Boice JD, Jr., Preston D, Davis FG, Monson RR. Frequent chest X-ray fluoroscopy and breast cancer incidence among tuberculosis patients in Massachusetts. *Radiation Research*. 1991;125(2):214-22.
55. Ronckers CM, Doody MM, Lonstein JE, Stovall M, Land CE. Multiple diagnostic X-rays for spine deformities and risk of breast cancer. *Cancer Epidemiol Biomarkers Prev*. 17. United States 2008. p. 605-13.
56. Henderson TO, Amsterdam A, Bhatia S, Hudson MM, Meadows AT, Neglia JP, et al. Systematic review: surveillance for breast cancer in women treated with chest radiation for childhood, adolescent, or young adult cancer. *Ann Intern Med*. 152. United States 2010. p. 444-55; W144-54.
57. Hildreth NG, Shore RE, Hempelmann LH. Risk of breast-cancer among women receiving radiation treatment in infancy for thymic enlargement. *Lancet*. 1983;2(8344):273.
58. Dores GM, Anderson WF, Beane Freeman LE, Fraumeni JF, Jr., Curtis RE. Risk of breast cancer according to clinico-pathologic features among long-term survivors of Hodgkin's lymphoma treated with radiotherapy. *Br J Cancer*. 103. England 2010. p. 1081-4.
59. Kenney LB, Yasui Y, Inskip PD, Hammond S, Neglia JP, Mertens AC, et al. Breast cancer after childhood cancer: a report from the Childhood Cancer Survivor Study. *Ann Intern Med*. 141. United States 2004. p. 590-7.
60. Ronckers CM, Erdmann CA, Land CE. Radiation and breast cancer: a review of current evidence. *Breast Cancer Research*. 2005;7(1):21-32.
61. Chowdhary A, Spence AM, Sales L, Rostomily RC, Rockhill JK, Silbergeld DL. Radiation associated tumors following therapeutic cranial radiation. *Surgical Neurology International*. 2012;3:48.
62. Mann I, Yates PC, Ainslie JP. Unusual Case of Double Primary Orbital Tumour. *The British Journal of Ophthalmology*. 1953;37(12):758-62.
63. Preston DL, Ron E, Yonehara S, Kobuke T, Fujii H, Kishikawa M, et al. Tumors of the nervous system and pituitary gland associated with atomic bomb radiation exposure. *Journal of the National Cancer Institute*. 2002;94(20):1555-63.
64. Shore RE, Albert RE, Pasternack BS. Follow-up study of patients treated by X-ray epilation for Tinea capitis; resurvey of post-treatment illness and mortality experience. *International Archives of Occupational and Environmental Health*. 1976;31(1):21-8.
65. Sadetzki S, Chetrit A, Freedman L, Stovall M, Modan B, Novikov I. Long-term follow-up for brain tumor development after childhood exposure to ionizing radiation for tinea capitis. *Radiation Research*. 2005;163(4):424-32.
66. Karlsson P, Holmberg E, Lundell M, Mattsson A, Holm LE, Wallgren A. Intracranial tumors after exposure to ionizing radiation during infancy: A pooled analysis of two Swedish cohorts of 28,008 infants with skin hemangioma. *Radiation Research*. 1998;150(3):357-64.
67. Neglia JP, Meadows AT, Robison LL, Kim TH, Newton WA, Ruymann FB, et al. Second neoplasms after acute lymphoblastic leukemia in childhood. *New England Journal of Medicine*. 1991;325(19):1330-6.
68. Neglia JP, Robison LL, Stovall M, Liu Y, Packer RJ, Hammond S, et al. New primary neoplasms of the central nervous system in survivors of childhood cancer: a report from the childhood cancer survivor study. *Journal of the National Cancer Institute*. 2006;98(21):1528-37.
69. WHO – Environment and Health Information System (ENHIS). *Incidence of Childhood Leukaemia - Code RPG4_Rad_E1*. 2009.
70. Miller RW, Young JL, Novakovic B. *Childhood-Cancer*. *Cancer*. 1995;75(1):395-405.
71. Richardson RB. Stem cell niches and other factors that influence the sensitivity of bone marrow to radiation-induced bone cancer and leukaemia in children and adults. *International Journal of Radiation Biology*. 2011;87(4):343-59.
72. Piu CH, editor. *Childhood leukemias*. New York, NY: Cambridge University Press; 1999.
73. National Radiological Protection Board (NRPB). *Risk of leukemia and related malignancies following radiation exposure: Estimated for the UK population*. Chilton: Documents of the NRPB; 2003.
74. Bartley K, Metayer C, Selvin S, Ducore J, Buffler P. Diagnostic X-rays and risk of childhood leukaemia. *International Journal of Epidemiology*. 2010;39(6):1628-37.
75. Little MP, Weiss HA, Boice JD, Darby SC, Day NE, Muirhead CR. Risk of leukemia in Japanese atomic bomb survivors, in women treated for cervical cancer, and in patients treated for ankylosing spondylitis. *Radiation Research*. 1999;152(3):280-92.
76. Nowell PC. Discovery of the Philadelphia chromosome: a personal perspective. *Journal of Clinical Investigation*. 2007;117(8):2033-5.
77. Bapat S. *Cancer Stem Cells: Identification and Targets*. New Jersey: John Wiley and Sons; 2009.
78. Byrd JC, Mrózek K, Dodge RK, Carroll AJ, Edwards CG, Arthur DC, et al. Pretreatment cytogenetic abnormalities are predictive of induction success, cumulative incidence of relapse, and overall survival in adult patients with de novo acute myeloid leukemia: results from Cancer and Leukemia Group B (CALGB 8461). *Blood*. 2002;100(13):4325-36.

79. Fenaux P, Chastang C, Chevret S, Sanz M, Dombret H, Archimbaud E, et al. A randomized comparison of all transretinoic acid (ATRA) followed by chemotherapy and ATRA plus chemotherapy and the role of maintenance therapy in newly diagnosed acute promyelocytic leukemia. *The European APL Group. Blood.* 1999;94(4):1192-200.
80. Rosati E, Sabatini R, Rampino G, Tabilio A, Di Ianni M, Fettucciari K, et al. Constitutively activated Notch signaling is involved in survival and apoptosis resistance of B-CLL cells. *Blood.* 113. United States 2009. p. 856-65.
81. Brenner DJ, Doll R, Goodhead DT, Hall EJ, Land CE, Little JB, et al. Cancer risks attributable to low doses of ionizing radiation: Assessing what we really know. *Proceedings of the National Academy of Sciences of the United States of America.* 2003;100(24):13761-6.
82. Little MP, Wakeford R, Tawn EJ, Bouffler SD, de Gonzalez AB. Risks Associated with Low Doses and Low Dose Rates of Ionizing Radiation: Why Linearity May Be (Almost) the Best We Can Do. *Radiology.* 2009;251(1):6-12.
83. Pearce MS, Salotti JA, Little MP, McHugh K, Lee C, Kim KP, et al. Radiation exposure from CT scans in childhood and subsequent risk of leukaemia and brain tumours: a retrospective cohort study. *Lancet.* 2012;380(9840):499-505.
84. Roitt I, Brostoff J, Male D. *Immunology. Fourth Edition ed.* U.S.A.: Mosby; 1996.
85. Purton L, Scadden D. *The haematopoietic stem cell niche.* Cambridge: Harvard Stem Cell Institute: Stembook; 2008.
86. Mendelson A, Frenette PS. Hematopoietic stem cell niche maintenance during homeostasis and regeneration. *Nat Med.* 20. United States 2014. p. 833-46.
87. Komorniczak M: http://upload.wikimedia.org/wikipedia/commons/6/63/Hematopoiesis_EN.svg.
88. Doulatov S, Notta F, Laurenti E, Dick JE. Hematopoiesis: a human perspective. *Cell Stem Cell.* 10. United States: 2012 Elsevier Inc; 2012. p. 120-36.
89. King KY, Goodell MA. Inflammatory modulation of HSCs: viewing the HSC as a foundation for the immune response. *Nature Reviews Immunology.* 2011;11(10):685-92.
90. Majeti R, Park CY, Weissman IL. Identification of a hierarchy of multipotent hematopoietic progenitors in human cord blood. *Cell Stem Cell.* 2007;1(6):635-45.
91. Hao QL, Zhu J, Price MA, Payne KJ, Barsky LW, Crooks GM. Identification of a novel, human multilymphoid progenitor in cord blood. *Blood.* 2001;97(12):3683-90.
92. Heylmann D, Roedel F, Kindler T, Kaina B. Radiation sensitivity of human and murine peripheral blood lymphocytes, stem and progenitor cells. *Biochimica Et Biophysica Acta-Reviews on Cancer.* 2014;1846(1):121-9.
93. D'Arena G, Musto P, Cascavilla N, Di Giorgio G, Zandoli F, Carotenuto M. Human umbilical cord blood: immunophenotypic heterogeneity of CD34+ hematopoietic progenitor cells. *Haematologica.* 1996;81(5):404-9.
94. Doulatov S, Notta F, Eppert K, Nguyen LT, Ohashi PS, Dick JE. Revised map of the human progenitor hierarchy shows the origin of macrophages and dendritic cells in early lymphoid development. *Nature Immunology.* 2010;11(7):585-U52.
95. Harfouche G, Martin MT. Response of normal stem cells to ionizing radiation: A balance between homeostasis and genomic stability. *Mutation Research-Reviews in Mutation Research.* 2010;704(1-3):167-74.
96. Kashiwakura I, Kuwabara M, Inanami O, Murakami M, Hayase Y, Takahashi TA, et al. Radiation sensitivity of megakaryocyte colony-forming cells in human placental and umbilical cord blood. *Radiation Research* 2000;153(2):144-52.
97. Takahashi K, Monzen S, Hayashi N, Kashiwakura I. Correlations of Cell Surface Antigens with Individual Differences in Radiosensitivity in Human Hematopoietic Stem/Progenitor Cells. *Radiation Research* 2010;173(2):184-90.
98. Kato K, Omori A, Kashiwakura I. Radiosensitivity of human hematopoietic stem/progenitor cells. *Journal of radiological protection* 2013;33(1):71-80.
99. Dick JE. Stem cell concepts renew cancer research. *Blood.* 2008;112(13):4793-807.
100. Milyavsky M, Gan OI, Trottier M, Komosa M, Tabach O, Notta F, et al. A Distinctive DNA Damage Response in Human Hematopoietic Stem Cells Reveals an Apoptosis-Independent Role for p53 in Self-Renewal. *Cell Stem Cell.* 2010;7(2):186-97.
101. Tothova Z, Gilliland DG. FoxO Transcription Factors and Stem Cell Homeostasis: Insights from the Hematopoietic System. *Cell Stem Cell.* 2007;1(2):140-52.
102. Cheng T, Rodrigues N, Shen H, Yang Y, Dombkowski D, Sykes M, et al. Hematopoietic stem cell quiescence maintained by p21cip1/waf1. *Science.* 287. United States 2000. p. 1804-8.
103. Nijnik A, Woodbine L, Marchetti C, Dawson S, Lambe T, Liu C, et al. DNA repair is limiting for hematopoietic stem cells during ageing. *Nature.* 2007;447(7145):686-90.
104. Rossi DJ, Bryder D, Seita J, Nussenzweig A, Hoeijmakers J, Weissman IL. Deficiencies in DNA damage repair limit the function of hematopoietic stem cells with age. *Nature.* 2007;447(7145):725-9.
105. Fialkow PJ. Stem cell origin of human myeloid blood cell neoplasms. *Verhandlungen der Deutschen Gesellschaft für Pathologie.* 1990;74:43-7.
106. Lobo NA, Shimono Y, Qian D, Clarke MF. The biology of cancer stem cells. *Annual Review of Cell and Developmental Biology.* 2007;23:675-99.

2

Use of x-rays in paediatric diagnostic imaging

The use of IR in medical applications has resulted in a significant improvement of patient care. Several epidemiological studies provided evidence for adverse health effects of moderate and high doses of IR exposure (see chapter 1). However, the characterization of health effects of IR at low levels, as used in medical diagnostics, is more difficult due to the statistical uncertainties associated with the small excess risks at low doses. As the use of IR in diagnostic medicine continuously increases over the years, the risk of low dose IR became of societal importance. In this second chapter, we will focus on the increasing number of paediatric computed tomography (CT) scans and the associated cancer risks of low levels of low linear energy transfer (LET) IR (e.g. x-rays), as used in CT imaging in children.

2.1

Medical radiation burden

In the 1890s, Wilhelm Conrad Roentgen, Henri Becquerel and Marie and Pierre Curie discovered man-made x-rays and naturally occurring radioactivity, which laid the foundation for the use of ionizing radiation in medicine. The discovery of x-rays resulted in the construction of x-ray machines, nowadays used to image structures in the human body. As a result, IR has been increasingly applied in medicine for diagnosis and therapy during the last century. Hence, medical radiation exposure has become an important component of the total radiation exposure of the population and the use of IR in medicine continues to increase over the years (1). The average radiation exposure in Belgium is 5.45 mSv/year per caput. The population burden due to medical diagnostic procedures amounts up to 2.66 mSv/inhabitant per year, of which 2.46 mSv/year is attributable to the radiology dose burden and 0.2 mSv/year to diagnostic nuclear medicine procedures (2). The radiation quality used in diagnostic radiology is defined as low-LET radiation. LET is a measure of the density of energy deposition along the radiation track of a given type of IR in matter. Low-LET radiation deposits less energy in the cell along the radiation path and is considered less destructive per radiation track than high-LET radiation. It is this kind of low-LET radiation, including x-rays and γ -rays, producing sparse ionizations throughout a cell which is subject of this PhD research.

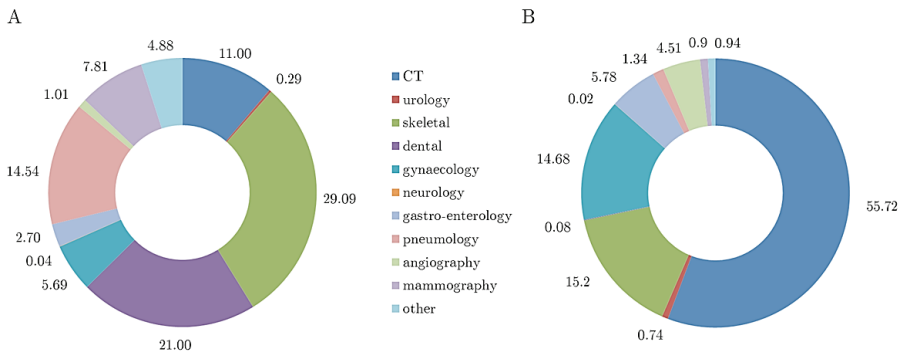


FIGURE 2.1

A. Frequency distribution of the different radiology examinations in Belgium (% of the annual 16.4 million procedures).
B. Contribution of the different radiology procedures to annual radiology dose burden (% of the annual radiology population dose of 2.46 mSv/year, which is the medical radiation burden in Belgium without 0.2 mSv/year from diagnostic nuclear medicine). Figure from (4).

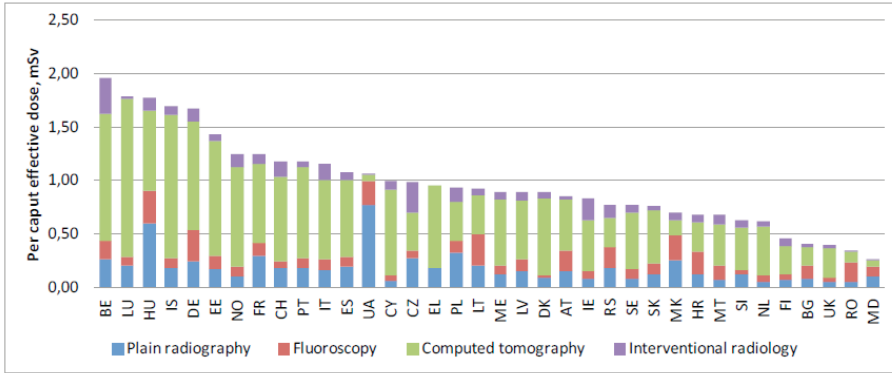


FIGURE 2.2

The effective dose per caput for the 36 participating countries of the DDMED 2 survey. The contribution of fluoroscopy and interventional radiology were not available for Greece (EL). The graph illustrates the high medical radiation burden in Belgium (3).

The main contributor to the medical radiology dose burden in Belgium is CT (55.72%), while only 11% of the 16.4 million radiological procedures each year are CT scans (see Figure 2.1). The high CT contribution in Belgium is comparable with the data published in the Dose Datamed 2 (DDM2) project report in 2010 on radiodiagnostic procedures in 36 European countries (3). The DDM2 project showed that CT examinations are the largest contributor to the collective medical x-ray radiation burden in Europe, representing 55% of the annual effective dose. The total annual frequency of x-ray procedures in the European countries is 1.1 examination per caput, while the frequency in Belgium is 1.5 examination per caput.

Thus, in comparison with neighbouring countries, the annual frequency of medical examinations per caput in Belgium is relatively high. Belgian inhabitants receive more than 3 times the average medical radiation dose per caput of the Netherlands, which was estimated as 1.96 mSv and 0.63 mSv respectively in the DDM2 report in 2010 (Figure 2.2) (3).

The high medical radiation burden in Belgium is due to the use of increasingly sophisticated medical imaging, computed tomography (CT) in particular, which improves the quality of diagnosis. Every year, on the average 1 out of 5 Belgian inhabitants undergoes a CT examination and every inhabitant undergoes on the average one RX examination (5). CT

examinations result in higher organ doses than conventional RX examinations. Both imaging techniques use diagnostic x-rays, but a CT image is acquired by combining rotation of the x-ray source around the patient, producing human body images in cross-sections after computerised reconstruction. For comparison, a CT abdomen and RX abdomen examination results in an effective dose of 12 mSv and 0.82 mSv respectively (1). To put this radiation burden of CT in perspective, one CT abdomen examination corresponds to approximately 1600 days (or 4.5 years) of natural background exposure.

The increasing frequency of radiological examinations and the corresponding high radiation burden, have put special attention on the management of patient dose in diagnostic radiology at national and international level. There are three factors making especially CT examinations the focus of recent concern (6):

- CT scans contribute to a large extent to the high amount of radiation exposure in diagnostic imaging (see Figure 2.1).
- The indications for CT scans and the number of CT scans are increasing rapidly (7).
- CT examinations can be performed by using a wide range of techniques, resulting in different levels of radiation exposure. Both scanner design and clinical protocol factors affect the radiation dose to the patient. Traditionally a higher dose corresponds with an increase in image quality in CT imaging. However, above a certain level of image quality, the decrease in image noise with increasing radiation dose will have no effect on diagnostic accuracy of the CT examination while the exposure may have been unnecessarily high, especially in children (5).

This is of special importance for the paediatric patient population, as children are more susceptible to radiation-induced carcinogenesis compared to adults. In this PhD, a population of paediatric patients undergoing a CT examination is considered, therefore we will focus on this specific population in the following sections.

2.2**Issues related to CT imaging in children**

Because of its proven diagnostic value, CT became an indispensable tool in modern medicine. The growing use of CT in paediatric radiology has been driven by new and improved imaging techniques, enabled by the advent of spiral and multi-slice CT (MSCT) scanning. MSCT allows faster imaging, resulting in less motion artefacts and reduction of the need for general anaesthesia in young children. Due to the shorter scanning time, it is also possible to extend the scope of some examinations, which allows to image larger volumes (e.g. staging of malignant lymphoma in children, which requires staging of neck and the entire trunk in one scan). Furthermore, MSCT allows to scan the same volumes with a better isotropic resolution, so organs can be evaluated in different planes. Children have smaller organs and less fat, resulting in less contrast between organs of similar density. This means that the improvement of image quality is even more advantageous in the paediatric patient group. Unfortunately, the ease of image acquisition results sometimes in unnecessary exposure of patients.

2.2.1**Frequency of CT imaging in children**

Limited data are available on the frequency of medical diagnostic x-ray procedures in Belgian children. The data of the UNSCEAR 2013 report on percentages of medical examinations in children are presented in Table 2.1 (8). There exists a large variation among countries, but in summary 3 - 10% of all medical radiation procedures are performed on children.

In 2011, 2 044 219 CT examinations were performed (190.1 per 1000 inhabitants) in Belgium of which 25 492 in children (age 0 to 12 years), corresponding to approximately 1 - 2% of CT procedures. The percentages of childhood CT scans reported in literature are higher, 6% of CT examinations are presumably performed in children (6, 8). However, former data are mainly based on studies from the USA where CT is more frequently used in children. A German study reported a similar lower percentage of paediatric CT examinations in the order of only 1% of all CT scans as in Belgium (9), which is again much smaller than in the USA. However, as described previously, although CT scanning represents just a small pro-

portion of the x-ray imaging examinations, it represents the main source of medical IR exposure.

A survey of the Netherlands and Germany showed that the most frequent type of paediatric CT examination is head CT (50-60%), followed by chest (17%) and only 7% of CT scans is performed for abdomen indications (6, 9). Thus, most paediatric CT examinations are performed to scan the head region, whereas CT scans of the abdomen are quite rare for children (Figure 2.3). On the contrary, almost 60% of the paediatric CT examinations in the USA were performed for abdomen indications. In most European countries, ultrasound (US) is performed by radiologists, which is widely accepted and frequently used for abdomen indications in children if possible.

<i>Examination</i>	<i>Percentage performed on children (%)</i>	<i>Examination</i>	<i>Percentage performed on children (%)</i>
RADIOGRAPHY		CT SCANNING	
Chest (posterior-anterior)	9	CT head	8
Chest (lateral)	10	CT abdomen	4
Limbs and joints	15	CT thorax	5
Lumbar spine (anterior-posterior)	7	CT spine	3
Thoracic spine (anterior-posterior)	12	ANGIOGRAPHY	
Cervical spine (anterior-posterior)	9	Non-cardiac angiography	2
Head	19	Cardiac angiography	4
Abdomen	13	Cerebral angiography	2
Upper gastrointestinal	3	NUCLEAR MEDICINE	
Lower gastrointestinal	3	Not available	
Cholecystography	2	RADIOTHERAPY	
Pelvis/hip	9	Not available	
Urography	7		

TABLE 2.1

Percentage of various types of medical examinations performed on infants and children (0-15 years old) in well-developed countries, as published in UNSCEAR 2013 (8).

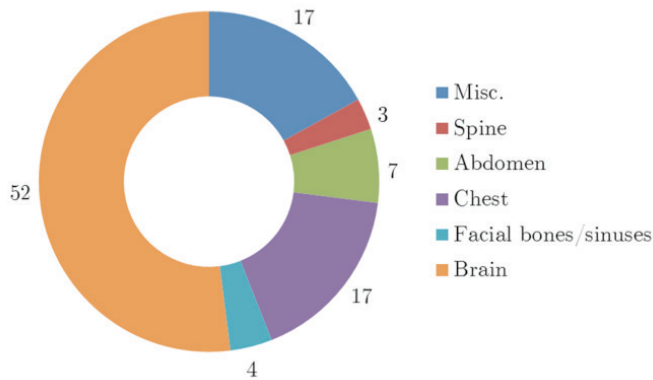
**FIGURE 2.3**

Illustration of the frequency distribution (%) for different types of paediatric CT examination in Germany. Data from (6).

2.2.2

Why are age-appropriate CT settings required for children?

When medical equipment and procedures are designed or set-up with an adult patient in mind, these settings can result in significantly higher doses for paediatric patients. Moreover, for a given dose, there is a significant difference in cancer risk from radiation exposure in children, compared to adults. There are several underlying reasons for this difference in cancer risk (see also chapter 1) (10):

- Tissues and organs of children are growing and developing, which makes them more sensitive to radiation effects than those that are fully mature and differentiated. Especially the thyroid gland, brain and breast tissue are structures with an increased sensitivity to radiation in growing children (see chapter 1). The increased sensitivity varies

with age, with the younger ages being more at risk. Some of these regions are routinely involved in chest CT imaging, such as thyroid and breast tissue. Furthermore, breast tissue might also be included in the uppermost part of a CT abdomen scan despite the fact that this is not clinically indicated (11). Also scatter may affect the organs close to the scanning area and specific attention should be paid when scanning newborns and infants in spiral CT mode with multi-slice CT scanners, as the additional exposure from overscanning effects can mount up to 20-30 % due to the short scan ranges (12).

- Children have a longer life expectancy to express the oncogenic effect of radiation exposure. Radiation exposure for elderly people doesn't carry the same risk, because most of the radiation-induced solid malignancies will not occur within the first decade after exposure. Radiation-induced leukaemia generally occurs with a minimum latency of about 2-3 years, while solid tumours only start to appear a minimum of 10 to 15 years after exposure (8). Moreover, the cancer risk is assumed to be cumulative over a lifetime, so each CT examination contributes to the lifetime exposure (11). This makes the risk more significant for the younger populations, for whom the risks are higher and there is more opportunity for repeated imaging.
- Identical CT settings provide higher organ doses in children compared to adults, due to their smaller cross-section. Although children absorb less radiation than adults, their organs are smaller and the actual dose to the organ is higher (12). The latter is illustrated in Figure 2.4, which shows the difference in effective dose between infants and adults versus x-ray tube voltage (kV) for a constant mAs value. Note that the patient effective dose increases by about a factor of five when the x-ray tube voltage increases from 80 to 140 kVp (13). The effective dose for infants is much higher than in adults for the same kVp settings.

In 2001, a number of surveys showed that adjustment of CT protocols for paediatric patients were not routinely made based on variations in size of children (14-16). The exposure parameters used in paediatrics were too high in comparison with adult protocols (17), even though a lower dose can provide equivalent image quality (6, 18). Since then, numerous recommendations have been published to adapt exposure settings in accordance with patient size and there is a strong radiation protection awareness

among CT users of paediatric radiology today. This is mainly the result of extensive campaigns at national and international level. An initiative definitely worth mentioning in this context, is the Image Gently campaign (see www.imagegently.org). Nevertheless, dose reduction in paediatric CT imaging remains a challenging topic that will be addressed in the Discussion of this PhD dissertation (see chapter 9).

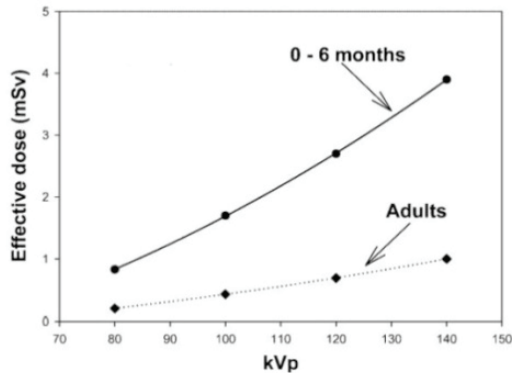


FIGURE 2.4

Effective dose versus x-ray tube voltage for infants and adult patients having a head CT examination with constant 340 mAs. Figure from (13).

2.3

Dose Reference Levels (DRLs) in paediatric CT imaging

The optimisation of patient protection in paediatric CT imaging requires the application of examination-specific scan protocols tailored to patient age or size, scan region and clinical indication in order to ensure that the dose to each patient is as low as reasonably achievable (ALARA) for the clinical purpose of the CT examination. Dose reference levels (DRLs) are a practical tool to compare the existing protocols between different radiology centres and to promote the development of new and improved protocols. The levels are expected not to be exceeded for standard patients when good and normal practice regarding diagnostic and technical performance

is applied. A DRL value is advisory, and when the value is exceeded regularly, this does not mean necessarily a case of unacceptable practice. Rather, the practice requires explanation, review, or possibly a new approach (19). In the following paragraphs we present the practical dose quantities used to monitor CT practice, national and international DRLs, in order to outline current practice in paediatric CT imaging.

2.3.1

Dose quantities in CT imaging

DRLs should be set in terms of the practical dose quantities used to monitor CT practice: volume weighted CT Dose Index ($CTDI_{vol}$, expressed in mGy) and Dose-Length Product (DLP in mGycm), as commonly displayed by CT scanners. $CTDI_{vol}$ is a standardized measure of radiation dose output of a CT scanner which allows the user to compare radiation output of different CT scanners. DLP represents the product of $CTDI_{vol}$ and the scan length. These quantities are not patient doses, but dose indicators characterising radiation exposure in CT. CTDI and DLP are specified in relation to dose measurements in the standard CT dosimetry phantoms, which are acrylic cylinders with diameters of 16 cm (commonly referenced for adult head protocols) and 32 cm (commonly referenced for adult body protocols). However, the large 32 cm dosimetry phantom underestimates dose in paediatric CT. A standard 16 cm phantom is a reasonable presentation of paediatric patient size, but phantoms with smaller diameters (between 8 and 16 cm) would provide a better representation of younger age groups, such as infants (12).

CTDI is quantity which represents the mean dose within a CT slice. It is defined as the integral of the dose profile along a line parallel to the axis of rotation (z-axis) for a single rotation, divided by the nominal thickness of the x-ray beam (19):

$$CTDI = \frac{1}{Nh} \int_{-\infty}^{+\infty} D(z) dz$$

Where N represents the number of slices simultaneously scanned for MSCT, h is the nominal slice thickness and $D(z)$ represents the dose profile along the z-axis. The weighted CTDI ($CTDI_w$) reflects the weighted sum of two thirds peripheral dose and one third central dose in a 100-mm range in the acrylic CT dosimetry phantoms.

$$CTDI_w = \frac{1}{3} CTDI_{100,c} + \frac{2}{3} CTDI_{100,p}$$

The $CTDI_w$ defined above assumes procedures consisting of contiguous slices, which is normally the case for axial scans. However, the table movement per rotation, defined as helical pitch, should be taken into account for helical CT (20). Pitch is the table movement per rotation divided by the slice thickness (multiplied by N for a MSCT scanner). To account for the effect of pitch in helical CT scanning, the indicator $CTDI_{vol}$ was introduced (21):

$$CTDI_{vol} = \frac{CTDI_w}{pitch} \text{ (mGy)}$$

CTDI (in any form) is an estimate of average radiation dose only in the irradiated volume. Risk from IR exposure in CT imaging, however, is more closely related to the total amount of the radiation dose (i.e. energy) deposited in the patient (20). The indicator DLP gives a better representation of the overall energy delivered by a given scan protocol. Since $CTDI_{vol}$ represents the average dose per tube rotation, DLP can be easily derived by taking into account the scan length (21):

$$DLP = CTDI_{vol}(mGy) \times scan \ length \ (cm)$$

2.3.2

National DRLs

National DRLs are based on large scale surveys of the dose parameters representing typical practice for a patient group (e.g. adults or children of different ages) at a range of representative national CT centres for a specific type of CT examination, taking into account different CT scanners and scanning protocols. National DRLs (NDRLs) are commonly set at the third quartiles of the national distribution (22) (see Figure 2.5). As such, NDRLs are not optimum doses, but nevertheless they are helpful in identifying potentially unusual practice (the highest 25% of the distribution). NDRLs are intended to promote awareness, dose audit and serve as a basis for improving patient radiation protection, while maintaining required diagnostic quality.

In 2007-2009, a multicentre study was set up in Belgium to evaluate CT exposure of children by investigating radiological practice and patient doses for five common CT examinations over four age ranges (0-1 y; 1-5 y; 5-10 y and 10-15y) (12). The survey revealed a strong radiation protection awareness among the CT users today and all centres adapted their CT

exposure parameters when children were scanned. This is encouraging, however, large differences in dose distributions between the different centres were observed.

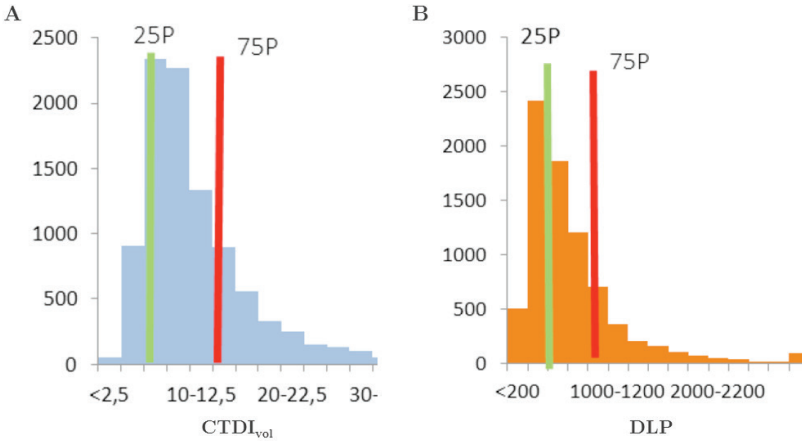


FIGURE 2.5

Illustration of CTDI_{vol} and DLP (for the total examination) frequency distribution used for the determination of the NDRLs for abdomen CT examinations in Belgium (paediatric frequency distribution were not available). 25P = 25th percentile, 75P = 75th percentile. Figure from (23).

Since 2006, the Federal Agency of Nuclear Control (FANC) in Belgium has started studies on patient dosimetry in radiology, in order to assess the patient dose received by the most common CT examinations. These surveys are conducted periodically and in the meantime, already three iterations were completed. Based on this national benchmarking, NDRLs were determined for standard paediatric CT examinations. Table 2.2 presents the national DRLs after the third iteration of the patient dosimetry study. The 75th percentiles of the analysed patient dose distributions represent the NDRLs, as identified the European MED guidelines (97/43/Euratom). In addition, the 25th percentiles are presented, defined as target values. These target values represent good clinical practice and demonstrate that optimisation should go further than the NDRLs.

CT examination	CTDI _{vol}		DLP (total investigation)	
	Percentile 25	Percentile 75	Percentile 25	Percentile 75
Cranium (brain)	21	44.5	350	755
Sinus	2.2	6.0	28	75
Chest	1.3	3.6	33	125
Abdomen	3.2	6.7	120	320

TABLE 2.2

Belgian DRLs for paediatric CT examinations based on the third patient dosimetry CT survey (source: www.fanc.fgov.be).

2.3.3

European DRLs

Several European countries published NDRLs for paediatric CT imaging (9, 24-28). In the framework of the DDM2 project, a European wide survey on the availability of these national DRLs was performed in 36 countries (29). This survey revealed that only 39% of the countries have established DRLs for paediatric x-ray examinations and 45% of EU and EFTA countries (Iceland, Norway, Switzerland). However, no Belgian DRLs for paediatric radiology were included in the survey (they were probably not published at that time). The results of the DDMED 2 project show that there is still a long way to go to update and establish European DRLs for paediatric CT imaging. The minimum over maximum ratios show large variations for some specific ages and procedures, e.g. CT chest examination for newborns. The results of the survey in terms of DRLs are presented in Table 2.3. Up to now, no European DRLs for paediatric CT imaging were published. In order to consolidate what is available at the moment and to provide guidance on what actions are needed for using DRLs to further enhance the radiation protection of children, the European Commission funded the PiDRL (European Diagnostic Reference Levels for Paediatric Imaging) project to establish European DRLs for paediatric patients.

CT examination	DLP (mGycm)	Age				
		0	1	5	10	15
Head	range	270 - 340	270 - 470	470 - 700	620 - 900	850 - 920
	min/max	1.3	1.7	1.3	1.5	1.1
Chest	range	12 - 200	28 - 200	55 - 230	105 - 370	200 - 205
	min/max	16.7	7.1	4.2	3.5	1.0
Abdomen	range	27 - 130	70 - 166	125 - 230	240 - 400	400 - 500
	min/max	4.8	2.3	1.8	1.7	1.3

TABLE 2.3

Range of DRLs for paediatric patients, in terms of DLP. The values are based on national surveys conducted in Austria, France, Ireland, the Netherlands, UK and Switzerland (29).

2.4

Overview of epidemiological studies on paediatric CT imaging

As the field of epidemiology advances, a better understanding of the health effects of low-dose exposures is the next challenge (30). Up to now, there are a few epidemiological studies dealing with leukaemia and cancer risks related to CT x-ray exposure of children which will be presented in the following paragraphs.

In 2012, Pearce *et al.* published in *The Lancet* the results of a record linkage study of leukaemia and brain cancer incidence after childhood CT exposure (31). The authors focussed on leukaemia and brain tumours, since red bone marrow and brain are highly radiosensitive tissues in children (as described in chapter 1), and the short latency period of leukaemia (and to an extent brain cancer). The average follow-up time was a little under 10 years and the cohort of this epidemiological study comprised of 178 604 children (0 – 21 years) without previous malignant disease, who underwent a CT scan between 1985 and 2002 in various hospitals in the UK. The collection of CT settings was not possible for every individual patient from the electronic database during the study period. Therefore typical CT

settings from two national surveys, together with data from a series of hybrid computational phantoms (reference male and female between 0 and 22 years) and Monte Carlo radiation transport techniques were used to estimate absorbed doses to the red bone marrow and brain. Significant dose responses were reported for leukaemia and brain cancers, see Figure 2.6. The data of Pearce *et al.* confirm that the cancer risk associated with CT x-ray examination of children is very small, but not zero. The individual risk is very small and far outweighed by the benefit of the diagnosis, provided the scan is clinically justified. The estimated lifetime risk for leukaemia from one paediatric CT scan based on the LSS data was about 1 in 10 000 (32), which is in good agreement with the estimate of approximately 1 in 10 000 of Pearce *et al.* (31). The lifetime risk estimate for brain cancer in the study of Pearce *et al.* was 1 in 10 000, however, the average length of follow-up in this study was only 8 – 10 years (25). The study of children epilited with x-rays for the treatment of tinea capitis highlighted that only 10 % of the final risk of brain cancer shows up in the first decade after irradiation (33). This would indicate that the risk for brain cancer reported by Pearce *et al.* is certainly an underestimate.

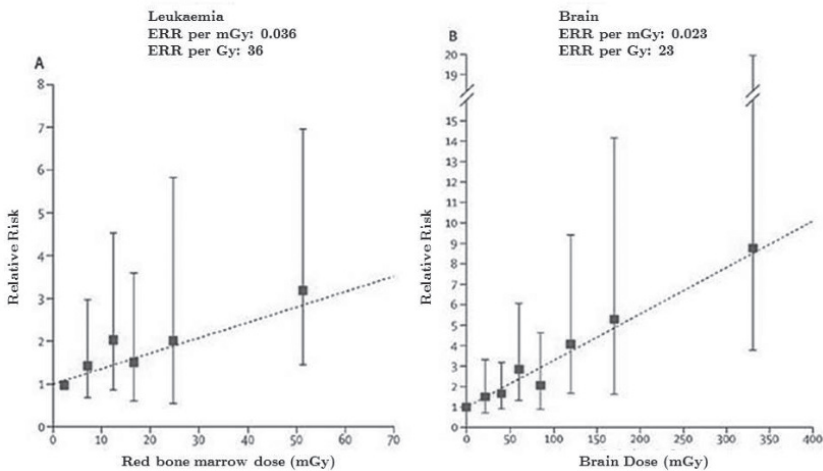


FIGURE 2.6

Relative risk of leukaemia and brain tumours in relation to estimated radiation doses to the red bone marrow and brain (mGy). Left graph – Leukaemia, Right graph – Brain tumours. The dotted line represents the fitted linear dose-response (ERR per mGy). Data from (31).

An Australian linkage study, with a mean follow-up 9.5 years, was conducted by Mathews *et al.* (34). The study cohort included 10 939 680 people, from which 680 211 (6.2%) were children and adolescents allocated into the CT exposed group and 18% of the exposed group had more than one scan. An increase of 24% in cancer incidence was reported for exposed compared to unexposed individuals. The largest incidence risk was found for brain cancers, although incidence was also increased significantly for cancers of the digestive organs, melanoma, soft tissue, female genital organs, urinary tract, thyroid, Hodgkin lymphoma, other lymphoid cancers, all leukaemias and myelodysplasias. However, no separate increase in incidence risk for breast cancer was reported. It seems implausible that increased radiation risks were reported for melanoma, which is not known to be associated with radiation, but not for breast cancer, a radiosensitive site.

When we compare the ERR per mGy of the Australian study with the study of Pearce *et al.* in the UK, similar estimates were found for leukaemia; Australian ERR of 0.039 (1 year lag) versus UK ERR of 0.036 (2 year lag). For brain cancers, the ERR per mGy was also comparable for a 5 year lag period, Australian ERR of 0.021 versus UK ERR of 0.023. However, the ERR for brain tumours are higher in both epidemiological studies compared to the LSS results for a 10 year lag period, which is more appropriate for brain cancers (e.g. Australian ERR of 0.015 compared to LSS ERR of 0.006). This points to the phenomenon of 'reverse causation', this means that cancers may have been caused by the medical indications prompting the CT scan rather than by the CT dose (35).

Finally, there were also the studies of Huang *et al.* (36) and Krille *et al.* (37). The first authors evaluated the association between a paediatric head CT scan and the risk of a malignant and benign brain tumour in a Taiwan cohort of 24 418 participants under 18 years of age who underwent a head CT examination between 1998 and 2006 (36). The risk of a brain tumour was 2.6 times higher in the exposed cohort than in the unexposed cohort after 8 year follow-up. In the same study, the risks of leukaemia and all cancers combined were increased as well. Krille *et al.* assessed the risk of developing cancer, specifically leukaemia, tumours of the central nervous system and lymphoma, before the age of 15 years in children previously exposed to CT in a German cohort of 44 584 children (37). They reported standardised incidence ratios (SIR) using incidence rates from the general

population. For leukaemia, the SIR was 1.72 and for brain tumours, the SIR was 1.35.

An overview of the differences in study designs, exposed cohorts and epidemiological risk estimates between the four presented studies can be found in Table 2.4.

Besides the limited dosimetry and short follow-up time, one of the major limitations in these studies is the lack of information about indications for the CT scans and the consequent potential for “reverse causation”. The authors of the mentioned publications tried to reduce the reverse causation by using a latency period to exclude patients from the cohort who had an exit date of less than 1 or 2 years in the case of leukaemia or less than 1, 2 or 5 years for brain tumours after the first scan, depending on the study (see Table 2.4). Furthermore, the adolescents with ages above 18 years as reported in the studies of Pearce *et al.* (31) and Mathews *et al.* (34), can no longer be considered as children and certainly not for brain tumours, where the susceptibility decreases as brain development nears completion.

TABLE 2.4

Comparison of the cohort composition and the risk estimates for leukaemia and CNS or brain tumours for the four described epidemiological cohort studies on cancer risk after CT scans in childhood. Table from (37).

	UK	Australia	Taiwan	Germany
Cohort				
Size	178 604	10 939 680	122 086	44 584
Exposed	178 604	680 211	24 418 (head CT)	44 584
Age at exposure	0 to <22	0 to <19	0 to <18	0 to <14
Follow-up period	1985 - 2008	1985 - 2007	1998 - 2008	1980 - 2010
Leukaemia				
Risk estimate	3.18	1.23	1.90	1.72
95% CI	1.46 - 6.94	1.08 - 1.41	0.82 - 4.40	0.89 - 3.01
Latency	2 years	1 year	2 years	2 years
Brain and CNS tumours				
Risk estimate	2.82	2.13	2.56	1.35
95% CI	1.33 - 6.03	1.88 - 2.41	1.44 - 4.45	0.54 - 2.78
Latency	5 years	1 year	2 years	2 years

Journey *et al.* tried to deal with the bias by indication and studied a cohort of 67 274 children who had a first CT before the age of 10 years from 2000 to 2010 in 23 French radiology departments (35). The cancer risk related to childhood CT was estimated and the influence of cancer-predisposing factors (PFs) (from discharge diagnoses) on the radiation-related risk was examined. The adjustment for PFs resulted in different estimates of the ERR. For an exclusion period of 2 years after the first CT scan and adjusting for all PFs, the ERR per mGy in the study of Journey *et al.* changed from 0.022 to 0.012 for CNS cancer, from 0.057 to 0.047 for leukaemia and from 0.018 to 0.008 for lymphoma (35). Although a dose-response trend was suggested for the risk of CNS cancer (but not for haematological cancers), no significant effect was actually observed. The ERR estimated for leukaemia, without any adjustment for PF, appeared comparable with the estimates from the UK study of Pearce *et al.* for children under 10 years of age at the first scan (31). These results confirm the need to consider the existence of PFs in estimating the cancer risks potentially induced by CT scans. However, the median follow-up was only 4 years in the French study, which is too short to provide any conclusive results about radiation-induced cancer risks.

These recent epidemiological studies on childhood CT exposure have raised criticism with respect to the results in issues such as reverse causation, short follow-up periods, potentially missed exposure information and the absence of individual patient dosimetry. Epidemiological studies make it possible to estimate the expected magnitude of potential risk, and besides the recent studies presented above, additional studies are underway (38). The European FP7 project, EPI-CT (Epidemiological study to quantify risks for paediatric computerised tomography and to optimise doses) will offer opportunities to better address the current limitations (<http://epi-ct.iarc.fr/>). Because the risks associated with low doses of IR from CT scans are expected to be small, this multinational collaborative study is undertaken to ensure sufficient statistical power. The project includes nine national cohorts, including some of the previously mentioned cohorts, and has following objectives:

- Establish a large multinational cohort of more than 1 million patients who received CT scans during childhood.
- Develop individual estimates of organ-specific doses from paediatric CT scans using improved methods for dose estimation for paediatric patients.

- Evaluate the radiation-related risk of cancer in the cohort and pilot test biological markers of CT-irradiation effects.
- Develop methods to characterise quality of CT images in relation to the corresponding examination dose.
- Provide recommendations for a “harmonised” approach to CT dose optimisation for paediatric patients in Europe.

Despite limitations, estimates are all we will have in the near future and even if they are only approximately, they are important at a time of increasing concern about the major increase in the collective dose of diagnostic CT scanning. These epidemiological studies are an important piece of additional evidence to show that low doses of radiation do carry some (admittedly small) risk, which must be taken into account (39). Furthermore, we passed an important bridge in the field of low dose radiation risks, since it is no longer tenable to claim that CT risks are “too low to be detectable and may be non-existent”. The conclusion of these epidemiological studies is that the individual risks are small but real (40). Since the associated risks are small, we can conclude that if a CT examination is clinically justified, there is no doubt that its benefits will by far exceed its risks.

2.5

Estimation of radiation risk in paediatric radiology: the BEIR VII model

As described in the previous section, the quantification of the risk of low dose IR exposure (< 100 mSv) remains complex. So far, no epidemiological evidence has invalidated the risk predictions extrapolated from studies at high doses under the linear dose-response assumption (31, 41). However, the described epidemiological studies are inherently difficult and large uncertainties remain to be solved.

The most widely accepted model of low-dose risk estimation using current scientific evidence is predominantly based on LSS data, with a linear extrapolation of the risks at high doses down to low doses, with no threshold (42, 43). The use of this linear no-threshold (LNT) model is the main paradigm of radiation protection and still subject of an active debate (44, 45). However, despite the lack of extensive epidemiological evidence, the LNT model remains the most reasonable assumption regarding the dose-response relationship at low levels.

A model for estimating the theoretical lifetime attributable risk (LAR) due to low-dose and low LET radiation exposure is provided in the Biological Effects of Ionizing Radiation (BEIR) VII report (42). This report represents the seventh in a series of reports from the National Research Council (NRC) prepared to advise the United States government on the relationship between exposure to IR and human health. This seventh report is an update on the older BEIR V report (NRC 1990), using new information from epidemiologic and experimental research that has accumulated during the previous 14 years. Since the 1990 BEIR V report, substantial new information on radiation-induced cancer has become available from the Hiroshima and Nagasaki survivors, slightly less than half of whom were alive in 2000. Of special importance are cancer incidence data from the Hiroshima and Nagasaki tumour registries. The risk estimation predominantly relies on LSS data, although other medically exposed cohorts were also taken into account for the risk assessment of breast and thyroid cancer. The use of LSS data has several advantages like the large size of the exposed cohort, including men, women and children, the extensive large follow-up, a wide range of doses and the whole body exposure resulting in an opportunity to assess cancer risks to several specific sites (42). In the BEIR VII report, a distinction is made between cancer incidence and cancer mortality rates, and the risk is dependent on gender and age (see Figure 2.7). In the framework of this PhD, a paediatric population exposed to CT imaging was studied. The LAR method of the BEIR VII committee was the best choice to estimate radiation risks since patient's age and gender can be taken into account. Based on the Monte Carlo simulated organ doses, site-dependent LAR of cancer incidence and mortality can be calculated for the organs in the field of view of CT scanning.

The extrapolation from a high acute dose at a high dose rate as in the LSS studies to either a low dose or to a low dose rate can be embodied into a single correction factor, namely DDREF. For solid cancers, the BEIR VII committee proposes that risks are divided by a DDREF of 1.5 when estimating risks for the relatively low doses in medical exposures (< 100 mGy) (46, 47). However, there remains uncertainty in the appropriate value of a DDREF for adjusting the low-dose risks based on linear estimates; ICRP and NRC propose a value of 2, while UNSCEAR suggests even a DDREF of no more than 3. For the risk calculations performed in the framework of this PhD, a DDREF of 2 was chosen.

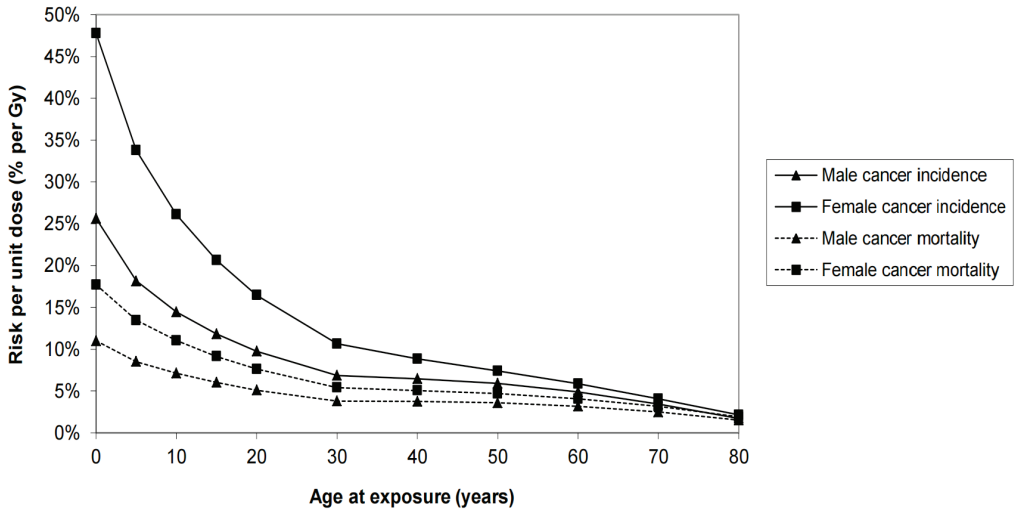


FIGURE 2.7

Overall cancer incidence and mortality attributable to radiation exposure for all solid cancers and leukaemia for males (▲) and for females (■). Data from (41, 42).

A lot of studies reported lifetime cancer risk estimates associated with low dose CT exposure as a function of age at exposure (14, 48, 49). These risk estimates were based on age-specific, gender-specific and organ-specific cancer risks derived primarily from the Japanese A-bomb survivors (14). The results of these 'risk projection studies' are not so far from the lifetime risk estimates for CT based on the epidemiological data (see 2.4), which are rescaled to the lifetime risk attributable to a single CT examination (40). For example, Brenner *et al.* estimated in 2001 a lifetime leukaemia risk of about 1 in 10 000 for one paediatric head CT (14), which is comparable with an estimated risk of 1 in 7500 lifetime risk with the data of Pearce *et al.* when a comparable age at exposure was taken into account (31, 40). The lifetime brain tumour risk in the study of Brenner *et al.* was 1 in 2000, compared with the 1 in 1000 lifetime estimate calculated with the data of Pearce *et al.* (31, 40). We can conclude that the standard method of estimating radiation risks in the risk projection studies, yields fairly reasonable results. Given the fact that we will have to wait several more dec-

ades for epidemiologically based lifetime risks (when follow-up times of 20, 30 or 40 years after exposure are reached), we will have to rely on this standard risk estimation method for several years to come (40). However, it should be noted that we must be cautious with the prediction of thousands of radiation-induced cancer and cancer deaths in the population in future years based on these risk models, a statement well addressed by Hendee and O'Connor in Radiology (41). For example, Berrington de Gonzalez *et al.* predicted 29 000 additional cancers and 14 500 cancer deaths caused by CT examinations each year (42). These predictions raised serious health concerns among the public and provokes anxiety in patients and families. Predictions of the effects of low doses of ionizing radiation should disclose all of the limitations in the current state of knowledge about low dose radiation effects. In the meantime, efforts should be made with respect to justification of a CT examination in children and optimisation of CT doses in paediatric radiology.

2.6

References

1. UNSCEAR. *Sources and effects of ionizing radiation*. New York: 2008.
2. Federal Agency of Nuclear Control (FANC) Belgium. Available from: www.fanc.fgov.be.
3. DDM2. *DoseDataMed 2 Project, Report Part 1: European Population Dose*. 2014.
4. *Personal communication with Federal Agency of Nuclear Control (FANC) Belgium - Thanks to Petra Willems*. 2015.
5. RIZIV. *Medische Beeldvorming: Rationeel voorschrijven. Sensibilisering voor het blootstellingsrisico aan ioniserende straling*. Brussel. 2010.
6. Nievelstein RAJ, van Dam IM, van der Molen AJ. *Multidetector CT in children: current concepts and dose reduction strategies*. *Pediatric Radiology*. 2010;40(8):1324-44.
7. Larson DB, Johnson LW, Schnell BM, Salisbury SR, Forman HP. *National trends in CT use in the emergency department: 1995-2007*. *Radiology*. 2011;258(1):164-73.
8. UNSCEAR. *Sources, Effects and Risks of ionizing radiation*. New York: United Nations Scientific Committee on the Effects of Atomic Radiation, 2013.
9. Galanski M, Nagel HD, Stamm G. *Paediatric CT exposure practice in the Federal Republic of Germany. Results of a nation-wide survey in 2005/06*. Medizinische Hochschule Hannover; 2006.
10. Brody AS, Frush DP, Huda W, Brent RL, Amer Acad P. *Radiation risk to children from computed tomography*. *Pediatrics*. 2007;120(3):677-82.
11. Frush DP, Donnelly LF, Rosen NS. *Computed tomography and radiation risks: What pediatric health care providers should know*. *Pediatrics*. 2003;112(4):951-7.
12. Buls N BH, Mommaert C, Malchair F, Clapuyt P, Everarts P. *CT paediatric doses in Belgium: a multi-centre study*. Federal Agency of Nuclear Control (FANC). 2010.
13. Huda W. *Dose and image quality in CT*. *Pediatric Radiology*. 2002;32(10):709-13.
14. Brenner DJ, Elliston CD, Hall EJ, Berdon WE. *Estimated risks of radiation-induced fatal cancer from pediatric CT*. *American Journal of Roentgenology*. 2001;176(2):289-96.
15. Paterson A, Frush DP, Donnelly LF. *Helical CT of the body: Are settings adjusted for pediatric patients?* *American Journal of Roentgenology*. 2001;176(2):297-301.
16. Rogers LF. *Taking care of children: Check out the parameters used for helical CT*. *American Journal of Roentgenology*. 2001;176(2):287.
17. Hollingsworth C, Frush DP, Cross M, Lucaya J. *Helical CT of the body: a survey of techniques used for pediatric patients*. *American Journal of Roentgenology*. 2003;180(2):401-6.
18. Singh S, Kalra MK, Moore MA, Shailam R, Liu B, Toth TL, et al. *Dose Reduction and Compliance with Pediatric CT Protocols Adapted to Patient Size, Clinical Indication, and Number of Prior Studies*. *Radiology*. 2009;252(1):200-8.
19. Khong PL, Ringertz H, Donoghue V, Frush D, Rehani M, Appelgate K, et al. *ICRP publication 121: radiological protection in paediatric diagnostic and interventional radiology*. *Annals of the ICRP*. 2013;42(2):1-63.
20. Goldman LW. *Principles of CT: radiation dose and image quality*. *Journal of Nuclear Medicine Technology*. 2007;35(4):213-25..
21. AAPM. *Report no. 96: The Measurement, Reporting, and Management of Radiation Doses in CT*. American Association of Physicists in Medicine; 2008.
22. IPEM. *IPEM Report 88: Guidance on the establishment and use of dose reference levels for medical x-ray examinations*. Institute of Physics and Engineering in Medicine; 2004.
23. *Personal communication with Federal Agency of Nuclear Control (FANC) Belgium on the third iteration of periodic patient CT dosimetry surveys in Belgium - Thanks to Thibault Vanaudenhove*. 2015.
24. Shrimpton PC, Hillier MC, Lewis MA, Dunn M. *National survey of doses from CT in the UK: 2003*. *British Journal of Radiology*. 2006;79(948):968-80.
25. Brisse HJ, Aubert B. *[CT exposure from pediatric MDCT: results from the 2007-2008 SFIPP/ISRN survey]*. *Journal de Radiologie*. 2009;90(2):207-15.
26. Treier R, Aroua A, Verdun FR, Samara E, Stuessi A, Trueb PR. *Patient doses in CT examinations in Switzerland: implementation of national diagnostic reference levels*. *Radiation Protection Dosimetry*. 2010;142(2-4):244-54.
27. Yakoumakis E, Karlatira M, Gialousis G, Dimitriadis A, Makri T, Georgiou E. *Effective dose variation in pediatric computed tomography: dose reference levels in Greece*. *Health Physics*. 2009;97(6):595-603.
28. Verdun FR, Gutierrez D, Vader JP, Aroua A, Alamo-Maestre LT, Bochud F, et al. *CT radiation dose in children: a survey to establish age-based diagnostic reference levels in Switzerland*. *European Radiology*. 2008;18(9):1980-6.
29. DDM2. *Dose DataMed 2 Project, Report Part 2: Diagnostic Reference Levels (DRLs) in Europe*. 2014.
30. Ron E. *Ionizing radiation and cancer risk: Evidence from epidemiology*. *Radiation Research*. 1998;150(5):S30-S41.

31. Pearce MS, Salotti JA, Little MP, McHugh K, Lee C, Kim KP, et al. Radiation exposure from CT scans in childhood and subsequent risk of leukaemia and brain tumours: a retrospective cohort study. *Lancet*. 2012;380(9840):499-505.
32. Hall EJ, Brenner DJ. Cancer risks from diagnostic radiology. *British Journal of Radiology*. 2008;81(965):362-78.
33. Ron E, Modan B, Boice JD, Jr, Alfandary E, Stovall M, Chetrit A, et al. Tumors of the brain and nervous system after radiotherapy in childhood. *New England Journal of Medicine*. 1988;319(16):1033-9.
34. Mathews JD, Forsythe AV, Brady Z, Butler MW, Goergen SK, Byrnes GB, et al. Cancer risk in 680 000 people exposed to computed tomography scans in childhood or adolescence: data linkage study of 11 million Australians. *British Medical Journal*. 2013;346.
35. Journy N, Rehel JL, Ducou Le Pointe H, Lee C, Brisse H, Chateil JF, et al. Are the studies on cancer risk from CT scans biased by indication? Elements of answer from a large-scale cohort study in France. *British Journal of Cancer*. 2015;112(1):185-93.
36. Huang WY, Muo CH, Lin CY, Jen YM, Yang MH, Lin JC, et al. Paediatric head CT scan and subsequent risk of malignancy and benign brain tumour: a nation-wide population-based cohort study. *British Journal of Cancer*. 2014;110(9):2354-60.
37. Krille L, Dreger S, Schindel R, Albrecht T, Asmussen M, Barkhausen J, et al. Risk of cancer incidence before the age of 15 years after exposure to ionising radiation from computed tomography: results from a German cohort study. *Radiation Environmental Biophysics*. 2015;54(1):1-12.
38. Meulepas JM, Ronckers CM, Smets AM, Nievelstein RA, Jahnen A, Lee C, et al. Leukemia and brain tumors among children after radiation exposure from CT scans: design and methodological opportunities of the Dutch Pediatric CT Study. *European Journal of Epidemiology*. 2014;29(4):293-301.
39. Hall EJ, Brenner DJ. Cancer risks from diagnostic radiology: the impact of new epidemiological data. *British Journal of Radiology*. 2012;85(1020):E1316-E7.
40. Brenner DJ, Hall EJ. Cancer risks from CT scans: now we have data, what next? *Radiology*. 2012;265(2):330-1.
41. Brady Z, Ramanauskas F, Cain TM, Johnston PN. Assessment of paediatric CT dose indicators for the purpose of optimisation. *British Journal of Radiology*. 2012;85(1019):1488-98.
42. *Health Risks from Exposure to Low Levels of Ionizing Radiation: BEIR VII Phase 2: The National Academies Press; 2006.*
43. *The 2007 Recommendations of the International Commission on Radiological Protection. ICRP publication 103. Annals of the ICRP. 37. England 2007. p. 1-332.*
44. Tubiana M, Feinendegen LE, Yang CC, Kaminski JM. The Linear No-Threshold Relationship Is Inconsistent with Radiation Biologic and Experimental Data. *Radiology*. 2009;251(1):13-22.
45. Brenner DJ, Doll R, Goodhead DT, Hall EJ, Land CE, Little JB, et al. Cancer risks attributable to low doses of ionizing radiation: Assessing what we really know. *Proceedings of the National Academy of Sciences of the United States of America*. 2003;100(24):13761-6.
46. Hoel DG. Comments on the DDREF Estimate of the BEIR VII Committee. *Health Physics*. 2015;108(3):351-6.
47. Little MP, Wakeford R, Tawn EJ, Bouffler SD, Berrington de Gonzalez A. Risks associated with low doses and low dose rates of ionizing radiation: why linearity may be (almost) the best we can do. *Radiology*. 2009;251(1):6-12.
48. Berrington de Gonzalez A, Mahesh M, Kim KP, Bhargavan M, Lewis R, Mettler F, et al. Projected cancer risks from computed tomographic scans performed in the United States in 2007. *Archives of Internal Medicine*. 2009;169(22):2071-7.
49. Miglioretti DL, Johnson E, Williams A, Greenlee RT, Weinmann S, Solberg LI, et al. The Use of Computed Tomography in Pediatrics and the Associated Radiation Exposure and Estimated Cancer Risk. *Jama Pediatrics*. 2013;167(8):700-7.

3

Biomarkers of x-ray induced DNA damage and repair

As described in the previous chapters, IR is a known carcinogen but the understanding of health risks at low doses and dose-rates remains controversial in view of the restricted amount of epidemiological data. It is anticipated that significant insights will emerge from radiation biomarker studies. European initiatives, such as DoReMi and MELODI have supported the introduction of sensitive assays and biomarkers to shed new light on the cellular and molecular responses at low doses (1). A biomarker is defined as “any measurement reflecting an interaction between a biological system and a potential hazard, which may be chemical, physical, or biological. The measured response may be functional and physiological, biochemical at the cellular level, or a molecular interaction” (2). Within this PhD, we will focus on biomarkers of exposure, which are available at a certain time point after IR exposure and can be used to validate a correlation between exposure and biological response (1).

3.1**The DNA damage response**

The integrity of an individual's genome is continuously challenged by both endogenous and exogenous DNA damaging agents. Damaging agents can induce a wide variety of lesions in the DNA, such as single strand breaks (SSBs), double strand breaks (DSBs), oxidative lesions and pyrimidine dimers (3). The DNA damage induced by IR exposure is due to the direct effect of radiation on DNA molecules, which accounts for 30-40% of lesions, or by the generation of free radicals in intracellular H₂O that in turn damage DNA, which accounts for 60-70% (4). The ratio of SSBs:DSBs induced by IR is 20:1 (5). Of the various forms of damage induced by IR, the DNA DSB is considered to be the principle cytotoxic lesion, since inaccurate repair or lack of repair of DSB can lead to mutations or cell death (6). Furthermore, there is experimental evidence for a causal link between the generation of DSBs and the induction of mutations and chromosomal translocations with tumorigenic potential (7-9). In order to maintain the genomic integrity of the DNA, cells have an integrated network of signaling pathways to counteract the genotoxic effects of the lesions induced by IR exposure, known as the DNA damage response (DDR). Although the majority of lesions are effectively repaired, the advent of a single DSB poses such a threat to cell survival that DNA damage checkpoint proteins have to be activated to bring the cell into arrest. This provides time for repair to proceed or, in the case of overwhelming damage, apoptosis programs are started (10).

The DDR provides a mechanism for transducing a signal from a sensor (DNA-damage binding protein) that in turn triggers the activation of a 'mediator/transducer' system (protein kinase cascade), to target eventually a series of downstream 'effectors' that determine the cellular outcome of DNA damage caused by radiation (see Figure 3.1). The three main effector outcomes are 1) cell-cycle arrest to slow down progression in cell cycle in order to provide time for repair, followed by the activation of DNA repair by recruiting DNA repair proteins to the DNA DSB or cellular senescence; or 2) the triggering of programmed cell death (apoptosis).

The signalling of DNA DSBs is fundamental for cells and the DDR pathway exhibits a critical function on the protection against human cancer, as indicated by the high cancer predisposition of individuals with germ-line

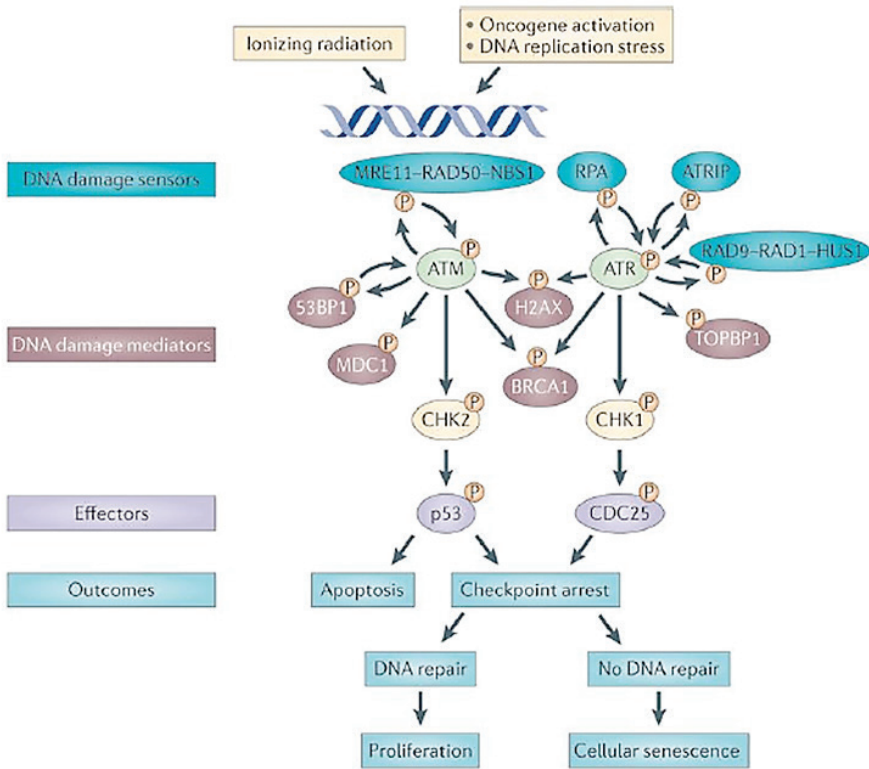


FIGURE 3.1

The general organization of the DNA-damage response pathway. The presence of a DSB is recognized by a sensor, which transmits the signal to a series of downstream effector molecules through a transduction cascade of DNA damage mediators, to activate signalling mechanisms for cell-cycle arrest and induction of repair, or cell death. The central role of ATM and ATR in DNA damage response is illustrated. Figure from (11).

mutations in DDR genes (12, 13). The signalling network is highly regulated and provides an accessible classification system of sensors, signal transducers, mediators and effectors; however, several publications indicate that many proteins satisfy the criteria of more than one category, pointing towards a series of highly cooperative pathways with overlapping functions (10). In the following sections, we give an overview of the major proteins involved in DDR in response to DNA DSBs.

3.1.1**DNA damage sensors and transducers**

Members of the phosphatidylinositol 3-kinase like kinase (PIKK) serine/threonine protein kinase family play an important role in different stages of DNA signalling. This protein kinase family includes DNA-dependent protein kinase catalytic subunit (DNA-PKcs), the ATM and ATM- and Rad3-related (ATR) protein kinases. While ATM and DNA-PKcs are critical for the signalling of DSBs, ATR is mainly activated by single-stranded DNA (ssDNA) regions that arise from stalled replication forks or processing of bulky lesions (10) (see Figure 3.1). It has been shown that when ATM activity is compromised, DNA PKcs can compensate to a certain degree for the defective ATM in some situations (14).

There remains controversy about the proteins that initially sense the DNA DSBs and start the signalling response. Critical roles in the detection of DNA damage have been ascribed to the Mre11/Rad50/Nbs1 (MRN) complex and the Ku70/80 proteins function as sensors of DSBs, which are also involved in the processing of DNA break ends (12). The MRN complex recruits ATM via the interaction with the C-terminus of Nbs1, while Ku70/80 recruits DNA PKcs to DNA lesion sites (15). A similar sensing process exists for ATR, where ATR is recruited to ssDNA regions marked with Replication Protein A (RPA) via a process that requires the ATR interacting protein (ATRIP), Rad17 and the so-called 9-1-1 complex of Rad1-Rad9 and Hus1, that stimulate the kinase activity of ATR (see Figure 3.1).

Because cells derived from Ataxia Telangiectasia (AT) patients display hypersensitivity to ionizing radiation, and defects in cell cycle checkpoint activation, ATM is considered to be a key protein kinase involved in DSB responses (16). In undamaged cells, ATM forms an inactive dimer (or multimer). When DSBs are generated and ATM interacts with Nbs1, the effective concentration of ATM increases and ATM is autophosphorylated on serine 1981 leading to its dissociation in kinase active monomers (10). In addition to the phosphorylation process, there occurs also dephosphorylation of ATM by several phosphatases such as protein phosphatase 2A (PP2A), which is necessary for the regulation of ATM activity (17) (see Figure 3.2). Experimental evidence has showed that the MRN complex is required for ATM auto-phosphorylation and for retention of ATM on chromatin following DNA damage. This suggests that the MRN complex functions indeed as a sensor upstream of ATM during the early stages of the DNA damage response (18, 19). Activated ATM monomers have been

shown to phosphorylate hundreds of proteins, including proteins involved in checkpoint activation (e.g. p53 and Chk2) and DNA-repair proteins (20).

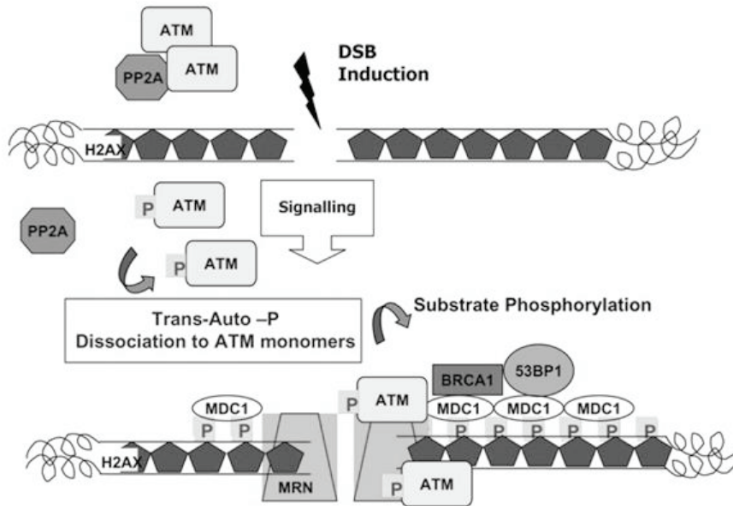


FIGURE 3.2

Activation of ATM kinase. Under physiological conditions, ATM exists as a dormant dimer in association with PP2A. In response to DSB ATM autophosphorylates, resulting in the release of active ATM monomers, which phosphorylate H2AX (γ H2AX). A positive feedback amplification loop arises, with γ H2AX recruiting ATM to sites of DSB, where it phosphorylates substrates such as MDC1, 53BP1 and BRCA1. Data from (10).

A critical target of ATM is the phosphorylation of the C-terminus of the histone variant H2AX (γ -H2AX), although this step can also be carried out by DNA PKcs or ATR. H2AX is among the earliest of substrates to become phosphorylated following DSB induction, achieving a plateau within 30 min. This leads to a positive feedback amplification loop, in which γ -H2AX functions as a binding site for the BRCA1 C-terminal (BRCT) domains of the Mediator of DNA damage Checkpoint 1 (MDC1) protein (21), illustrated in Figure 3.3. Positioning of MDC1 at the DSB creates a docking site for additional repair proteins and recruits the MRN-ATM complex to the DSB site, where activated pATM phosphorylates a large number of ‘mediator’ substrates, such as p53 binding protein 1 (53BP1) and Breast

Cancer early onset-1 (BRCA1). MDC1 counteracts the dephosphorylation of γ -H2AX by PP2A and possible other phosphatases. γ -H2AX serves as a platform for signalling onto which DDR proteins are concentrated to amplify the initial signal (22). It is illustrated in Figure 3.2 that the phosphorylation of H2AX orchestrates the retention of many DDR proteins at sites of DSBs. This cascade of reactions spreads H2AX phosphorylation over a distance of a few megabase-long domains (23). This clustering of DDR proteins is commonly referred to as irradiation-induced foci (IRIF). The modified mediator proteins then amplify the DNA damage signal and transduce the signals to downstream effectors such as Rad51, Artemis, Chk2 and p53 (24).

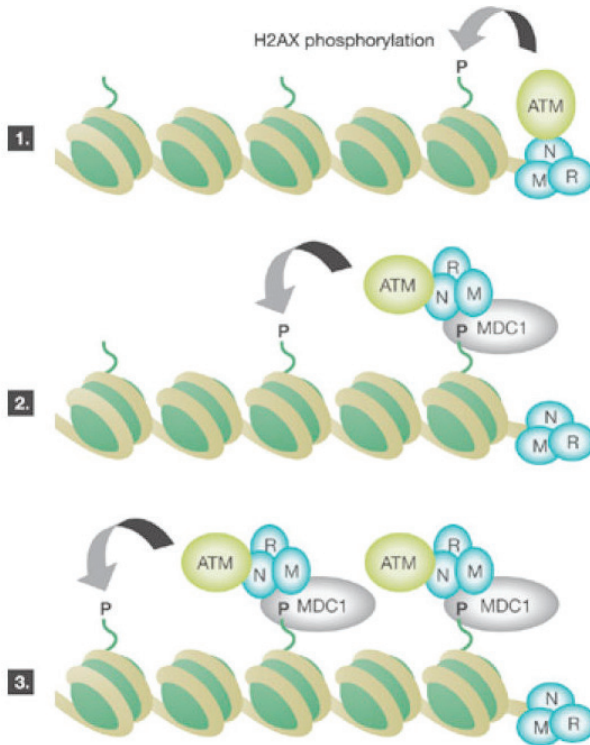


FIGURE 3.3

Model of MDC1-regulated phosphorylation of H2AX. In the first step, the MRN complex binds at the DNA ends and recruits ATM, which phosphorylates H2AX. Afterwards, MDC1 binds proximal phosphorylated H2AX and recruits more MRN-ATM, which phosphorylates more distal H2AX. This cascade of events contributes to the spreading of γ -H2AX to more distal chromatin regions. Figure from (23).

3.1.2

DNA damage effectors

As described above, the induction of DNA DSBs leads to the activation and integration of a diverse network of proteins. This culminates in the activation of effector pathways, including cell cycle checkpoint responses to allow DNA repair or, in certain cases, the initiation of apoptotic programs (25). The overall function of cell cycle checkpoints is to detect damaged or abnormally structured DNA, and to coordinate cell-cycle progression with DNA repair. Typically, cell-cycle checkpoint activation slows or arrests cell-cycle progression, thereby allowing time for appropriate repair mechanisms to correct the radiation-induced lesions before they are passed on to the next generation of daughter cells.

3.1.2.1

Cell cycle checkpoints

The control of the mammalian cell cycle division is subjected to numerous cyclin-dependent kinase (cyclin-Cdk) complexes, which regulate the movement through the cell cycle (see Figure 3.4). To ensure fidelity of DNA replication and chromosome segregation, cell cycle checkpoint arrest ensures the activation of surveillance mechanisms to prevent progression through the cell cycle until critical processes have been completed (26). The cell possesses several checkpoints, namely the G₁/S, intra-S-phase and

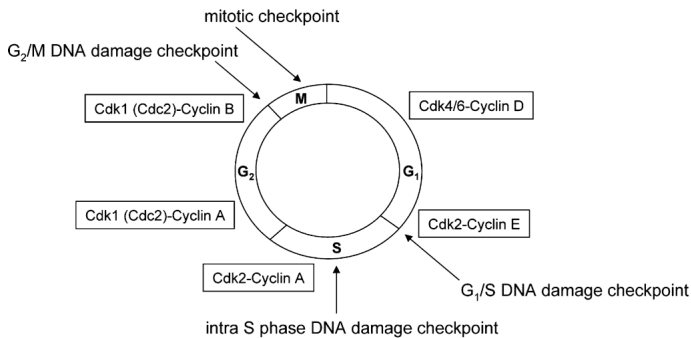


FIGURE 3.4

Control of the cell division cycle by cyclin-Cdks and their regulation by cell cycle checkpoints In the early G₁ phase of the cell cycle, Cdk4/6–Cyclin D complexes are active. Subsequently, entry into and progression through S phase are regulated by Cdk2–Cyclin E and Cdk2–Cyclin A, respectively, while the onset of mitosis is governed by Cdk1 (Cdc2)–Cyclin B. Figure from (28).

G2/M restriction points. When a cell arrives at a cell cycle checkpoint, it must assess whether its genome is fit for division, or whether it must allow time for DNA repair (27). Checkpoint activation is based in the inhibition of the cyclin-Cdk complexes, which regulate the movement through cell cycle.

In the presence of DNA damage, the G1/S checkpoint prevents replication of cells that were in G1 at the time of DNA damage to progress into S-phase. The checkpoint is mediated by two distinct signal transduction pathways, the Chk1/Chk2-Cdc25A-Cdk2 pathway (29) and a second pathway centred on tumour suppressor p53. The G1 arrest is a consequence of the inhibition of Cdk2, repressing the release of the G1/S phase-promoting E2F transcription factor (28, 30, 31).

During the S-phase, damaged DNA inhibits replicative DNA synthesis, which is referred to as an *intra-S-phase checkpoint*. Downregulation of CDC25A subsequently causes inactivation of the S-phase-promoting Cdk2 –cyclinE and prevents loading of Cdc45 on replication origins (29).

The *G2/M checkpoint* prevents the cells from entering into mitosis and transducing DNA damage to daughter cells. The checkpoint is subject to the Chk1/Chk2-Cdc25c-Cdk1 pathway. The arrest is achieved through Cdk1-cyclinB kinase inhibition of the Cdc25c phosphatase (28, 29).

3.1.2.2

DNA repair pathways

IR can induce different types of DNA lesions, which require different repair pathways. Base damage and DNA SSBs can be repaired by ‘base-excision repair’ (BER). Other excision repair mechanisms are ‘nucleotide excision repair’ (NER) and ‘mismatch repair’ (MMR), however the latter repair pathways are less important in the framework of IR induced DNA damage. DNA DSBs are the most serious and lethal types of DNA damage, since a single DSB is sufficient to kill a cell or disturb its genomic integrity. In the following paragraphs, we will focus on the two major repair pathways for DSBs in mammalian cells: homologous recombination (HR) and non-homologous end-joining (NHEJ). The HR pathway is error free but requires an intact homologous template, while the error prone NHEJ is the most prominent pathway for DSB repair in mammalian cells and does not require a homologous sequence to guide the repair (19, 30) (see Figure 3.5).

Homologous recombination (HR): HR-mediated repair is characterized by deriving the correct sequence from a homologous strand of intact DNA, which allows high-fidelity repair of DSBs. Thus, HR is typically error-free and occurs without loss of genetic information. Because HR depends on the existence of sister-chromatids to provide repair templates, it must occur during the late S-phase and G2-phase. The production of ssDNA requires the initial nuclease activity of the CtIP-MRN complex. DNA lesions are recognized by the MRN complex, and transmits the signal to mediators such as ATM and ATR. These mediators phosphorylate repair factors including H2AX and CtIP-interacting protein (CtIP), BRCA1 and exonuclease 1 (EXO1). HR requires the phosphorylation of CtIP at serine 327 by Cdk, for the recruitment of BRCA1 and commitment to HR (27). Endonucleolytic cleavage by the MRN complex allows resection, which is mediated by CtIP and EXO1 in the presence of BRCA1 and Bloom's syndrome helicase (BLM). The single-stranded DNA generated by resection is rapidly coated by RPA and subsequently replaced by Rad51 in the presence of BRCA2. Rad 51 and its paralogs, such as XRCC3, are critical in homology searching to identify a homologous sequence and mediate invasion of the sister chromatid. When a homologous sequence is found, the invaded strand is extended by DNA polymerase and ligated to form D-loop structures. There is an exchange of the damaged strands, such that each strand is now paired with a homologous template. The damaged strands are then extended and ligated, restoring the original double strand (23).

Non-homologous end-joining (NHEJ): In contrast to the HR pathway, DNA repair through NHEJ is thought to occur rapidly throughout the cell cycle. The Ku70/80 heterodimer binds with high affinity to broken DNA termini in a non-sequence-dependent manner. Binding of Ku to the DNA recruits the catalytic subunit of DNA PKcs to the DSB site, leading to the activation of DNA PKcs serine-threonine kinase activity by binding to the DNA. ATM-mediated phosphorylation of H2AX and the recruitment of 53BP1 protects DSB ends from being resected. It is noteworthy that in the absence of Ku, DNA-PKcs bind to DNA termini, albeit with a 100-fold lower affinity (31). The activated DNA PKcs facilitate then the recruitment of other repair factors to the DSB site, such as Artemis, the XRCC4/DNA ligase 4 complex and XRCC4-like factor (XLF). Artemis facilitates end processing and, subsequently, DNA ligase 4 (LIG4), XRCC4 and XLF ligate the broken DNA termini to complete repair (32). It has been suggested that in mammals, the MRN complex, which possesses nuclease and hel-

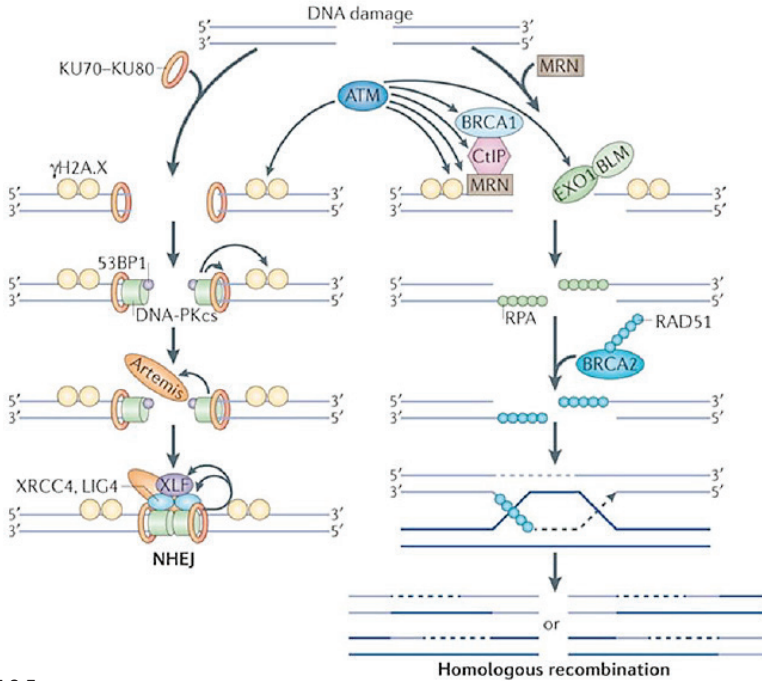


FIGURE 3.5

Illustration of DNA double-strand break (DSB) repair pathways in mammals. DSBs are predominantly repaired by either an error-prone pathway - non-homologous end-joining (NHEJ), or an error free pathway - homologous recombination (HR) (32).

icase activities and localizes at nuclear foci that are associated with DSB, is involved in the processing of the broken DNA ends in both HR and NHEJ (33). Although NHEJ efficiently rejoins the DSB ends, it often causes a loss of genetic information due to the loss of a few nucleotides at each broken end. NHEJ is the most common pathway in higher eukaryotes, and predominates in most stages of the cell cycle, particularly in G₀ and G₁ (34).

How cells regulate the choice between HR and NHEJ repair pathways is not well understood, although both the 53BP1 and BRCA1 proteins can play a key role in this choice (20). Over the past decade, a number of alternative DSB repair mechanisms were identified. These include alternative end joining pathways, also known as backup NHEJ, which operate independently of factors such as DNA-PKcs, XRCC4 and LIG4 (35). They are suspected to be more error-prone than the classical NHEJ pathway. Furthermore, single-strand annealing and break-induced replication were recently observed in mammalian cells where they may contribute to DSB repair (36, 37), especially in association with replication.

3.1.2.3**Apoptosis**

Apoptosis is known as a 'programmed cell death' and represents an ordered suicidal process that results in the destruction and removal of damaged cells. Apoptosis plays a major role in the maintenance of tissue homeostasis and the removal of cells during certain developmental processes, such as during lymphocyte development and differentiation. Moreover, it appears to be exploited by the damage response to specifically remove cells containing a threshold level of DNA damage. Thereby apoptosis limits the potential for the damaged cells to accumulate mutations that might lead to carcinogenesis and to prevent the transfer of defective genetic material to daughter cells. Apoptosis is often viewed as a mechanism for eliminating severely damaged cells that might otherwise threaten the health of the organism in which the threshold level of damage required to trigger apoptosis seems to be highly cell type-dependent (38). There are various experimental systems, which show that defects in the execution of apoptosis increase cancer incidence (39, 40).

Apoptosis is characterised by morphological changes, including plasma membrane blebbing, peripheral condensation of the nuclear DNA without disassembly of the nuclear envelope, chromatin condensation and cleavage of the nucleus into membrane-enclosed structures, known as apoptotic bodies (41). These changes distinguish apoptosis from necrotic cell death, which can also result from DNA damage. Necrosis is considered as "uncontrolled" cell death, resulting in a loss of membrane integrity, swelling of cellular organelles and disruption of the cells. During necrosis, the cellular contents are released uncontrolled into the cell's environment which can result in a strong inflammatory response in the surrounding tissue (42). Apoptosis is a complex process that can proceed through at least two main pathways (extrinsic and intrinsic), each of which can be regulated at multiple levels (43).

The primary regulators of apoptosis are proteins belonging to a group known as the B-cell CLL/lymphoma 2 (Bcl-2) family, including both pro- as well as anti-apoptotic molecules (44). The ratio between pro- and anti-apoptotic family members determines whether or not a cell will undergo apoptosis. Apoptosis regulators also include death receptors on the cell surface which bind to death signalling molecules, as part of the extrinsic apoptotic pathway. Apoptosis is characterized by the activation of the members of a specialised family of cysteine aspartyl proteases, the cas-

pases. Active caspases are heterodimeric, consisting of large and small subunits generated by caspase-mediated cleavage. Sequential activation of caspases plays a central role in the execution-phase of cell apoptosis, with a potential for amplification of apoptotic signals through caspase cascades. In human cells caspases 8 and 9 play key regulatory roles in these cascades, whereas other members of the family perform effector roles downstream (40).

A brief overview of the extrinsic and intrinsic apoptotic pathways can be found in Figure 3.6. In the extrinsic pathway, death signals from the surrounding environment of the cell bind to death receptors on the surface of the cell membrane. This causes the conversion of inactive pro-caspase-8 into active caspase-8. Caspase-8 then goes on to activate caspase-3, which begins the caspase cascade that leads to apoptosis.

In addition to its cell cycle regulatory functions, p53 serves as a regulator of the apoptosis and plays a key role in both extrinsic and intrinsic pathways. In the intrinsic pathway, typically initiated by DNA damage, p53 is activated, escapes degradation and enables the activation of its

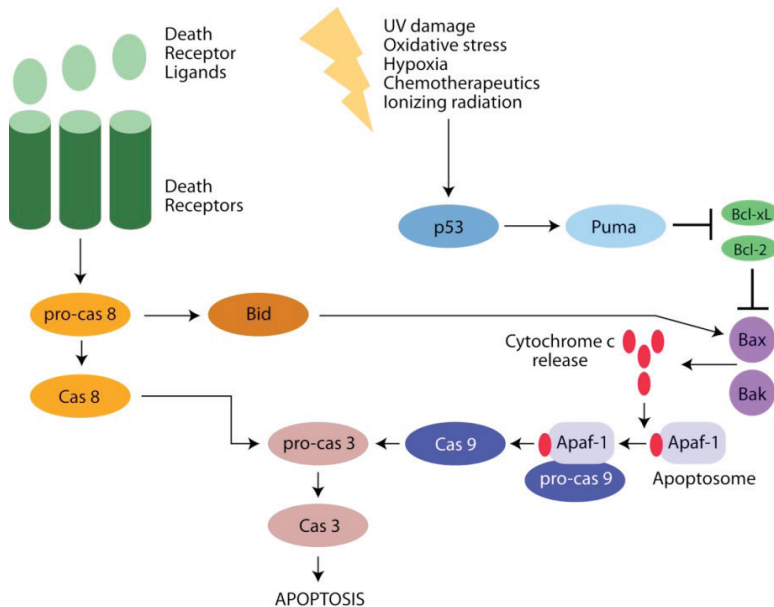


FIGURE 3.6

Model of the intrinsic and extrinsic apoptotic pathways (45).

target genes involved in apoptosis; e.g. pro-apoptotic Bcl-2-associated X (Bax), Bcl-2 homologous antagonist killer (Bak), p53 up-regulated modulator of apoptosis (Puma), Noxa, and apoptotic protease activating factor 1 (Apaf1). The activation of the pro-apoptotic protein Bax by p53, initiates the release of cytochrome c from the mitochondria. Apaf-1 and the released cytochrome c combine to form a complex known as the apoptosome. This apoptosome causes the conversion of inactive pro-caspase-9 into active caspase-9. Caspase-9 then goes on to activate caspase-3 in a similar manner to the extrinsic pathway.

Thus, once activated, initiator caspases 8 and 9 in turn activate the executioner caspases: caspases-3, -6, and -7 (46). Caspase-3 and the other executioner caspases are required for initiating the hallmarks of the degradation phase of apoptosis, and are indispensable for apoptotic chromatin condensation and DNA fragmentation. Thus, caspase-3 is an essential executioner caspase that initiates a caspase cascade, necessary for certain processes associated with the dismantling of the cell and the formation of apoptotic bodies (47).

3.2

Chromatin structure and DNA repair

One of the striking features of the eukaryotic cell nucleus, which carries and reads the genetic information, is its functional and structural complexity. The human genome contains some 35 000 genes and 3.2 billion base pairs of DNA (48). The packing of the human DNA into chromatin is an extremely efficient way to store the DNA within the nucleus of approximately 5 to 10 μm (see Figure 3.7). The primary protein components of chromatin are histones that compact the DNA into a nucleosome. The nucleosome core particle represents the first level of chromatin organization and is composed of two copies of each of histones H2A, H2B, H3 and H4 (the core histones) (49). Nucleosome cores are separated by linker DNA of variable length and are associated with the fifth histone H1, which is bound to the DNA as it enters each nucleosome core particle. This forms a chromatin subunit known as a chromatosome. The next level of chromatin organization is the 30-nm fibre, which is composed of packed nucleosome arrays arranged as a two-start helical model, and mediated by core histone internucleosomal interactions (50).

The organization of DNA into chromatin is not only important for resolving spatial and organization problems, but it is also essential for the functional utilization of the DNA and the proper coordination of its metabolic activities (51). Several chromatin states are likely to be regulated and maintained in a tissue-specific manner, making the DNA accessible to the transcription machinery during specific periods of the cell cycle and at precise locations. During interphase, the chromatin is structurally decondensed and distributed throughout the nucleus to allow gene transcription and DNA replication in preparation for cell division. Most of the euchromatin in interphase nuclei appears to be in the form of 30-nm fibers, organized into large loops. About 10% of the euchromatin, containing the

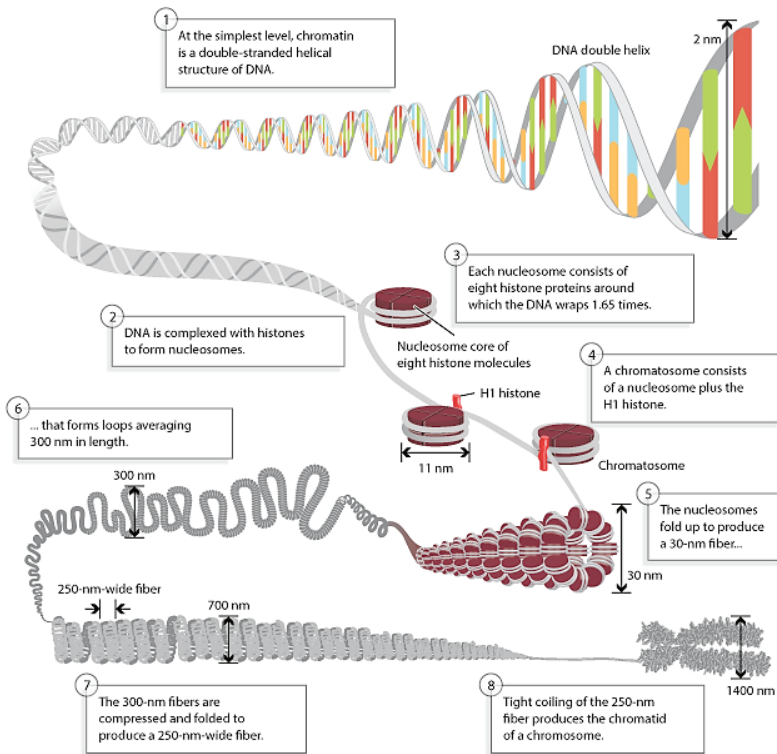


FIGURE 3.7

Illustration of DNA packing into chromatin and chromosomes. DNA wraps around proteins called histones to form units called nucleosomes. These units condense into a chromatin fibre, which condenses further to form a chromosome. Figure from (53).

genes that are actively transcribed, is in a more decondensed state (the 10-nm conformation) that allows transcription. In contrast to euchromatin, about 10% of interphase chromatin (called heterochromatin) is in a very highly condensed state that resembles the chromatin of cells undergoing mitosis. Heterochromatin is transcriptionally inactive and contains highly repeated DNA sequences, such as those present at centromeres and telomeres (52).

DDR takes place within the complex organization of the chromatin, and it is clear from work in many model systems that chromatin structure and nucleosome organisation represent a significant barrier to the efficient detection and repair of DSBs (20). The structure of the chromatin in eukaryotic cells affects the accessibility of DNA and therefore has consequences for all cellular activities, including DNA repair (3). A more open and accessible chromatin should facilitate both the generation of DNA modifications by endogenous and exogenous agents and the initiation of the repair, while more condensed and compact chromatin might protect against damage generation, but at the same time hinder and retard the detection by repair enzymes.

The influence of the chromatin structure on damage generation and repair was demonstrated for DNA DSBs induced by ionizing radiation (54). Furthermore, chromatin condensation by hypertonic shock was shown to impede the repair of oxidative generated DNA base modifications (55). In the last years, several small-molecule modulators of the chromatin structure have been identified and tested for therapeutic applications in tumour therapy. An example of these compounds is 'resveratrol' (3,5,4'-trihydroxystilbene) that induces a more condensed chromatin compaction and therefore potentially decreases the accessibility of the DNA (56). The influence of resveratrol on damage generation and repair has not been studied in detail, but primary studies show that resveratrol decreases the repair rates, while damage generation remained unchanged (57). The influence of the chromatin status on DNA repair will be further explored in the discussion section (see chapter 11).

3.3**Detection of x-ray effects at DNA level**

A variety of tests can be applied to determine the initial radiation-induced DNA damage, its repair, the cellular outcome and the associated 'radiosensitivity'. There are several endpoints that can be used as radiosensitivity markers, depending on the assay that is used: radiation-induced DNA damage, cell survival, chromosomal aberrations, direct and late effects after *in vivo* exposure. The kind of assay that should be used, will depend on the study design such as the time window after exposure, the required sensitivity and specificity and the available biological material. The haematopoietic system contains some of the most radiosensitive and easily sampled cells in the human body. Furthermore, circulating lymphocytes are a synchronous G₀ population with a relatively long life span to preserve the DNA damage. Therefore, peripheral blood lymphocytes have been widely used for the detection of radiation-induced DNA damage. Cytogenetic analysis of lymphocytes as a biomarker of IR exposure, covers a set of long-established techniques. To this group of assays belong the dicentric assay, the scoring of stable chromosome aberrations such as translocations with chromosome 'painting' and the micronucleus (MN) assay. Another group of biomarkers comprise DNA damage and repair assays, such as the comet assay, pulsed-field gel electrophoresis (PFGE) and the γ -H2AX foci assay. Other assays, representing the effect on cell survival, apoptosis and epigenetic processes can also be used. In the following sections, the main focus is on the cytokinesis-block micronucleus assay (CBMN) and the γ -H2AX foci assay, as these two assays were used as biomarker for this PhD research.

3.3.1**Mutagenic effects: cytogenetic assays**

Cytogenetics focus on the study of chromosomes and several cytogenetic biomarkers have been routinely used as biomarkers of exposure (58). The fact that most established human carcinogens, such IR, are genotoxic and capable of inducing chromosomal damage is the primary rationale of using these assays. Furthermore, epidemiological studies suggest that a high frequency of chromosome aberrations (CAs) is predictive for an increased cancer risk which supports the link between increased frequency of cy-

togenetic alterations and cancer risk (59). CAs are structural aberrations resulting from un- or misrepaired radiation-induced DSBs, comprising chromosome- and chromatid-type breaks and rearrangements, usually analysed by transmitted light microscopy of Giemsa-stained metaphase slides or by fluorescence microscope using fluorescence in situ hybridization (FISH) techniques. The dicentric assay is considered as the 'gold standard' for biological dosimetry and is based on the analysis of dicentric chromosomes in metaphase cells. In addition to its application in biological dosimetry, cytogenetic analysis is also used to determine chromosomal sensitivity. The concept that genetic susceptibility to cancer development is related to genomic instability was initially supported by rare disorders, such as Ataxia Telangiectasia and Xeroderma Pigmentosum. Several studies showed that both disorders are associated with *in vivo* and *in vitro* chromosomal instability and defective DNA repair capacity (60). The extent of genetic damage reflects critical events for carcinogenesis, such as an impaired ability to remove damaged DNA or failure to correctly rejoin DNA breaks, which have the potential to be cytogenetically detectable (60, 61).

The G_0 or the cytokinesis-block MN assay in human lymphocytes is one of the most commonly used methods for measuring chromosomal damage and sensitivity. The assay is based on the *in vitro* culturing of peripheral blood lymphocytes, that are stimulated to divide with phytohaemagglutinin (PHA) after irradiation. After the completion of one nuclear division, cells are blocked from performing cytokinesis by the addition of cytochalasin B and will consequently appear as binucleated (BN) cells. Cytochalasin B is an inhibitor of the microfilament ring assembly required for the completion of cytokinesis (62). MN originate from chromosome fragments or whole chromosomes that fail to engage with the mitotic spindle and therefore lag behind when the cell divides (60). Several studies demonstrated that radiation-induced MN are predominantly derived from acentric fragments (63) and the observed MN in PBL are mainly the result of un- or misrepaired DSBs by the NHEJ repair pathway (64). Compared to other cytogenetic assays, the quantification of MN has several advantages, including speed and ease of analysis, no requirement for metaphase cells and reliable identification of BN cells which completed only one nuclear division. The latter prevents confounding effects caused by differences in cell division kinetics because expression of the genetic damage end points is dependent on completion of nuclear division (65). Over the past 20 years, the CBMN assay has evolved into a comprehensive method for measuring several outcomes, such as chromosome breakage,

DNA misrepair, chromosome loss, apoptosis, gene amplification through nuclear buds (NBUDs) and nucleoplasmic bridges (NPBs) as biomarker of dicentric chromosomes resulting from telomere end-fusions or DNA misrepair (66) (see Figure 3.8). The CBMN assay requires BN cells, so in principle, MN can be detected in all types of cells, as long as they are capable to divide after *in vitro* stimulation. In the framework of this PhD, a new method to perform the CBMN assay in HSPCs was developed.

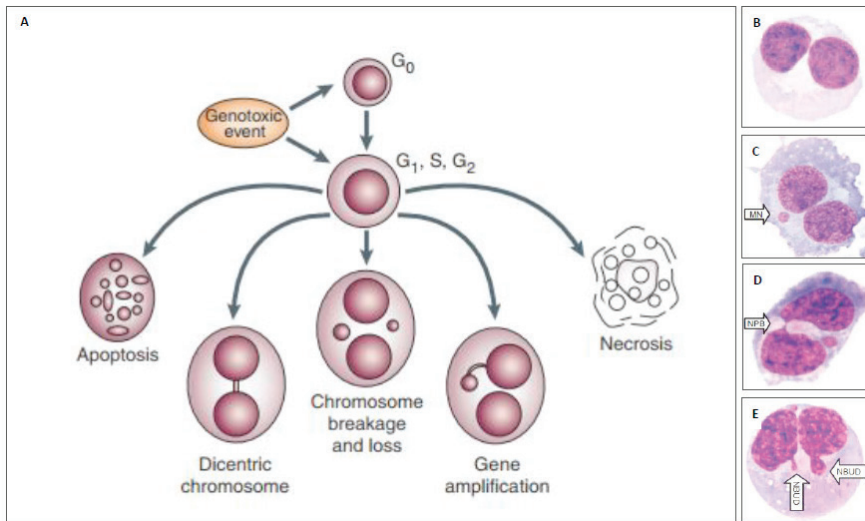


FIGURE 3.8

A. The various possible fates of the CBMN assay following exposure to cytotoxic/genotoxic agents such as IR: the measurement of chromosome breakage and loss (MN), dicentric chromosomes (NPB) gene amplification (NBUDs), necrosis and apoptosis. Microscopic images of **B.** binucleated (BN) cell; **C.** BN cell containing one MN; **D.** BN cell containing a NPB and a MN; **E.** BN cell containing NBUDs and a MN. Figure from (66).

3.3.2**The γ -H2AX foci assay to detect DNA DSB damage and repair**

The phosphorylation of the histone variant H2AX at the site of DNA DSBs, as described in 3.1.1, leads to the formation and accumulation of γ -H2AX foci in the cell nucleus within a few minutes after IR exposure. The maximum yield of foci is detected within 0.5 - 1h after irradiation, depending on the dose and cell type, and after this time point, the number of foci usually decreases to baseline levels within days (67). The scoring of γ -H2AX foci can be used as a direct endpoint to assess the formation of damage after IR exposure, whereas its persistence with time in irradiated samples can be used to evaluate DNA repair kinetics. Application of the γ -H2AX foci assay for both endpoints was used in this PhD research.

3.3.2.1**The role of γ -H2AX in the DDR**

The histone variant H2AX was the first and most prominent protein for which foci formation at the site of a DSB was described. Phosphorylation of H2AX at its C-terminal Ser-139 residue is mediated by DNA damage activated protein kinases ATM, ATR and DNA-PKcs to form γ -H2AX (see also 3.1.1) (37). This phosphorylation event is restricted to a chromosomal region surrounding an unrepaired DSB however, it involves hundreds to thousands of histone modifications within this region, resulting in a microscopically detectable distinct spot or 'focus' of several hundred nanometres diameter following immunostaining against γ -H2AX (68). As described in previous paragraphs of this chapter, phosphorylation of histone H2AX is critical for facilitating the assembly of specific DNA-repair complexes on damaged DNA. This was supported by experiments in targeted H2AX mice in which H2AX^{-/-} mice were radiation sensitive and showed a reduced capacity to repair DSBs (69). A short summary of the biological functions that have been suggested for H2AX, based on (70):

- *Concentration of DNA damage signalling and repair proteins at DSBs, such as MDC1, resulting in the positive feedback loop that extends H2AX phosphorylation over a megabase region around the DSB (37, 51, 71).*

- *Signal amplification and transduction to enhance the sensitivity of the DNA damage-induced G2 cell cycle checkpoint.* The γ -H2AX dependent recruitment of 53BP1 could facilitate the activation of the cell cycle checkpoint in situations with low levels of DNA damage when checkpoint effectors (Chk1/Chk2) are not sufficiently activated (72).
- *Implementation of an Artemis-dependent pathway required for the repair of a subset of radiation-induced DNA DSBs with slow kinetics during the G₁-phase of the cell cycle by NHEJ.* Since Artemis interacts with 53BP1; γ -H2AX and 53BP1 may act as scaffolds to maintain Artemis at the DSB site (73).
- *Recruitment of cohesin to promote sister chromatid-dependent HR.* Rapid phosphorylation of H2AX results in a large zone of modified chromatin surrounding the DNA DSB, to which cohesin can be recruited to hold the broken chromatin in close proximity to its undamaged sister (74).
- *Chromatin remodelling to assist DSB processing,* by recruiting the chromatin remodelling complexes INO80 and SWR1 (75).
- γ -H2AX functions as a chromatin anchor to prevent the separation of break ends and enhance repair fidelity (72).

When repair is completed, γ -H2AX should be reverted to H2AX. The molecular mechanism of this elimination remains to be established, currently it is not clear whether dephosphorylation takes place directly in the nucleosome, or whether it requires removal of γ -H2AX from chromatin (reviewed in (76)). In contrast to γ -H2AX foci formation, the elimination is much slower. It is known that about 60% of initial IR-induced DSBs are transient with rejoining half-lives of the order of minutes, whereas the other 40% are persistent with rejoining half-lives of the order of hours (4). In principle, the elimination of γ -H2AX in mammalian cells can be done either directly by dephosphorylation of γ -H2AX or indirectly by replacing γ -H2AX in the nucleosome with H2AX followed by rapid dephosphorylation of H2AX protein after its displacement from chromatin (51, 76).

3.3.2.2

Technical aspects of γ -H2AX foci detection

There is a close correlation between the number of DNA DSBs and γ -H2AX foci, and between the rate of foci loss and DSB repair, resulting in a sensi-

tive assay to monitor DSB formation and repair in individual cells after IR exposure. The demonstration of precise γ -H2AX localization to the sites of DNA DSBs was achieved by the means of a laser scissor experiment, where DSBs were introduced through a pulsed laser microbeam. Subsequent immunocytochemistry showed that γ -H2AX forms precisely along this track of DSBs (68). The formation of γ -H2AX foci has been detected in fibroblasts and peripheral lymphocytes following radiation doses as low as 1 mGy, and the increase in foci yields is strongly dose-dependent (65, 72). Each individual γ -H2AX spot represents one (or more) DNA DSB. Although γ -H2AX foci are observed by 3 min post irradiation in G_0/G_1 -phase cells (e.g. lymphocytes), their detection is difficult at this time due to the small size of the spots. The best time point for foci scoring is probably 30 min post exposure, when most of the induced foci are still present and have reached a size and intensity that allow reliable scoring (5, 70). However, there exists considerable variation among the time points of maximal γ -H2AX foci formation (70) and it is important to note that the levels of foci may vary substantially between different cell types and also technical differences can play an important role. Differences in immunostaining protocols and reagents may produce differences in signal to noise ratios. Furthermore, differences in magnification and the optical resolution of the microscope and camera used for foci scoring can affect the detection of small spots. Furthermore, the sensitivity of the technique depends largely on the variability of foci levels in unirradiated cells, which points again to the fact that the technique is cell type dependent (70).

In general, lymphocytes have several advantages that make them most suitable for evaluating γ -H2AX foci formation. First, a considerable amount of cells can be easily obtained within a short time frame before and after exposure. Second, the use of lymphocytes avoids cell cycle effects, since unstimulated lymphocytes are a synchronous populations of non-cycling cells (G_0). Third, the percentage of nucleosomal H2AX variant was reported to be small in lymphocytes, resulting in a low γ -H2AX background (77).

The most frequently used techniques to score foci are immunofluorescence microscopy and intensity-based assays, such as flow cytometry. Microscopic foci quantification can be performed by manual scoring through the eye piece of the microscope, manual scoring of digital microscope images or by automated scoring using image analysis software (37). The main disadvantage of manual foci scoring by fluorescence microscopy is its time-consuming character. Furthermore, it requires some training

and to avoid subjectivity slides have to be coded. There is an ongoing intensive development of high throughput γ -H2AX foci scoring systems to automate microscopic evaluation. Automatic scoring could exclude the scorer-subjectivity together with the time-consuming character of manual scoring. In all cases of microscopic scoring, it is important to define and maintain strict scoring criteria and this requires an extensive optimisation of spot counting when scoring software is used.

Analysis by flow cytometry may be quicker. However, it is not as sensitive as microscopy, which has the advantage to discriminate objects such as foci from background staining spots (78). Certainly for the detection of DNA damage after low dose exposure as in diagnostic radiology, where foci signals can be elusive, a sensitive scoring method is more appropriate. Furthermore, attempts have been made to quantify DSB formation using H2AX by Western blotting. However, Western blotting techniques are, just like flow cytometry, hampered by the inherent background staining that arises from S-phase cells, which can differ between cell types and can be affected by the activation of cell cycle checkpoint arrest following radiation exposure (79).

Recently, live cell imaging of cells expressing fluorescent fusion proteins that are recruited to the sites of DSB has enabled detailed studies of the spatio-temporal dynamics of foci formation (80).

3.3.2.3

Double immunostaining of 53BP1/ γ -H2AX foci

Since H2AX is phosphorylated following activation of the DDR, γ -H2AX provides a powerful tool to monitor the presence of DNA damage. However, artefactual foci formation in the absence of a DSB can occur by non-specific staining or aggregate formation of the primary or secondary antibody. A possible cause for these artefacts could be the non-specific binding of the γ -H2AX antibody (Ab) with parts of the endoplasmic reticulum and/or Golgi vesicles (67). During S-phase, ATR activation occurs at ss-regions of DNA and γ -H2AX can be observed during normal replication, suggesting that phosphorylation of H2AX is not exclusively DSB dependent (25, 81). However, the γ -H2AX staining that arises in S-phase cells is more diffuse and pan nuclear compared to the discrete foci at DSBs after IR exposure (5). Furthermore, early apoptotic DNA breakage can also give rise to foci patterns that may sometimes be scored as residual IRIF (81).

Besides the before mentioned limitations, the γ -H2AX foci assay is a reliable and sensitive monitor of DSB formation and repair if careful optimisation of the immunostaining conditions is performed. Furthermore, the use of a double immunostaining for two foci-forming markers could validate the signal and reduce strongly the impact of artefacts, which enhances the sensitivity of the technique. Radiation-induced γ -H2AX foci co-localise very reliably with 53BP1 foci (83, 84), the latter DDR protein can be used as an alternative or, in situation where accuracy is of crucial importance, as an additional marker of DSBs through double immunostaining.

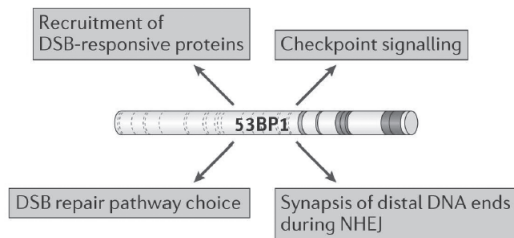


FIGURE 3.9

Different functions of 53BP1 in the DNA damage response. First, 53BP1 recruits additional DNA double-strand break (DSB) signalling and repair proteins to the site of DNA damage. Second, 53BP1 promotes ATM-dependent checkpoint signalling, especially at low levels of DNA damage. Third, it is a key player in DSB repair pathway choice. Fourth, 53BP1 promotes the synapsis of distal DNA ends during NHEJ. Figure from (85).

Hence, 53BP1 represents a second, highly useful IRIF marker. In undamaged cells, 53BP1 is present as pan-nuclear staining, which is low in intensity since the protein is distributed diffusely throughout the nucleus (79). The latter can cause higher background 53BP1 foci levels, when 53BP1 is not quantified in combination with another IRIF marker. Following radiation exposure, 53BP1 concentrates at DSBs, where it becomes visible as defined IRIF (86, 87). 53BP1 acts as a mediator and effector of the DSB response and is recruited to damaged chromatin and protects genomic instability by regulating DSB repair pathway choice by mutual antagonism with BRCA1 (85) (see Figure 3.9). 53BP1 can be advantageous over single γ -H2AX foci scoring for DSB repair analysis since it is not, or only weakly, retained at the ssDNA regions generated during replication (78). MRN and MDC1 can also be used for IRIF analysis but the foci

are less obvious either because they take longer to form (as in the case of MRN) or the currently available antibodies are sub-optimal (as in the case of MDC1) (78).

As already mentioned in the first paragraph, soon after the discovery of γ -H2AX, Rogakou *et al.* reported the induction of apoptotic γ -H2AX (82). The subcellular distribution of γ -H2AX in apoptotic cells was further investigated by Solier and Pommier, leading to the identification of the 'apoptotic ring' which contains γ -H2AX as an early chromatin modification during apoptosis (82). This γ -H2AX apoptotic ring appears in an early phase of apoptosis and follows a progression that we can subdivide in three phases: (1) the 'ring staining' that occurs only in a fraction of the cell without alteration of nuclear size, (2) the 'ring' is followed by a panstaining of the nucleus, which retains its overall morphology and size, (3) the panstaining persists within apoptotic bodies. An important finding of Solier *et al.* was that 53BP1 does not co-localize with γ -H2AX in the apoptotic ring (88). This suggested molecular and mechanistic differences between γ -H2AX induction after primary DNA damage and during apoptosis. In a subsequent study, the same research group could demonstrate that the apoptotic H2AX response does not recruit the DDR factors, because MDC1 (which normally binds to γ -H2AX in response to DNA DSB induction and amplifies the DDR, see 3.1.1) is cleaved by caspase-3 (89). The decrease of MDC1 during apoptosis and the fact that it is not recruited to γ -H2AX could explain why 53BP1 does not co-localize with apoptotic γ -H2AX. However, the functional relevance of γ -H2AX formation during apoptosis remains unknown. The scoring of co-localising 53BP1/ γ -H2AX foci can rule out the misclassification of early apoptotic DNA breakage as residual IRIF.

3.4

Ethical considerations for biomarker studies in children

Biomarker studies in children raise a number of particular ethical considerations related to the collection of biological samples, informed consent, and how to convey information about low-dose cancer risk to the parents, as the level of scientific knowledge is inadequate to quantify the risk (90). The ethics of research involving children has a long and profound history including important debates that made compelling arguments for and against (91). Current statements on the ethical conduct of research

issued by various national and professional bodies generally include a section outlining the special requirements for the inclusion of children in research, with the following three general protection guidelines (90):

- Sound justification - the presumption that children should not be included in research unless there is a compelling reason to do so.
- Informed consent - Only adults are presumed to have the capacity to act autonomously, whereas children are not presumed to have this capacity. In general, consent is given on their behalf by parents or legal guardians, usually supplemented by the positive affirmation of the child where possible (92).
- Prior ethics review.

For a paediatric patient population, the subject of this PhD research, there are a number of barriers to cross compared to studies on adult subjects, such as: fewer study subjects (only 1-2% of the CT examinations are performed in children), unique ethical challenges, difficulties in sample-collection methods, and small tissue-sample volumes. Biomarker studies require the use of biological samples. In case of the γ -H2AX foci assay, preferably peripheral blood lymphocytes are used. The problem of repeated blood sampling in children before and after CT exposure can be addressed by using the catheter for contrast agent administration (flushed) to collect the blood samples, eliminating the need for additional venepuncture. Efforts have been made to optimize the assay on exfoliated buccal cells which can be obtained by commercially available kits or a mouth-wash technique (93). However, pilot studies are warranted to prove the applicability of this technique in the dose range relevant to CT procedures and the collected cells originate only from one anatomical site. This makes them currently only appropriate for the assessment of DNA damage related to high-dose x-ray exposure to the head and neck region (93, 94). Furthermore, buccal cells are likely to have higher background levels of DNA DSBs as they are more directly exposed to other environmental, nutritional and life-style factors (70, 95).

3.5

References

1. Pernet E, Hall J, Baatout S, Benotmane MA, Blanchardon E, Bouffler S, et al. Ionizing radiation biomarkers for potential use in epidemiological studies. *Mutation Research-Reviews in Mutation Research*. 2012;751(2):258-86.
2. Strimbu K, Tavel JA. What are biomarkers? *Current Opinion in Hiv and Aids*. 2010;5(6):463-6.
3. Dinant C, Houtsmuller AB, Vermeulen W. Chromatin structure and DNA damage repair. *Epigenetics & Chromatin*. 2008;1.
4. Ward JF. DNA damage produced by ionizing radiation in mammalian cells: identities, mechanisms of formation, and reparability. *Progress in Nucleic Acid Research and Molecular Biology*. 1988;35:95-125.
5. Lobrich M, Shibata A, Beucher A, Fisher A, Ensminger M, Goodarzi AA, et al. gammaH2AX foci analysis for monitoring DNA double-strand break repair: strengths, limitations and optimization. *Cell Cycle* 2010;9(4):662-9.
6. Jackson SP. Sensing and repairing DNA double-strand breaks - Commentary. *Carcinogenesis*. 2002;23(5):687-96.
7. Richardson C, Jasin M. Frequent chromosomal translocations induced by DNA double-strand breaks. *Nature*. 2000;405(6787):697-700.
8. Vamvakas S, Vock EH, Lutz WK. On the role of DNA double-strand breaks in toxicity and carcinogenesis. *Critical Reviews in Toxicology*. 1997;27(2):155-74.
9. Khanna KK, Jackson SP. DNA double-strand breaks: signaling, repair and the cancer connection. *Nature Genetics*. 2001;27(3):247-54.
10. Riches LC, Lynch AM, Gooderham NJ. Early events in the mammalian response to DNA double-strand breaks. *Mutagenesis*. 2008;23(5):331-9.
11. Sulli G, Di Micco R, di Fagagna FdA. Crosstalk between chromatin state and DNA damage response in cellular senescence and cancer. *Nature Reviews Cancer*. 2012;12(10).
12. De la Torre C, Pincheira J, Lopez-Saez JF. Human syndromes with genomic instability and multiprotein machines that repair DNA double-strand breaks. *Histology and Histopathology*. 2003;18(1):225-43.
13. Knoch J, Kamenisch Y, Kubisch C, Berneburg M. Rare hereditary diseases with defects in DNA-repair. *European Journal of Dermatology*. 2012;22(4):443-55.
14. Callen E, Jankovic M, Wong N, Zha S, Chen H-T, Difilippantonio S, et al. Essential Role for DNA-PKcs in DNA Double-Strand Break Repair and Apoptosis in ATM-Deficient Lymphocytes. *Molecular Cell*. 2009;34(3):285-97.
15. Mordes DA, Cortez D. Activation of ATR and related PIKKs. *Cell Cycle*. 2008;7(18):2809-12.
16. Shiloh Y. ATM and related protein kinases: safeguarding genome integrity. *Nature Reviews. Cancer*. 3. 2003;3(3):155-68.
17. Goodarzi AA, Jonnalagadda JC, Douglas P, Young D, Ye R, Moorhead GB, et al. Autophosphorylation of ataxia-telangiectasia mutated is regulated by protein phosphatase 2A. *EMBO Journal* 2004;23(22): 4451-61.
18. Uziel T, Lerenthal Y, Moyal L, Andegeko Y, Mittelman L, Shiloh Y. Requirement of the MRN complex for ATM activation by DNA damage. *EMBO Journal*. 2003;22(20):5612-21.
19. Iijima K, Ohara M, Seki R, Tauchi H. Dancing on damaged chromatin: functions of ATM and the RAD50/MRE11/NBS1 complex in cellular responses to DNA damage. *Journal Radiation Research*. 2008;49(5):451-64.
20. Price BD, D'Andrea AD. Chromatin Remodeling at DNA Double-Strand Breaks. *Cell*. 2013;152(6):1344-54.
21. Lou ZK, Minter-Dykhouse K, Franco S, Gostissa M, Rivera MA, Celeste A, et al. MDC1 maintains genomic stability by participating in the amplification of ATM-dependent DNA damage signals. *Molecular Cell*. 2006;21(2):187-200.
22. Celeste A, Fernandez-Capetillo O, Kruhlak MJ, Pilch DR, Staudt DW, Lee A, et al. Histone H2AX phosphorylation is dispensable for the initial recognition of DNA breaks. *Nature Cell Biology*. 2003;5(7):675-U51.
23. West AG, van Attikum H. Chromatin at the crossroads. Meeting on Signalling to Chromatin Epigenetics. *EMBO Reports*. 2006;7(12):1206-10.
24. Kobayashi J, Iwabuchi K, Miyagawa K, Sonoda E, Suzuki K, Takata M, et al. Current topics in DNA double-strand break repair. *Journal Radiation Research* 2008;49(2):93-103.
25. Petrini JHJ, Stracker TH. The cellular response to DNA double-strand breaks: defining the sensors and mediators. *Trends in Cell Biology*. 2003;13(9):458-62.
26. Caspari T, Carr AM. Checkpoints: How to flag up double-strand breaks. *Current Biology*. 2002;12(3):R105-R7.
27. Santivasi WL, Xia F. Ionizing radiation-induced DNA damage, response, and repair. *Antioxidants & Redox Signaling*. 2014;21(2):251-9.
28. Poehlmann A, Roessner A. Importance of DNA damage checkpoints in the pathogenesis of human cancers. *Pathology, Research and Practice*. 2010;206(9):591-601.
29. Shimada M, Nakanishi M. DNA damage checkpoints and cancer. *Journal of Molecular Histology*. 2006;37(5-7):253-60.

30. Bohgaki T, Bohgaki M, Hakem R. DNA double-strand break signaling and human disorders. *Genome Integrity*. 2010;1(1): 15.
31. Yaneva M, Kowalewski T, Lieber MR. Interaction of DNA-dependent protein kinase with DNA and with Ku: biochemical and atomic-force microscopy studies. *EMBO Journal*. 1997;16(16):5098-112.
32. Chowdhury D, Choi YE, Brault ME. Charity begins at home: non-coding RNA functions in DNA repair. *Nature Reviews. Molecular Cell Biology* 2013;14(3):181-9.
33. Karagiannis TC, El-Osta A. Double-strand breaks: signaling pathways and repair mechanisms. *Cellular and Molecular Life Sciences*. 2004;61(17):2137-47.
34. Lieber MR, Ma Y, Pannicke U, Schwarz K. Mechanism and regulation of human non-homologous DNA end-joining. *Nature Reviews. Molecular Cell Biology*. 2003;4(9):712-20.
35. Schieler A, Iliakis G. DNA double-strand-break complexity levels and their possible contributions to the probability for error-prone processing and repair pathway choice. *Nucleic Acids Research*. 2013;41(16):7589-605.
36. Kuhar R, Gwiadzda KS, Humbert O, Mandt T, Pangallo J, Brault M, et al. Novel fluorescent genome editing reporters for monitoring DNA repair pathway utilization at endonuclease-induced breaks. *Nucleic Acids Research*. 2014;42(1).
37. Rothkamm K, Barnard S, Moquet J, Ellender M, Rana Z, Burdak-Rothkamm S. DNA damage foci: Meaning and significance. *Environmental and Molecular Mutagenesis*. 2015;56(6):491-504.
38. Norbury CJ, Hickson ID. Cellular responses to DNA damage. *Annual Review of Pharmacology and Toxicology*. 2001;41:367-401.
39. Wirtz S, Nagel G, Eshkind L, Neurath MF, Samson LD, Kaina B. Both base excision repair and O6-methylguanine-DNA methyltransferase protect against methylation-induced colon carcinogenesis. *Carcinogenesis*. 2010;31(12):2111-17.
40. Roos WP, Kaina B. DNA damage-induced cell death: from specific DNA lesions to the DNA damage response and apoptosis. *Cancer Letters*. 2013;332(2):237-48.
41. Glucksmann A. Cell deaths in normal vertebrate ontogeny. *Biological reviews of the Cambridge Philosophical Society*. 1951;26(1):59-86.
42. Zing WX, Thompson CB. Necrotic death as a cell fate. *Genes & Development*. 2006;20(1):1-15.
43. Elmore S. Apoptosis: A Review of Programmed Cell Death. *Toxicologic pathology*. 2007;35(4):495-516.
44. Gross A, McDonnell JM, Korsmeyer SJ. BCL-2 family members and the mitochondria in apoptosis. *Genes & Development*. 1999;13(15):1899-911.
45. Panayi ND, Mendoza EE, Breshears ES, Burd R. *Aberrant Death Pathways in Melanoma, Recent Advances in the Biology, Therapy and Management of Melanoma*, 2013. ISBN: 978-953-51-0976-1, Available from: <http://www.intechopen.com/books/recent-advances-in-the-biology-therapy-and-management-of-melanoma/aberrant-death-pathways-in-melanoma>
46. Brentnall M, Rodriguez-Menocal L, De Guevara R, Cepero E, Boise L. Caspase-9, caspase-3 and caspase-7 have distinct roles during intrinsic apoptosis. *BMC Cell Biology*. 2013;14(1):1-9.
47. Porter AG, Janicke RU. Emerging roles of caspase-3 in apoptosis. *Cell Death Differ*. 1999;6(2):99-104.
48. Schneider R, Grosschedl R. Dynamics and interplay of nuclear architecture, genome organization, and gene expression. *Genes & Development*. 2007;21(23):3027-43.
49. Kornberg RD. Chromatin structure: a repeating unit of histones and DNA. *Science*. 1974;184(4139):868-71.
50. Marino-Ramirez L, Kann MG, Shoemaker BA, Landsman D. Histone structure and nucleosome stability. *Expert Review of Proteomics*. 2005;2(5):719-29.
51. Kinner A, Wu W, Staudt C, Iliakis G. Gamma-H2AX in recognition and signaling of DNA double-strand breaks in the context of chromatin. *Nucleic Acids Research*. 2008;36(17):5678-94.
52. Cooper G. *The Cell: A molecular approach*. 2nd Edition ed. Sunderland (MA): Sinauer Associates; 2000.
53. Pierce B. *Genetics: A conceptual approach*. 2nd Edition ed. Freeman W, editor. New York. 2004.
54. Falk M, Lukasova E, Kozubek S. Chromatin structure influences the sensitivity of DNA to gamma-radiation. *Biochimica Et Biophysica Acta-Molecular Cell Research*. 2008;1783(12):2398-414.
55. Amouroux R, Campalans A, Epe B, Radicella JP. Oxidative stress triggers the preferential assembly of base excision repair complexes on open chromatin regions. *Nucleic Acids Research*. 2010;38(9):2878-90.
56. Park S-J, Ahmad F, Philp A, Baar K, Williams T, Luo H, et al. Resveratrol Ameliorates Aging-Related Metabolic Phenotypes by Inhibiting cAMP Phosphodiesterases. *Cell*. 2012;148(3):421-33.
57. Keuser B, Khobta A, Galle K, Anderhub S, Schulz I, Pauly K, et al. Influences of histone deacetylase inhibitors and resveratrol on DNA repair and chromatin compaction. *Mutagenesis*. 2013;28(5):569-76.
58. Norppa H. Cytogenetic biomarkers. *IARC Scientific Publications*. 2004(157):179-205.
59. Bonassi S, Hagmar L, Stromberg U, Montagud AH, Tinnerberg H, Fornì A, et al. Chromosomal aberrations in lymphocytes predict human cancer independently of exposure to carcinogens. *European Study Group on Cytogenetic Biomarkers and Health. Cancer Research*. 2000;60(6):1619-25.

60. El-Zein R, Vral A, Etzel CJ. Cytokinesis-blocked micronucleus assay and cancer risk assessment. *Mutagenesis*. 2011;26(1):101-6.
61. Solomon E, Borrow J, Goddard AD. Chromosome-aberrations and cancer. *Science*. 1991;254(5035):1153-60.
62. Fenech M, Morley A. Solutions to the kinetic problem in the micronucleus assay. *Cytobios*. 1985;43(172-173):233-46.
63. Fenech M, Morley AA. Kinetochores detection in micronuclei – An alternative method for measuring chromosome loss LOSS. *Mutagenesis*. 1989;4(2):98-104.
64. Vral A, Fenech M, Thierens H. The micronucleus assay as a biological dosimeter of in vivo ionising radiation exposure. *Mutagenesis*. 2011;26(1):11-7.
65. Hsu TC, Johnston DA, Cherry LM, Ramkissoon D, Schantz SP, Jessup JM, et al. Sensitivity to genotoxic effects of bleomycin in humans – Possible relationship to environmental carcinogenesis. *International Journal of Cancer*. 1989;43(3):403-9.
66. Fenech M. Cytokinesis-block micronucleus cytome assay. *Nature Protocols*. 2007;2(5):1084-104.
67. Barnard S, Bouffler S, Rothkamm K. The shape of the radiation dose response for DNA double-strand break induction and repair. *Genome Integrity*. 2013;4:1-.
68. Rogakou EP, Boon C, Redon C, Bonner WM. Megabase chromatin domains involved in DNA double-strand breaks in vivo. *Journal of Cell Biology*. 1999;146(5):905-16.
69. Celeste A, Petersen S, Romanienko PJ, Fernandez-Capetillo O, Chen HT, Sedelnikova OA, et al. Genomic instability in mice lacking histone H2AX. *Science*. 2002;296(5569):922-7.
70. Rothkamm K, Horn S. gamma-H2AX as protein biomarker for radiation exposure. *Annali Dell Istituto Superiore Di Sanita*. 2009;45(3):265-71.
71. Paull TT, Rogakou EP, Yamazaki V, Kirchgessner CU, Gellert M, Bonner WM. A critical role for histone H2AX in recruitment of repair factors to nuclear foci after DNA damage. *Current Biology*. 10. 2000;10(15):886-95.
72. Fernandez-Capetillo O, Chen HT, Celeste A, Ward I, Romanienko PJ, Morales JC, et al. DNA damage-induced G2-M checkpoint activation by histone H2AX and 53BP1. *Nat Cell Biology*. 2002;4(12):993-7.
73. Riballo E, Kuhne M, Rief N, Doherty A, Smith GC, Recio MJ, et al. A pathway of double-strand break rejoining dependent upon ATM, Artemis, and proteins locating to gamma-H2AX foci. *Molecular Cell*. 2004;16(5):715-24.
74. Lowndes NF, Toh GW. DNA repair: the importance of phosphorylating histone H2AX. *Current Biology*. 2005;15(3):R99-R102.
75. van Attikum H, Gasser SM. The histone code at DNA breaks: a guide to repair? *Nature Reviews. Molecular Cell Biology*. 2005;6(10):757-65.
76. Svetlova MP, Solovjeva LV, Tomilin NV. Mechanism of elimination of phosphorylated histone H2AX from chromatin after repair of DNA double-strand breaks. *Mutation Research*. 2009;685(1-2):54-60.
77. Valdiguiesias V, Giunta S, Fenech M, Neri M, Bonassi S. gammaH2AX as a marker of DNA double strand breaks and genomic instability in human population studies. *Mutation Research/Reviews in Mutation Research*. 2013;753(1):24-40.
78. Redon CE, Weyemi U, Parekh PR, Huang D, Burrell AS, Bonner WM. gamma-H2AX and other histone post-translational modifications in the clinic. *Biochimica Et Biophysica Acta-Gene Regulatory Mechanisms*. 2012;1819(7):743-56.
79. Goodarzi AA, Jeggo PA. Irradiation induced foci (IRIF) as a biomarker for radiosensitivity. *Mutation Research*. 2012;736(1-2):39-47.
80. Neumaier T, Swenson J, Pham C, Polyzos A, Lo AT, Yang PA, et al. Evidence for formation of DNA repair centers and dose-response nonlinearity in human cells. *Proceedings of the National Academy of Sciences of the United States of America*. 2012;109(2):443-8.
81. Ciccia A, Elledge SJ. The DNA damage response: making it safe to play with knives. *Molecular Cell*. 2010;40(2):179-204.
82. Rogakou EP, Nieves-Neira W, Boon C, Pommier Y, Bonner WM. Initiation of DNA fragmentation during apoptosis induces phosphorylation of H2AX histone at serine 139. *Journal of Biological Chemistry*. 2000;275(13):9390-5.
83. Horn S, Barnard S, Brady D, Prise KM, Rothkamm K. Combined analysis of gamma-H2AX/53BP1 foci and caspase activation in lymphocyte subsets detects recent and more remote radiation exposures. *Radiation Research*. 2013;180(6):603-9.
84. de Feraudy S, Revet I, Bezrookove V, Feeney L, Cleaver JE. A minority of foci or pan-nuclear apoptotic staining of gammaH2AX in the S phase after UV damage contain DNA double-strand breaks. *Proceedings of the National Academy of Sciences*. 2010;107(15):6870-5.
85. Panier S, Boulton SJ. Double-strand break repair: 53BP1 comes into focus. *Nature Reviews. Molecular Cell Biology*. 2014;15(1):7-18.
86. Markova E, Schultz N, Belyaev IY. Kinetics and dose-response of residual 53BP1/gamma-H2AX foci: Co-localization, relationship with DSB repair and clonogenic survival. *International Journal of Radiation Biology*. 2007;83(5):319-29.

87. Schultz LB, Chehab NH, Malikzay A, Halazonetis TD. p53 binding protein 1 (53BP1) is an early participant in the cellular response to DNA double-strand breaks. *Journal of Cell Biology*. 2000;151(7):1381-90.
88. Solier S, Sordet O, Kohn KW, Pommier Y. Death receptor-induced activation of the Chk2- and histone H2AX-associated DNA damage response pathways. *Molecular and Cellular Biology*. 2009;29(1):68-82.
89. Solier S, Pommier Y. MDC1 cleavage by caspase-3: a novel mechanism for inactivating the DNA damage response during apoptosis. *Cancer Research*. 2011;71(3):906-13.
90. Sly PD, Eskenazi B, Pronczuk J, Sram R, Diaz-Barriga F, Machin DG, et al. Ethical issues in measuring biomarkers in children's environmental health. *Environmental Health Perspectives*. 2009;117(8):1185-90.
91. McCormick RA. Experimentation in children: sharing in sociality. *Hastings Center Report*. 1976;6(6):41-6.
92. De Lourdes Levy M, Larcher V, Kurz R. Informed consent/assent in children. Statement of the Ethics Working Group of the Confederation of European Specialists in Paediatrics (CESP). *European Journal of Pediatrics*. 2003;162(9):629-33.
93. Gonzalez JE, Roch-Lefevre SH, Mandina T, Garcia O, Roy L. Induction of gamma-H2AX foci in human exfoliated buccal cells after in vitro exposure to ionising radiation. *International Journal of Radiation Biology*. 2010;86(9):752-9.
94. Yoon AJ, Shen J, Wu H, Angelopoulos C, Singer SR, Chen R et al. Expression of activated checkpoint kinase 2 and histone 2AX in exfoliative oral cells after exposure to ionizing radiation. *Radiation Research* 2009;171(6):771-5.
95. Dhillon VS, Thomas P, Fenech M. Comparison of DNA damage and repair following radiation challenge in buccal cells and lymphocytes using single-cell gel electrophoresis. *International Journal of Radiation Biology* 2004;80(7):517-28

4

Aim of the research

During the past decades, computed tomography has revolutionized the world of medical imaging. The CT usage in the US and the UK increased a 20-fold and a 12-fold respectively, over the past two decades (1). The increase in CT usage in Belgium is comparable, approximately 2 million CT examinations are performed annually (2). However, the high x-ray doses associated with CT usage have raised health concerns (3). This is of particular importance for the paediatric patient population, recognized as one of the most important target groups in medical radiation protection. Children have a higher sensitivity compared to adults regarding radiation-induced malignancies and the associated risk for exposure induced death (4). Moreover, children have a longer life expectancy in which they can develop radiation-related cancer and they can receive higher radiation doses than necessary if CT settings are not adjusted according to their smaller body size.

The results of several ongoing epidemiologic studies on paediatric CT imaging have recently been published. Pearce *et al.* estimated the leukaemia and brain tumour risk associated with childhood CT imaging (5). The bottom line in this study was that there were significant linear associations between the radiation dose to the brain and the brain tumour excess

relative risk, and between the bone marrow dose and the leukaemia excess relative risk. Although the individual risks were small, in view of the high number of CT scans the radiation risk associated with paediatric CT imaging is a public health issue. Unfortunately, the limitations of epidemiology inherent to low dose exposure, make it extremely difficult to directly quantify health risks from low-dose CT exposure (6). For the extrapolation of radiation risks to very low doses ($\leq 1\text{mGy}$) and to substantiate the epidemiological evidence for radiation effects at low doses of the order of 20 mGy, we are forced to rely on radiobiological evidence and biophysical arguments. An alternative approach to estimate the dose response relationship after low dose CT exposure, can be based on cellular and molecular biomarker studies of the biological mechanisms underlying the health effects of radiation exposure. Therefore, a first aim of this PhD project was to assess the *in vivo* biological effects and estimate cancer risks associated with paediatric CT imaging. Biomarker studies in children raise a number of ethical constraints, therefore, technical issues can be equally challenging as well. Therefore, a prior *in vitro* study was set-up in order to overcome the practical constraints and to adapt and optimise the existing protocols for paediatric CT settings.

As indicated by several epidemiological studies on high dose and high dose rate exposure (e.g. LSS cohort), there is a clear age-at-exposure effect which makes children considerably more sensitive compared to adults regarding radiation-induced malignancies. The UNSCEAR committee dedicated a special volume on the paediatric target group in their 2013 report, showing that for at least 25% of tumour types, children are clearly more sensitive (4). A second aim of this PhD project was to get more insight in the intrinsic higher radiosensitivity of children compared to adults. The most prominent malignancy is leukaemia with a latency period of only 2 to 3 years. Together with the positive association reported by Pearce *et al.* (5) between radiation dose from CT scans and leukaemia in children, it is of particular importance to study the radiation sensitivity of HSPCs. As HSPCs cells self-renew throughout life, accumulation of DNA damage can compromise their genomic integrity, which makes these cells a major target for radiation-induced carcinogenesis.

4.1**References**

1. Hall EJ, Brenner DJ. *Cancer risks from diagnostic radiology: the impact of new epidemiological data. British Journal of Radiology.* 2012;85(1020):E1316-E7.
2. *Personal communication with Federal Agency of Nuclear Control (FANC) Belgium - Thanks to Petra Willems.* 2015.
3. Brenner DJ, Hall EJ. *Current concepts - Computed tomography - An increasing source of radiation exposure. New England Journal of Medicine.* 2007;357(22):2277-84.
4. UNSCEAR. *Sources, Effects and Risks of ionizing radiation.* New York: United Nations Scientific Committee on the Effects of Atomic Radiation, 2013.
5. Pearce MS, Salotti JA, Little MP, McHugh K, Lee C, Kim KP, et al. *Radiation exposure from CT scans in childhood and subsequent risk of leukaemia and brain tumours: a retrospective cohort study. Lancet.* 2012;380(9840):499-505.
6. Brenner DJ, Doll R, Goodhead DT, Hall EJ, Land CE, Little JB, et al. *Cancer risks attributable to low doses of ionizing radiation: Assessing what we really know. Proceedings of the National Academy of Sciences of the United States of America.* 2003;100(24):13761-6.

5

Outline of the research

The use of sensitive biomarkers for the assessment of direct x-ray effects in patients gives valuable information on dose-effect relationships for diagnostic x-rays. Earlier work has demonstrated that the γ -H2AX foci assay is a sensitive technique to determine the effects of CT exposure at molecular level, namely the induction of DNA DSBs (1-3). DSBs are considered to be the most deleterious cellular effects of radiation exposure, because they can result in loss or rearrangement of genetic information, leading to cell death or carcinogenesis.

Before the start of a biomarker study on a paediatric patient population, *in vitro* feasibility studies were required to optimise the γ -H2AX foci assay as a biomarker of DNA damage to investigate the effects of CT x-rays in children in a multicentre setting. The application of biomarkers to this end implies a critical evaluation of a number of technical issues: the logistics of biological sample collection in a paediatric radiology setting, processing and storing of blood samples, the validity and reliability of the biomarker γ -H2AX for DNA DSBs in the low-dose range, as well as the impact of potential confounding factors, such as contrast agent administration. The results of this feasibility study are presented in the first paper: EPI-CT: IN VITRO ASSESSMENT OF THE APPLICABILITY OF THE γ -H2AX FOCI ASSAY AS CELLULAR MARKER

FOR EXPOSURE IN A MULTICENTRE STUDY OF CHILDREN IN DIAGNOSTIC RADIOLOGY. This paper is part of Workpackage 5 'Biological Mechanisms' of the EU funded FP7 EPI-CT (Epidemiological study to quantify risks for paediatric computerised tomography and to optimise doses) project.

In order to determine the number of x-ray induced DNA DSBs in children's lymphocytes undergoing a CT examination, a prospective multicentre study was set up in Belgium. Herein, the γ -H2AX foci assay was used as an *in vivo* effect biomarker for radiation-induced DSBs. Individual blood dose estimates were obtained for every patient by creating patient-specific 3D voxel models based on the CT images of the paediatric patients by using ImpactMC simulation software 1.3.1. Organ volumes were segmented in the original CT images and organ dose deposition was calculated based on the Monte Carlo dose distribution. BEIR VII age and gender specific risk models (4) were used to assess the lifetime attributable risk (LAR) of cancer incidence and mortality associated with the CT examination of every individual patient. The results of this study are presented in a second paper: γ -H2AX FOCI AS IN VIVO EFFECT BIOMARKER IN CHILDREN EMPHASIZE THE IMPORTANCE TO MINIMIZE X-DOSES IN PAEDIATRIC CT IMAGING.

In a last part of this PhD project, we investigated further the higher radiosensitivity of children compared to adults, by comparing the DNA repair and chromosomal radiosensitivity at a cellular level in T-lymphocytes from newborns and adults. Furthermore, the high radiosensitivity of children with respect to radiation-induced leukaemia, warrants studies on the response of HSPCs to DNA damage induced by IR as well as on the mutagenic consequences of DNA misrepair. In order to evaluate the chromosomal radiosensitivity of HSPCs, we developed a micro-culture CBMN assay for purified CD34⁺ cells. The results of these *in vitro* studies are presented in the third paper: RADIATION SENSITIVITY OF HUMAN CD34⁺ CELLS VERSUS PERIPHERAL BLOOD T-LYMPHOCYTES.

5.1**References**

1. Rothkamm K, Balroop S, Shekhdar J, Fernie P, Goh V. Leukocyte DNA damage after multi-detector row CT: A quantitative biomarker of low-level radiation exposure. *Radiology*. 2007;242(1):244-51.
2. Lobrich M, Rief N, Kuhne M, Heckmann M, Fleckenstein J, Rube C, et al. In vivo formation and repair of DNA double-strand breaks after computed tomography examinations. *Proceedings of the National Academy of Sciences of the United States of America*. 2005;102(25):8984-9.
3. Beels L, Bacher K, De Wolf D, Werbrouck J, Thierens H. gamma-H2AX Foci as a Biomarker for Patient X-Ray Exposure in Pediatric Cardiac Catheterization Are We Underestimating Radiation Risks? *Circulation*. 2009;120(19):1903-9.
4. *Health Risks from Exposure to Low Levels of Ionizing Radiation: BEIR VII Phase 2: The National Academies Press; 2006.*

PAR

RTI

Original Research

6

PAPER I

EPI-CT: *in vitro* assessment of the applicability of the γ -H2AX-foci assay as cellular biomarker for exposure in a multicentre study of children in diagnostic radiology

Charlot Vandevoorde¹, Maria Gomolka², Ute Roessler², Daniel Samaga², Carita Lindholm³, Marie Fernet⁴, Janet Hall⁵, Eileen Pernot^{6,7,8}, Houssein El-Saghire⁹, Sarah Baatout⁹, Ausrele Kesminiene¹⁰, Hubert Thierens¹

¹ Ghent University, UGent, Belgium

² Federal Office for Radiation Protection, BfS, Germany

³ Radiation and Nuclear Safety Authority, STUK, Finland

⁴ Institut Curie, Inserm U612, France

⁵ Centre de Recherche en Cancérologie de Lyon - UMR Inserm 1052 - CNRS 5286, France

⁶ Centre for Research in Environmental Epidemiology, CREAL, Spain

⁷ Universitat Pompeu Fabra (UPF), Barcelona, Spain

⁸ CIBER Epidemiología y salud Pública (CIBERESP), Barcelona, Spain

⁹ Radiobiology Unit, Belgian Nuclear Research Centre, SCK-CEN, Belgium

¹⁰ Centre International de Recherche sur le Cancer, France

Published in International Journal of Radiation Biology 2015;91(8): 653-63

EPI-CT: *in vitro* assessment of the applicability of the γ -H2AX-foci assay as cellular biomarker for exposure in a multicentre study of children in diagnostic radiology

ABSTRACT

Purpose: A feasibility study on the application of the γ -H2AX foci assay as an exposure biomarker in a prospective multicentre paediatric radiology setting.

Materials and methods: A set of *in vitro* experiments was performed to evaluate technical hurdles related to biological sample collection in a paediatric radiology setting (small blood sample volume), processing and storing of blood samples (effect of storing blood at 4°C), the reliability of foci scoring for low-doses (merge γ -H2AX/53BP1 scoring), as well as the impact of contrast agent administration as potential confounding factor. Given the exploratory nature of this study and the ethical constraints related to paediatric blood sampling, blood samples from adult volunteers were used for these experiments. In order to test the feasibility of pooling the γ -H2AX data when different centres are involved in an international multicentre study, two intercomparison studies in the low-dose range (10-500 mGy) were performed.

Results: Determination of the number of x-ray induced γ -H2AX foci is feasible with one 2 ml blood sample pre- and post- computed tomography (CT) scan. Lymphocyte isolation and fixation on slides is necessary within 5h of blood sampling to guarantee reliable results. The possible enhancement effect of contrast medium on the induction of DNA DSB in a patient study can be ruled out if radiation doses and the contrast agent concentration are within diagnostic ranges. The intercomparison studies using *in vitro* irradiated blood samples showed that the participating laboratories, executing successfully the γ -H2AX foci assay in lymphocytes, were able to rank blind samples in order of lowest to highest radiation dose based on mean foci/cell counts. The dose response of all intercomparison data shows that a dose point of 10 mGy could be distinguished from the sham irradiated control ($p = 0.006$).

Conclusions: The results demonstrate that it is feasible to apply the γ -H2AX foci assay as a cellular biomarker of exposure in a multicentre prospective study in paediatric CT imaging after validating it in an *in vivo* international pilot study on paediatric patients.

INTRODUCTION

Epidemiological data of the atomic bomb survivors (Life Span Study) and medically exposed populations summarized in the UNSCEAR report clearly indicate that high doses of ionizing radiation (IR) enhance cancer risks in humans (Preston et al., 2007, Thompson et al., 1994, Ron et al., 1998, Richardson and Hamra, 2010, UNSCEAR 2008). These studies have laid the foundation of the linear non-threshold (LNT) model, used in radiological protection for risk estimations at low-dose exposure, implying a linear relationship between dose and biological effect without a dose threshold. Although the LSS has provided valuable insights into the quantitative effects of exposure to IR at higher dose ranges, considerable uncertainties remain about the health effects of exposure at low-dose and/or low-dose rates. As described by Brenner *et al.* (Brenner et al., 2003), extraordinarily large population cohorts would be required to determine low-dose cancer risks in epidemiological studies. In order to obtain adequate statistical precision and power, the required sample size increases approximately as the inverse square of the dose. Other factors influencing power in epidemiological radiation effect studies include variability of the data - that can create background noise - and the frequency of the health outcomes (cancer and non-cancer diseases) to be observed (Motulsky, 2010).

The health risks of low-dose IR exposure are relevant for a broad range of medical, environmental and occupational exposed populations and are therefore of societal importance. For an average person worldwide, diagnostic x-ray applications represent the largest portion of radiation exposure coming from man-made irradiation sources and remain a topic of concern in the medical world and public press (Brenner and Hall, 2007, Lin, 2010, UNSCEAR, 2013). The growing use of CT scans for paediatric patients over the past two decades is an important issue (Brenner, 2003), since the lifetime cancer risk estimates might be a factor of 2 to 3 times higher for children compared to a population of all ages. This estimation is based on a lifetime risk projection model combining the risks of all tumour types together (UNSCEAR, 2013). The increased

sensitivity for children is due to a number of factors including the higher number of rapidly dividing cells, smaller body dimensions leading to less tissue shielding towards external exposure and their longer life expectancy to develop radiation-induced cancer. Concomitantly, the increased sensitivity of children and adolescents to IR might potentiate and reveal more clearly the effects of IR at low doses than in adults. Recently a number of studies were published dealing with the long-term risk of radiation-induced cancer following CT scans in childhood (Mathews et al., 2013, Pearce et al., 2012, Huang et al., 2014). Despite some study limitations, the results reported by the UK cohort study and the Australian linkage study were consistent with the LSS results. However, it remains very difficult to assess the potential of small radiation-induced changes in cancer risk in the low-dose range.

For the extrapolation of radiation risks to very low doses ($\leq 1\text{mGy}$) and to substantiate the epidemiological evidence for radiation effects at low doses of the order of 10 mGy, we are forced to rely on radiobiological evidence and biophysical arguments (Brenner, 2009, Pernot et al., 2012). IR can induce a variety of DNA damage either directly or indirectly through ionization events produced by radiation-induced reactive oxygen species (ROS). Double strand breaks (DSB) are considered as the most deleterious DNA lesions induced by IR exposure. Prior studies in the low-dose range have demonstrated effects of CT exposure at molecular level, including the induction of DNA DSB (Rothkamm et al., 2007, Beels et al., 2012, Geisel et al., 2012, Löbrich et al., 2005). The phosphorylation of the histone variant H2AX at the site of a DNA DSB leads to the formation and accumulation of γ -H2AX foci in the cell nucleus within three minutes after DNA damage (Rogakou et al., 1998, Su, 2006). γ -H2AX foci induced in peripheral T-lymphocytes by interventional x-ray exposure were used as a biomarker of DNA damage in a group of paediatric patients who underwent cardiac catheterization (Beels et al., 2009). Low-dose hypersensitivity was observed for this paediatric patient group, which challenges the LNT hypothesis and stresses the importance of non-targeted effects as the bystander effect at low doses (Beels et al., 2009).

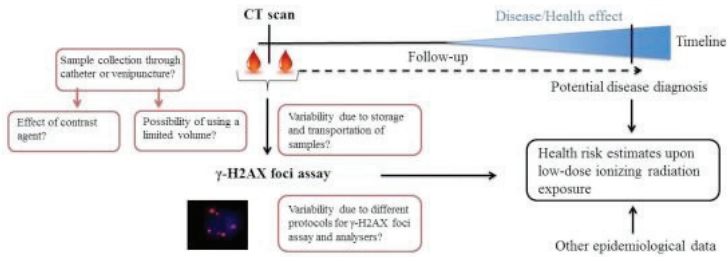


FIGURE 1

Logistical and technical questions related to the use of γ -H2AX foci in blood samples as biomarkers of exposure in a multicentre molecular epidemiology study assessing the health effects of CT scans.

In the framework of the EU funded FP7 project EPI-CT (Epidemiological study to quantify risks for paediatric computerised tomography and to optimise doses), a multi-national large scale epidemiological cohort study was set up with the aim to investigate possibly late health effects associated to CT scan exposure in childhood and adolescence in a population of 1 million paediatric CT patients (<http://epi-ct.iarc.fr/>). Using Picture Archiving and Communication Systems (PACS) national cohorts were assembled retrospectively and prospectively, until 2013, in nine European countries. The indications for CT scan are being reviewed to identify scans related to the diagnosis of cancer, in order to rule out potential reverse causation. Patients will be followed over time to ascertain information on leukaemia and cancer incidence. In addition to the extensive epidemiological and dosimetric efforts undertaken in this project, one of the goals of the project is to perform pilot tests for different biomarkers of exposure and to assess their sensitivity in the low-dose range in order to clarify the biological mechanisms behind low-dose hypersensitivity reported in some paediatric patients. It is anticipated that significant insights will emerge from the integration of epidemiological and biological research, made possible by molecular epidemiology studies incorporating biomarkers and bioassays (Pernot et al., 2012). Biomarkers of exposure, effects and susceptibility could be integrated into

epidemiological studies in order to improve dosimetry, health outcome diagnosis and homogeneity of the population, respectively, leading to an increased study power and accuracy of the risk estimates. In this paper, we present the results of *in vitro* feasibility studies to use the γ -H2AX foci assay as a biomarker of DNA damage to investigate the effects of CT x-rays in children in a multicentre setting. The application of biomarkers to this end implies a critical evaluation of a number of technical issues: the logistics of biological sample collection in a paediatric radiology setting, processing and storing of blood samples, the validity and reliability of the biomarker γ -H2AX in the low-dose range, as well as the impact of potential confounding factors, such as contrast agent administration, mentioned in Figure 1. Furthermore, in order to test the feasibility of pooling the γ -H2AX data when different centres are involved in an international multicentre study, we performed two independent intercomparison studies in the low-dose range among the participants of the EPI-CT project. In this paper we report on the results of the experiments performed to solve the technical issues of using the γ -H2AX foci assay as a molecular epidemiology biomarker in a paediatric radiology setting and the results of the low-dose intercomparison studies.

	Blood Separation Technique	Fixative	First Ab	Second Ab	Nuclear Counterstain	Scoring System
Lab 1	EasyColl (Density: 1.077 g/ml) (#L6135) Biochrom, Berlin, Germany	2% Paraformaldehyde (#P6148) Sigma Aldrich, Taufkirchen Germany	γ -H2AX (Ser139) Rabbit mAb (#9718# 1:200) Cell Signalling, Frankfurt, Germany	Goat-Anti-Rabbit Alexa Fluor 555 (#4413) (1:1000) Cell Signalling, Frankfurt, Germany	Hoechst 33342 (#B2261-52mG) Sigma Aldrich, Taufkirchen, Germany	Zeiss Axio Imager.Z2, 40x; Metafer vers. 3.10.1 Metasystems, Altulussheim, Germany
Lab 2	Histopaque (Density: 1.077 g/ml) (#H8889) Sigma Aldrich, St Louis, MO, USA	2% Formaldehyde (#F8775) Sigma Aldrich, St Louis, MO, USA	Anti- γ -H2AX (Ser139) (#05-636) Mouse mAb Millipore, Temecula, CA, USA	Goat-Anti-Mouse AlexaFluor488 (#A-11029) (1:500) Molecular Probes, Eugene, USA	Vectashield Propidium Iodide (#H-1300) Vector Laboratories, Burlingame, CA, USA	Zeiss Axio Imager.Z1, 63x/1.30 oil objective Metafer 4 vers. 3.8.6 Metasystems, Altulussheim, Germany
Lab 3	RosetteSep Human T-cell Enrichment Cocktail (#15061) and RosetteSep DM-L Density Medium (Density: 1.081 g/ml) (#15705) Stemcell Technologies, Grenoble, France	3% Paraformaldehyde (#P6148) Sigma Aldrich, Bornem, Belgium	Purified anti-H2AX phosphorylated (Ser139) Mouse mAb (#613402) (1:500) Biologend, Erembodegem, Belgium	Rabbit-Anti-Mouse TRITC (#R0270) (1:1000) Dakocytomation, Glostrup, Denmark	Fluoromount (#F4680) + DAPI (#D9542) Sigma Aldrich, Bornem, Belgium	Olympus BX60 fluorescence microscope 100x/1.30 oil lens
Lab 4	RosetteSep Human T-cell Enrichment Cocktail (#15061) and RosetteSep DM-L Density Medium (Density: 1.081 g/ml) (#15705) Stemcell Technologies, Grenoble, France	2% Paraformaldehyde (#P6148) Sigma Aldrich, Lyon, France	Anti-phospho-histone H2AX (Ser139) Mouse mAb (#05-636-1) (1:500) Millipore, Molesheim, France	Goat-Anti-Mouse AlexaFluor488 (#A-11029) (1:500) Molecular Probes, Eugene, USA	Vectashield + DAPI (#H-1200) Vector Laboratories, Les Ulis, France	Leica SP5 AOBs, tandem scanner

TABLE 1

Overview of the different γ -H2AX protocols used by the various partners of the project.

MATERIALS AND METHODS

Blood samples

Although the main goal of this study was to validate the use of the γ -H2AX foci assay for large paediatric studies, we used samples from adult donors in the first instance to assess inter-laboratory and methodological issues. This choice is justified by ethical considerations (Edwards and McNamee, 2005) given the exploratory nature of this study regarding blood volume, sample collection, storage and analytical conditions, that do not necessarily require samples from children. Informed consent was obtained from all healthy adult volunteers, in accordance with local ethical guidelines.

γ -H2AX foci analysis

All participating research centres followed their own protocol of lymphocyte isolation, fixation, γ -H2AX foci staining and scoring techniques. Details of the different protocols used by the various partners can be found in Table I. Most of the partners had experience with γ -H2AX foci analysis in purified blood lymphocytes, except for Lab 4, who used γ -H2AX foci analysis up to now only for cell lines.

Adaptation of the γ -H2AX foci protocol for multicentre paediatric studies in diagnostic radiology

Reduction of blood sample volume

In a previous study from Beels *et al.* (Beels *et al.*, 2012), two consecutive blood samples were collected after CT examination through the catheter used for contrast agent administration to avoid an additional venepuncture. After the CT scan, the first blood sample was not used because of possible dilution of the blood with contrast agent and to avoid stagnation. Because of the small blood volume of very young children, the local Ethical Committee restricts blood sampling for biomarker studies of effects of CT x-rays in children to a single small blood sample of 2 ml

before and after the CT examination. Blood circulation is faster in children compared to adults, which ensures a lower risk of getting stagnated blood. We collected one blood sample before CT and two consecutive (interval of 5 min) blood samples of 2 ml - a small sample volume aimed at mimicking the limited volume that would be available from children - from two adult patients 5 min after their CT examination through the catheter used for contrast agent administration (after flushing). The blood samples were kept for 30 min at 37°C in a water bath, followed by 15 min in ice water (0°C). Afterwards, the γ -H2AX foci protocol as described for Lab 3 in Table I was applied.

Effect of storing blood samples at 4°C

First, we investigated the effect of storing whole blood samples at 4°C for several hours before blood separation, on the foci yield in a set of *in vitro* experiments using blood samples from four healthy donors. For every time point, one blood sample was sham-irradiated. Blood samples were irradiated with 100 mGy Co-60 γ -rays at a dose rate of 170 mGy/min, incubated at 37°C for 30 min and arrested on iced water (0°C) for 15 min. Afterwards, the blood samples were kept at 4°C for 0, 5 and 24h before the start of the T-lymphocyte isolation according to the γ -H2AX foci protocol of Lab 3 (Table I). Afterwards, a second set of *in vitro* experiments was set up in order to mimic the shipping conditions in case blood samples need to be transported to another laboratory in the framework of a multicentre study. For these experiments, blood samples of three adult healthy volunteers were irradiated under the same conditions as in the first set of experiments, incubated at 37°C for 30 min and arrested on ice water (0°C) for 15 min. Part of the whole blood was kept at 4°C for 24h before lymphocyte isolation was started, while the other part underwent T-lymphocyte isolation directly after the ice water arrest. Half of the isolated T-lymphocytes were stored in cRPMI with 10% foetal calf serum (FCS) at 4°C for 24h. Afterwards the γ -H2AX foci protocol of Lab 3 was applied (see Table I).

Validation of the γ -H2AX foci immunostaining and scoring

Discrimination between artefacts and DNA damage induced γ -H2AX foci remains a critical point especially in the low-dose range. To validate the γ -H2AX foci data obtained by manual scoring with an Olympus BX60 fluorescence microscope, a double staining of the microscopic slides was performed. In the standard protocol of Lab 3, the γ -H2AX protein is stained with a secondary antibody conjugated with the red fluorophore Tetramethyl Rhodamine Isothiocyanate (TRITC) (Sigma-Aldrich, Diegem, Belgium). For the double immunostaining a second protein, the p53 binding protein 1 (53BP1) (Abcam, Cambridge, UK), is stained with the green fluorescent marker Fluorescein Isothiocyanate (FITC) (Sigma-Aldrich, Diegem, Belgium). The 53BP1 protein acts, together with MDC1, as mediator/adaptor protein that promotes DNA repair and regulates cell cycle checkpoints (Markova et al., 2007, Solier and Pommier, 2014) and the co-localisation of 53BP1 and γ -H2AX foci will allow to distinguish artefacts from real DNA DSB. For this validation experiment, we irradiated blood samples of four donors with 25 mGy and 500 mGy Co-60 γ -rays at a dose rate of 170 mGy/min, incubated at 37°C for 30 min and arrested on 0°C (ice water) for 15 min. For each irradiated sample, a sham-irradiated control sample was taken into account.

Effect of contrast agent

A venepuncture for blood sampling is a very distressing experience for children. As described earlier (Beels et al., 2012), pre- and post-CT blood samples are needed in order to determine the induced number of DNA DSB by CT x-rays. In order to limit the number of venepunctures, blood samples can be collected through the catheter for contrast agent administration. An *in vitro* experiment was set up to investigate the possible interference of iodinated contrast agent and the corresponding emission of secondary radiation in CT imaging on the induction of DNA DSB. Blood samples from three healthy volunteers were mixed with 4 different concentrations of a frequently used contrast agent (Ultravist 300,

Bayer Schering Pharma, Mijdrecht, The Netherlands), resulting in concentrations of 0, 5, 10, 20 mg iodine per ml blood. Samples were subsequently irradiated *in vitro* with 100 kV x-rays (dose rate of 20 mGy/min) at different dose levels (5, 10, 50 mGy). A radiation quality of 100 kVp with 2 mm Al filtration was used generated by a Philips MG420 x-ray generator coupled to a MCN420 tube (Philips Medical Systems, Anderlecht, Belgium). One blood sample was sham-irradiated for every condition. The iodine concentrations used in the experiment were calculated based on the volumes used in clinical practice. After irradiation, blood samples were kept at 37°C in a water bath for 30 min to allow DNA damage signalling. Afterwards, DNA repair was arrested by cooling the samples at 0°C (iced water) for 15 min.

In vitro intercomparison of different γ -H2AX foci protocols for a molecular epidemiological study in diagnostic radiology

A first intercomparison was organised in order to investigate whether the existing γ -H2AX protocols (blood separation technique, fixation, immunostaining and scoring) of different EPICT partners would produce similar foci frequencies. In a second intercomparison study, the aim was to test the feasibility of sending isolated lymphocytes in an overnight shipment and to evaluate the ability of the different participants to quantify DNA damage induced by low-dose x-ray exposure.

First intercomparison study

We performed the first intercomparison at Ghent University and four different partner research centres participated: Bundesamt fuer Strahlenschutz, Germany (BfS), Institut Curie, France (IC), Radiation and Nuclear Safety Authority, Finland (STUK) and Ghent University, Belgium (UGent). Blood samples from the same adult healthy donor were irradiated with 100 mGy and 500 mGy Co-60 γ -rays with a dose rate of 170 mGy/min at Ghent University. After irradiation, blood samples were incubated at 37°C for 30 min and arrested on ice water (0°C). Each

participant followed in Ghent its own protocol of lymphocyte isolation and γ -H2AX foci protocols as presented in Table I. All participants evaluated their samples on their own scoring platforms at home, using an automated microscope system and/or manual scoring.

Second intercomparison study

For the second intercomparison study, irradiation experiments were performed at STUK (Finland). Blood from an adult healthy donor was collected and lymphocytes were isolated with Histopaque density gradient separation (Sigma-Aldrich Co., St Louis, MO, USA). Four biological replicates from the same donor were set up per dose point and cells remained in pure FCS (Sigma-Aldrich, St Louis, MO, USA) throughout the irradiation and shipment (each laboratory obtained approximately 5×10^5 cells per replicate). Irradiation was performed with 135 kV x-rays (generator: Isovolt 320HS, Seifert; X-ray tube: MB 350/1, Thales; filters: 2.203 mmAl and 0.232 mmCu) at 37 °C with 10, 30, 50, 100 mGy (dose rate: 35.3 mGy/min). One sample served as control and was sham irradiated. After irradiation, cells were kept at 37°C for 30 min, put on iced water (0°C) for 15 min and kept cooled until and during shipment. For shipment, samples were packed together with Styrofoam boxes containing frozen cool packs in order to keep the temperature below 6°C in order to diminish foci loss during transportation. Care was taken to avoid freezing of samples. Each pack of blood samples also contained a temperature logger to control the temperature during transport. Samples were coded before sending and decoding was performed after evaluation. Upon arrival of samples, each laboratory performed the γ -H2AX assay according to its own protocol. In case of manual scoring it was intended to evaluate 100 cells/dose/replicate, in total 400 cells/dose for all 4 replicates. For the automated scoring, 500 cells/dose/replicate, in total 2000 cells/dose for all 4 replicates had to be evaluated. In this set-up a biological replicate meant four independent irradiated lymphocyte samples from the same donor per dose point. Lab 1 applied two classifiers with

different sensitivity settings for the automated scoring with the Metafer scoring system.

Statistical analyses

Differences between two datasets were tested for significance with a Mann-Whitney U test for unpaired datasets, while a Wilcoxon signed-rank test was used for paired datasets. For experimental data including more than two variables, a Kruskal-Wallis test was used. The slopes of linear regression fit of different scoring methods was compared by using the F-statistics. Statistically significance was considered for $p < 0.05$. Coefficients of variation were calculated from the dispersion of the frequency distribution of the γ -H2AX foci scoring and the arithmetic mean of the distribution. All statistical calculations were performed with the SPSS program, version 22 (SPSS Inc., USA), GPower version 3.1.5 (Universität Düsseldorf, Germany) for power calculations, R Studio 3.1.2 and Microsoft Excel 2010 (Microsoft Corporation, USA).

RESULTS

Adaptation of the γ -H2AX foci protocol for multicentre paediatric studies in diagnostic radiology

Reduction of blood sample volume

To investigate the feasibility of using one small blood sample for the γ -H2AX foci assay instead of a consecutive sampling as reported by Beels *et al.* (Beels *et al.*, 2012), one blood sample of 2 ml before CT and two blood samples of 2 ml were taken from two adult patients after a CT examination (DLP (Dose Length Product) patient 1: 1090 mGy \cdot cm; DLP patient 2: 374 mGy \cdot cm). RosetteSep T-lymphocyte separation resulted in a yield of approximately 10^6 cells/ml of blood. For every replicate, foci were manually scored in at least 240 cells over two microscopic slides. To rule out the possible dilution with contrast agent or the effects of stagnation the number of foci of the first and second 2 ml blood sample after CT were compared: patient 1: 1.46 foci/cell (95% CI: 1.29-1.63) and 1.34 foci/cell (95% CI: 1.14-1.54) post-CT versus 0.90 foci/cell (95% CI: 0.78-1.02) pre-CT, patient 2: 0.88 foci/cell (95% CI: 0.71-1.05) and 0.83 foci/cell (95% CI: 0.72-0.94) post-CT versus 0.57 foci/cell (95% CI: 0.48-0.66) pre-CT. Based on the overlapping 95% confidence intervals in the two consecutive post-CT blood samples, it can be concluded that determination of the number of x-ray induced γ -H2AX foci in patients is feasible with one 2 ml blood sample before and 5 min after CT scan.

Effect of storing blood samples at 4°C

In most *in vivo* γ -H2AX foci studies, blood separation was performed almost directly after blood sampling and incubation. However, in the framework of large multicentre studies, direct access to an on-site laboratory for blood separation is not always feasible immediately after CT exposure. Therefore, the effect of storing the samples at 4°C (in the refrigerator) over a certain period was investigated. For the different time points at least 400 cells were scored over 2 slides for each donor. Results are presented in Figure 2-a. Compared

to direct isolation the average foci yield induced by 100 mGy γ -rays in the blood of four healthy donors has not changed significantly after 5h applying the Wilcoxon signed-rank test ($p = 0.180$). On the contrary, an incubation period of 24h induced a statically significant decrease in the average number of foci (38%, $p = 0.032$). The results show that keeping a blood sample at 4°C (e.g. in a refrigerator) for a few of hours (up to 5h) has no significant effect on the number of γ -H2AX foci. However, leaving a whole blood sample overnight in the refrigerator reduces the foci yield significantly. For a multicentre study we can conclude that lymphocyte isolation is necessary on the day of the blood sampling to guarantee reliable results. In a second set of experiments the influence of storing blood samples for 24h at 4°C was investigated for both isolated lymphocytes and whole blood samples to test if the shipment of purified lymphocytes to other laboratories would provide better results with respect to foci yields compared to whole blood samples (Figure 2-b). The storage of whole blood samples for 24h at 4°C results again in a significant reduction in the average number of foci, while the experiments on isolated lymphocytes provide similar results compared to the protocol with direct assessment of γ -H2AX foci.

Validation of the γ -H2AX foci immunostaining and scoring

The validation experiments show that γ -H2AX-TRITC foci co-localise with 53BP1-FITC foci, as illustrated in Figure 3. Scoring of sham-irradiated samples results in a mean value of 0.86 γ -H2AX-TRITC foci/cell (95% CI: 0.75-0.97), 1.05 53BP1-FITC foci/cell (95% CI: 0.87-1.23) and 0.71 co-localised foci/cell (95% CI: 0.56-0.85). An *in vitro* radiation dose of 25 mGy γ -rays gives a mean value of 1.53 γ -H2AX-TRITC foci/cell (95% CI: 1.31-1.74), 1.86 53BP1-FITC foci/cell (95% CI: 1.62-2.09) and 1.34 co-localised foci/cell (95% CI: 1.16-1.52), while a radiation dose of 500 mGy results in 7.34 γ -H2AX-TRITC foci/cell (95% CI: 7.05-7.63), 7.24 53BP1-FITC foci/cell (95% CI: 6.98-7.50) and 6.57 co-localised foci/cell (95% CI: 6.31-6.83) (Figure 3-d). When taken all data together, 86.4% (95% CI: 81.6% - 91.2%) of γ -H2AX foci

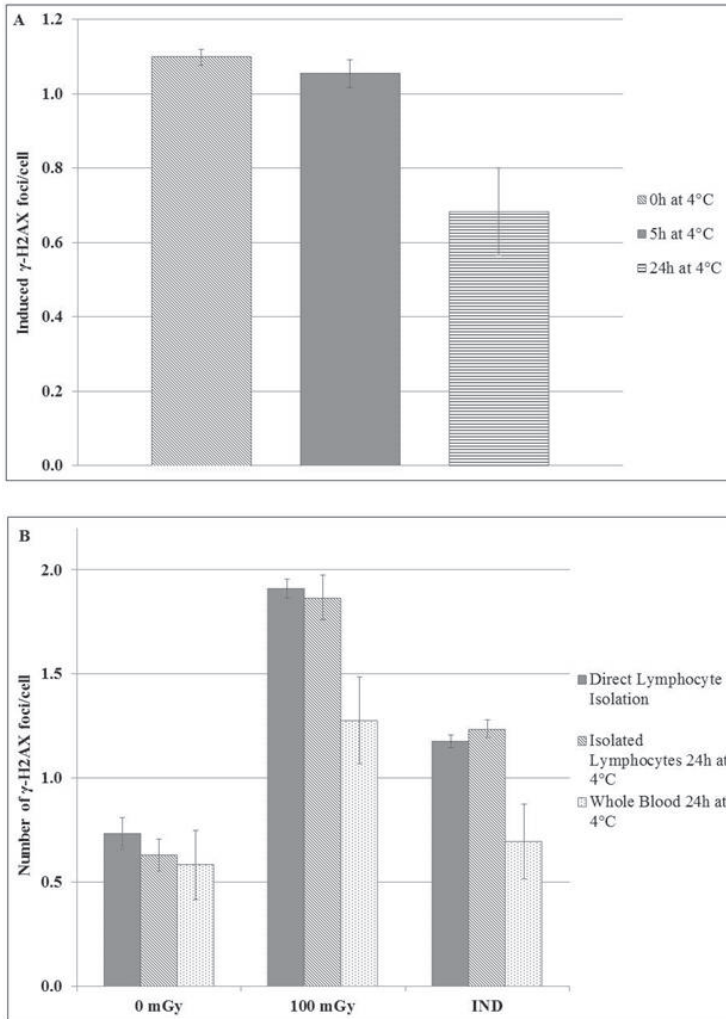


FIGURE 2

A: The mean induced number of γ -H2AX foci after in vitro irradiation of blood samples of four donors with 100 mGy, 30 min at 37°C and then storing at 4°C for 0, 5 and 24h. Error bars represent standard deviations for the inter-individual variation among the four donors.

B: Three different methods were tested after 30 min incubation at 37°C and arrest on ice water (0°C): 1) the full γ -H2AX protocol was applied directly after incubation, 2) lymphocytes were isolated and stored at 4°C for 24h, 3) whole blood was stored at 4°C for 24h. The corresponding mean numbers of γ -H2AX foci among three different donors for 0mGy, 100mGy and the induced yield are presented. Error bars represent standard deviations.

were confirmed by 53BP1-foci scoring and represent real DNA DSB. This indicates that γ -H2AX foci scoring is a sensitive and reliable technique for the visualisation of DNA DSB after low-dose exposure. However, the added value of using a double γ -H2AX-53BP1 immunostaining should be further explored in the future. The scoring of merged foci reduces to a certain extent the rate of false positives, but increases the reliability that the observed spots are indeed DNA DSB and enhances the sensitivity of foci scoring in the low-dose range by reducing the impact of artefacts.

Effect of contrast agent

The iodine contrast agent concentrations used in this experiment were based on the physiological concentrations after administration to patients in clinical practice. The blood samples containing the contrast agent were exposed to x-ray doses in the diagnostic range for CT scans. We observed no enhancement of γ -H2AX foci as a function of the concentration of iodinated contrast agent (Figure 4). At least 400 cells were scored over 2 slides for every experimental condition. Kruskal-Wallis analysis showed no statistical significant increase in γ -H2AX foci numbers with increasing

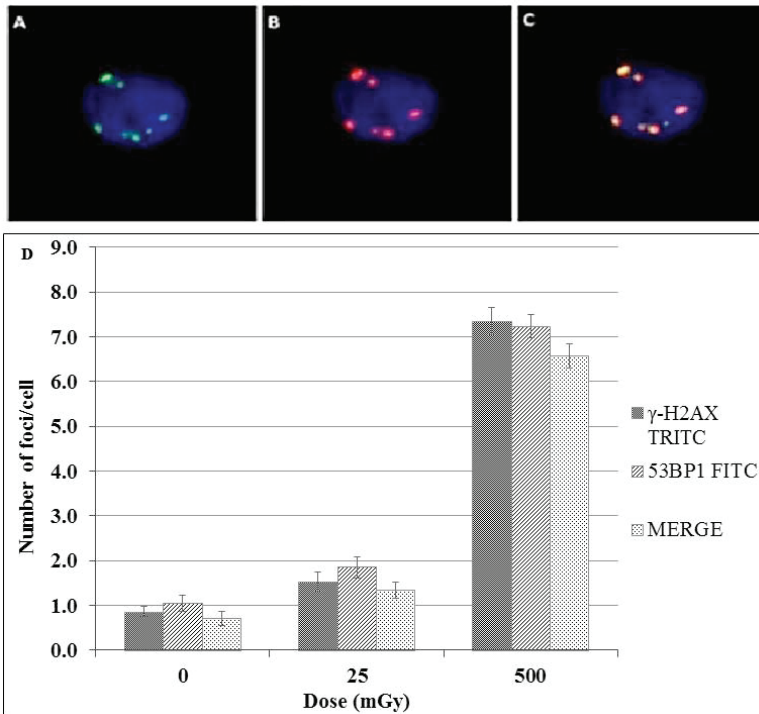


FIGURE 3

Captured images of the Olympus BX60 fluorescence microscope (100x/1.30 oil lens) of A) 53BP1-FITC staining, B) γ -H2AX-TRITC staining and C) merged in T-lymphocytes. The graph (D) illustrates the mean γ -H2AX-TRITC foci, 53BP1-FITC foci and the merged foci of four different donors, error bars represent the corresponding standard deviations.

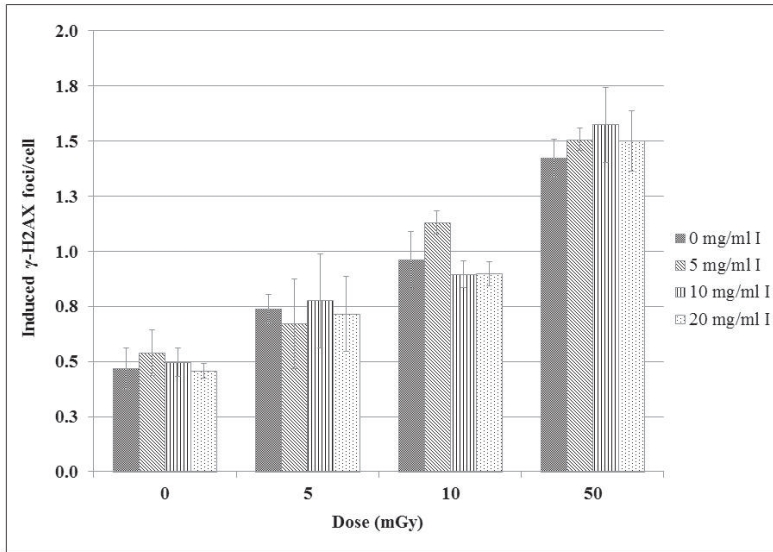


FIGURE 4

Illustration of the *in vitro* γ -H2AX foci yield for different contrast agent concentrations (0, 5, 10, 20 mg/ml I) and different dose points (0, 5, 10, 50 mGy), in the range of clinical practice. The error bars represent standard deviations derived from the statistical uncertainty on inter-individual variation among three donors.

iodine concentrations for the different radiation doses. Thus the observed data do not indicate a possible enhancement effect of contrast medium on the induction of DNA DSB in a patient study if radiation doses and the amount of Ultravist 300 contrast agent used are within those used for normal ranges for these procedures.

In vitro intercomparison study of different γ -H2AX protocols for a molecular epidemiological study

First intercomparison study

All the partner research centres used their own γ -H2AX foci assay protocol at Ghent University and the resulting slides were thereafter analysed in their own laboratory. One partner had no experience with γ -H2AX foci analysis in purified blood lymphocytes and their techniques

optimised for use in cell lines did not produce satisfactory results in terms of number of cells/slide and staining of foci and thus were excluded from subsequent comparisons. Figure 5 shows that all the other partners had a working γ -H2AX protocol appropriate for possible future collaborative multicentre studies to assess DNA DSB induced *in vivo* in purified lymphocytes from patients. Very similar levels of γ -H2AX foci were found after exposure to 100 and 500 mGy according to the standard protocol and preferred scoring technique of each laboratory. The histograms in Figure 5 represent the mean number of foci for at least 350 cells in case of automated scoring (Laboratories 1 and 2) and at least 200 cells in case of manual score (Laboratories 1 and 3). An analysis of the foci frequency distributions of the irradiated samples showed no systematic differences in the coefficient of variation between the participating laboratories and between the

results of automated and manual scoring: 0.1 Gy 1.71-2.53 versus 1.43-3.26; 0.5 Gy 0.53-1.12 versus 0.52-0.60.”

Second intercomparison study

The three institutes that succeeded in the 1st intercomparison study also participated in the 2nd intercomparison study using the same experimental γ -H2AX protocol (Table 1). The set-up for the 2nd intercomparison study was different: isolated lymphocytes in pure FCS were irradiated by one partner (STUK) and sent as overnight shipments to the other participants for processing and scoring. In this set of experiments the response in the low-dose range, as used in diagnostic radiology, was further explored (10-100 mGy x-rays). The laboratory at STUK kept the samples in the cold room (5-6 °C) until next day to mimicking the shipment circumstances. The other two laboratories received the samples within 24h and

the temperature loggers showed profiles ranging from 0.5 to 6 °C during shipment. Figure 6 shows the γ -H2AX foci yields obtained by the different partners of the project. Per dose point, on the average 360 cells were evaluated in case of manual scoring and 1600 cells in case of automated scoring. A power analysis was performed based on mean values of 0.34 and 0.56 foci/cell for 0 and 10 mGy respectively. This power analysis resulted in a required scoring sample size of 205 cells per dose point to be able to discern a dose of 10 mGy from background levels, when considering a power of 0.80 ($\alpha=0.05$, $\beta=0.20$).

One of the major differences with the first intercomparison is that isolated lymphocytes in pure FCS were irradiated for the second intercomparison study instead of whole blood samples. Indeed, a blood separation after 24h together with the shipment conditions results in an inferior quality of lymphocyte separation. Furthermore the second intercomparison study was

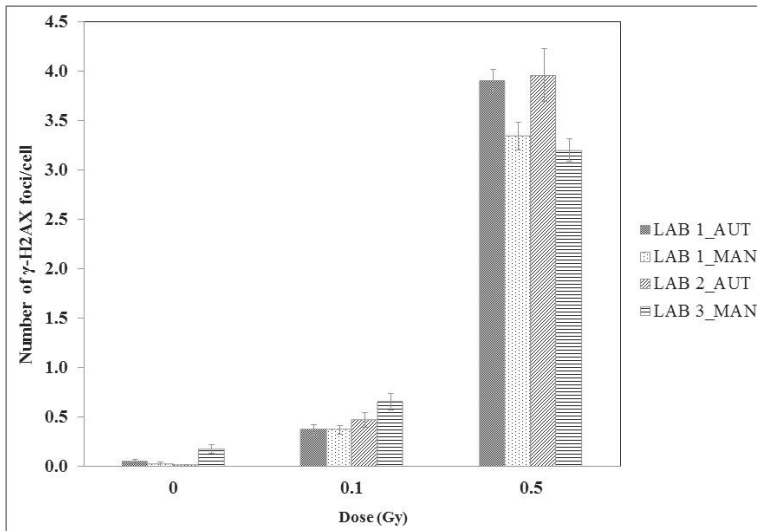


FIGURE 5

The number of γ -H2AX foci obtained by three different partners as a function of radiation doses of 0, 100 and 500 mGy. The error bars represent the standard error of the mean (SEM) of three different slides scored per condition.

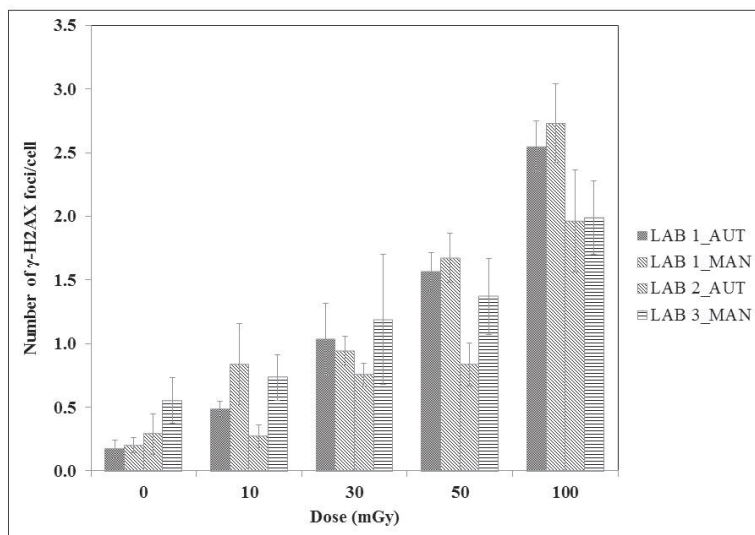


FIGURE 6

Number of γ -H2AX foci yields scored as a function of low radiation doses (0, 10, 30, 50 and 100 mGy) obtained by the different partners of the project. Error bars represent the standard deviations among the four different replicates per dose point.

performed in the diagnostic x-ray dose range, instead of the higher 0.1 and 0.5 Gy doses used in the first intercomparison study. The different laboratories were able to rank the blind samples in order of lowest to highest radiation dose based on mean foci/cell counts over the four replicates, except Lab 2 was not able to distinguish 10 mGy from the sham irradiated control. However, the results of Lab 2 were impaired to a certain degree by equipment failure during sample processing. The γ -H2AX foci levels averaged over the four replicates obtained with different protocols and scoring methods of the three participating labs show a statistical significant difference between sham irradiation and the dose of 10 mGy (Mann Whitney U test: $p = 0.001$).

The data collected by participant 1 allowed comparing manual against automated scoring on a Metafer4 scoring platform. Comparison of the linear regression fits (presented in Fig 7) with F-statistics shows good accordance between classifier 1 and manual scoring ($p = 0.371$), while the foci yields obtained with classifier 2 with higher sensitivity were clearly too high compared to the

manual scoring ($p < 0.05$). This illustrates the importance of careful optimization of Metafer classifier settings for automated scoring of γ -H2AX foci.

Although the four data sets presented in Figure 6 show a similar dose dependence the results obtained by the different laboratories and scoring method are significantly different except for the 30 mGy dose point when applying a Kruskal-Wallis analysis. The results of the intercomparison study highlight the importance of standardization of γ -H2AX assay protocols and application of quality assurance procedures to obtain foci yields, which can be shared in a multicentre setting.

The induced γ -H2AX foci levels obtained by averaging the results of the participants for every dose point are presented in Figure 8. Regression analysis shows a linear relationship between the radiation dose and the number of γ -H2AX foci induced in the isolated lymphocytes ($R^2 = 0.998$) in the dose range from 0 mGy to 100 mGy.

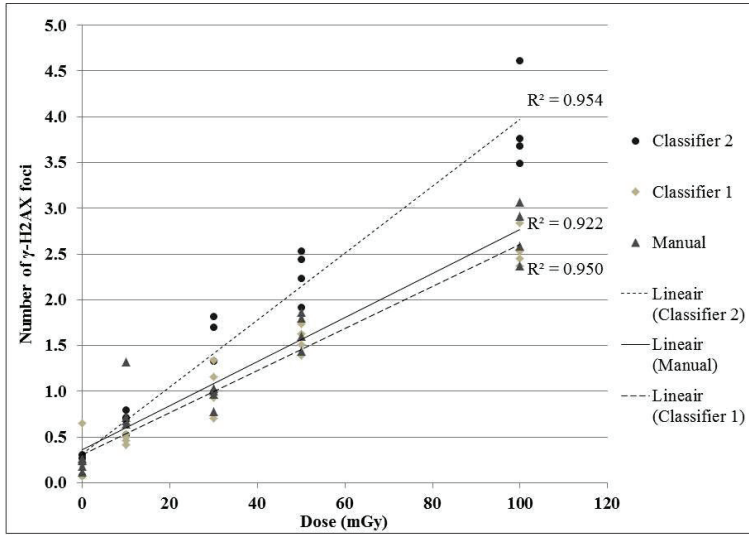


FIGURE 7

The γ -H2AX foci yields of the four replicates obtained with automated scoring by using 2 different classifiers and with manual scoring on Metasystems Metafer4 scoring platform. The lines are the result of a linear least squares fit to the data of Lab 1. R^2 values are based on the γ -H2AX foci yields of the four replicates, to illustrate the dispersion of the data points around the fit.

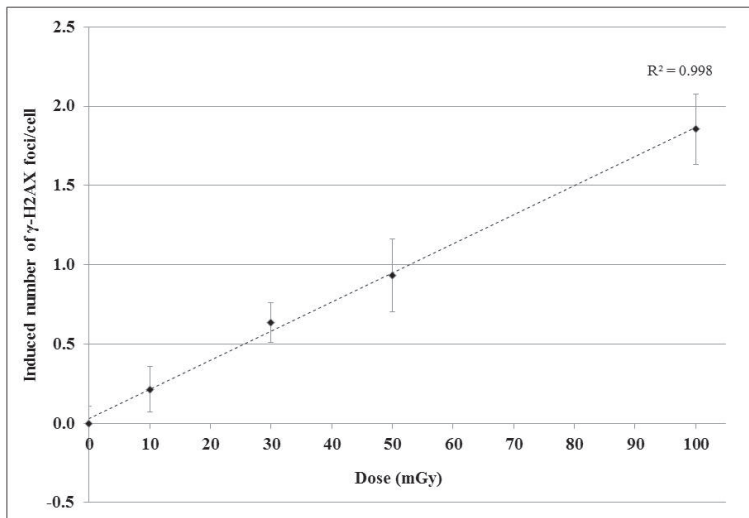


FIGURE 8

Linear regression of the dose response curve of all participating labs. The error bars represent the standard deviations on the mean among the three laboratories.

DISCUSSION

One of the aims of the EU FP7 project EPI-CT is to investigate the feasibility of using biomarkers of exposure in a multicentre molecular epidemiological study in order to better understand mechanisms underlying the response to low-dose irradiation effects in paediatric patients undergoing CT imaging. Many studies have already demonstrated the relevance and sensitivity of using the formation and persistence of γ -H2AX as a surrogate endpoint to detect and quantify DNA damage after low-dose radiation exposure. The post-translational modification of the histone protein H2AX in response to the formation of DSB can be detected by a number of immunological approaches including immune-coupled FACS analysis (Haddy et al., 2014) or as in this study immunofluorescence microscopy. The γ -H2AX foci assay is currently the most sensitive assay to investigate low-dose exposure induced DSB after CT x-ray exposure. Rothkamm *et al.* demonstrated a detection sensitivity of manual γ -H2AX foci scoring by fluorescence microscopy to radiation doses as low as 1 mGy (Rothkamm and Lobrich, 2003) and recently Halm *et al.* (Halm et al., 2014) described a dose dependent increase in γ -H2AX foci in a pilot study of three CT exposed children to blood doses of 0.22 – 1.22 mGy.

The use of biomarkers in multicentre molecular epidemiology studies is limited by access to appropriate biological samples. In many situations there is only a small time window of opportunity to collect the samples as the study subject may no longer be available or conditions may have changed (Pernot et al., 2012). Particularly in children, the study population in the EPI-CT project, an additional desirable characteristic is the possibility of using non-invasive procedures to collect biological samples. Currently we still depend on blood sampling to perform a highly sensitive γ -H2AX foci assay. Efforts have been made to optimize the assay on exfoliated buccal cells which can be obtained by commercially available kits or a mouthwash technique (Gonzalez et al., 2010) and γ -H2AX has been measured in eye-brow hair root bulbs in the context of pharmacodynamic studies involving PARP inhibitors (Fong et al., 2009). However neither of the above

mentioned biological samples have been proven to be informative in the dose range relevant to CT procedures and these samples are only appropriate for the assessment of DNA damage related to high-dose x-ray exposure to the head and neck region.

In the present paper, the problem of repeated bloodsampling was addressed by using the catheter for contrast agent administration (flushed) to collect the blood samples, eliminating the need for additional venepuncture. However, the catheter for blood collection in young children is not a perfect solution as it can be occluded after administration of contrast agent. Moreover, it is important that the possible influence of contrast agent administration on DNA DSB formation can be ruled out, which is still subject of debate (Grudzenski et al., 2009, Jost et al., 2009, Joubert et al., 2005, Deinzer et al., 2014). Iodine-containing contrast agents strongly attenuate x-rays and are commonly used in CT imaging to better delineate anatomical structures from their surrounding tissue. Our results show no significant increase in γ -H2AX foci numbers with increasing iodine concentration. These findings confirm the results of Jost *et al.* (Jost et al., 2009) showing no biological dose-enhancing effect when both radiation and contrast dose were in the diagnostic range (0.025, 0.05 and 0.1 Gy). However, a statistically significant increase in γ -H2AX foci and dicentric chromosomes was reported by these authors when a dose of 50 mg I/ml blood (outside the local iodine concentration range used for CT) and a high dose of 1 Gy (outside the diagnostic imaging dose range) were used.

Performing clinical studies in children is challenging and limited by low consent rates from parents, the small amount of blood volume and the difficulties associated with blood sampling. In many countries, an informed consent has to be signed by one of the parents for children below the age of 12 years, which requires detailed explanations of study aims and protocols. The limited blood volume in small children (0.27 l – 4.5 l as published in ICRP 89 (Valentin, 2002)) obliged us to carry out the γ -H2AX foci assay in a small blood volume. Our results demonstrate that it is technically feasible to perform the assay with only 2 ml of blood taken before and after

the CT examination. This is in accordance with the sample volumes used the recent pilot study of Halm *et al.* (Halm *et al.*, 2014) in which 2 ml blood samples were collected from children before and 1h after CT.

One of the major drawbacks of using γ -H2AX foci in a molecular epidemiological study, is the limited persistence of the signal after irradiation. This problem was also addressed by Roch-Lefèvre *et al.* (Roch-Lefevre *et al.*, 2010) as a critical issue for the application of the γ -H2AX assay for biological dosimetry in case of an accidental exposure. They reported an inhibition of γ -H2AX signal loss up to 24h when the blood was incubated on ice after an irradiation with 500 mGy γ -rays. In contrast whilst we could demonstrate that there was no loss in γ -H2AX foci signal when the blood samples of four different donors after irradiation with 100 mGy γ -rays were kept at 4°C up to 5h after exposure, a significant decrease in γ -H2AX signal was noted after 24h incubation at 4°C. Moreover, keeping the blood samples on ice for 24h can result in difficulties during blood separation due to extensive haemolysis (Olson *et al.*, 2011). The current results open up the possibility of transporting the blood samples at 4°C from the hospital to an equipped laboratory, keeping in mind that lymphocyte separation is required on the same day of blood sample collection. After lymphocyte separation it is possible to ship the purified lymphocyte overnight (within 24h) at 4°C to another laboratory without γ -H2AX signal loss.

In case blood sampling is only possible a few hours and not within 5-30 min post-CT, the scored gamma-H2AX foci will be reduced due to the DNA DSB repair kinetics. To cope with this decrease, more information on the kinetics of gamma-H2AX foci after low-dose x-ray exposure is needed and a subject for future research.

In a large scale context a quick and objective quantification of the γ -H2AX signals in cells would be particularly interesting. There is an ongoing intensive development of high throughput γ -H2AX foci scoring systems to automate microscopic evaluation. Automated scoring would exclude the scorer-subjectivity together with the time-consuming character of manual scoring, which are the major limitations of the γ -H2AX

foci scoring to date. Sample size calculation based on the mean γ -H2AX foci yields obtained in the second intercomparison study, revealed that at least 200 cells per case should be scored in order to be able to discern a dose of 10 mGy from a sham-irradiated control. This is reasonable considering the statistical resolution at low doses. However, many studies in literature count not more than 100 cells per sample. As discussed previously, analysis by flow cytometry may be quicker, however, it is not as sensitive as microscopy, which has the advantage of being able to discriminate objects such as discrete foci from background fluorescence (Redon *et al.*, 2012). Certainly for the detection of DNA damage after low-dose exposure as in diagnostic radiology, where the number of foci is small and the size of the biological sample is a limiting factor, a sensitive scoring method is more appropriate. In the intercomparison exercises, two participants performed manual scoring and two laboratories performed automated scoring. The results of the present study indicate a satisfactory agreement between manual and automated scoring obtained in one of the participating laboratories ($p = 0.093$), suggesting an opportunity for automated γ -H2AX foci scoring in a low-dose molecular epidemiological study. A carefully designed and well trained classifier is essential for a good correlation between manual and automated scoring. The selection of the classifier depends on the microscope magnification and the quality of the samples and is therefore specific for the laboratory. However, an extensive optimisation of spot counting on the Metasystem scoring platforms and exchange of classifiers between laboratories is required to make automated scoring applicable at a larger scale. It is recognised that there are several variables to consider when data collected from different laboratories are compared (reagents and methods) and each laboratory has predetermined criteria for foci scoring (Barnard *et al.*, 2014). By organising intercomparison studies and training, we can try to improve quality assurance, however some variation will be unavoidable in a multicentre context.

As already mentioned, the presence of background and staining artefacts on the microscopic slides, can impede the foci quantification and

may affect the reproducibility of the assay. In this study in addition to γ -H2AX, 53BP1 was used as a surrogate marker for DNA DSB. 53BP1 is a well known DNA damage response (DDR) factor, which is recruited to nuclear structures at the site of DNA damage and forms readily visualised ionizing radiation-induced foci. Within the DNA damage response mechanism, 53BP1 is classified as an adaptor/mediator, required for processing of the DNA damage response signal and as a platform for the recruitment of other repair factors (Gupta et al., 2014). We selected this protein, because 53BP1 foci are formed very quickly in response to IR, compared to MRE11/RAD50/NBS1 and BRCA1 foci (Celeste et al., 2003). For a radiation dose of 25 and 500 mGy in the present experimental set-up most of the radiation induced foci showed overlap in fluorescence images. An additional interesting characteristic of performing γ -H2AX/53BP1 double immunostaining, is the possibility to make a morphological distinction between DNA-repair and apoptosis as 53BP1 is not present in the apoptotic ring as reported by Solier and Pommier (Solier and Pommier, 2014). By scoring 'merged' γ -H2AX/53BP1 foci in G0 lymphocytes one can be sure that the observed spot represents a DNA DSB attributable to the radiation exposure (Chua et al., 2011, Rothkamm et al., 2007, Horn et al., 2013). Our results validated that the 'conventional' γ -H2AX foci scoring method is a reliable technique to score DNA DSB after low-dose exposure. However, further research is needed to test if the scoring of merged foci within a multicentre study would increase the uniformity in scoring results among the partners.

In the last few years, several laboratory intercomparison studies were organised in order to compare laboratories' dose-assessment performances of the γ -H2AX foci assay as a triage tool in biological dosimetry (Ainsbury et al., 2014, Rothkamm et al., 2013a, Rothkamm et al., 2013b). These intercomparison studies provided valuable input for the shipment and processing of the samples in the current study. For shipment, lymphocytes were packed together with frozen cool packs in order to keep the temperature below 10°C and each package contained a temperature logger and dosimeter, as described in the Mul-

tibiodose Guidance (www.multibiodose.eu). The initial experiments of Rothkamm *et al.* (Rothkamm et al., 2013a) showed that several laboratories encountered difficulties in sample processing due to extensive haemolysis when whole blood was irradiated, incubated and shipped. This was also observed in the current experiments after storing blood samples at 4°C for 24h. For this reason, we used freshly isolated lymphocytes in the second intercomparison study. In addition, we should keep in mind that radiation doses used in diagnostic radiology are much lower than the doses used in these emergency exercises. We show here for the first time in an intercomparison exercise in the low-dose range that laboratories with highly optimized protocols can detect a damage response at least down to 10 mGy. This is essential for a large scale multicentre molecular epidemiological study, in particular when using biomarkers of exposure at very low doses.

In the context of large international studies, it is crucial to organise intercomparison studies to investigate whether existing γ -H2AX protocols would produce similar foci frequencies and to test the feasibility of sending samples in an overnight shipment. The first intercomparison study showed comparable results for radiation doses of 100 and 500 mGy when every partner applied its own protocol. In the second intercomparison, the transport of samples exposed to doses in the diagnostic range was further explored and demonstrated the feasibility of the foci assay to distinguish low-dose diagnostic x-ray exposures in a multicentre setting. In the first intercomparison foci yields were systematically lower compared to the other data obtained in this study. A possible explanation could be differences in experimental conditions between the UGent laboratory and partner sites or related to variation in radiosensitivity among the donors involved in the different experiments.

DNA DSB are considered to be the most deleterious cellular damage of x-rays because misrepaired DNA DSB are the principal lesions of importance in the induction of gene mutations and chromosomal rearrangements, including translocations, which are linked to genomic instability and tumorigenesis (Richardson and Jasin, 2000). However, before the γ -H2AX foci assay can be

widely applied to obtain cancer risk estimations after low-dose exposure the link between the repair of ionizing radiation-induced DNA DSB and carcinogenesis needs to be further explored (Haddy et al., 2014).

In conclusion, we have shown that it is feasible to apply the γ -H2AX foci assay as a potential cellular biomarker of exposure in a multicentre prospective study of the effects of paediatric CT imaging if the γ -H2AX foci results can be validated in an *in vivo* pilot study on paediatric patients.

ACKNOWLEDGEMENTS

The research leading to these results has received funding from the European Union's Seventh Framework Programme for research, technological development and demonstration (FP7/2007–2013) under grant agreement number 269912-EPI-CT: Epidemiological study to quantify risks for paediatric computerized tomography and to optimise doses. Marjo Perälä (STUK), Frank Bunk and Ingrid Baumgartner (BfS) are acknowledged for their technical support, analysis of γ -H2AX foci and improvement of automated scoring.

DECLARATION OF INTEREST

The authors report no declarations of interest.

REFERENCES

- AINSBURY, E. A., AL-HAFIDH, J., BAJINSKIS, A., BARNARD, S., BARQUINERO, J. F., BEINKE, C., DE GELDER, V., GREGOIRE, E., JAWORSKA, A., LINDHOLM, C., LLOYD, D., MOQUET, J., NYLUND, R., OESTREICHER, U., ROCH-LEFEVRE, S., ROTHKAMM, K., ROMM, H., SCHERTHAN, H., SOMMER, S., THIERENS, H., VANDEVOORDE, C., VRAL, A. & WOJCIK, A. 2014. Inter- and intra-laboratory comparison of a multibiosidometric approach to triage in a simulated, large scale radiation emergency. *Int J Radiat Biol* 90:193-202.
- BARNARD, S., AINSBURY, E. A., AL-HAFIDH, J., HADJIDEKOVA, V., HRISTOVA, R., LINDHOLM, C., MONTEIRO GIL, O., MOQUET, J., MORENO, M., ROSSLER, U., THIERENS, H., VANDEVOORDE, C., VRAL, A., WOJEWODZKA, M. & ROTHKAMM, K. 2014. The first gamma-H2AX biosidometry intercomparison exercise of the developing European biosidometry network RENE. *Radiat Prot Dosimetry* [cited 2014 Nov 3] DOI: 10.1093/rpd/ncu259.
- BEELS, L., BACHER, K., DE WOLF, D., WERBROUCK, J. & THIERENS, H. 2009. gamma-H2AX Foci as a Biomarker for Patient X-Ray Exposure in Pediatric Cardiac Catheterization Are We Underestimating Radiation Risks? *Circulation* 120:1903-1909.
- BEELS, L., BACHER, K., SMEETS, P., VERSTRAETE, K., VRAL, A. & THIERENS, H. 2012. Dose-length product of scanners correlates with DNA damage in patients undergoing contrast CT. *Eur J Radiol* 81:1495-1499.
- BRENNER, D. J. 2009. Extrapolating radiation-induced cancer risks from low doses to very low doses. *Health Phys* 97:505-509.
- BRENNER, D. J., DOLL, R., GOODHEAD, D. T., HALL, E. J., LAND, C. E., LITTLE, J. B., LUBIN, J. H., PRESTON, D. L., PRESTON, R. J., PUSKIN, J. S., RON, E., SACHS, R. K., SAMET, J. M., SETLOW, R. B. & ZAIDER, M. 2003. Cancer risks attributable to low doses of ionizing radiation: Assessing what we really know. *Proc Natl Acad Sci U S A* 100:13761-13766.
- BRENNER, D. J. & HALL, E. J. 2007. Current concepts - Computed tomography - An increasing source of radiation exposure. *N Engl J Med* 357:2277-2284.
- CELESTE, A., FERNANDEZ-CAPETILLO, O., KRULAK, M. J., PILCH, D. R., STAUDT, D. W., LEE, A., BONNER, R. F., BONNER, W. M. & NUSSENZWEIG, A. 2003. Histone H2AX phosphorylation is dispensable for the initial recognition of DNA breaks. *Nat Cell Biol* 5:675-U51.
- CHUA, M. L., SOMAIAH, N., AHERN, R., DAVIES, S., GOTHARD, L., YARNOLD, J. & ROTHKAMM, K. 2011. Residual DNA and chromosomal damage in ex vivo irradiated blood lymphocytes correlated with late normal tissue response to breast radiotherapy. *Radiother Oncol* 99:362-6.
- DEINZER, C. K., DANOVA, D., KLEB, B., KLOSE, K. J. & HEVERHAGEN, J. T. 2014. Influence of different iodinated contrast media on the induction of DNA double-strand breaks after in vitro X-ray irradiation. *Contrast Media Mol Imaging* 9:259-67.
- EDWARDS, S. D. & MCNAMEE, M. J. 2005. Ethical concerns regarding guidelines for the conduct of clinical research on children. *J Med Ethics* 31:351-354.
- FONG, P. C., BOSS, D. S., YAP, T. A., TUTT, A., WU, P., MERGUI-ROELVINK, M., MORTIMER, P., SWAISLAND, H., LAU, A., O'CONNOR, M. J., ASHWORTH, A., CARMICHAEL, J., KAYE, S. B., SCHELLENS, J. H. & DE BONO, J. S. 2009. Inhibition of poly(ADP-ribose) polymerase in tumors from BRCA mutation carriers. *N Engl J Med* 361:123-34.
- GEISEL, D., ZIMMERMANN, E., RIEF, M., GREUPNER, J., LAULE, M., KNEBEL, F., HAMM, B. & DEWEY, M. 2012. DNA double-strand breaks as potential indicators for the biological effects of ionising radiation exposure from cardiac CT and conventional coronary angiography: a randomised, controlled study. *Eur Radiol* 22:1641-1650.
- GONZALEZ, J. E., ROCH-LEFEVRE, S. H., MANDINA, T., GARCIA, O. & ROY, L. 2010. Induction of gamma-H2AX foci in human exfoliated buccal cells after in vitro exposure to ionising radiation. *Int J Radiat Biol* 86:752-759.
- GRUDZENSKI, S., KUEFNER, M. A., HECKMANN, M. B., UDER, M. & LOBRICH, M. 2009. Contrast medium-enhanced radiation damage caused by CT examinations. *Radiology* 253:706-14.
- GUPTA, A., HUNT, C. R., CHAKRABORTY, S., PANDITA, R. K., YORDY, J., RAMNARAIN, D. B., HORIKOSHI, N., PANDITA, T. K. 2014. Role of 53BP1 in the regulation of DNA double-strand break repair pathway choice. *Radiat Res* 181:1-8.
- HADDY, N., TARTIER, L., KOSCIELNY, S., ADJADI, E., RUBINO, C., BRUGIERES, L., PACQUEMENT, H., DIALLO, I., DE VATHAIRE, F., AVERBECK, D., HALL, J. & BENHAMOU, S. 2014. Repair of ionizing radiation-induced DNA damage and risk of second cancer in childhood cancer survivors. *Carcinogenesis* 35:1745-9.
- HALM, B. M., FRANKE, A. A., LAI, J. F., TURNER, H. C., BRENNER, D. J., ZOHREBIAN, V. M. & DIMAURO, R. 2014. gamma-H2AX foci are increased in lymphocytes in vivo in young children 1 h after very low-dose X-irradiation: a pilot study. *Pediatr Radiol* 44:1310-7.
- HORN, S., BARNARD, S., BRADY, D., PRISE, K. M. & ROTHKAMM, K. 2013. Combined analysis of gamma-H2AX/53BP1 foci and caspase activation in lymphocyte subsets detects recent and more remote radiation exposures. *Radiat Res* 180:603-9.
- HUANG, W. Y., MUO, C. H., LIN, C. Y., JEN, Y. M., YANG, M. H., LIN, J. C., SUNG, F. C. & KAO, C. H. 2014. Paediatric head CT scan and subsequent risk of malignancy and benign brain tumour: a nation-wide population-based cohort study. *Br J Cancer* 110:2354-60.
- JOST, G., GOLFFIER, S., PIETSCH, H., LENGSELD, P., VOTH, M., SCHMID, T. E., ECKARDT-SCHUPP, F. & SCHMID, E. 2009. The influence of x-ray contrast agents in computed tomography on the induction of dicentric and gamma-H2AX foci in lymphocytes of human blood samples. *Phys Med Biol* 54:6029-39.
- JOUBERT, A., BISTON, M. C., BOUDOU, C., RAVANAT, J. L., BROCHARD, T., CHARVET, A. M., ESTEVE, F., BALOSSO, J. & FORAY, N. 2005. Irradiation in presence of iodinated contrast agent results in radiosensitization of endothelial cells: consequences for computed tomography therapy. *Int J Radiat Oncol Biol Phys* 62:1486-96.

- LIN, E. C. 2010. Radiation Risk From Medical Imaging. *Mayo Clinic Proceedings*, 85, 1142-1146.
- LÖBRICH, M., RIEF, N., KÜHNE, M., HECKMANN, M., FLECKENSTEIN, J., RÜBE, C., UDER, M. 2005. In vivo formation and repair of DNA double-strand breaks after computer tomography examinations. *P Natl Acad Sci USA* 102:8984-8989.
- MARKOVA, E., SCHULTZ, N. & BELYAEV, I. Y. 2007. Kinetics and dose-response of residual 53BP1/gamma-H2AX foci: Colocalization, relationship with DSB repair and clonogenic survival. *Int J Radiat Biol* 83:319-29.
- MATHEWS, J. D., FORSYTHE, A. V., BRADY, Z., BUTLER, M. W., GOERGEN, S. K., BYRNES, G. B., GILES, G. G., WALLACE, A. B., ANDERSON, P. R., GUIVER, T. A., MCGALE, P., CAIN, T. M., DOWTY, J. G., BICKERSTAFFE, A. C. & DARBY, S. C. 2013. Cancer risk in 680 000 people exposed to computed tomography scans in childhood or adolescence: data linkage study of 11 million Australians. *Br Med J* 346:f2360.
- MOTULSKY, H. 2010. *Intuitive biostatistics: a nonmathematical guide to statistical thinking*. New York, Oxford University Press.
- OLSON, W. C., SMOLKIN, M. E., FARRIS, E. M., FINK, R. J., CZARKOWSKI, A. R., FINK, J. H., CHIANESE-BULLOCK, K. A. & SLINGLUFF, C. L., JR. 2011. Shipping blood to a central laboratory in multicenter clinical trials: effect of ambient temperature on specimen temperature, and effects of temperature on mononuclear cell yield, viability and immunologic function. *J Transl Med*, 9: Article Number 26.
- PEARCE, M. S., SALOTTI, J. A., LITTLE, M. P., MCHUGH, K., LEE, C., KIM, K. P., HOWE, N. L., RONCKERS, C. M., RAJARAMAN, P., CRAFT, A. W., PARKER, L. & DE GONZALEZ, A. B. 2012. CT scans in childhood and subsequent risk of leukaemia and brain tumours: a retrospective cohort study. *Lancet* 380:499-505.
- PERNOT, E., HALL, J., BAATOUT, S., BENOTMANE, M. A., BLANCHARDON, E., BOUFFLER, S., EL SAGHIRE, H., GOMOLKA, M., GUERTLER, A., HARMS-RINGDAHL, M., JEGGO, P., KREUZER, M., LAURIER, D., LINDHOLM, C., MKACHER, R., QUINTENS, R., ROTHKAMM, K., SABATIER, L., TAPIO, S., DE VATHAIRE, F. & CARDIS, E. 2012. Ionizing radiation biomarkers for potential use in epidemiological studies. *Mutat Res Rev Mutat Res* 751:258-86.
- PRESTON, D. L., RON, E., TOKUOKA, S., FUNAMOTO, S., NISHI, N., SODA, M., MABUCHI, K. & KODAMA, K. 2007. Solid cancer incidence in atomic bomb survivors: 1958-1998. *Radiat Res* 168:1-64.
- REDON, C. E., WEYEMI, U., PAREKH, P. R., HUANG, D., BURRELL, A. S. & BONNER, W. M. 2012. gamma-H2AX and other histone post-translational modifications in the clinic. *Biochim Biophys Acta* 1819:743-56.
- RICHARDSON, C. & JASIN, M. 2000. Frequent chromosomal translocations induced by DNA double-strand breaks. *Nature* 405:697-700.
- RICHARDSON, D. B. & HAMRA, G. 2010. Ionizing Radiation and Kidney Cancer among Japanese Atomic Bomb Survivors. *Radiat Res* 173:837-42.
- ROCH-LEFEVRE, S., MANDINA, T., VOISIN, P., GAETAN, G., GONZALEZ MESA, J. E., VALENTE, M., BONNESOEUR, P., GARCIA, O., VOISIN, P. & ROY, L. 2010. Quantification of gamma-H2AX Foci in Human Lymphocytes: A Method for Biological Dosimetry after Ionizing Radiation Exposure. *Radiat Res*, 174:185-94.
- ROGAKOU, EP, PILCH, DR., ORR, AH., IVANOVA, VS., BONNER, WM. 1998. DNA double-stranded breaks induce histone H2AX phosphorylation on serine 139. *J Biol Chem* 273:5858-5868.
- RON, E., PRESTON, D. L., KISHIKAWA, M., KOBUE, T., ISEKI, M., TOKUOKA, S., TOKUNAGA, M. & MABUCHI, K. 1998. Skin tumor risk among atomic-bomb survivors in Japan. *Cancer Causes Control*, 9:393-401.
- ROTHKAMM, K., BALROOP, S., SHEKHAR, J., FERNIE, P. & GOH, V. 2007. Leukocyte DNA damage after multi-detector row CT: A quantitative biomarker of low-level radiation exposure. *Radiology* 242:244-51.
- ROTHKAMM, K., BARNARD, S., AINSBURY, E. A., AL-HAFIDH, J., BARQUINERO, J. F., LINDHOLM, C., MOQUET, J., PERALA, M., ROCH-LEFEVRE, S., SCHERTHAN, H., THIERENS, H., VRAL, A. & VANDERSICHEL, V. 2013a. Manual versus automated gamma-H2AX foci analysis across five European laboratories: Can this assay be used for rapid biodosimetry in a large scale radiation accident? *Mutat Res Genet Toxicol Environ Mutagen* 756:170-3.
- ROTHKAMM, K., HORN, S., SCHERTHAN, H., ROSSLER, U., DE AMICIS, A., BARNARD, S., KULKA, U., LISTA, F., MEINEKE, V., BRASELMANN, H., BEINKE, C. & ABEND, M. 2013b. Laboratory Intercomparison on the gamma-H2AX Foci Assay. *Radiat Res* 180:149-55.
- ROTHKAMM, K. & LOBRICH, M. 2003. Evidence for a lack of DNA double-strand break repair in human cells exposed to very low x-ray doses. *Proc Natl Acad Sci U S A* 100:5057-62.
- SOLIER, S., POMMIER, Y. 2014. The nuclear gamma-H2AX apoptotic ring: implications for cancer and autoimmune diseases. *Cell Mol Life Sci* 71:2289-97.
- SU, T. 2006. Cellular responses to DNA damage: One signal, multiple choices. *Annu Rev Genet* 40: 187-208.
- THOMPSON, D. E., MABUCHI, K., RON, E., SODA, M., TOKUNAGA, M., OCHIKUBO, S., SUGIMOTO, S., IKEDA, T., TERASAKI, M., IZUMI, S. & PRESTON, D. L. 1994. Cancer incidence in atomic-bomb survivors 2. solid tumors, 1958-1987. *Radiat Res* 137:S17-S67.
- UNSCEAR 2008. Sources and effects of ionizing radiation. New York, NY: Report to the General Assembly of the United Nations.
- UNSCEAR 2013. Sources and effects of ionizing radiation. New York, NY: Report to the General Assembly of the United Nations.
- VALENTIN, J. 2002. Basic anatomical and physiological data for use in radiological protection: reference values: ICRP Publication 89. *Annals of the ICRP* 32:1-277.

7

PAPER II

γ -H2AX foci as *in vivo* effect biomarker in children emphasize the importance to minimize x-ray doses in paediatric CT imaging

Vandevoorde C¹, Franck C¹, Bacher K¹, Breyssem L², Smet MH², Ernst C³, De Backer A⁴, Van De Moortele K⁵, Smeets P⁶, Thierens H¹

¹ Ghent University, Department of Basic Medical Sciences

² University Hospital Louvain, Radiology Department

³ University Hospital Brussels, Radiology Department

⁴ General Hospital Sint-Lucas Ghent, Radiology Department

⁵ General Hospital Sint-Jan Bruges, Radiology Department

⁶ Ghent University Hospital, Radiology Department

Published in European Radiology 2015;25(3):800-11

γ -H2AX foci as *in vivo* effect biomarker in children emphasize the importance to minimize x-ray doses in paediatric CT imaging

ABSTRACT

Objectives: Investigation of DNA damage induced by CT x-rays in paediatric patients versus patient dose in a multicentre setting.

Methods: From 51 paediatric patients (median age, 3.8 years) who underwent a CT abdomen or CT chest examination in one of the five participating radiology departments, blood samples were taken before and shortly after the examination. DNA damage was estimated by scoring γ -H2AX foci in peripheral blood T-lymphocytes. Patient-specific organ and tissue doses were calculated with a validated Monte Carlo program. Individual lifetime attributable risks (LAR) for cancer incidence and mortality were estimated according to the BEIR VII risk models.

Results: Despite the low CT doses, a median increase of 0.13 γ -H2AX foci/cell was observed. Plotting the induced γ -H2AX foci versus blood dose indicated a low-dose hypersensitivity, supported also by an *in vitro* dose-response study. Differences in dose levels between radiology centres were reflected in differences in DNA-damage. LAR of cancer mortality for the paediatric chest CT and abdomen CT cohort was 0.08 and 0.13 ‰ respectively.

Conclusion: CT x-rays induce DNA damage in paediatric patients even at low doses and the level of DNA damage is reduced by application of more effective CT dose reduction techniques and paediatric protocols.

Key Points:

1. CT induces a small, significant number of DNA DSBs in children.
2. More effective CT dose reduction results in less DNA damage.
3. Risk estimates according to the LNT hypothesis, may represent underestimates

Abbreviations and Acronyms:

DNA: deoxyribonucleoside acid
LSS: lifespan study
LNT: linear-no-threshold
 γ H2AX: phosphorylated histone subtype H2A isoform X
DSB: double-strand break
BEIR: biological effects of ionizing radiation
LAR: lifetime attributable risk
ATCM: automatic tube current modulation
RPMI: Roswell Park Memorial Institute
PFA: paraformaldehyde
RAM-TRITC: rabbit-anti-mouse tetramethyl rhodamine isothiocyanate
DAPI: 4',6-diamidino-2-phenylindole
53PB1: p53 binding protein 1
ICRP: international commission on radiological protection
DLP: dose-length product
DRL: dose reference level
CTDIvol: computed tomography dose index (volume)

INTRODUCTION

The introduction of computed tomography (CT) has tremendously improved diagnostic imaging. However, the high x-ray doses associated with CT procedures have raised health concerns [1]. This is of particular importance for the paediatric patient population, recognized as one of the most important target groups in medical radiation protection. Technological developments in CT have substantially increased diagnostic applications and accuracy in paediatric patients. Children have a higher radiosensitivity compared to adults regarding x-ray induced malignancies and the associated risk for exposure induced death [2]. Therefore, optimisation and justification of CT protocols for children is a topic of high importance in daily clinical practice [3]. An initiative worth mentioning in this context, is the Image Gently campaign of the Alliance for Radiation Safety in Paediatric Imaging, that tries to change practice by increasing awareness of the opportunities to reduce radiation dose in the imaging of children [4]. Several studies have shown that the use of CT dose reduction techniques in paediatric CT imaging lowers the physical radiation dose [5, 6]. However it remains unexplored if they also have an impact on the DNA damage induced by CT x-rays in children.

A recent study in the United Kingdom has linked the exposure from x-rays in CT scanning during childhood with the development of brain tumours and leukaemia [7]. However, the risk assessments at low doses remain subject of active debate. The lifespan study (LSS) of atomic bomb survivors showed a roughly linear relationship between cancer mortality and high doses of high dose rate radiation for an adult population [8]. This resulted in the linear-no-threshold (LNT) hypothesis, implying a linear relationship between dose and biological effect without a dose threshold. Despite the considerable uncertainties and divergent views regarding the health effects and applicability of the LNT theory at low doses, the model is used for risk estimation by the international radiation protection community and referred as the main paradigm of radiation protection [9].

The use of sensitive biomarkers for the assessment of early x-ray effects in patients gives valuable information on dose-effect relationships for diagnostic x-rays. Earlier work has demonstrated that the γ -H2AX foci assay can be used to determine the effects of CT exposure at molecular level, namely the induction of DNA double-strand breaks (DSBs) [10-13]. DSBs are considered to be the most deleterious cellular effects of x-rays, because they can result in loss or rearrangement of genetic information, leading to cell death or carcinogenesis [14]. The phosphorylation of the histone variant H2AX is one of the earliest stages in the cellular response to DSBs and one γ -H2AX focus represents one DNA DSB, which can be quantified by immunofluorescence microscopy [15].

A prospective multicentre study was set up in order to determine the number of x-ray induced DNA DSBs in children undergoing a CT chest or CT abdomen examination. Herein, the γ -H2AX foci assay was used as an effect biomarker for radiation-induced DSBs. Blood doses were determined by a patient specific full Monte Carlo dose simulation in order to correlate the induced DNA damage with the individual blood dose. BEIR VII age and gender specific risk models were used to assess the lifetime attributable risk (LAR) of cancer incidence and mortality associated with the CT examination of every individual patient.

MATERIALS AND METHODS

A. Assessment of DNA DSBs in pre- and post-CT blood samples of paediatric patients

Study Population

The study population consisted of 51 children undergoing a CT exam of the chest (41) or abdomen (10) in one of the five participating radiology centres (March 2012 through July 2013) (Table 1). The small number of CT abdomen patients is caused by the fact that magnetic resonance imaging (MRI) was the preferred imaging modality of the majority of participating radiologists for abdomen investigations, to avoid ionizing radiation

exposure. Exclusion criteria were present or past leukaemia or lymphoma and radiochemotherapy within the last year. The median age of the patient group was 3.8 years (range 0.1 - 12.5 years). Before blood sampling, an informed consent was signed by one of the parents of the children. The prospective multicentre study was approved by the local review boards of the participating hospitals and the institutional review board of Ghent University Hospital acted as central Ethical Committee.

state-of-the-art CT systems with dose reduction techniques and adapted paediatric protocols resulted in low- or even ultra-low CT doses.

Sample collection

Blood samples (2 mL) were collected through the catheter for contrast agent administration. One blood sample was taken before CT, to determine the baseline level of DSBs, and one approximately 5 min after the examination (the catheter was always flushed before sampling). Due to oc-

	CT Chest	CT Abdomen
Demographic patient data		
<i>Age, y</i>	3.00 (0.10 - 12.20)	7.1 (1.80 - 12.10)
<i>Weight, kg</i>	13.50 (2.40 - 40.00)	24.00 (8.80 - 68.50)
<i>Length, cm</i>	93.50 (45.50 - 160.00)	123.50 (76.50 - 167.00)
<i>Males</i>	30	7
<i>Females</i>	11	3

TABLE 1

Demographic data of the paediatric patients included in the study.

CT Equipment and acquisition protocols

All the participating radiology departments used contemporary state-of-the-art low dose CT systems. The following CT scanners were used in this study: Siemens Somatom Definition Flash and Sensation 64 (Siemens Medical Solutions, Germany), Toshiba Aquilion (Toshiba Medical Systems, Japan) and three centres used the GE Discovery CT750 HD (GE Healthcare, USA). Every radiology department used his own, optimized paediatric CT protocol with low kVp settings (median values; CT chest 80 kV: range 80-120 kV; CT abdomen 100 kV: range 100-120 kV), low fixed tube currents or automatic tube current modulation (ATCM), adapted pitch values and scan lengths restricted to the region of interest. Iterative reconstruction technology was applied in two of the institutions, resulting in ultra-low doses (VEO reconstruction from GE Healthcare). Individual CT parameters for the patients of the study are presented in Table 2 and 3 for CT chest and abdomen respectively. The combination of

conclusion, blood sampling through the catheter was not possible for more than half of the patients, especially very young children. For these patients an additional venepuncture after the CT exam was necessary. The blood samples were kept at 37°C for 30 minutes to allow DNA damage signalling. Afterwards, DNA repair was arrested by cooling the samples at 0°C for 15 minutes. Blood was transported at 4°C, with an elapsed time no longer than 3h from collection to processing. Before processing, samples were coded allowing blind scoring later on.

Detection of DNA DSBs

The method is based on the phosphorylation of the histone variant H2AX after DSB formation and follows previously published protocols [11, 16, 17]. In order to be able to work with a homogeneous cell population, T-lymphocytes were isolated from the blood with the RosetteSep Human T-Cell Enrichment Cocktail (StemCell Technologies, France) and resuspended in com-

CT Chest

Patient Number		Tube current (mA)	Exposure time (s)	Tube voltage (kV)	Pitch	Collimation (mm)	Type of CT scanner
1	A	80	0.4	100	1.375	40	GE Discovery CT750 HD
	B*	60	0.4	100	1.375	40	GE Discovery CT750 HD
2		80	0.4	80	1.375	40	GE Discovery CT750 HD
3		35	0.6	100	1.375	40	GE Discovery CT750 HD (VEO)
4		30	0.4	100	0.984	40	GE Discovery CT750 HD
5		25	0.6	100	0.984	40	GE Discovery CT750 HD
6		38.3 (ATM)	0.5	80	1.375	40	GE Discovery CT750 HD
7		75	0.4	100	0.984	40	GE Discovery CT750 HD (VEO)
8		111.82 (ATM)	0.6	80	1.370	40	GE Discovery CT750 HD
9		86.86 (ATM)	0.6	80	1.375	40	GE Discovery CT750 HD
10		79	0.6	100	1.375	40	GE Discovery CT750 HD
11		94.98 (ATM)	0.6	120	1.375	40	GE Discovery CT750 HD
12		119.25 (ATM)	0.6	120	1.375	40	GE Discovery CT750 HD
13		22.47 (ATM)	0.4	80	0.516	40	GE Discovery CT750 HD (VEO)
14		22.58 (ATM)	0.4	80	0.516	40	GE Discovery CT750 HD (VEO)
15		18.90 (ATM)	0.4	80	0.516	40	GE Discovery CT750 HD (VEO)
16		31.54 (ATM)	0.4	80	0.516	40	GE Discovery CT750 HD (VEO)
17		10	0.4	80	0.984	40	GE Discovery CT750 HD (VEO)
18		41.42 (ATM)	0.4	80	0.984	40	GE Discovery CT750 HD (VEO)
19		19.66	0.4	80	0.516	40	GE Discovery CT750 HD (VEO)
20		61.69 (ATM)	0.4	80	0.516	40	GE Discovery CT750 HD (VEO)
21		24	0.4	80	0.516	40	GE Discovery CT750 HD (VEO)
22		37.67	0.4	80	0.516	40	GE Discovery CT750 HD (VEO)
23		39.15 (ATM)	0.4	80	0.516	40	GE Discovery CT750 HD (VEO)
24		31.13	0.4	80	0.516	40	GE Discovery CT750 HD (VEO)
25		10	0.4	80	0.984	40	GE Discovery CT750 HD (VEO)
26		35.84 (ATM)	0.4	80	0.516	40	GE Discovery CT750 HD (VEO)
27		21.58	0.4	80	0.516	40	GE Discovery CT750 HD (VEO)
28		29.81 (ATM)	0.4	80	0.516	40	GE Discovery CT750 HD (VEO)
29		33.30 (ATM)	0.4	80	0.516	40	GE Discovery CT750 HD (VEO)
30		122.32 (ATM)	0.285	120	0.900	38.4	Siemens Somatom Definition Flash
31		73.28 (ATM)	0.5	100	1.400	38.4	Siemens Somatom Definition Flash
32		163.19 (ATM)	0.5	100	1.200	38.4	Siemens Somatom Sensation 64
33		63.42 (ATM)	0.5	100	1.400	38.4	Siemens Somatom Definition Flash
34		124.31 (ATM)	0.5	100	1.400	38.4	Siemens Somatom Definition Flash
35		48.31 (ATM)	0.5	100	1.200	38.4	Siemens Somatom Definition Flash
36		160.54 (ATM)	0.5	100	1.200	38.4	Siemens Somatom Definition Flash
37		127.81 (ATM)	0.5	100	1.200	38.4	Siemens Somatom Definition Flash
38		89.89 (ATM)	0.5	100	1.200	38.4	Siemens Somatom Definition Flash
39		77.12 (ATM)	0.5	100	1.200	38.4	Siemens Somatom Definition Flash
40		157.67 (ATM)	0.5	80	1.200	38.4	Siemens Somatom Definition Flash
41		138.39 (ATM)	0.5	80	1.200	38.4	Siemens Somatom Definition Flash

ATM: Automatic Tube current Modulation

VEO: Iterative Reconstruction

* problems with contrast agent administration

TABLE 2

Individual CT parameters for all paediatric patients of present study undergoing a CT chest examination.

CT Abdomen

Patient Number		Tube current (mA)	Exposure time (s)	Tube voltage (kV)	Pitch	Collimation (mm)	Type of CT scanner
1		70.5	0.6	100	1.375	40	GE Discovery CT750 HD
2		325	0.8	100	0.984	40	GE Discovery CT750 HD
3		120	0.5	100	0.844	32	Toshiba Aquilion
4	A	188.63 (ATM)	0.5	120	0.900	38.4	Siemens Somatom Definition Flash
	B*	349.5 (ATM)	0.285	100	0.600	38.4	Siemens Somatom Definition Flash
5		184.21 (ATM)	0.5	100	0.900	38.4	Siemens Somatom Definition Flash
6	A	49.7 (ATM)	0.5	100	1.200	38.4	Siemens Somatom Definition Flash
	B*	47.38 (ATM)	0.5	100	1.200	38.4	Siemens Somatom Definition Flash
7		152.32 (ATM)	0.5	100	1.200	38.4	Siemens Somatom Definition Flash
8		105.69 (ATM)	0.5	100	1.400	38.4	Siemens Somatom Definition Flash
9		122.55 (ATM)	0.5	100	1.400	38.4	Siemens Somatom Definition Flash
10		75.92 (ATM)	0.5	100	1.200	38.4	Siemens Somatom Definition Flash

ATM: Automatic Tube Current Modulation

* One scan with and one scan without contrast agent administration

TABLE 3

Individual CT parameters for all paediatric patients of present study undergoing a CT abdomen examination.

plete RPMI cell culture medium (84% RPMI-1640, 15% Foetal Calf Serum, 1% L-glutamine, 50U/mL penicillin and 50µg/mL streptomycin; Life Technologies, Belgium). For immunofluorescence staining, 250 µL of the resuspended T-lymphocytes was centrifuged onto poly-L-lysine coated slides (VWR International, Belgium). The slides were fixed in 3% paraformaldehyde (PFA) (Sigma-aldrich, Belgium) for 20 minutes and stored overnight in 0.5% PFA. Fixation should immobilize antigens while retaining the lymphocytes as close to their natural state as possible. The next day, slides were permeabilised by dropping 100 µL of 0.2% Triton-X-100 (Sigma-Aldrich, Belgium). This permeabilisation step is required because the anti- γ -H2AX antibody binding requires intracellular access to detect the γ -H2AX protein. The immunofluorescence staining was performed with an unlabelled primary mouse monoclonal anti- γ -H2AX antibody (1:500; Biolegend, Belgium) which specifically binds to the target γ -H2AX protein, followed by a secondary Rabbit Anti-Mouse (RAM) - TRITC antibody (1:1000; DakoCytomation, Denmark). This secondary antibody carries the (TRITC) fluorophore, recognizes the primary anti- γ -H2AX antibody and binds to it. Subsequently, the lymphocyte nucleus was counterstained with -6,4 %2diamidino-2-phenylindole (DAPI) in slow-fade mounting medium (Sigma-Aldrich, Belgium). DAPI is a blue fluorescent stain specific for DNA. Microscopic scoring was performed manually with an Olympus BX60 fluorescence microscope with an Olympus 100x/1.30 oil lens. The images were viewed using Cytovision software and captured with a digital camera (Applied Imaging, USA). Ten optical sections were obtained for each field of vision (Z-stack sections of 1.03 µm). Different images of one blinded slide were stored and on average 250 cells were scored manually for γ -H2AX foci. More than 250 cells were scored for every condition and the number of γ -H2AX foci induced by CT x-rays was obtained by subtracting the pre-scan foci yield from the post-scan foci yield after decoding. The scoring procedure was validated by double immunostaining for both γ -H2AX and p53 binding protein 53) 1BP1), to discriminate between background artefacts and small γ -H2AX

foci. The experiments demonstrated that the γ -H2AX-TRITC foci coincide with 53BP-1FITC foci, resulting in a statistical significant agreement between the number of double stained foci (merge) and the number of individual γ -H2AX-TRITC foci (results not shown).

B. *In vitro* dose response study on umbilical cord blood samples

For the validation of the *in vivo* results, a set of *in vitro* experiments was performed. Unfortunately, it was not possible to have access to blood samples with a larger volume than 2 mL from young children, due to ethical constraints. Since umbilical cord blood is physiologically and genetically part of the foetus, we can consider this as blood of a newborn [18]. Therefore, umbilical cord blood samples were irradiated *in vitro* in order to compare the γ -H2AX foci dose response after *in vivo* and *in vitro* exposure. Cord blood samples from three healthy donors were exposed to 1, 2, 4, 6, 8, 10, 15, 20 and 500 mGy and one blood sample was sham-irradiated. A radiation quality of 100-kVp x-rays and 2 mm Al filtration was used, with a Philips MG420 x-ray generator coupled to a MCN420 tube. The irradiation was carried out in a 37°C water bath. Calibration was performed with an NE2571 Farmer ionization chamber (Thermo Electron, Altrincham, UK). The irradiated blood samples were kept for 30 minutes at 37°C, followed by 15 minutes on ice water to simulate the situation of patient blood samples after *in vivo* exposure. The same γ -H2AX foci protocol and scoring method as described for the *in vivo* study was applied. The use of cord blood for *in vitro* experiments was approved by the institutional review board.

C. Patient dosimetry

Calculation of blood and organ doses induced by CT x-rays by full Monte Carlo simulation

The blood dose was calculated as a weighted sum of doses to the largest blood containing organs with the percentage of blood pool as weighting factor, namely lungs (12.5%), heart (10%), liv-

er (10%) and remainder (67.5%) [19]. In order to obtain individual organ dose estimates, an individualized full Monte Carlo patient dose simulation was set up using ImpactMC simulation software 1.3.1 (CT Imaging GmbH, Germany). In the latter software, patient-specific 3D voxel models are created based on the CT images acquired during CT examination [20]. For the simulation of the CT scan, actual scan parameters such as tube voltage (kV), tube current - exposure time product (mAs) and pitch, are retrieved from the DICOM header of the CT images. The individual mA values of all the reconstructed CT slices were used in order to take into account the tube current modulation of the CT scanner. More than 10^{10} photons were simulated in order to minimize the uncertainty in the Monte Carlo results. The patient specific dose distribution was determined by multiplying the air-kerma normalized dose distribution from the simulations with the actual air-kerma value (mGy) measured free-in-air in the iso-center of the scanner by using a pencil ionization chamber (RaySafe Xi CT detector, Unfors RaySafe, Sweden). In addition to the organ doses needed for the blood dose evaluation, doses to other organs and tissues of interest according to the BEIR VII risk models were also calculated with this Monte Carlo patient dose simulation. Organ volumes were segmented in the original CT images and organ dose deposition was calculated based on the Monte Carlo dose distribution. For the bone marrow, all bony structures in the field of view were segmented and the bone marrow dose was calculated as the weighted sum of the doses to these structures with the percentage of bone marrow in these compartments as weighting factor [21]. To account for differences in photon absorption in bone and bone marrow, the obtained value was corrected for the ratio of mass absorption coefficients in soft tissue and bone [22].

Calculation of effective dose

To compare the dose levels of the CT procedures in the current study with similar procedures in different hospitals and countries, the effective dose was calculated for the total group of CT chest and CT abdomen patients. Effective

dose is a quantity reflecting the stochastic risk associated with an exposure to ionizing radiation at a population level. The effective doses of the paediatric populations under study were derived from the individual DLP values by using the conversion factors published by Deak et al. as function of kVp, imaging region and age for ICRP publication 103 recommendations [23].

D. Risk estimation

Individual LAR of cancer incidence and mortality related to a chest or abdomen CT scan were calculated according to the BEIR VII risk models for different cancer types, taking into account age-dependent incidence and mortality rates within the Euro-American population [24]. Input for these risk assessments were the simulated organ doses and the age of the individual patients. The LAR data from BEIR VII were adapted for a dose and dose-rate effectiveness factor of 2 as proposed by the ICRP [25].

E. Statistical Analysis

Statistical analysis was performed with Microsoft Office Excel 2010 (Microsoft Corporation, USA) and Statistical Package for Social Sciences software version 22 (SPSS Inc., USA). Poisson statistics were applied to calculate the statistical accuracy of the number of x-ray induced γ -H2AX foci. The differences between the pre- and post-CT data sets were evaluated for significance with the paired sample Wilcoxon signed-rank test (95% confidence level). Linear regression analysis was applied to evaluate age dependence. A p-value less than 0.05 was considered as statistically significant.

RESULTS

A. Assessment of DNA DSBs in pre- and post-CT blood samples of paediatric patients

An increase in DNA DSBs was observed for every patient, except for one CT chest patient with a very low blood dose of 0.14 mGy. The median pre-exposure level was 0.56 foci/cell (range 0.23 - 1.20 foci/cell) and the post-exposure level was 0.72 foci/cell (range 0.31 - 1.44 foci/cell). The pre- and post- CT exposure foci levels are presented in Figure 1 for every individual patient. The median number of induced foci representing DNA DSBs induced by CT was 0.13 foci/cell (range -0.07 - 0.49 foci/cell) and the median blood dose 0.94 mGy (range 0.14 - 8.85 mGy). Present study shows that nearly every CT procedure induces DNA DSBs in T-lymphocytes of paediatric patients. A Wilcoxon signed-rank test showed a statistically significant difference in the mean level of DNA DSBs pre-CT and the mean level post-CT per patient ($p < 0.001$). Moreover, the number of induced DSBs is strongly blood dose dependent as illustrated in Figure 2.

To investigate the intrinsic higher radiosensitivity of children decreasing with age, the number of induced γ -H2AX foci was divided by the calculated blood dose and plotted versus age of the paediatric patient. The linear fit in Figure 3 indicates a diminishing trend of the foci-over-dose ratio versus age, however regression analysis showed that the decrease of the foci-over-dose ratio versus age was not statistically significant ($p = 0.204$).

B. In vitro dose response study on umbilical cord blood samples

The results of the *in vitro* irradiation of umbilical cord blood, repeated for 3 different donors, are also presented in Figure 2. The *in vivo* and *in vitro* dose response curves show both an initial sharp increase with dose and appear not linear at all. The dashed line in Figure 2 represents an extrapolation according to the LNT hypothesis of the *in vitro* dose response of γ -H2AX foci in cord blood at higher doses (5.68 γ -H2AX foci/cell for 0.5 Gy) to zero. This shows clearly that the foci numbers in the low-dose range are much higher than expected from the LNT extrapolation of high dose behaviour.

PART II

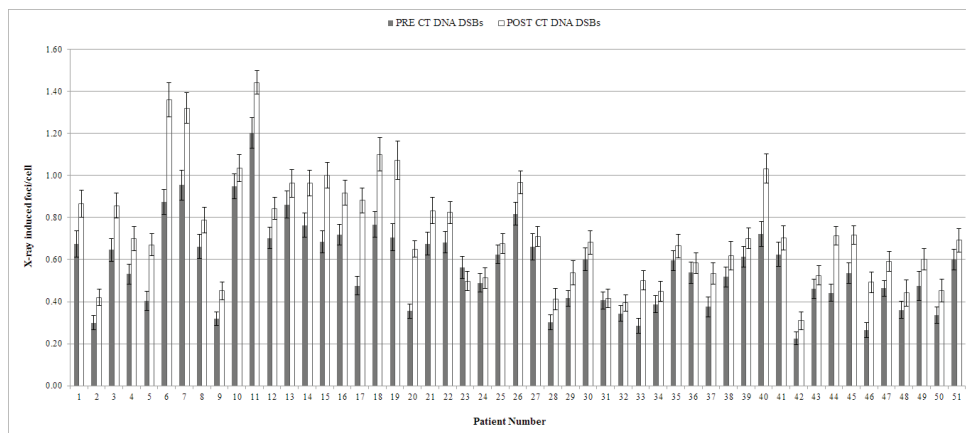


FIGURE 1

Comparison of γ -H2AX-foci levels pre- and post-CT x-ray exposure for every individual patient of the study. Error bars represent standard deviations on foci yields calculated following Poisson statistics.

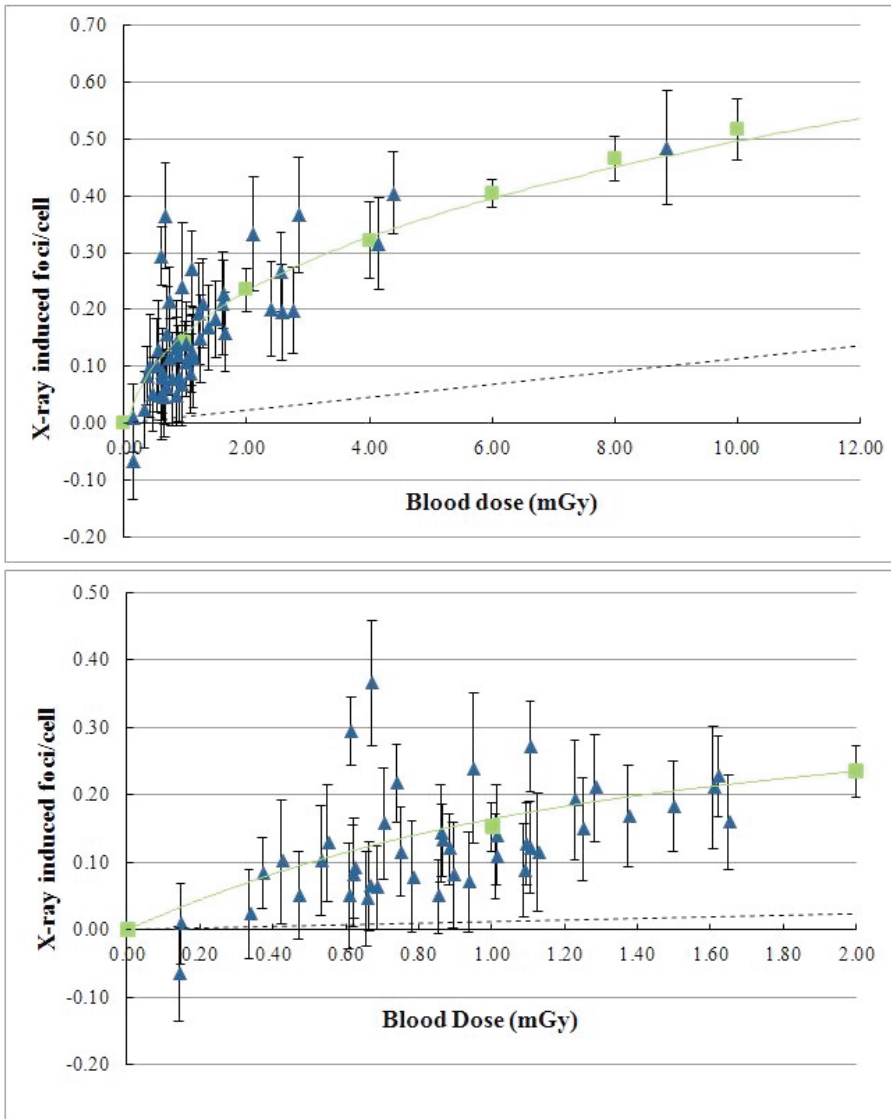


FIGURE 2

(a) The mean number of γ H2AX-foci per cell induced by in vivo x-ray exposure plotted versus the Monte Carlo calculated blood dose for every paediatric patient undergoing a CT chest or CT abdomen (in blue). The whiskers represent standard deviations derived from the statistical accuracy of the scored number of foci in the blood samples taken before and after CT examination (Poisson statistics). The dose-response curve after in vitro x-ray irradiation of cord blood is also shown (in green). The whiskers of the in vitro study represent SDs among the three different donors. The dashed line represents a linear extrapolation based on the γ -H2AX foci induced in cord blood after an in vitro dose of 0.5 Gy, based on the LNT hypothesis. Since a large part of the data are clustered in 0-2 mGy range, this range is presented as a separate figure (b).

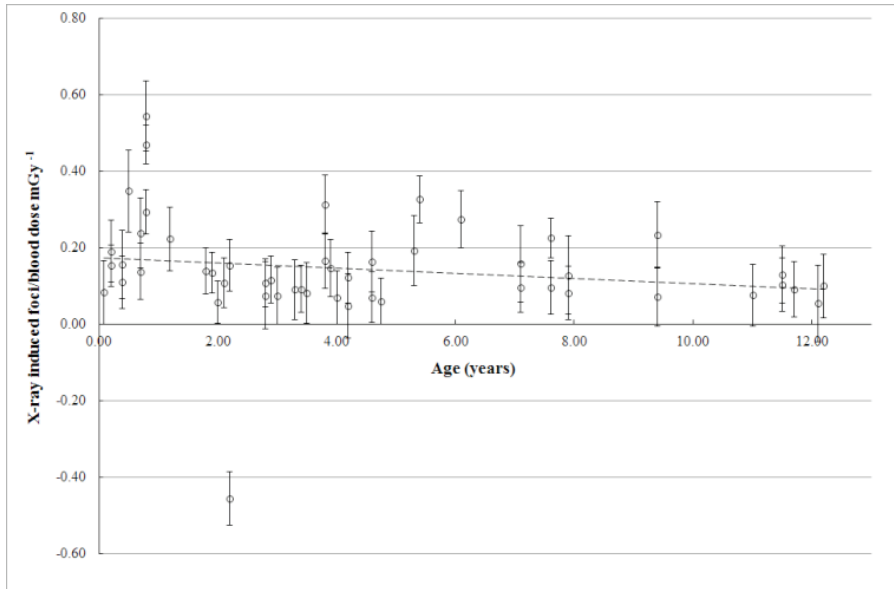


FIGURE 3

The number of γ -H2AX foci normalized to blood dose, as a function of age of the paediatric patients. The dashed line is the result of a linear fit.

PART II

C. Patient dosimetry

Monte Carlo calculations resulted in a median blood dose for CT chest patients of 0.86 mGy (0.14 – 2.84 mGy) and for CT abdomen patients of 1.62 mGy (0.66 – 8.85 mGy). The median effective dose value for the CT chest patient cohort was 1.14 mSv (range 0.17 mSv – 3.10 mSv). For the CT abdomen patient cohort, the median effective dose value was higher, namely 2.82 mSv (range 1.18 mSv – 10.55 mSv). A comparison of these values with literature data confirms that in present study patient doses were low [26, 27]. All participating centres used state-of-the-art low dose equipment and specific paediatric protocols, resulting in very low CTDI_{vol} and DLP values of the patients compared with the national dose reference levels (DRLs) (Table 4). Reference levels are typically set at the 75th percentile of the dose distribution from a conducted survey. The median CTDI_{vol} and DLP values in the current study are below the 75th percentile values and close to the 25th percentile, which represents good clinical

practice. However, substantial differences in dose sparing equipment and imaging protocols for children resulted in differences in patient doses and corresponding DNA damage. Figure 4 shows a clear correlation between both parameters when comparing the data for the different participating hospitals. This figure emphasizes that the use of more powerful dose reduction techniques and protocols involving a lower patient dose, results also in less radiation effects for paediatric patients according to the DNA damage effect biomarker.

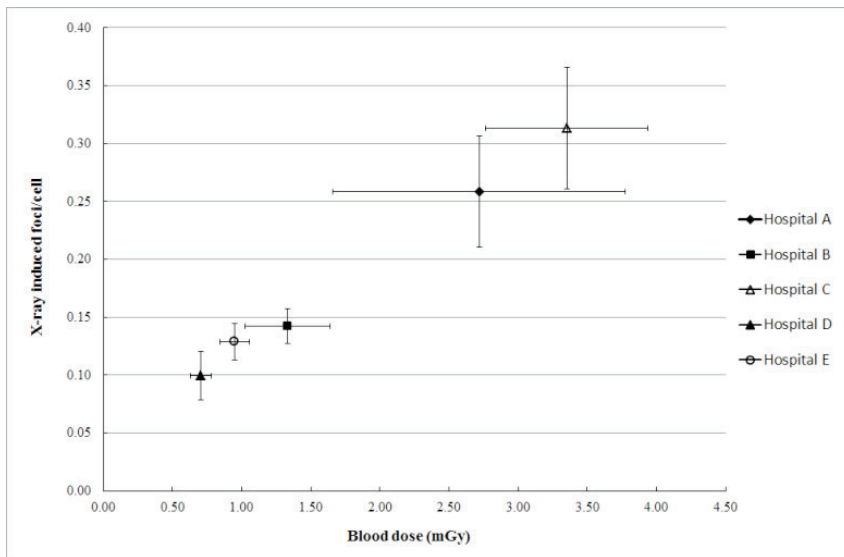
D. Risk estimation

Based on the Monte Carlo calculated organ doses, individual lifetime attributable risk values for cancer incidence and mortality according to the BEIR VII risk models were calculated for every patient. The BEIR VII report provides a method to estimate LAR of cancer incidence and mortality based on the organ doses associated with the radiation exposure and a patient's age at

	CT Chest	CT Abdomen
CTDIvol (mGy)		
25 th percentile	1.85	2.80
75 th percentile (DRL)	5.00	6.75
study data	1.54 (0.22-4.07)	4.17 (1.11-13.98)
DLP (mGycm)		
25 th percentile	40.00	100.00
75 th percentile (DRL)	130.00	315.00
study data	24.80 (4.57-130.36)	315 (33.00-698.82)

TABLE 4

Comparison of the median CTDIvol (mGy) and DLP (mGycm) values of the CT chest and CT abdomen investigations in this study with the national DRLs (75th percentile) in Belgium. As an indication of good clinical practice, also the 25th percentile is presented.

**FIGURE 4**

The mean γ -H2AX foci per cell induced by CT x-rays plotted against the mean patient blood dose for participating centres. The CT equipment used by the participating centres was as follows: hospital A - GE Discovery CT750 HD, hospital B - GE Discovery CT750 HD (VEO), hospital C - Siemens Somatom Definition Flash and Toshiba Aquilion, hospital D - GE Discovery CT750 HD (VEO), hospital E - Siemens Somatom Definition Flash and Sensation 64. Whiskers represent the standard deviation on the mean of foci numbers and blood doses.

the time of exposure. Table 5 represents the median LAR values of cancer incidence and mortality related to leukaemia and different types of solid cancer of organs in the field of view based on the simulated organ doses. The range of LAR values over the patient cohorts is indicated between brackets. For the total patient cohort undergoing

a CT chest examination the LAR values for cancer incidence and mortality are respectively 0.17 per thousand and 0.08 per thousand. For the total group of paediatric patients undergoing a CT abdomen examination the LAR incidence and mortality are respectively 0.32 per thousand and 0.13 per thousand.

CT Chest				
	LAR _{incidence} ‰	LAR _{mortality} ‰	LAR _{incidence} ‰	LAR _{mortality} ‰
	Male (30)		Female (11)	
<i>Age, y</i>	3.20 (0.20 - 11.50)		2.00 (0.10 - 12.20)	
<i>Blood dose, mGy</i>	0.81 (0.14 - 2.84)		0.86 (0.55 - 2.56)	
<i>Stomach</i>	0.007 (0.001 - 0.017)	0.004 (0.001 - 0.009)	0.011 (0.005 - 0.033)	0.006 (0.003 - 0.019)
<i>Liver</i>	0.005 (0.001 - 0.011)	0.003 (0.001 - 0.008)	0.002 (0.001 - 0.005)	0.002 (0.001 - 0.005)
<i>Lung</i>	0.034 (0.006 - 0.130)	0.035 (0.006 - 0.131)	0.088 (0.049 - 0.275)	0.077 (0.043 - 0.241)
<i>Breast</i>	0.159 (0.048 - 0.415)	0.037 (0.011 - 0.097)
<i>Thyroid</i>	0.011 (0.002 - 0.032)	...	0.078 (0.043 - 0.141)	...
<i>Remainder</i>	0.037 (0.005 - 0.094)	0.014 (0.002 - 0.034)	0.038 (0.020 - 0.146)	0.014 (0.008 - 0.055)
<i>Leukemia</i>	0.002 (0.000 - 0.007)	0.001 (0.000 - 0.004)	0.002 (0.001 - 0.003)	0.001 (0.000 - 0.002)
<i>All cancers</i>	0.099 (0.015 - 0.287)	0.055 (0.009 - 0.184)	0.378 (0.171 - 1.016)	0.137 (0.067 - 0.417)
CT Abdomen				
	LAR _{incidence} ‰	LAR _{mortality} ‰	LAR _{incidence} ‰	LAR _{mortality} ‰
	Male (7)		Female (3)	
<i>Age, y</i>	7.10 (1.80 - 12.10)		7.90 (6.10 - 11.00)	
<i>Blood dose, mGy</i>	1.61 (0.66 - 8.85)		1.38 (1.09 - 4.15)	
<i>Stomach</i>	0.018 (0.007 - 0.058)	0.009 (0.004 - 0.030)	0.010 (0.008 - 0.035)	0.006 (0.005 - 0.020)
<i>Colon</i>	0.089 (0.035 - 0.337)	0.043 (0.017 - 0.158)	0.045 (0.028 - 0.110)	0.021 (0.013 - 0.051)
<i>Liver</i>	0.014 (0.006 - 0.047)	0.010 (0.004 - 0.033)	0.005 (0.002 - 0.013)	0.004 (0.002 - 0.011)
<i>Lung</i>	0.018 (0.011 - 0.065)	0.018 (0.011 - 0.063)	0.067 (0.031 - 0.068)	0.059 (0.027 - 0.059)
<i>Prostate</i>	0.024 (0.004 - 0.075)	0.005 (0.001 - 0.032)
<i>Uterus</i>	0.008 (0.005 - 0.021)	0.002 (0.001 - 0.005)
<i>Ovary</i>	0.021 (0.009 - 0.042)	0.011 (0.005 - 0.023)
<i>Bladder</i>	0.054 (0.010 - 0.176)	0.012 (0.002 - 0.037)	0.039 (0.002 - 0.099)	0.011 (0.006 - 0.028)
<i>Remainder</i>	0.077 (0.015 - 0.274)	0.027 (0.005 - 0.096)	0.100 (0.029 - 0.273)	0.025 (0.012 - 0.071)
<i>Leukemia</i>	0.008 (0.002 - 0.029)	0.003 (0.001 - 0.018)	0.005 (0.004 - 0.015)	0.002 (0.002 - 0.009)
<i>All cancers</i>	0.318 (0.091 - 1.047)	0.131 (0.046 - 0.445)	0.329 (0.263 - 0.677)	0.130 (0.108 - 0.277)

TABLE 5

LAR of cancer incidence and mortality following the BEIR VII model, associated with x-ray exposure from CT chest and CT abdomen examinations for the cohort of paediatric patients included in the study. Values are median (range), based on the individual simulated organ doses and the age of the individual patients.

DISCUSSION

Our study provides evidence that CT induces DNA damage in paediatric patients, even at low doses (blood doses in the range of 0.15 - 8.85 mGy). Several studies reported γ -H2AX foci induction by CT x-ray exposure in adult patients [10-13, 28]. However none of them investigated the DNA damage induced by CT radiation exposure in paediatric patients, nor the ultra-low dose region evaluated in current study. There was already a small scale pilot study with blood samples from ten paediatric patients undergoing CT examinations, in which chromosome analysis in lymphocytes showed a significant increase in dicentric frequencies and excess acentric fragments [29]. However, the mean blood dose of the cohort of ten children in the study of Stephan *et al.* was 12.9 mGy compared to the low mean blood dose of 1.35 mGy for the 51 patients in the current study.

Currently, the vast majority of publications use the concept of effective dose to assess CT radiation burden. However, effective dose calculations can never be linked to an individual patient exposure, as reference phantoms need to be used and the quantity effective dose is designed for risk estimation in a population. To interpret the *in vivo* γ -H2AX foci data, it is very important to have an accurate blood dose calculation for every patient, which takes into account the patient's anatomy, different types of CT scanners, dose reduction technologies and various types of CT protocols. However, the latter analysis cannot be performed by using effective dose. This was accomplished by a Monte Carlo simulation of radiation transport in patient specific 3D voxel models derived from the CT images. For dosimetry of paediatric patients the use of voxel models is a substantial improvement compared to dose calculation based on anthropomorphic paediatric standard phantoms, as the full Monte Carlo simulation takes into account the real anatomy of the patient.

In addition the results of present study show that lower patient doses related to more effective CT dose reduction strategies for paediatric patients result also in a similar decrease in DNA DSBs as effect biomarker. It is internationally rec-

ognized that CT dose optimization is essential, especially for children taking into account not only dose reduction but also diagnostic image quality. A number of CT dose surveys showed substantial differences between practices for the same type of examination, suggesting that not all institutions have suitably optimized their CT protocols [30, 31]. Dose saving strategies are continuously evolving in terms of imaging techniques as well as dose management and the result of the present study, stress the importance of dose reduction in paediatric CT imaging. As already shown by the values of the calculated blood doses and the comparison of DLP and $CTDI_{vol}$ values with national DRLs, paediatric CT radiation doses were substantially low in all participating radiology departments. One of the institutions (hospital D in Figure 4) achieved very low doses (mean blood dose, 0.71 mGy) by using iterative reconstruction for all CT examinations, however only CT chest patients were recruited in this institution. For the patient cohort of institution D, a very low mean level of induced γ -H2AX foci per cell (0.10 foci/cell) was recorded. Hospital E achieved a mean blood dose of 0.95 mGy corresponding with 0.13 induced foci/cell and the data for this hospital are a mixture of CT chest and CT abdomen investigations. For both types of examination DLP values in this hospital were very low compared to the DRL (reported in Table 4). The median DLP value for CT abdomen patients in hospital E was 60.00 mGycm (range, 33.00 - 87.20 mGycm), which is lower than the 25th percentile of 100 mGycm.

When the number of induced γ -H2AX foci is plotted versus blood dose, the data point to a low-dose hypersensitivity. The observed low-dose hypersensitive response in paediatric CT is in agreement with the data of a previous study on paediatric patients undergoing a cardiac catheterization [17]. The *in vitro* dose response curve on umbilical cord blood shows the same behaviour in the low-dose range and supports the *in vivo* results.

The observed low dose hypersensitivity challenges the LNT hypothesis, assuming less DNA-damage, and can be explained by the "bystander effect" [32]. Genetic/epigenetic changes occur not only in cells hit by the ionizing particles but also in non-irradiated cells that are neighbouring

directly-hit cells. The bystander effect amplifies the effects of radiation by increasing the number of affected cells, due to cell-cell communication or soluble factors released by irradiated cells. Bystander effects are observed after co-cultivation of irradiated and non-irradiated cells and transfer of medium from irradiated to non-irradiated cells [33, 34]. For cells in direct contact, bystander signalling can occur through gap-junctional intercellular communication [35, 36]. A second route by which bystander responses are mediated is through the release of soluble factors from cells that have been irradiated. These factors have been extensively studied and several of these key molecules are central players involved in stress responses and cell-cell signalling, which are not generally specific to radiation exposure [35]. Moreover, many aspects of bystander mediated response have close parallels to inflammatory responses. This was recently shown in a gene set enrichment analysis, that highlighted different gene expression profiles in whole blood samples irradiated with low and high doses of x-rays. Functional analysis of genes differentially expressed at 0.05 Gy showed the enrichment of chemokine and cytokine signalling [37]. In a study of Mancuso *et al.*, DNA damage, apoptosis and tumour induction were observed in the shielded cerebellum of mice heterozygous for *Patched* after partial-body irradiations [38]. This indicates that bystander effects *in vivo* have carcinogenic potential.

A possible confounder in present study could be the increase in DSB levels due to the administration of contrast agent and the corresponding emission of secondary radiation in CT imaging. However, previous studies showed that there was no biological dose enhancing effect if radiation and contrast agent are within the diagnostic range [11,39].

Epidemiological data indicate a higher relative risk of cancer per unit of radiation dose for children compared to adults and children have also a longer lifetime for radiation-related cancer to occur [2]. We observed a non-significant age-dependency in our present study of x-ray induced DNA DSBs. To study age dependence, the study population should be broadened and a more uniform distribution of the ages is required.

Using the calculated organ doses, the LAR for cancer mortality in the paediatric patient population undergoing a low dose chest or abdomen CT was of the order of 0.1‰ according to the BEIR VII data assuming the LNT hypothesis. The thyroid gland, breast tissue and gonads are structures that have an increased sensitivity to radiation in growing children. Some of these regions, as thyroid and breast tissue, are routinely involved in CT chest scanning. Miglioretti *et al.* [27] calculated radiation exposure and LAR for cancer incidence from a random sample of paediatric CT scans. The calculated lifetime attributable risks reported in this paper are an order of magnitude higher than those reported in the current study: CT abdomen 1-4 ‰ versus 0.3 ‰ (median), CT chest 2-3 ‰ versus 0.1-0.4 ‰ (median boys-girls). The main reason for the lower risk estimates in the current study are lower patient doses compared to the work of Miglioretti *et al.* [27]. They reported a mean ED of 12.5 mSv for CT abdomen and 6.3 mSv for CT chest, where in present work median ED values were 2.8 mSv and 1.1 mSv respectively. The lower doses and corresponding risk estimates in current work reflect the use of contemporary state-of-the-art low-dose CT equipment and the successful implementation of dose reduction strategies for paediatric CT imaging by the participating radiology departments (as illustrated in Table 4).

Large uncertainties are associated with the risk estimates summarized in Table 5. The BEIR VII committee estimates that the excess cancer mortality due to radiation can be estimated within a factor of two (at 95% confidence level). For leukaemia the corresponding factor is four. The LNT model applied by the BEIR VII committee is based mainly on epidemiological data for radiation induced cancers in the atomic bomb survivors in the dose range of about 100 mSv to 2.5 Sv [8]. For lower doses involved in diagnostic radiology epidemiological data are not available to support the LNT model mainly owing to the necessary sample size [40]. Application of the LNT hypothesis in the low dose range may lead to an overestimation of the risk in case of the existence of a dose threshold or an underestimate in case of cooperative multicellular radiation effects such as bystander effects. It is anticipated that signifi-

cant insights in dose response and cancer risks in the low dose range will emerge from molecular epidemiology studies incorporating biomarkers and bioassays [41]. The low dose hypersensitivity observed in the γ -H2AX foci dose response of present study indicates that LAR estimates based on the LNT model may potentially underestimate the risks of paediatric CT imaging.

For conclusions with respect to the risk of stochastic effects of x-rays present study has limitations. Biological damage in T-lymphocytes reflects only the damage in one tissue, namely the blood. However, we may assume that DNA damage and repair in peripheral blood lymphocytes is representative for other normal tissues [42]. Using the γ -H2AX foci assay, only DNA DSBs induced by CT x-rays are detected but not the outcome of the DNA repair process. DNA DSBs are considered to be particularly biologically important because their repair is more difficult than other types of DNA damage. Cells have evolved mechanisms to monitor genome integrity and they respond to DNA damage by activating a complex DNA damage response pathway. Erroneous repair of DNA DSBs can result in chromosomal rearrangements, including translocations, which are associated with tumorigenesis [43]. An increase in chromosomal aberrations, due to a defect in DNA repair as observed in Ataxia Telangiectasia (AT) patients, leads to genetic instability, which in turn enhances the rate of cancer development [44]. In the framework of cancer risk, a direct assessment of mutations in DNA or chromosomal aberrations induced by CT x-rays in paediatric patient's lymphocytes would provide added value taking into account the mutagen-carcinogen link. However, this kind of studies is not obvious in view of the low sensitivity of contemporary mutagenicity assays.

Present study emphasizes the need to optimize and minimize radiation exposure in paediatric CT imaging: lower patient doses entail less DNA damage in children. This implies justification of the indications for which medical imaging involving ionizing radiation is used. From a patient's perspective, the benefits of a medically necessary CT scan far exceed the small radiation-induced cancer risk. However, some studies suggest that a third of paediatric CT scans

are unnecessary [1]. This indicates that the referring physician and radiologist should consider whether the exam is truly clinically indicated and was not recently performed in another hospital. Furthermore, they should check if no alternative diagnostic procedure might be available, not involving ionizing radiation such as ultrasound and MRI. When CT is indicated, great care should be taken to optimize radiation exposures in order to minimize the risk for carcinogenic effects later in life. Strategies to optimize radiation doses in paediatric CT imaging are: adjustment of the CT parameters to the child's size (guidelines on individual size/weight parameters [45]), the scan length should be restricted to the region of interest and dose reduction techniques should be implemented taking into account the required image quality (ATCM, iterative reconstruction and/or adaptive collimation). The observations of present work should encourage medical practitioners to maximize the benefit-to-risk ratio of CT imaging in paediatric radiology.

ACKNOWLEDGEMENTS

We wish to thank all patients and their parents to participate in this study. We express also our gratitude to Hilde Vandenhout, Ilse Roebben and the nurses of the participating hospitals for their help with the collection of blood samples. A special thank you to Dr. Wim Decaluwe from the neonatology department at AZ Sint-Bruges, for his support and dedication to this study. Furthermore, we acknowledge the master thesis students for their help with processing of the blood samples. Above all, we would like to thank Virginie De Gelder and Sofie De Langhe for their practical support. The study was financially supported by the Federal Agency of Nuclear Control, Belgium (CO-90-09-2329-00).

REFERENCES

- Brenner DJ, Hall EJ (2007) Current concepts - Computed tomography - An increasing source of radiation exposure. *N Engl J Med* 357:2277-2284
- UNSCEAR (2013) Sources, Effects and Risks of ionizing radiation. Report to the General Assembly of the United Nations. New York
- Nivelstein RAJ, van Dam IM, van der Molen AJ (2010) Multidetector CT in children: current concepts and dose reduction strategies. *Pediatr Radiol* 40:1324-1344
- Strauss KJ, Goske MJ, Kaste SC, et al (2010) Image Gently: Ten Steps You Can Take to Optimize Image Quality and Lower CT Dose for Pediatric Patients. *Am J Roentgenol* 194:868-873
- Gay F, Pavia Y, Pierrat N, Lasalle S, Neuenschwander S, Brisse HJ (2014) Dose reduction with adaptive statistical iterative reconstruction for paediatric CT: phantom study and clinical experience on chest and abdomen CT. *Eur Radiol* 24:102-111
- Brady SL, Moore BM, Yee BS, Kaufman RA (2014) Pediatric CT: Implementation of ASIR for Substantial Radiation Dose Reduction While Maintaining Pre-ASIR Image Noise. *Radiology* 270:223-231
- Pearce MS, Salotti JA, Little MP, et al (2012) Radiation exposure from CT scans in childhood and subsequent risk of leukaemia and brain tumours: a retrospective cohort study. *Lancet* 380:499-505
- Preston DL, Shimizu Y, Pierce DA, Suyama A, Mabuchi K (2012) Studies of Mortality of Atomic Bomb Survivors. Report 13: Solid Cancer and Noncancer Disease Mortality: 1950-1997. *Radiat Res* 178:AV146-AV172
- Morgan WF, Bair WJ (2013) Issues in Low Dose Radiation Biology: The Controversy Continues. A Perspective. *Radiat Res* 179:501-510
- Rothkamm K, Balroop S, Shekhdar J, Fernie P, Goh V (2007) Leukocyte DNA damage after multi-detector row CT: A quantitative biomarker of low-level radiation exposure. *Radiology* 242:244-251
- Beels L, Bacher K, Smeets P, Verstraete K, Vral A, Thierens H (2012) Dose-length product of scanners correlates with DNA damage in patients undergoing contrast CT. *Eur J Radiol* 81:1495-1499
- Lobrich M, Rief N, Kuhne M, et al (2005) In vivo formation and repair of DNA double-strand breaks after computed tomography examinations. *Proceedings of the National Academy of Sciences of the United States of America* 102:8984-8989
- Kuefner MA, Grudzenski S, Hamann J, et al (2010) Effect of CT scan protocols on x-ray-induced DNA double-strand breaks in blood lymphocytes of patients undergoing coronary CT angiography. *Eur Radiol* 20:2917-2924
- Rothkamm K, Horn S (2009) gamma-H2AX as protein biomarker for radiation exposure. *Ann Ist Super Sanita* 45:265-271
- Rothkamm K, Lobrich M (2003) Evidence for a lack of DNA double-strand break repair in human cells exposed to very low x-ray doses. *Proceedings of the National Academy of Sciences of the United States of America* 100:5057-5062
- Beels L, Werbroeck J, Thierens H (2010) Dose response and repair kinetics of gamma-H2AX foci induced by in vitro irradiation of whole blood and T-lymphocytes with X- and gamma-radiation. *Int J Radiat Biol* 86:760-768
- Beels L, Bacher K, De Wolf D, Werbroeck J, Thierens H (2009) gamma-H2AX Foci as a Biomarker for Patient X-Ray Exposure in Pediatric Cardiac Catheterization Are We Underestimating Radiation Risks? *Circulation* 120:1903-1909
- Carroll PD, Nankervis CA, Iams J, Kelleher K (2012) Umbilical cord blood as a replacement source for admission complete blood count in premature infants. *Journal of Perinatology* 32:97-102
- Valentin J (2002) Basic anatomical and physiological data for use in radiological protection: reference values: ICRP Publication 89. *Annals of the ICRP* 32:1-277
- Deak P, van Straten M, Shrimpton PC, Zankl M, Kalender WA (2008) Validation of a Monte Carlo tool for patient-specific dose simulations in multi-slide computed tomography. *Eur Radiol* 18: 759-772
- Cristy M (1981) Active bone-marrow distribution as a function of age in humans. *Phys Med Biol* 26:389-400
- Seuntjens J, Thierens H, Vanderplaetsen A, Segart O (1987) Conversion factor F for X-ray beam qualities, specified by peak tube potential and HVL value. *Phys Med Biol* 32:595-603
- Deak PD, Smal Y, Kalender WA (2010) Multisection CT Protocols: Sex- and Age-specific Conversion Factors Used to Determine Effective Dose from Dose-Length Product. *Radiology* 257:158-166
- National Research Council (2006) Health Risks from Exposure to Low Levels of Ionizing Radiation: BEIR VII Phase 2. The National Academies Press Washington, DC
- International Commission on Radiological Protection (2007) The 2007 Recommendations of the International Commission on Radiological Protection. ICRP publication 103. *Ann ICRP* 37 (2-4)
- Thomas KE, Wang B (2008) Age-specific effective doses for pediatric MSCT examinations at a large children's hospital using DLP conversion coefficients: a simple estimation method. *Pediatr Radiol* 38:645-656
- Miglioretti DL, Johnson E, Williams A, et al (2013) The Use of Computed Tomography in Pediatrics and the Associated Radiation Exposure and Estimated Cancer Risk. *JAMA Pediatr* 167:700-707
- Geisel D, Zimmermann E, Rief M et al (2012) DNA double-strand breaks as potential indicators for the biological effects of ionising radiation exposure from cardiac CT and conventional coronary angiography: a randomised, controlled study. *Eur Radiol* 22:1641-1650

- Stephan G, Schneider K, Panzer W, Walsh L, Oestreicher U (2007) Enhanced yield of chromosome aberrations after CT examinations in paediatric patients. *Int J Radiat Biol* 83:281-287
- Shrimpton PC, Hillier MC, Lewis MA, Dunn M (2006) National survey of doses from CT in the UK: 2003. *Br J Radiol* 79:968-980
- Pages J, Buisson N, Osteaux M (2003) CT doses in children: a multicentre study. *Br J Radiol* 76:803-811
- Morgan WF (2012) Non-targeted and Delayed Effects of Exposure to Ionizing Radiation: I. Radiation-Induced Genomic Instability and Bystander Effects In Vitro. *Radiat Res* 178:AV223-AV236
- Little JB, Azzam EI, de Toledo SM, Nagasawa H (2005) Characteristics and mechanisms of the bystander response in monolayer cell cultures exposed to very low fluences of alpha particles. *Radiation Physics and Chemistry* 72:307-313
- Sokolov MV, Smilenov LB, Hall EJ, Panyutin IG, Bonner WM, Sedelnikova OA (2005) Ionizing radiation induces DNA double-strand breaks in bystander primary human fibroblasts. *Oncogene* 24:7257-7265
- Prise KM, O'Sullivan JM (2009) Radiation-induced bystander signalling in cancer therapy. *Nature Reviews Cancer* 9:351-360
- Azzam EI, de Toledo SM, Little JB (2001) Direct evidence for the participation of gap junction-mediated intercellular communication in the transmission of damage signals from alpha-particle irradiated to nonirradiated cells. *Proc Natl Acad Sci U S A* 98:473-478
- El-Sagheer H, Thierens H, Monsieurs P, Michaux A, Vandevoorde C, Baatout S (2013) Gene set enrichment analysis highlights different gene expression profiles in whole blood samples X-irradiated with low and high doses. *Int J Radiat Biol* 89:628-638
- Mancuso M, Pasquali E, Leonardi S et al (2008) Oncogenic bystander radiation effects in Patched heterozygous mouse cerebellum. *Proc Natl Acad Sci U S A* 105:12445-12450
- Jost G, Golfier S, Pietsch H et al (2009) The influence of x-ray contrast agents in computed tomography on the induction of dicentric and gamma-H2AX foci in lymphocytes of human blood samples. *Phys Med Biol* 54:6029-6039
- Brenner D, Doll R, Goodhead D et al (2003) Cancer risks attributable to low doses of ionizing radiation: Assessing what we really know. *Proc Natl Acad Sci U S A* 100: 13761-13766
- Pernot E, Hall J, Baatout S et al (2012) Ionizing radiation biomarkers for potential use in epidemiological studies. *Mutat Res* 751: 258-286
- Rübe CE, Grudzinski S, Kühne M et al (2008) DNA double-strand break repair of blood lymphocytes and normal tissues analysed in a preclinical mouse model: implication for radiosensitivity testing. *Clin Cancer Res* 14:6546-6555
- Richardson C, Jasin M (2000) Frequent chromosomal translocations induced by DNA double-strand breaks. *Nature* 405: 697-700
- Khanna KK, Jackson SP (2001) DNA double-strand breaks: signalling, repair and the cancer connection. *Nature Genetics* 27: 247-253
- Singh S, Kalra MK, Moore MA et al (2009) Dose reduction and compliance with pediatric CT protocols adapted to patient size, clinical indication, and number of prior studies. *Radiology* 252: 200-208

8

PAPER III

**Radiation sensitivity of human
CD34+ cells versus peripheral
blood T-lymphocytes of
newborns and adults: DNA repair
and mutagenic effects**

Vandevoorde C¹, Vral A¹, Vandekerckhove B², Philippé J², Thierens H¹

¹ Ghent University, Department of Basic Medical Sciences

² Ghent University, Department of Clinical Chemistry, Microbiology and Immunology

Submitted to Radiation Research

Radiation sensitivity of human CD34+ cells versus peripheral blood T-lymphocytes of newborns and adults: DNA repair and mutagenic effects

ABSTRACT

As haematopoietic stem and progenitor cells (HSPCs) self-renew throughout life, accumulation of genomic alterations can potentially give rise to radiation carcinogenesis. In this study we examined DNA double-strand break (DSB) induction and repair as well as mutagenic effects of ionizing radiation (IR) in HSPCs (CD34+) and T-lymphocytes from the umbilical cord of newborns. The age dependence of these DNA damage repair endpoints was investigated by comparing newborn T-lymphocytes with adult peripheral blood T-lymphocytes. As umbilical cord blood (UCB) contains T-lymphocytes that are practically all phenotypically immature, we examined the radiation response of separated naive (CD45RA+) and memory lymphocytes (CD45RO+). The number of DNA DSB was assessed by the microscopic scoring of γ -H2AX/53BP1 foci 0.5 h after low-dose exposure, while DNA repair was studied by scoring the number of residual γ -H2AX/53BP1 foci 24 h post-exposure. Mutagenic effects were studied by the cytokinesis block micronucleus (CBMN) assay.

Both HSPCs and newborn T-lymphocytes showed statistically significant lower endogenous levels of DNA DSBs and MN compared to adult T-lymphocytes. No significant differences in the number of DNA DSB induced by low-dose (100-200 mGy) exposure were observed between the three different cell types. However, residual γ -H2AX/53BP1 foci levels 24 h post IR were significantly lower in HSPCs compared to newborn T-lymphocytes, while newborn T-lymphocytes showed significant higher foci yields than adult T-lymphocytes. No significant differences in the level of radiation-induced micronuclei at 2 Gy were observed between CD34+ cells and newborn T-lymphocytes. However, newborn T-lymphocytes showed a significantly higher number of MN, compared to adult T-lymphocytes. These results confirm that HSPC quiescence promotes mutagenesis after ionizing radiation exposure. Furthermore, we can conclude that the peripheral T-lymphocytes from newborns are significantly more radiosensitive than peripheral T-lymphocytes of adults. Using the results of the comparative study of the radiation-induced DNA damage repair endpoints in naive (CD45RA+) and memory T-lymphocytes (CD45RO+), we could demonstrate that the observed differences between newborn and adult T-lymphocytes can be explained by the immunophenotypic change of T-lymphocytes with age, which is presumably linked with the remodelling of the closed chromatin structure of naive T-lymphocytes.

INTRODUCTION

The paediatric patient population is recognized as one of the most critical target groups in medical radiation protection. Epidemiological study data, summarized in the UNSCEAR 2013 report, show clearly that for a given dose the risk for a radiation-induced malignancy and especially for leukaemia is seriously higher in children than in adults: 2-3 times for solid tumours (however, not all solid cancers show age-at-exposure effects) and 3-5 times for haematological malignancies (1). These observations are thought to be linked to the fact that children are in a phase of active development of organs and tissues. This variance of cancer risk with age-at-exposure was also observed in a series of animal studies (2).

A recent study in the United Kingdom has assessed the risks of leukaemia and brain tumours after CT scans in childhood and young adulthood (3). These malignancies are considered as endpoints of great concern during childhood, due to the high radiosensitivity of red bone marrow and brain at young ages. Especially red marrow, which contains haematopoietic stem and progenitor cells (HSPCs), is of critical interest owing to the well-documented induction of a range of leukaemia types by ionizing radiation, especially myeloid leukaemias (AML and CML) (4). Stem cells are a major target of radiation-induced carcinogenesis. As HSPCs cells self-renew throughout life, accumulation of DNA damage can compromise their genomic integrity. In this way, proper regulation of DNA damage responses in HSPCs is crucial to avoid bone marrow failure and prevent malignant transformation, resulting in leukaemia. Furthermore, appropriate regulation of the cell cycle is essential for homeostasis. Under steady-state conditions, stem cells are mainly in dormancy to avoid exhaustion, known as a quiescent state (5). A hierarchical model has been proposed for blood, where tissue homeostasis requires continual replenishment of mature blood cells from a rare population of marrow residing quiescent cells, which are vastly outnumbered by the dividing progenitor population which lead to the differentiated cells. The finding that leukemic stem cells can also be quiescent like normal haematopoietic stem cells adds additional support

to the notion that some types of AML may arise from the primitive cell compartment, before full lineage commitment has occurred. Alternatively, it is also possible that AML could arise from committed progenitors if stem cell self-renewal programs are established during the leukemogenic process (6).

The high radiosensitivity of children with respect to radiation-induced leukaemia warrants studies on the response of HSPCs to DNA damage induced by ionizing radiation as well as on the mutagenic consequences of DNA misrepair. However only limited data are currently available (7-9). HSPCs are usually characterized by their CD34 antigen and specified as CD34+ cells, which are present in bone marrow (BM), umbilical cord blood (UCB) and in low amounts in the peripheral blood (PB) (10). They have emerged as a model system for studying stem cell biology since they can be purified based on the unique CD34+ cell surface marker.

Whether cellular responses to ionizing radiation change with age remains largely unknown. A recent study of Bakhmutsky *et al.*, showed that peripheral blood lymphocytes (PBL) from newborns (UCB samples) showed a statistically significant increased number of radiation-induced chromosome aberrations compared to adult PB (APB) T-lymphocytes (11). However, UCB or newborn T-lymphocytes differ from APB T-lymphocytes in their immunophenotypic profile. In particular, UCB contains T-lymphocytes that are phenotypically immature and express the naive RA isoform of the CD45 molecule (CD45RA⁺), while APB contains a higher number of CD45RO⁺ memory cells (12).

In present study, induction and repair of DNA double-strand breaks (DSBs) after in vitro exposure to ionizing radiation were evaluated by scoring the radiation-induced and residual γ -H2AX/53BP1 foci 24 h post-irradiation for HSPCs (CD34⁺) compared to newborn T-lymphocytes, both isolated from UCB. In addition, the mutagenic effect of ionizing radiation on UCB CD34⁺ and newborn T-lymphocytes was evaluated with the cytokinesis-blocked micronucleus (CBMN) assay. To investigate if there exists an age dependency in radiation-induced DNA damage, repair and mutagenic effects in T-lympho-

cytes, the γ -H2AX/53BP1 foci and CBMN assays were also applied to PB T-lymphocytes of adults. In order to find an explanation for the observed age dependence, the immunophenotypic difference of T-lymphocytes with age was examined by flow cytometric analysis of the composition of the UCB and APB T-lymphocyte subpopulations with respect to naive CD45RA⁺ and memory CD45RO⁺ subsets. Furthermore, we were able to evaluate for the first time radiation-induced residual DNA DSBs and mutagenic endpoints in separated human naive CD45RA⁺ and memory CD45RO⁺ subpopulations to allow interpretation of the observed age dependent difference in radiosensitivity of T-lymphocytes between newborns and adults.

MATERIALS AND METHODS

Sample collection and isolation of cells

Human CD34⁺ HSPC were isolated from UCB following the guidelines of the Ethical Commission of Ghent University Hospital (Belgium). UCB (70-90 ml) was collected from full-term newborns through the umbilical cord at time of delivery. Afterwards, mononuclear cells were obtained by density gradient centrifugation (Density: 1.077 g/ml, Lymphoprep, Axis-Shield) and HSPCs were purified by using CD34⁺ immunomagnetic beads (human CD34 MicroBeadKit, Miltenyi Biotec) to achieve a purity > 95%.

Adult peripheral blood samples were collected from healthy volunteers from whom informed consent was obtained prior to the experiments. Donors were non-smokers and had no history of radiotherapy treatment within the last ten years. CD3⁺ T cells were isolated from UCB and APB using the RosetteSep[™] Human T Cell Enrichment Cocktail (Stemcell Technologies) by negative selection after density gradient centrifugation (Density: 1.081 g/ml, RosetteSep[™] Density Medium, Stemcell Technologies). Unwanted cells are targeted for removal with Tetrameric Antibody Complexes recognizing CD16, CD19, CD36, CD56, CD66b and glycophorin A on red blood cells (RBCs), resulting in a highly enriched population of CD3 T-lymphocytes (purity > 98%).

Since umbilical cord blood is physiologically and genetically part of the foetus, we can consider this as blood of a newborn (13). For simplicity we will refer to the UCB T-lymphocytes as “T newborns” and APB T-lymphocytes as “T adults”.

CD4⁺ T-lymphocyte subsets were isolated from the peripheral blood (50 ml) of healthy adult donors by using first RosetteSep[™] Human CD4⁺ T Cell Enrichment Cocktail (Stemcell Technologies) to obtain CD4⁺ T-lymphocytes from whole blood by negative selection (purity > 95%). Afterwards, the isolated CD4⁺ cells were labelled with CD45RO and CD45RA immunomagnetic beads (human CD45RO MicroBeadKit and human CD45RA MicroBeadKit, Miltenyi Biotec) to obtain naive (CD45RA⁺) and memory (CD45RO⁺) CD4⁺ cells (purity > 85%).

Flow cytometric immunophenotyping

T-lymphocyte subpopulations of newborns and adults were determined by means of flow cytometry using the following panel of monoclonal antibodies: CD45RA-FITC/CD45RO-PE/CD3-PerCP/CD8-PC7/CD4-APC (BD Biosciences). Briefly, 50 μ l of whole blood was simultaneously stained with 5 μ l of the mAb panel and incubated for 20 minutes at room temperature, in dark. After incubation, the red blood cells were lysed (BD Pharm Lyse[™], BD Biosciences) and washed with Cellwash (BD Biosciences) before the samples were analysed. Data were acquired on a BD FACSCanto[™] II flow cytometer (BD Biosciences) and at least five thousand T-lymphocyte events were scored.

In vitro irradiation

For the assessment of the number of γ -H2AX/53BP1 foci induced by low-dose x-irradiation, isolated T-lymphocyte populations of UCB (n=6) and adult PB (n=7) were resuspended in cRPMI (Gibco) + 10% FCS (Gibco) and CD34⁺ cells (n=7) in cIMDM (Gibco) + 10% FCS and exposed to 100 or 200 mGy x-rays. In every experiment, one cell sample served as a sham irradiated control sample. The samples were kept for 30 min at 37°C in a humidified 5% CO₂ atmosphere incubator (Thermo Scientific) after irradiation to obtain the maximum number

of γ -H2AX/53BP1 foci, followed by an arrest on ice water (0°C) for 15 min.

A repair time of 24 h was considered to study the residual number of γ -H2AX/53BP1 foci in the different cell types. To this end, after isolation, CD34+ cells (n=6), newborn (n=6) and adult (n=6) T-lymphocyte populations were suspended in appropriate medium as described in previous paragraph and irradiated with 4 Gy x-rays. Again, one sample served as a sham irradiated control. After irradiation, the cells were kept in a humidified 5% CO₂ atmosphere incubator at 37°C for 24h, followed by an arrest on ice water (0°C).

One of the most frequently used tests for the assessment of in vitro chromosomal radiosensitivity is the CBMN assay. For this set of experiments, isolated cells (n=7, for all cell types) were resuspended in appropriate medium as described above and irradiated with 2 Gy x-rays, while one sample served as a sham irradiated control sample in every experiment.

In all the irradiation experiments, a radiation quality of 100 kVp x-rays with 2mm Al filtration was used generated by a Philips MG420 x-ray generator coupled to a MCN420 tube (Philips Medical Systems). All irradiations were carried out in a water bath at 37°C (Lauda GMBH & Co) and calibration was performed with a NE2571 Farmer ionization chamber (Thermo Electron). The dose rate was 20 mGy/min for doses up to 200 mGy and 0.6 Gy/min for the higher doses (2 and 4 Gy).

γ -H2AX/53BP1 Foci Assay

After irradiation and incubation, cells were centrifuged on poly-L-lysine coated slides (VWR International) in a concentration of 600,000 cells/ml. The slides were fixed in PBS (Sigma-Aldrich) containing 3% paraformaldehyde (PFA) (Sigma-Aldrich) for 20 min and stored overnight in PBS containing 0.5% PFA. The next day, slides were washed with PBS for 10 min and treated with 0.2% Triton X-100 (Sigma-Aldrich) solution in PBS for 10 min. Thereafter, cells were blocked by washing them three times for 10 min in PBS containing 1% Bovine Serum Albumin (BSA) (Roche). Immunohistochemistry staining was performed using primary antibodies (Ab) against

γ -H2AX (1:500, Mouse mAb, Biolegend) and p53 binding protein 1 (53BP1) (1:500, Rabbit pAb, Abcam). Slides were incubated with the primary Ab for 1 h at room temperature. After washing the cells three times in PBS containing 1% BSA the slides were incubated for 1 h at room temperature with secondary antibodies, Tetramethyl Rhodamine Isothiocyanate (TRITC) goat-anti-mouse Ab (1:1000, Sigma-Aldrich) for γ -H2AX staining and highly cross-adsorbed Alexa Fluor 488 goat-anti-rabbit (1:1000, Invitrogen) for 53BP1 staining. Afterwards, the slides were rinsed three times in PBS and mounted in a solution of Fluoromount (Sigma-Aldrich) containing 2% 4',6-Diamidino-2-Phenylindole (DAPI) (Sigma-Aldrich).

Slides were stored in a cool and dark place before image capturing to allow the mounting medium to dry and to avoid fading of the fluorescent signal. Slides were scanned by a Metafer 4 System (Metasystems) equipped with a 63x/1.30 oil objective. Images were obtained automatically by using MetaCyte software, however merged foci were scored manually on the raw training files. First, cells were selected as positives based on the nucleus morphology visible in the DAPI channel. Secondly, co-localizing foci were scored by projecting TRITC and Alexa Fluor 488 sections on top of each other. The scoring of γ -H2AX/53BP1 co-localized foci increases the reliability that the observed spots are indeed DNA DSB and enhances the sensitivity of foci scoring by reducing the impact of artefacts and false positives. In each experiment, at least 250 cells were scored over two slides in randomly selected fields of view.

'96-well Plate' Cytokinesis Block Micro-nucleus Assay

It is difficult to obtain a sufficient number of CD34+ cells after immunomagnetic purification of one UCB sample in order to perform several CBMN cultures in parallel. To overcome this problem, we developed a micro-culture CBMN assay in which isolated cells were cultured in a small volume of 200 μ l in a 96-well plate. The methodology is based on a protocol published by Fenech (14).

After isolation and irradiation, T-lymphocytes and their corresponding subtypes were seeded in a concentration of 500,000 cells/ml in a F-bottom shape 96-well plate (CELLSTAR[®] Tissue Culture Plates, Greiner Bio-One). Isolated cells were cultured in 200 μ l RPMI supplemented with 0.5% antibiotics (penicillin and streptomycin, Gibo), 1% L-glutamine (Sigma-Aldrich), 1% sodium pyruvate (100 mM, Gibo), 0.1% β -mercaptoethanol (50 mM, Gibco). In case of naive and memory T-lymphocytes, 50 μ L/ml interleukin-2 (Roche) was added to the cultures. Mitotic division of T-lymphocytes was stimulated by adding 10 μ L/ml phytohaemagglutinin (PHA) (Gibo). Cells were incubated at 37°C with lids loose in a humidified incubator containing 5% CO₂. Cytochalasin B (Sigma-Aldrich) was added to the cultures after 23 h at a final concentration of 6 μ g/ml and 50 μ l of fresh culture medium (pre-heated to 37 °C) was added to each well. CD34⁺ HSPCs were cultured in a similar way, however, cIMDM containing 10% FCS was used as culture medium and a combination of recombinant hematopoietic cytokines, 100 ng/ml stem cell factor (SCF), 100 ng/ml FLT3 ligand (Flt3L) and 20 ng/ml thrombopoietin (TPO) (all cytokines from Peprotech), were used in order to stimulate the expansion of the HSPCs. Furthermore, CD34⁺ HSPCs were grown in a different well plate than the T cells, a U-shaped 96 well-plate (BD Biosciences). Determination of HSPC cycle stage by flow cytometry after first stimulation showed a division rate comparable to that of T-lymphocytes (data not shown). Based on these findings cytochalasin B was added at the same time point of 23 h as for the T-lymphocyte cultures.

After 72 h total incubation time, the cultures were resuspended gently to reduce cellular clumping and harvested for slide preparation. A cell suspension of 250 μ l was applied to a slide by cytocentrifugation (Cellspin, Tharmac) at 1000 rpm for 5 min. Slides were air dried horizontally for 8 min, fixed in 10/1 methanol/acetic acid (Merck) for 12 min and again allowed to air dry. Thereafter, slides were stained in Giemsa's Azur Eosin Methylene blue solution (Merck) and micronuclei were scored in binucleated (BN) cytokinesis blocked cells under the microscope using a 400x magnification. At least 1000 BN cells

were scored from various slides per condition by two independent readers.

Statistical Analysis

The results from the individual experiments were averaged and the corresponding standard deviation of the mean (SEM) calculated. The 2-tailed Mann-Whitney test was performed to investigate the significance of differences in biomarker scores. The results were considered as significantly different at $p < 0.05$. Statistical analysis of the data was performed using the Statistical Package for Social Sciences (SPSS) version 22.0

RESULTS

DNA DSB formation after low-dose x-ray exposure

γ -H2AX foci formation is a highly sensitive technique to evaluate DNA DSB formation and repair. Moreover, the γ -H2AX foci co-localize with other DNA repair factors such as 53BP1, which confirms that the observed focus is a DNA DSB and no staining artefact. In a first set of experiments the foci numbers induced in HSPCs and T-lymphocytes from newborns and adults by 100 and 200 mGy x-rays were compared. The pre-existing, endogenous DNA DSBs were analysed

in all three cell types, illustrated in Figure 1. The number of endogenous γ -H2AX/53BP1 foci levels was significantly lower in CD34+ cells (MWU, $p < 0.05$) and T newborns (MWU, $p < 0.05$) compared to T adults. These data are in line with other studies that reported lower levels of endogenous DSBs in cord blood lymphocytes and HSPCs than in adult peripheral blood lymphocytes (7, 8, 15). Subsequently, the number of radiation-induced (RI) foci was determined by subtracting the endogenous foci levels from the foci counts in the irradiated samples. Figure 1 shows that the induction of DSBs is dose dependent, but for both doses the differences in induced foci levels among the different types of cells were not statistically significant (MWU, $p > 0.05$).

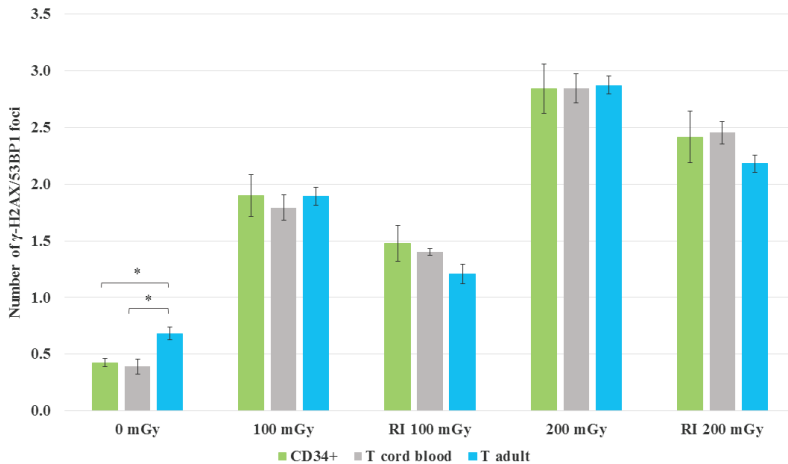


FIGURE 1

Mean number of γ -H2AX/53BP1 foci per nucleus at 30 min in the sham-irradiated control samples and after irradiation with 100 and 200 mGy x-rays. Radiation-induced (RI) foci levels were obtained by subtracting the number of endogenous γ -H2AX/53BP1 foci in the sham irradiated control samples from the γ -H2AX/53BP1 foci number scored in the irradiated samples. The number of endogenous γ -H2AX/53BP1 foci was significantly different between CD34+ ($n=7$) and T newborn ($n=5$) compared to T adult ($n=7$) ($* p < 0.05$). No statistical significant difference could be observed in RI foci levels between CD34+ ($n=4$), T newborn ($n=4$) and T adult ($n=5$) at the two dose points. Error bars represent standard error of the mean of the different donors (SEM).

Residual foci levels 24h post-irradiation in HSPCs, newborn and adult T-lymphocytes

The first set of experiments showed no detectable difference in the induction of γ -H2AX/53BP1 foci between HSPCs, T newborn and T adult. However, to assess the number of residual DNA DSBs, which may mark unrepaired or misrepaired sites, γ -H2AX/53BP1 foci were quantified at 24 h after irradiation with 4 Gy x-rays. A dose of 4 Gy was chosen for the DNA repair experiments, as this dose is often used for the estimation of radiosensitivity after in vitro irradiation of human lymphocytes (16). Again, co-localizing γ -H2AX and 53BP1 foci were scored to make sure that DNA DSBs were analysed (Figure 2). The sham-irradiated HSPCs and T-lymphocytes of newborns show again very low levels of foci compared to T-lymphocytes of adults (MWU, both p -values < 0.005) (Figure 3). At 24 h after 4 Gy irradiation, the number of radiation-induced

γ -H2AX/53BP1 foci in HSPCs (3.54 foci/cell) is significantly lower than in T-lymphocytes of newborns (7.13 foci/cell) (MWU, $p < 0.005$), indicating more repair in the first 24 h after irradiation in HSPCs. This is in agreement with data previously published by other research groups (8, 15). On the other hand, significantly higher foci levels of induced foci were observed 24 h post-exposure in T-lymphocytes of newborns compared to adults (5.77 foci/cell) (MWU, $p < 0.05$).

Residual foci levels 24h post-irradiation in CD45RA+ and CD45RO+ CD4+ T-lymphocytes

A possible explanation for the difference in residual foci levels 24 h post-irradiation between T-lymphocytes of newborns and adults could reside in the immune system immaturity. Therefore we performed an immunophenotypic study of the UCB and adult PB T-lymphocyte samples

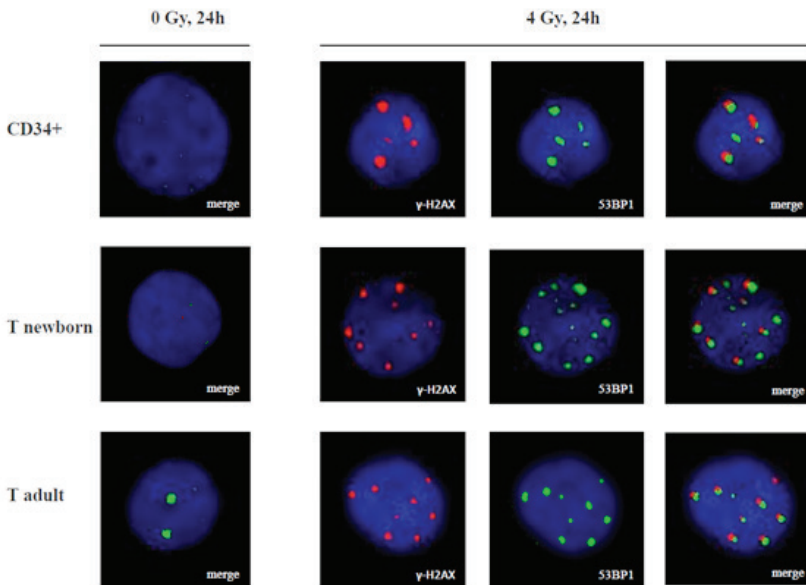


FIGURE 2

Immunofluorescence staining of γ -H2AX (red), 53BP1 (green) and the merged double-staining in CD34⁺, newborn and adult T-lymphocytes, 24h after 0 and 4 Gy irradiation.

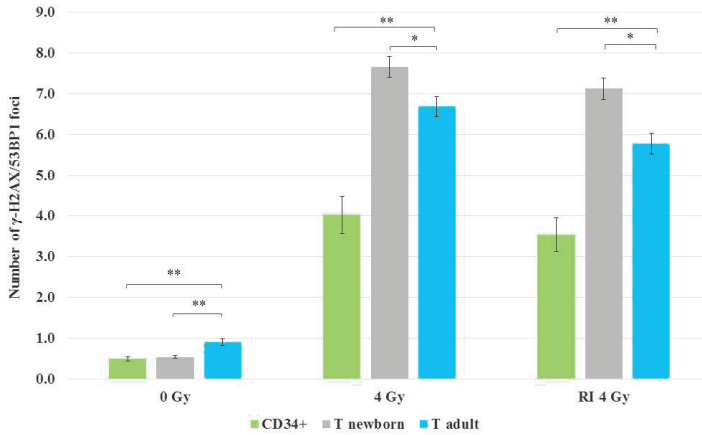


FIGURE 3

Mean number of residual DNA DSBs in CD34⁺ (n=6), T newborn (n=6) and T adult (n=6) 24h after 4 Gy x-ray irradiation. Error bars represent the standard error of the mean (SEM) of the six different donors. At least 250 nuclei were scored for each donor at each time point (* p < 0.05, ** p < 0.005).

by means of flow cytometry. The data, presented in Table 1, show that CD4⁺ and CD8⁺ T cells of newborns predominantly (> 98%) co-express the CD45RA antigen, while adult PB T-lymphocytes are composed by both CD45RA⁺ and CD45RO⁺ subpopulations. A different distribution of the CD45 isoforms was observed on CD4⁺ and CD8⁺ T-lymphocytes, with the CD45RA⁺ phenotype more expressed in CD8⁺ T cell population and the CD45RO⁺ phenotype more expressed on CD4⁺ T cells, which is in agreement with other studies (12, 17).

To evaluate whether the observed difference in residual DNA DSBs between newborn and adult T-lymphocytes could be explained by the composition of T-lymphocyte subsets, naive and memory CD4⁺ cells were isolated from adult peripheral blood samples of four donors in order to compare DNA repair of the two subsets. We selected the CD4⁺ subpopulation for this pilot study as the results in Table 1 show the high prevalence of helper-inducer CD4⁺ in both UCB

and adult PB samples and we want to avoid interference of the results by possible differences among the CD4⁺ and CD8⁺ subpopulations. A difference in residual DNA DSBs was observed for CD4⁺CD45RO⁺ and CD4⁺CD45RA⁺ cells (MWU, p < 0.05), shown in Table 2. The percentage of CD4⁺ cells expressing the CD45RO⁺ and CD45RA⁺ phenotype was determined by flow cytometry and these values were taken into account to calculate an 'estimated' overall CD4⁺ residual γ -H2AX/53BP1 foci level 24 h post-exposure. The calculated 'estimate' differs less than 10% from the CD4⁺ γ -H2AX/53BP1 foci levels, determined experimentally on the total CD4⁺ population (Table 2). These results indicate that a change of immunophenotypic profile of lymphocytes with age has an effect on DNA DSB repair.

Subpopulation	T newborns	T adults
CD4 ⁺	75.9 (68.2 - 81.5)	63.5 (52.8 - 69.8)
CD4 ⁺ RO ⁺	1.7 (0.5 - 6.1)	66.0 (33.2 - 75.4)
CD4 ⁺ RA ⁺	98.3 (92.8 - 99.9)	30.5 (19.9 - 64.9)
CD8 ⁺	34.5 (30.2 - 41.7)	22.0 (13.1 - 27.4)
CD8 ⁺ RO ⁺	0.2 (0.0 - 0.9)	36.0 (19.8 - 56.8)
CD8 ⁺ RA ⁺	99.7 (99.1 - 100.0)	64.0 (31.0 - 79.4)

TABLE 1

Expression of CD45RO and CD45RA on CD4 and CD8 T cell subsets. Data present median percentage values (with corresponding range).

PART II

	Subpopulation	RI γ -H2AX/53BP1 foci		%		Estimate CD4 ⁺
Donor 1	CD4 ⁺ RO ⁺	5.23	x	48.2	=	6.00
	CD4 ⁺ RA ⁺	6.78	x	51.3		
	CD4 ⁺	6.66				
Donor 2	CD4 ⁺ RO ⁺	5.96	x	75.8	=	6.40
	CD4 ⁺ RA ⁺	7.47	x	25.2		
	CD4 ⁺	6.83				
Donor 3	CD4 ⁺ RO ⁺	6.41	x	66.7	=	7.14
	CD4 ⁺ RA ⁺	8.04	x	35.6		
	CD4 ⁺	7.04				
Donor 4	CD4 ⁺ RO ⁺	5.54	x	66.8	=	6.31
	CD4 ⁺ RA ⁺	7.18	x	36.4		
	CD4 ⁺	6.75				
Mean	CD4 ⁺ RO ⁺	5.78 ± 0.25	x	64.4	=	6.46
	CD4 ⁺ RA ⁺	7.37 ± 0.26	x	37.1		
	CD4 ⁺	6.82 ± 0.08				

TABLE 2

Distribution of memory and naive cells, expressed as percentage number of adult CD4⁺ cells. The experimentally determined radiation-induced γ -H2AX/53BP1 foci values were multiplied with the corresponding percentage of the CD45 isoform, to obtain an estimated induced γ -H2AX/53BP1 foci yield for the overall CD4⁺ population of every adult donor.

Assessment of radiation-induced mutagenic effects in HSPCs, newborn and adult T-lymphocytes by the CBMN assay

The CBMN is an effective method to detect chromosomal damage in peripheral blood lymphocytes of humans exposed to ionizing radiation (18). However, no study reported the use of the CBMN assay to detect chromosomal damage in human CD34⁺ HSPCs after ionizing radiation exposure so far. For these experiments, isolated cells were irradiated with 2 Gy x-rays. Table 3 presents the number of spontaneous and radiation-induced MN in binucleated (BN) CD34⁺ HSPCs and T-lymphocytes of both newborns and adults for the different donors. Before irradiation, the cell cycle distribution of the HSPCs was determined by DNA flow cytometry analysis with propidium iodide (PI) and revealed similar distributions in HSPCs as in G0 T-lymphocytes, approximately 95% of the cells was in G1/G0, 3.2% in S-phase and 1.8% in G2/M-phase (data not shown). The spontaneous MN expression was significantly lower in CD34⁺ HSPCs (mean 11/1000 BN cells; MWU $p < 0.005$) and T-lymphocytes of newborns (mean 8/1000 BN cells; MWU $p < 0.005$) compared to adult T-lymphocytes (mean 18/1000 BN cells). No difference was observed between the MN yields induced by 2 Gy in HSPCs (mean 371/1000 BN cells) and newborn T lymphocytes (mean 351/1000 BN cells) (MWU, $p > 0.05$). However, MN yields were significantly lower in T-lymphocytes of adults (mean 275/1000 BN cells) compared to newborns (mean 351/1000 BN cells) (MWU $p < 0.05$) after 2 Gy irradiation.

Assessment of radiation-induced mutagenic effects in CD45RO⁺ and CD45RA⁺ CD4⁺ T-lymphocytes

To evaluate whether the observed difference in MN yields between newborn and adult T-lymphocytes could be explained by the composition of T cell subsets as discussed in the paragraph on DNA repair kinetics, naive and memory CD4⁺ cells were isolated from adult peripheral blood samples of four donors in order to compare the number of MN induced by 2 Gy in the two subsets. Results are presented in Table 4. A statistically significant difference was observed in the induced number of MN after 2 Gy x-rays between CD4⁺CD45RO⁺ cells and CD4⁺CD45RA⁺ cells ($p < 0.05$). An estimate of the expected number of MN for the CD4⁺ population was made based on the CD45RO⁺/CD45RA⁺ distribution of every individual donor. The difference between the estimated MN value and the actual observed number of induced MN in the total population of CD4⁺ cells was less than 10% for every donor.

Donor	Cell Type	Dose (Gy)	
		0	2
UCB1	CD34 ⁺	7	433
	T newborn	9	347
UCB2	CD34 ⁺	8	345
	T newborn	9	316
UCB3	CD34 ⁺	12	347
	T newborn	7	332
UCB4	CD34 ⁺	11	378
	T newborn	7	335
UCB5	CD34 ⁺	16	335
	T newborn	10	265
UCB6	CD34 ⁺	13	330
	T newborn	6	414
UCB7	CD34 ⁺	12	429
	T newborn	6	447
Mean (\pm SEM)	CD34 ⁺	11 (\pm 1)	371 (\pm 17)
	T newborn	8 (\pm 1)	351 (\pm 23)
AB1	T adult	18	255
AB2	T adult	13	198
AB3	T adult	16	265
AB4	T adult	16	262
AB5	T adult	14	351
AB6	T adult	26	299
AB7	T adult	26	297
Mean (\pm SEM)	T adult	18 (\pm 2)	275 (\pm 18)

TABLE 3

Number of micronuclei per 1000 BN cells in both the sham irradiated control samples and after 2 Gy x-ray irradiation, for 14 individual donors (7 UCB samples and 7 adult PB samples).

	Subpopulation	RI MN/1000 BN		%		Estimate CD4 ⁺
Donor 1	CD4 ⁺ RO ⁺	213	x	48.2	=	280
	CD4 ⁺ RA ⁺	346	x	51.3		
	CD4 ⁺	259				
Donor 2	CD4 ⁺ RO ⁺	229	x	75.8	=	253
	CD4 ⁺ RA ⁺	335	x	25.2		
	CD4 ⁺	263				
Donor 3	CD4 ⁺ RO ⁺	322	x	66.7	=	355
	CD4 ⁺ RA ⁺	395	x	35.6		
	CD4 ⁺	334				
Donor 4	CD4 ⁺ RO ⁺	259	x	66.8	=	295
	CD4 ⁺ RA ⁺	334	x	36.4		
	CD4 ⁺	312				
Mean	CD4 ⁺ RO ⁺	251 (±22)	x	64.4	=	287
	CD4 ⁺ RA ⁺	352 (±15)	x	37.1		
	CD4 ⁺	292 (±17)				

TABLE 4

Radiation-induced number of MN per 1000 BN cells after 2 Gy x-ray irradiation. Based on the percentage of CD45RO⁺ and CD45RA⁺ subpopulations, an estimate of the expected induced number of MN for CD4⁺ cells was made.

DISCUSSION

Leukaemia is, with an incidence of 2.6% in Europe (both sexes combined) (19), a relatively rare disease, but the IR-induced risk of cancer development is high for the hematopoietic tissue especially in children (excess relative risk (ERR)/Sv for childhood leukaemia of ~50) (20, 21). The bone marrow is likely to harbour HSPCs with acquired mutations as a direct result of genotoxic insults such as IR exposure. During the long lifespan of stem cells DNA damage-induced mutations accumulate and could initiate the leukemogenic process (6, 9, 22). Up to now, there are only a very limited numbers of studies that evaluate the DNA repair capacity and chromosomal radiosensitivity of human HSPCs. Most of the studies on the radiation sensitivity of HSPCs use colony formation in the framework of haematological recovery after ionizing radiation exposure (23, 24). The elimination of damaged HSPCs by apoptotic or necrotic death prevents long-term consequences of damage. The nonlethal DNA modifications which remain unrepaired or misrepaired can eventually lead to malignant disease (25). Therefore, the aim of this study was to characterize the DNA damage response and the mutagenic effects of IR exposure in HSPCs in comparison with T-lymphocytes from UCB and APB.

Present study shows that the number of residual DSBs 24 h post-exposure is significantly lower in HSPCs than in newborn T-lymphocytes pointing to more repair of DNA DSBs. This is possibly linked to differences in chromatin structure, which has a major influence on the cellular response to DNA damage (26). Indeed, intriguing evidence accumulates showing that stem cells use specific DDR mechanisms to ensure genomic integrity over lifetime and a possible defence mechanism could be their chromatin structure. For example, the nuclear organization of embryonic stem cells is globally open and permissive for gene expression, becoming more compact at different regions of the genome with differentiation. The open configuration allows different proteins to interact easily with chromatin, a very important process which could facilitate signalling of cell cycle arrest and DNA repair in damaged stem cells (9).

In the current study, purified HSPCs enriched for the glycosylated transmembrane protein CD34 have been used, as the enrichment of CD34⁺ cells is current practice in haematopoietic stem cell transplantation and to date one of the most efficient cell separation methods to study *in vitro* haematopoiesis. However, CD34⁺ cells are a heterogeneous mixture of cells at various stages of differentiation which are hierarchically organized in primitive human HSCs (Lin⁻CD34⁺CD38⁻CD90⁺CD45RA⁻), multipotent progenitors (MPP) (Lin⁻CD34⁺CD38⁻CD90⁺CD45RA⁻) and oligopotent progenitors (CD34⁺CD38⁺). Emerging evidence reveals that the radiation sensitivity of these three populations is different (10). Furthermore, the long lasting dogma that primitive human HSCs are believed to be Lin⁻CD34⁺CD38⁻ has recently been challenged by several groups who suggest that CD34⁺ HSCs originate from CD34⁻ HSCs (27). If we want to compare the current results on radiation sensitivity of HSPCs with the existing literature on DNA repair of HSCs, it is important to take into account that a heterogeneous population of CD34⁺ cells was used in the current study. The majority of the observed DNA damage response is attributable to the CD34⁺CD38⁺ progenitor fraction, since only a very small fraction as low as 3% of the enriched cells in this study will be CD34⁺CD38⁻ (28-30).

Milyavsky *et al.* showed that the DDR of human quiescent HSC population (Lin⁻CD34⁺CD38⁻CD90⁺CD45RA⁻) differs in multiple ways from more mature haematopoietic populations, such as progenitor/precursor cells (Lin⁻CD34⁺CD38⁺) (9). The authors observed significantly more residual γ -H2AX foci 12h after 3 Gy irradiation in HSC compared to the progenitor population, 7.1 versus 2.7 foci/nucleus respectively. These results are in line with our low residual foci level of 3.5 foci/cell 24h after 4 Gy in CD34⁺ HSPCs, from which the majority are progenitor cells (CD34⁺CD38⁺). Fast DNA repair kinetics of HSPCs was observed in a murine model by Mohrin *et al.* using the alkaline COMET assay (8). Furthermore, in a study of residual γ H2AX/53BP1 foci level in human CD133⁺ HSPCs from UCB, Vasilyev *et al.* concluded enhanced DNA repair capacity in HSCs compared to mature lymphocytes. CD133 is, just as CD34, a

marker found both in human progenitor and haematopoietic stem cells, which can be used alone or in combination with CD34 to enrich HSPCs (31, 32). Flow cytometer analysis of Becker *et al.* indicated that 80% of the purified CD34⁺ population, co-express CD34⁺CD133⁺ (33).

Another interesting field where the DNA DSB repair of haematopoietic stem cells is widely studied, is the age-dependent decline in stem cell function. Several studies reported an age-dependent accumulation of DNA damage in tissue stem cells leading to stem cell exhaustion (15, 34, 35). In particular, Rube *et al.* studied the formation and loss of γ -H2AX foci in different stem and progenitor populations exposed to ionizing radiation to gain insight into age dependent changes in DSB repair capacity (15). In both CD34⁺ and CD34⁻ cells obtained from UCB the number of endogenous γ -H2AX foci was generally low, which is in line with the results obtained in the current study on background levels of co-localizing γ -H2AX/53BP1 foci. Furthermore, the study of Rube *et al.* showed an increase of unrepaired DSBs with increasing donor age (newborns and healthy volunteers of 16-83 years old), which suggests that unrepaired DSBs accumulate continuously in CD34⁺ HSPCs and in the more mature CD34⁻ cells during physiological cell aging. The higher endogenous foci levels observed in present study in adult peripheral T-lymphocytes compared to HSPCs and T-lymphocytes of newborns support these findings.

In present work a new culture method for the CBMN assay requiring culture volumes of only 250 μ l was worked out. Comparison of the CBMN results obtained with this new culture method for adult T-lymphocytes (mean 275 MN/1000 BN cells for 2 Gy) shows a good agreement with previously published data obtained with the standard MN assay using 5 mL whole blood cultures (mean 277 MN/1000 BN cells for 2 Gy) (36). Fenech described in detail the standard method for the CBMN Cytome assay as applied to isolated lymphocyte cultures (14). In this protocol isolated lymphocytes were cultured in 750 μ l of culture medium in a density of 1 x 10⁶ cells per ml and duplicate cultures were set up per subject and/or dose point. However, since the number of CD34⁺ cells isolated from one umbilical cord

blood sample (70-90 ml) was approximately 1.5 x 10⁶ cells which had to be divided by two to obtain a sham-irradiated and 2 Gy dose sample, we had to work with smaller culture volumes of 250 μ l. The same methodology was applied for isolated T-lymphocytes.

The MN data obtained in present work indicate that a 2 Gy exposure induces the same amount of mutagenic effects in HSPCs as in newborn T-lymphocytes. Under steady-state conditions, the majority of HSPCs and T-lymphocytes are maintained in a quiescent state, in which the major pathway for DSB repair is nonhomologous end joining (NHEJ), a rapid but error-prone pathway of DSB repair. It is well known that NHEJ-mediated repair can be mutagenic and this was reflected in our CBMN results with high levels of radiation-induced MN (371 \pm 15 MN/1000 BN cells) in CD34⁺ HSPCs, which were comparable with newborn T-lymphocytes (351 \pm 23 MN/1000 BN cells). Micronucleus analysis in CD34⁺ cells was already used to assess the genotoxicity induced by benzoquinone (37). However, to our knowledge, this is the first study in which the CBMN assay was used to assess the chromosomal radiosensitivity of CD34⁺ cells after ionizing radiation exposure. The lower levels of spontaneous MN yields observed for both the HSPCs as the newborn T-lymphocytes compared to adult T-lymphocytes reflect the increase of baseline genotoxic damage with age.

One of the major findings of this work is the observed difference in cellular chromosomal radiosensitivity between T-lymphocytes of newborns and adults, with T-lymphocytes of newborns being more radiosensitive than T-lymphocytes of adults. Bakhmutsky *et al.* could show that newborns as a group have an elevated sensitivity for radiation-induced chromosome damage in peripheral blood lymphocytes compared to adults by scoring chromosome aberrations at doses of 1, 2, 3 and 4 Gy (11). Another interesting finding in the study of Bakhmutsky *et al.* was that sensitivity to radiation-induced chromosome damage does not change with age among adults. This indicates that the change in sensitivity with age appears to occur between birth and young adulthood rather than gradually over the years from birth to senescence. Similarly, a study on

rodents didn't show a difference in cancer susceptibility between adult and elderly rodents, while there was a dramatically higher risk of cancer for rodents in fetal period up to the age of sexual maturity compared to adult and elderly animals (2). This lack of an age effect among adult humans could be the result of the completion of growth and development.

Most of the T-lymphocytes of newborns are immunologically immature, known as naive T-lymphocytes, and express the CD45RA cell surface marker (12, 38). The immune system maintains both naive and memory T cells, so that individuals can establish an immune response to a variety of new antigens while keeping appropriate levels of memory T cells that recognise previously encountered pathogens. Naive and memory T cells can most simply be characterised by the reciprocal expression of the CD45RA or CD45RO isoforms. Once naive T cells encounter an antigen and become activated through the T cell receptor, they proliferate and generate effector T cells that are CD45RO⁺. A small proportion of these effector cells persist as memory cells which give an accelerated response upon a future encounter with the specific antigen. As individuals age and encounter more new antigens, the proportion of naive T cells declines and that of antigen experienced memory cells increases (17, 39). The proportion of the naive subpopulation in T cells gradually decreases from a high fraction (median of 89% in present study) at 0 to 3 months to about 50 % (median of 51% in present data) at 12 to 18 years. The gradual shift is most compelling in the CD4⁺ T cell subsets.

In this study, we studied for the first time the radiosensitivity of human CD4⁺CD45RO⁺ and CD4⁺CD45RA⁺ subpopulations of T-lymphocytes. We could demonstrate that the observed differences in foci 24 h post exposure and MN yields between newborn and adult T-lymphocytes are related to the immunophenotypic changes in T-lymphocyte composition with respect to naive and memory subsets. In agreement with our findings, studies in murine models could also show that naive lymphocytes are more radiosensitive than their memory counterparts (40-42). The main reason for the observed difference is attributable to the chromatin structure of the cells. The

organization of DNA into chromatin has a major influence on the cellular response to DNA damage (43). The ability of repair factors to detect DNA lesions and to be retained efficiently at breaks is determined by histone modifications around the DSBs and involves chromatin-remodelling events that facilitate repair by promoting chromatin accessibility (26). Closed chromatin formations impair DSB repair. The differentiation of naive to memory T cells requires chromatin remodelling. Rawlings *et al.* demonstrated that Stat5 proteins, essential for peripheral T cell proliferation, cannot access DNA in naive T cells and acquire this ability only after T cell receptor engagement (44). This transition is not associated with changes in DNA methylation or global histone modifications, but rather chromatin decondensation. Furthermore, Pugh *et al.* showed that opening chromatin with the histone deacetylase inhibitor (HDACi) valproic acid (VPA) following radiation exposure improved survival of naive T cells to the levels observed in effector memory T cells (40).

This study has several restrictions, we were not able to evaluate the radiosensitivity of the different subsets of the heterogeneous CD34⁺ cell population, due to the restriction on the number of cells obtained after isolation of UCB samples. Future research is needed to elucidate the DNA damage response of the different subsets of the human HSPCs population. To confirm that the observed age-effect in T-lymphocytes is gradual and partly determined by the shift in immunophenotypic profile of the lymphocytes, a more extensive study would be required using blood samples from children of all ages. However, ethical constraints limit the feasibility of such studies.

In conclusion, the obtained results confirm that HSPC quiescence promotes fast error prone DNA repair and mutagenesis after ionizing radiation exposure, which may trigger leukaemia development. Furthermore, one of the major findings of this work is the difference in radiation sensitivity between naive and memory T-lymphocytes, which sheds new light on our understanding of the radiation sensitivity of newborns compared to adults. Further work is required to provide better understanding on chromatin structures and the corresponding influence of chromatin remodelling on the radiation sensitivity of human HSPCs, naive and memory T-lymphocytes.

REFERENCES

1. UNSCEAR. *Sources, Effects and Risks of ionizing radiation*. New York: United Nations Scientific Committee on the Effects of Atomic Radiation, 2013.
2. Hattis D, Goble R, Russ A, Chu M, Ericson J. Age-related differences in susceptibility to carcinogenesis: A quantitative analysis of empirical animal bioassay data. *Environ Health Persp* 2004; 112:1152-8.
3. Pearce MS, Salotti JA, Little MP, McHugh K, Lee C, Kim KP, et al. Radiation exposure from CT scans in childhood and subsequent risk of leukaemia and brain tumours: a retrospective cohort study. *Lancet* 2012; 380:499-505.
4. Richardson RB. Stem cell niches and other factors that influence the sensitivity of bone marrow to radiation-induced bone cancer and leukaemia in children and adults. *Int J Radiat Biol* 2011; 87:343-59.
5. Cheshier SP, Morrison SJ, Liao XS, Weissman IL. In vivo proliferation and cell cycle kinetics of long-term self-renewing hematopoietic stem cells. *P Natl Acad Sci USA* 1999; 96:3120-5.
6. Dick JE. Stem cell concepts renew cancer research. *Blood* 2008; 112:4793-807.
7. Vasilyev SA, Kubes M, Markova E, Belyaev I. DNA damage response in CD133+stem/progenitor cells from umbilical cord blood: Low level of endogenous foci and high recruitment of 53BP1. *Int J Radiat Biol* 2013; 89:301-9.
8. Mohrin M, Bourke E, Alexander D, Warr MR, Barry-Holson K, Le Beau MM, et al. Hematopoietic Stem Cell Quiescence Promotes Error-Prone DNA Repair and Mutagenesis. *Cell Stem Cell* 2010; 7:174-85.
9. Milyavsky M, Gan OI, Trottier M, Komosa M, Tabach O, Notta F, et al. A Distinctive DNA Damage Response in Human Hematopoietic Stem Cells Reveals an Apoptosis-Independent Role for p53 in Self-Renewal. *Cell Stem Cell*. 2010; 7:186-97.
10. Heylmann D, Roedel F, Kindler T, Kaina B. Radiation sensitivity of human and murine peripheral blood lymphocytes, stem and progenitor cells. *BBA - Rev Cancer* 2014; 1846:121-9.
11. Bakhmutsky MV, Joiner MC, Jones TB, Tucker JD. Differences in Cytogenetic Sensitivity to Ionizing Radiation in Newborns and Adults. *Radiat Res* 2014; 181:605-16.
12. D'Areña G, Musto P, Cascavilla N, Di Giorgio G, Fusilli S, Zendoli F, et al. Flow cytometric characterization of human umbilical cord blood lymphocytes: immunophenotypic features. *Haematologica* 1998; 83:197-203.
13. Carroll PD, Nankervis CA, Iams J, Kelleher K. Umbilical cord blood as a replacement source for admission complete blood count in premature infants. *J Perinatol* 2012; 32:97-102.
14. Fenech M. Cytokinesis-block micronucleus cytome assay. *Nat Protoc* 2007; 2:1084-104.
15. Rube CE, Fricke A, Widmann TA, Furst T, Madry H, Pfreundschiuh M, et al. Accumulation of DNA Damage in Hematopoietic Stem and Progenitor Cells during Human Aging. *Plos One* 2011; 6:9.
16. Chua MLK, Horn S, Somaiah N, Davies S, Gothard L, A'Hern R, et al. DNA double-strand break repair and induction of apoptosis in ex vivo irradiated blood lymphocytes in relation to late normal tissue reactions following breast radiotherapy. *Radiat Environ Bioph* 2014; 53:355-64.
17. Shearer WT, Rosenblatt HM, Gelman RS, Oymopito R, Plaeger S, Stiehm ER, et al. Lymphocyte subsets in healthy children from birth through 18 years of age: The pediatric AIDS clinical trials group P1009 study. *J Allergy Clin Immun* 2003; 112:973-80.
18. El-Zein R, Vral A, Etzel CJ. Cytokinesis-blocked micronucleus assay and cancer risk assessment. *Mutagenesis* 2011; 26:101-6.
19. Ferlay J, Autier P, Boniol M, Heanue M, Colombet M, Boyle P. Estimates of the cancer incidence and mortality in Europe in 2006. *Ann Oncol* 2007; 18:581-92.
20. Harfouche G, Martin MT. Response of normal stem cells to ionizing radiation: A balance between homeostasis and genomic stability. *Mut Res-Rev Mutat* 2010; 704:167-74.
21. Wakeford R. The risk of childhood leukaemia following exposure to ionising radiation—a review. *J Radiol Prot* 2013; 33:1-25.
22. Niedernhofer LJ. DNA repair is crucial for maintaining hematopoietic stem cell function. *DNA Repair* 2008; 7:523-9.
23. Kashiwakura I, Kuwabara M, Inanami O, Murakami M, Hayase Y, Takahashi TA, et al. Radiation sensitivity of megakaryocyte colony-forming cells in human placental and umbilical cord blood. *Radiat Res* 2000; 153:144-52.
24. Takahashi K, Monzen S, Hayashi N, Kashiwakura I. Correlations of Cell Surface Antigens with Individual Differences in Radiosensitivity in Human Hematopoietic Stem/Progenitor Cells. *Radiat Res* 2010; 173:184-90.
25. Wakeford R. The cancer epidemiology of radiation. *Oncogene*. 2004;23(38):6404-28.
26. Schuler N, Ruebe CE. Accumulation of DNA Damage-Induced Chromatin Alterations in Tissue-Specific Stem Cells: The Driving Force of Aging? *Plos One* 2013; 8: e63932.
27. Takahashi M, Matsuoka Y, Sumide K, Nakatsuka R, Fujioka T, Kohno H, et al. CD133 is a positive marker for a distinct class of primitive human cord blood-derived CD34-negative hematopoietic stem cells. *Leukemia* 2014; 28:1308-15.
28. Hao QL, Shah AJ, Thiemann FT, Smogorzewska EM, Crooks GM. A Functional comparison of CD34(+)CD38(-) cells in cord blood and bone-marrow. *Blood* 1995; 86:3745-53.
29. Darena G, Musto P, Cascavilla N, DiGiorgio G, Zendoli F, Carotenuto M. Human umbilical cord blood: Immunophenotypic heterogeneity of CD34(+) hematopoietic progenitor cells. *Haematologica* 1996; 81:404-9.

30. Kato K, Takahashi K, Monzen S, Yamamoto H, Maruyama A, Itoh K, et al. Relationship between Radiosensitivity and Nrf2 Target Gene Expression in Human Hematopoietic Stem Cells. *Radiat Res* 2010; 174:177-84.
31. He X, Gonzalez V, Tsang A, Thompson J, Tsang TC, Harris DT. Differential gene expression profiling of CD34+ CD133+ umbilical cord blood hematopoietic stem progenitor cells. *Stem Cells Dev* 2005; 14:188-98.
32. Yin AH, Miraglia S, Zanjani ED, Almeida-Porada G, Ogawa M, Leary AG, et al. AC133, a novel marker for human hematopoietic stem and progenitor cells. *Blood* 1997; 90:5002-12.
33. Becker D, Elsasser T, Tonn T, Seifried E, Durante M, Ritter S, et al. Response of human hematopoietic stem and progenitor cells to energetic carbon ions. *Int J Radiat Biol* 2009; 85:1051-9.
34. Rossi DJ, Bryder D, Seita J, Nussenzweig A, Hoeijmakers J, Weissman IL. Deficiencies in DNA damage repair limit the function of haematopoietic stem cells with age. *Nature* 2007; 447:725-U15.
35. Sedelnikova OA, Horikawa I, Zimonjic DB, Popescu NC, Bonner WM, Barrett JC. Senescing human cells and ageing mice accumulate DNA lesions with unrepairable double-strand breaks. *Nat Cell Biol* 2004; 6:168-70.
36. Thierens H, Vral A, Deridder L. Biological dosimetry using the micronucleus assay for lymphocytes – Interindividual differences in dose-response. *Health Phys* 1991; 61:623-30.
37. Abernethy DJ, Kleymenova EV, Rose J, Recio L, Faiola B. Human CD34(+) hematopoietic progenitor cells are sensitive targets for toxicity induced by 1,4-benzoquinone. *Toxicol Sci* 2004; 79:82-9.
38. Lopez MC, Palmer BE, Lawrence DA. Phenotypic Differences Between Cord Blood and Adult Peripheral Blood. *Cytom Part B-Clin Cy*. 2009; 76:37-46.
39. Ben-Smith A, Gorak-Stolinska P, Floyd S, Weir RE, Lalor MK, Mvula H, et al. Differences between naive and memory T cell phenotype in Malawian and UK adolescents: a role for Cytomegalovirus? *BMC Infect Dis* 2008; 8:139.
40. Pugh JL, Sukhina AS, Seed TM, Manley NR, Sempowski GD, van den Brink MRM, et al. Histone Deacetylation Critically Determines T Cell Subset Radiosensitivity. *J Immunol* 2014; 193:1451-8.
41. Grayson JM, Harrington LE, Lanier JG, Wherry EJ, Ahmed R. Differential sensitivity of naive and memory CD8(+) T cells to apoptosis in vivo. *J of Immunol*. 2002; 169:3760-70.
42. DiSpirito JR, Shen H. Histone Acetylation at the Single-Cell Level: A Marker of Memory CD8(+) T Cell Differentiation and Functionality. *J Immunol* 2010; 184:4631-6.
43. Price BD, D'Andrea AD. Chromatin Remodeling at DNA Double-Strand Breaks. *Cell* 2013; 152:1344-54.
44. Rawlings JS, Gatzka M, Thomas PG, Ihle JN. Chromatin condensation via the condensin II complex is required for peripheral T-cell quiescence. *Embo J* 2011; 30:263-76.

PAR

General Discussion

9

Radiation risks in paediatric CT imaging

CT is a valuable and essential imaging modality for children since it can provide rapid, consistent and detailed information about nearly any organ system (1). As already described in the Introduction of this PhD, children are more radiosensitive than adults and the high x-ray doses associated with CT procedures have raised serious health concerns (2). Recent epidemiological studies have linked CT x-ray exposure during childhood to elevated cancer risks, especially to the development of brain tumours and leukaemia (see chapter 2) (3). However, carcinogenic risk assessment at low doses based on the LNT hypothesis is still subject of debate and several authors question the validity of the linear extrapolation down to low doses (4, 5). The assessment of low dose IR effects in humans is one of the major problems in radiation protection that remains to be clarified. In this respect, the development of sensitive biomarkers for assessment of x-ray effects can give valuable information on the low dose-effect relationship.

The latter methodology was applied in this PhD research to assess radiation risks in children. We used the γ -H2AX foci assay to detect early x-ray effects at DNA level to get more insight into the dose-effect relationship for diagnostic CT x-rays in children. In an prospective multicentre study in Belgium, we determined the number of CT x-ray induced DNA DSBs in

lymphocytes of children undergoing a chest or abdomen CT examination (paper 2). This study resulted in three key findings:

- CT induces a small, but statistical significant number of DNA DSBs in children's T-lymphocytes
- Risk estimates based on the LNT hypothesis may represent underestimates
- More effective CT dose reduction results in less DNA damage

In the following sections, we will discuss these findings in more detail, describe the associated uncertainties and put the obtained results in the current concept of low dose risk estimates in paediatric CT imaging.

9.1

Biomarker studies in paediatric diagnostic radiology

Children are a difficult study population for biomarker studies, since the use of biological samples of children raises a number of ethical issues. Therefore, only limited *in vivo* biomarkers studies of paediatric patients were published. These studies will be presented in the following paragraphs, together with the findings of our own research group.

Since its discovery, the γ -H2AX foci assay has been widely applied in fundamental and human population studies, because of the high sensitivity, efficiency and mechanistic relevance of the assay. It is generally accepted that one γ -H2AX focus represents one DNA DSB. DSBs are considered to be the most deleterious effect of x-ray exposure at DNA level, because they can result in loss or rearrangement of genetic information, chromosomal aberrations and gene mutations, which can eventually lead to carcinogenesis (6). In the framework of cancer risk assessment, detection of chromosomal aberrations or MN induced by diagnostic x-rays would allow a more direct mutagen-carcinogen link. However, the γ -H2AX foci assay is currently the best we can do, due to the lack of sensitivity of contemporary mutagenicity assays.

9.1.1**Behaviour of the γ -H2AX dose response in diagnostic studies on children**

The results of the *in vivo* γ -H2AX foci study on 51 paediatric patients (median age: 3.8 years) undergoing a CT examination (see paper 2), showed an increase in DNA DSBs for nearly every child except for one patient with a very low blood dose of 0.14 mGy (7). The initial sharp increase of the *in vivo* dose response was confirmed by *in vitro* γ -H2AX foci data on umbilical cord blood, representing blood of a newborn. The shape of the *in vivo* and *in vitro* dose response curves points to a low dose hypersensitivity, which is consistent with a previous study of our research group on 49 paediatric patients (median age: 0.75 years) undergoing a cardiac catheterization (8). Figure 1.1 combines the γ -H2AX data versus the blood doses of both studies. However, the blood doses of the paediatric CT study are much lower (average blood dose: 1.35 mGy) compared to the blood dose in the study of interventional cardiology of Beels *et al.* (average blood dose: 11.3 mGy). The *in vivo* dose response allowed us to explore further the very low dose range in the paediatric CT study. The data of both *in vivo* CT and interventional x-ray studies are in good agreement and show that the *in vivo* foci yields observed in the paediatric patients are without any doubt higher than expected from the linear extrapolation of high dose behaviour (dashed line in Figure 9.1). The results indicate a higher risk for low dose exposure than expected using the LNT model, which will be further discussed in 1.1.2 of this chapter.

Until recently, it was not known whether the low doses from CT exams could induce γ -H2AX foci *in vivo* in young children. However, several studies already reported γ -H2AX foci induction by CT x-ray exposure in adult patients (9-11). Unfortunately, lack of blood dose calculations and different experimental conditions make it impossible to directly compare the results obtained in these adult patient studies with the results obtained for young children presented in paper 2. Around the same time of our study, a small pilot study was published by Halm *et al.* who also found a significant induction of γ -H2AX foci in lymphocytes of three very young children (3 – 21 months) post CT (12). The reported blood doses were in the same low dose range as our dose estimates (0.22 – 1.22 mGy), however, blood samples were taken 1h post CT exam. In view of the low statistical power, the results of this study are very preliminary and no wide-reach-

ing conclusions can be drawn on the dose-response relationship between γ -H2AX foci and the corresponding radiation doses.

A few *in vivo* studies involving other biomarkers to determine low dose effects of diagnostic x-rays were already published.

A first group of *in vivo* biomarker studies deals with CA and MN induced by diagnostic RX examinations of children. Already in 1980, a significant increase in chromosomal aberrations was reported in a retrospective study of nine children exposed to high diagnostic x-ray doses for congenital skeletal anomalies compared to nine healthy control individuals ($p = 0.001$) (13). The mean age of the children was 13.2 years (range 7 – 17 years). The shorter the time since the last x-ray exposure, the higher was the frequency of chromosome type aberrations. Although the study population was small, it was already clear at that time that exposure of children to diagnostic x-rays may cause chromosomal damage. Chest radiographs represent the basic radiological examination of the thorax providing diagnostic information on the status of lung, heart and the skeletal system; and are the most frequently performed radiological examinations in children (14). Effective doses from chest radiographs are also very small, typically less than 1 mSv. The CBMN assay was used in a study of Gajski *et al.* (15) to assess different types of chromosomal damage in twenty children with pulmonary diseases exposed to diagnostic x-ray procedures. The average age of the study population was 11.30 ± 2.74 years and absorbed doses were estimated by using thermoluminescence and radiophotoluminescence dosimetry systems. Almost all children exhibited higher frequency of CBMN parameters (MN, NPBs and NBUDs) compared with the levels before diagnostic examination. However, it should be noted that the observed increase in MN, NPBs and NBUDs frequencies per 1000 BN cells is very low in this study; respectively 3.00 MN, 3.05 NPBs and 2.30 NBUDs per 1000 BN cells, and the increase was only statistically significant for a few of the patients. The results of this study suggest, together with a previous study from the same research group using the comet assay (16), that the radiation exposure of diagnostic chest RX may induce some damaging effects to the cell chromosome structure, even though the radiation doses in this type of procedure is very low.

A second group of *in vivo* biomarker studies investigated mutagenic radiation effects in children with congenital heart diseases (CHD) undergoing intensive radiological exposure, who are theoretically at a relatively higher radiation risk due to their cumulative radiation exposure in the

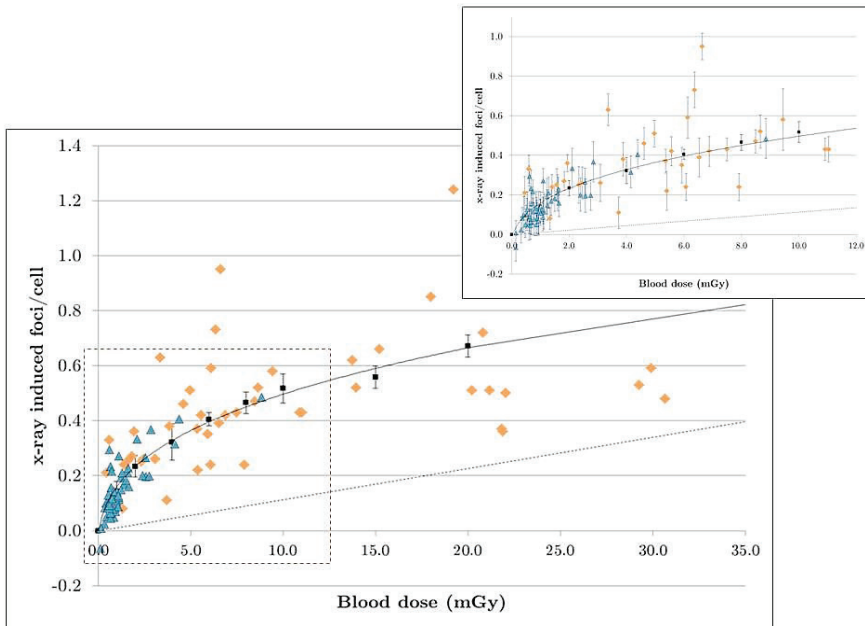


FIGURE 9.1

Comparison of x-ray induced γ -H2AX foci per cell versus calculated blood dose observed in the paediatric CT study (blue (7)) and the previous paediatric interventional cardiology study (orange (8)). The *in vitro* dose response curve is presented in black (■). Error bars are not shown in the overview figure, since they disturb the detail in the low dose region. The figure in the right corner zooms in on the low dose region, since most of the paediatric CT study data are clustered in this region (error bars are calculated based on Poisson statistics). The dashed line represents the behaviour according to the LNT hypothesis based on the γ -H2AX foci induced after an *in vitro* dose of 0.5 Gy (5.68 foci/cell). The error bars on the *in vitro* dose response curve represent SDs among three different donors.

early periods of life. Andreassi *et al.* (17) examined the frequency of CA and MN in patients with CHD. The mean frequency of CA and MN were higher in the exposed patients, showing that cardiac x-ray procedures are associated with a long lasting mark in the chromosomal damage of exposed children with CHD. The same research group published in 2010 a new study in which the MN assay was used as a biomarker of DNA damage before and 2h after catheterisation procedures in a subset of 18 patients (mean age 5.2 ± 5.7 years) (18). The micronucleated BN cell frequency was determined as the number of micronucleated cells per 1000 cells. The median micronucleus levels increased significantly after the procedure in comparison with the baseline (median effective MN value of 6‰ at base-

line versus 9‰ 2h after the procedure), but the median dose-area product (DAP) value of the paediatric procedure was high, 20 Gy cm².

A last study of cytogenetic biomarkers in children is of particular interest for this PhD research. A small scale pilot study was set up by Stephan *et al.* to determine whether CT could enhance the chromosome aberration yield in paediatric patients (19). Blood samples were taken from 10 children between 5 months and 15 years of age (median age: 8.4 years) before and after a CT scan. The mean blood dose of the 10 children was 12.9 mGy. Based on more than 20 000 analysed cells it was found that the frequencies of dicentric and acentric fragments were significantly increased after CT examination. The results demonstrate that CT examinations enhance the dicentric yields in peripheral lymphocytes of children. The detection of chromosomal anomalies induced by diagnostic x-rays in paediatric patients provides an interesting mutagen-carcinogen link. However, it should be noted that this kind of studies is not obvious in view of the low sensitivity of contemporary mutagenicity assays to detect the weak mutagenic effects induced by low dose exposure. The estimated blood dose of children after CT x-ray exposure is of the order of 0.1 - 10 mGy (based on our estimates in paper 2). To get meaningful results, chromosome and chromatid breaks should be analysed manually in 500 – 1000 metaphases/ per individual, which makes this kind of studies very labour intensive.

The observed low-dose hypersensitivity in both *in vivo* γ -H2AX foci studies in paediatric x-ray applications of our research group (7, 8) challenges the LNT hypothesis, which assumes less DNA damage than we observed, and can be explained by the bystander effect. The studies of the atomic bomb survivors have provided risk estimates that increase linearly for moderate to high doses (>50–100 mGy). However, this linear dose-response relationship based on the A-bomb data is very different in nature compared to the IR used in diagnostic radiology. The A-bomb survivors were mainly exposed to neutron and γ -rays, while 100 kV x-rays (corresponding to CT x-rays) were used through this PhD research. Estimates below this level are difficult to obtain directly from epidemiological data and BEIR VII indicates that “statistical limitations make it difficult to evaluate cancer risk in humans below this level” (20). However, for practical regulatory purposes, a linear model has been adopted for low doses and is used by the international radiation protection community. Nevertheless, this remains the main paradigm of radiation protection and as nicely described by Brenner *et al.*, a linear extrapolation could both underestimate

(hypersensitivity or bystander effect) or overestimate (adaptive response, threshold hypothesis or hormetic response) low-dose risks (21). Several radiobiological phenomena, challenge the assumption that the biological responses at high and low doses are proportional with radiation doses (22-24). Furthermore, this low dose hypersensitivity was also observed in an *in vitro* study of our research group, however, only when whole blood was irradiated with x-rays (25). On the contrary, when isolated T-lymphocytes were irradiated or when γ -rays were used, a linear dose response was observed. These findings suggest that biophysical differences in dose qualities and tissue environment might lead to a different radiation dose response. Nevertheless, the results of this PhD research support a hypersensitive response that is able to signal very small changes above endogenous level of DNA DSBs (26). The mechanisms of the radiation-induced bystander effect will be further discussed in the next section.

9.1.2**Low dose hypersensitivity indicates a bystander effect**

Already in 1992, the dogma that radiation-induced DNA damage is restricted to directly hit cells, has been challenged by the observation that similar effects can be seen in normal cells that were not directly traversed by the radiation track (27). In the following decades, evidence has built up for a novel biological phenomenon termed as bystander effect, in which genetic and biochemical changes not only occur in cells hit by ionizing particles but also in unexposed “bystander” cells, that are in close proximity to the directly hit cells. The fact that IR would only induce direct biological effects and subsequent health consequences as a result of energy deposition in the cell nucleus, is likely true for higher radiation doses, but at lower doses (<100 mGy) non-targeted effects may play a significant role (28, 29). A key characteristic of the bystander response in contrast to direct irradiation effects, is the dose–response relationship. Instead of an increased response with increasing radiation dose, the bystander response has been shown to be induced at very low doses (in the mGy range) and a further increase in radiation dose did not increase the effect (30). However, this hypothesis remains controversial and at high doses the effects will likely be overwhelmed by direct damage to cells (28). Also, it has been proposed that a binary mode of action may occur, with a simple on–off response, the probability of which increases with radiation dose (31). Bystander effects have been observed in a range of cell types and for several endpoints, such as sister chromatic exchanges, mutations, transformation, apoptosis, MN formation and genomic instability.

Co-culture experiments of irradiated and non-irradiation cells (32, 33), as well as medium transfer experiments (34) demonstrated that cell populations exposed to IR respond as an integrated tissue rather than separate individual cells, pointing to the role of the cellular communication. Microbeam irradiation could even demonstrate that gene mutations do occur following cytoplasmatic irradiation without crossing of the nucleus (28). The nature of the induced mutations in this study consisted mainly of base damage, suggesting the involvement of ROS. Several mechanisms have been assumed to mediate radiation-induced bystander effects, which are the result of cells receiving signals from irradiated cells through gap-junction mediated intercellular communication or the secretion of soluble factors (see Figure 9.2) (27). Several studies point to a crucial role of

membrane originating effects such as gap junctions and critical enzymes such as cyclooxygenase-2 (COX-2) (35, 36). Gap junction-mediated intercellular communication (GJIC) seems an appropriate mechanism for the mediation of bystander effects because they form clusters of intercellular membrane channels connecting the cytoplasm of two neighbouring cells. Gap junction channels consisting of connexin (Cx) proteins may mediate bystander effects by allowing the direct intercellular exchange of small molecules of up to 1000 – 1500 Da, such as cAMP, IP3 and Ca^{2+} (37). Another mechanism to transduce bystander signals is by soluble factors released from irradiated cells into the culture medium. Soluble factors like cytokines such as tumour necrosis factor α (TNF- α) (38), interleukin 6 (IL-6) (39), and IL-8 (40) and transforming growth factor- β 1 (TGF- β 1) (41) can be found in literature as mediators of the ‘paracrine’ bystander effect.

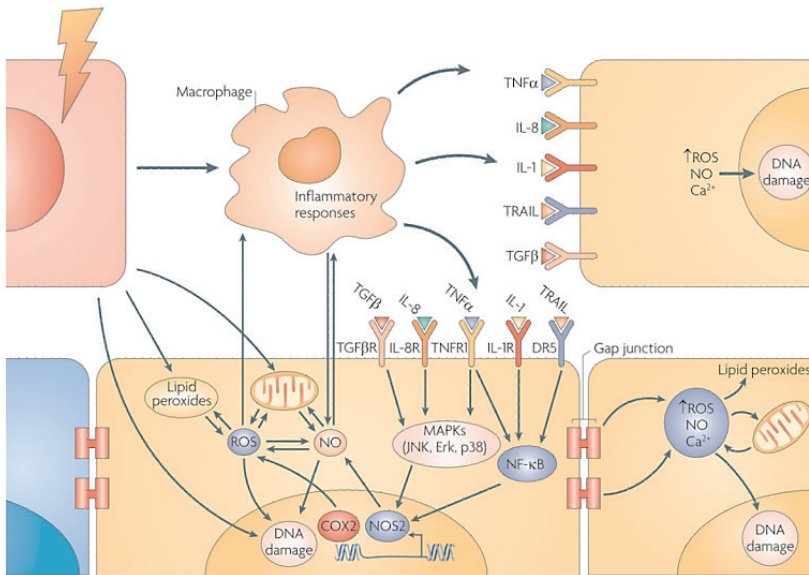


FIGURE 9.2

Underlying key pathways of the radiation-induced bystander effects. Signalling molecules are propagated among irradiated and neighbouring bystander cells through two key routes. The first one involves direct intercellular communication via gap junctions, the second one through diffusible secretion of cytokine signals in the surrounding matrix. Figure from (42).

Moreover, an underlying mechanism of the previously mentioned modes of bystander communication is the involvement of ROS. Several studies have indicated that the oxidative metabolism mediates signalling events leading to radiation-induced bystander effects. Normal oxidative metabolism is a key endogenous regulator of ROS and reactive nitrogen species (RNS) (35). Physical levels of both ROS and RNS play critical roles in numerous cellular functions. A disruption of the oxidative metabolism alters the homeostatic cellular redox and results in a state of oxidative stress. The role of free radicals in the bystander effect such as ROS released into the cell-culture medium has been shown by applying antioxidants such as superoxide dismutase or inhibitors of superoxide and NO generators (42, 43). Zhou *et al.* showed that treatment of bystander cells with a COX-2 inhibitor (NS-398) reduced the bystander effect (44). These results provide evidence that the COX-2-related pathway, which is essential in mediating cellular inflammatory response, is a critical signalling link for the bystander phenomenon.

The mechanisms of bystander signalling are now starting to be elucidated at the molecular level and several key molecules are known to have close parallels to inflammatory responses. For example, recent studies have shown that inflammatory macrophages are a potent source of microenvironmental reactive nitrogen and oxygen species that can damage bystander cells (43). Gene set enrichment analysis could demonstrate that different gene profiles were highlighted after low and high doses of x-rays in whole blood samples (44). Inflammatory and immune-related gene sets were higher ranked after low dose irradiation, whereas gene sets enriched at higher doses were 'classical' radiation pathways like p53 signalling, apoptosis and DNA damage and repair. Functional analysis of genes differentially expressed at low doses showed the enrichment of chemokine and cytokine signalling. Furthermore, there are several other candidate processes suggested in scientific literature that could at least in part mediate the non-targeted effects due to IR exposure, such as exosomes (45), DNA repair capacity (46) and/or mitochondrial dysfunction (47). It is most likely that multiple mechanisms are involved in bystander effects, depending on the biological endpoint being measured and the cell type (48). The bystander phenomenon implies that in the low dose range of diagnostic radiology a tissue radiation response is observed rather than a cellular DNA damage response. To gain more understanding of the biological mechanisms behind the observed low dose hypersensitivity in both *in vivo* paediatric

studies, it would be interesting to study differential gene profiles before and after CT examination in children.

The *in vitro* observed bystander effects are possibly linked with the longer-range effects observed in response to radiotherapy in humans, termed as the controversial abscopal or out-of-field distant bystander responses (49, 50). It has been reported that non-targeted tissues in partial body irradiated rodents also experienced stressful effects, including oxidative and oncogenic effects. A study of Mancuso *et al.* showed that apoptosis and tumour induction were observed in the shielded cerebellum of radio-sensitive mice after partial body irradiations (51, 52). This phenomenon indicates the carcinogenic potential of bystander responses *in vivo*, such as the induction of secondary cancers following radiotherapy.

9.1.3

Importance of blood dose calculation in biomarker studies

Biomarker studies require direct measurements on biological media, in our set-up peripheral whole blood. The γ -H2AX foci analysis of lymphocytes has the advantage that access to blood is easy and fast and does not require a massive medical intervention. In order to obtain a reliable interpretation of the *in vivo* γ -H2AX foci data in our paediatric CT study (paper 2) (7), it was very important to have an accurate blood dose calculation for every child. In this calculation, we had to take into account the patient's anatomy, different types of CT systems, dose reduction techniques and various types of CT protocols. To obtain an individual blood dose estimate for every patient, patient-specific 3D voxel models were created based on the CT images of the paediatric patients by using ImpactMC simulation software 1.3.1 (CT Imaging GmbH, Germany) (53). Organ volumes were segmented in the original CT images and organ dose deposition was calculated based on the Monte Carlo dose distribution, as illustrated in Figure 9.3. A density value and a mass attenuation coefficient is assigned to each voxel contained in the input volume. The density values are determined from the CT numbers using validated conversion curves.

The blood dose was calculated as a weighted sum of the doses of the largest blood-containing organs in the field of view with the percentage of blood pool in children as weighting factor. For CT chest and CT abdomen, these organs are lungs (12.5%), heart (10%), liver (10%) and remainder (67.5%) (54). The blood dose calculation in the 'remainder of the body'

was an important issue in our estimations. We considered the radiation dose outside the scan length as negligible, moreover, no voxel data are available outside the scanned volume since our voxel model was based on the CT images of the patients. The dose was calculated in the remaining volume (excluding lung, heart and liver) of the scan region and normalized over the total weight of the patient, excluding liver, heart and lungs. The latter methodology was validated and resulted in an uncertainty of about 10% (55).

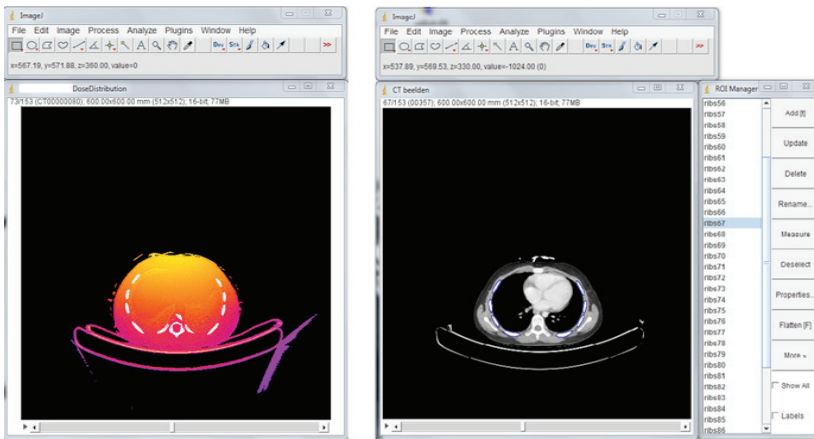


FIGURE 9.3

The left picture shows the typical dose distribution of a transversal slice of a chest CT scan represented by colour scales. The right picture illustrates the segmentation of the organs by drawing regions of interest on the same CT image.

Accurate assessment of the dose to the blood remains a challenge. It is already shown in radiotherapy patients that the dependence between dose and average incidence of γ -H2AX foci in lymphocytes was found to differ by as much as four-fold depending on the location of the irradiated site of the body. Lymphocyte distribution, circulation and migration through the different organs may explain these differences. An accurate blood dose calculation is needed to interpret the γ -H2AX foci results in lymphocytes and in an ideal situation, the biodistribution of lymphocytes through the

body should be taken into account. For example, lymphocytes that migrate more slowly in capillaries than in large vessels may receive a higher radiation dose (56-58). Assessment of dose to the blood remains a challenge since blood is a circulating fluid and none of the Monte Carlo simulation CT dose reconstruction programs that are currently available, such as ImpactMC and NCI-CT (59), can estimate dose to circulating fluids. The methodology applied in our paper 2 is the best we can do so far and provides a substantial improvement compared to standard software tools in which only anthropomorphic paediatric phantoms for discrete reference ages can be selected. The dosimetry tools ImPact (www.impactscan.org), ImpactDose (CT Imaging GmbH, Erlangen, Germany) and CT-Expo (Medizinische Hochschule, Hannover, Germany) offer anthropomorphic phantoms limited to newborn, child, adult male and adult female. Considering the diversity among the anatomy of paediatric patients, it is impossible to perform the dose estimations accurately for paediatric patients with only a few phantom models.

9.1.4

Paediatric patient data point to age-dependency in DNA damage induced by CT x-rays

Based on the paediatric CT data, we investigated if we could observe an intrinsic higher radiosensitivity decreasing with the age of the children included in study (7). The number of induced γ -H2AX foci was divided by the calculated blood dose and plotted versus age of the paediatric patient (see Figure 9.4). The linear fit indicated a decrease of the foci-over-dose ratio data versus age. The diminishing trend of induced foci with age remains present when patients are selected with blood doses in the range of 0-2 mGy, indicating that the observed tendency is not caused by the fact that blood doses are higher in larger volumes, e.g. older patients. These findings show small but observable age dependent DNA damage effects induced by CT x-rays, however, the regression analysis showed no statistical significance for the decrease with age.

The previously mentioned classical cytogenetic study of Stephan *et al.*, showed that CT examinations enhanced the dicentric yields in children aged up to 15 years (19). When the children were subdivided in two groups in the same study, those with an age of 0.4 to 9 years and from 10 to 15 years, it became obvious that the observed increase in CA was mainly con-

tributed by the younger age group, indicating that children younger than 10 years may be more radiation sensitive.

In the study of Bakhmutsky *et al.* regression analysis showed that significantly more translocated chromosomes, more dicentric and more colour junctions were observed for newborns as a group compared to adults as a group (60). Both studies support the findings that children are at higher risk of developing cancer associated with radiation exposure. The age effect will be further discussed in chapter 11 of the Discussion.

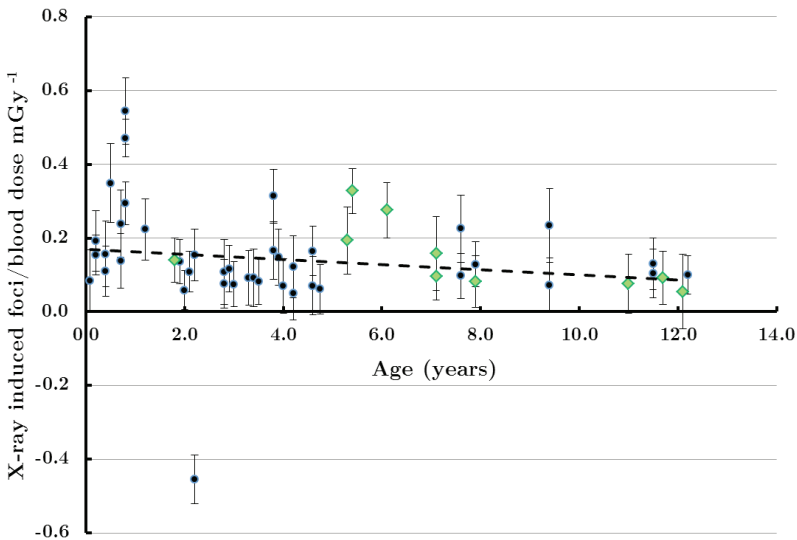


FIGURE 9.4

The number of γ -H2AX foci normalized to blood dose, as a function of age of the 41 CT chest patients and 10 CT abdomen patients included in the paediatric CT study (7). The dashed line is the result of a linear fit.

9.2**Uncertainties in paediatric radiation risk assessment**

The lifetime attributable risk of cancer incidence and mortality associated with a chest or abdomen CT scan were estimated for each individual paediatric patient in paper 2. The estimations were based on the calculated organ doses of each patient and the risk models from the National Academy, referred to as the BEIR VII risk models (20). The committee judged in their seventh report on the health effect of low levels of low LET IR (< 100 mGy) that the LNT model provided the most reasonable description of the relationship between low-dose exposure to IR and the incidence of solid cancers induced by IR. For leukaemia, the committee adopted a linear-quadratic model. Data from epidemiological studies (atomic bomb survivor studies, medical, occupational and environmental radiation studies) were used to express the dependence of risk on radiation dose, sex and age at exposure.

The LSS cohort plays a principal role in the development of risk models by the BEIR committee. The updated risk estimates did not change significantly from the BEIR V estimates published in 1990 (61), but the confidence intervals have narrowed as the result of the availability of additional data. For 2 of the 11 evaluated cancers, namely breast and thyroid cancer, models were based on pooled analyses that included data on both the LSS cohort and medically exposed persons. Data from additional medical studies and from studies of nuclear workers were evaluated and found to be compatible with BEIR VII models (20).

The BEIR VII risk models allow to compare cancer risks from radiation exposure of medical x-rays and natural background cancer risks. This allows a comparison between potential negative effects from e.g. a childhood CT scan with the hazards of everyday living. The dose-effect model of the BEIR VII report assumes that risk caused by the exposure is proportional to the baseline risk as well as to the exposure, with some modifications. This is in line with the ERR model, a product of both baseline risk and dose, which is for this reason often referred to as the multiplicative model. Table 9.1 shows the expected number of radiation induced cancers based on BEIR VII risk estimates from an exposure to 0.1 Gy in a population of 100 000 persons with an age range distribution similar to that of the entire US population, compared with the number of naturally occurring cancers (62). This table illustrates that the number of radiation-induced

cancers is very small compared to the number of naturally occurring cancers, what makes the detection of this excess very difficult. On average, assuming a sex and age distribution similar to the entire US population, BEIR VII lifetime risk calculation predicts that approximately 1 person in 100 would be expected to develop cancer (solid cancer or leukaemia) from a dose of 100 mGy above background, while approximately 42 out of 100 individuals would develop solid cancer or leukaemia from other causes.

	All solid cancer		Leukaemia	
	Males	Females	Males	Females
Excess cases (including non-fatal cases) from exposure to 0.1 Gy	800 (400, 1600)	1300 (690, 2500)	100 (30, 300)	70 (20, 250)
Number of cases in the absence of exposure	45 500	36 900	830	590
Excess deaths from exposure to 0.1 Gy	410 (200, 830)	610 (300, 1200)	70 (20, 220)	50 (10, 190)
Number of deaths in the absence of exposure	22 100	17 500	710	530

TABLE 9.1

BEIR VII lifetime attributable risk estimates of incidence and mortality for all solid cancers and leukaemia for a population of mixed ages, with 95% subjective confidence intervals. The subjective confidence intervals reflect the most important sources of uncertainty (statistical variation, DDREF and method of transport). Number of cases or deaths are expressed per 100 000 persons. Figure from (20).

Site-specific solid cancer and leukaemia lifetime risk for cancer incidence and mortality resulting from a single dose of 100 mGy at several specific ages can be estimated by using Tables 12D-1 and 12D2 of the BEIR VII report (20). Figure 9.5 shows that these risk estimates depend both on sex and age at exposure, with higher risks for females and for those exposed at younger ages. The committee's estimates are obtained by calculating a weighted mean of linear estimates based on relative and absolute risk transport, and reducing them by a DDREF of 1.5. For thyroid cancer, the BEIR VII Committee used only an ERR model to quantify risk, while for breast cancer only an EAR model based on a pooled analysis of eight cohorts was used (63). It is surprising that the LAR for lung cancer is nearly

twice as high for females compared to males, even though the baseline risk shows a reverse pattern. This is possibly attributable to statistical anomalies or other biases in LARs estimated with high uncertainty. Estimates for persons exposed at age 10 are more than twice as high as those for persons exposed at ages 30 or 50. Since current models don't allow further decrease after age 30, the difference in LAR for persons exposed at ages 30 and 50 is not so high.

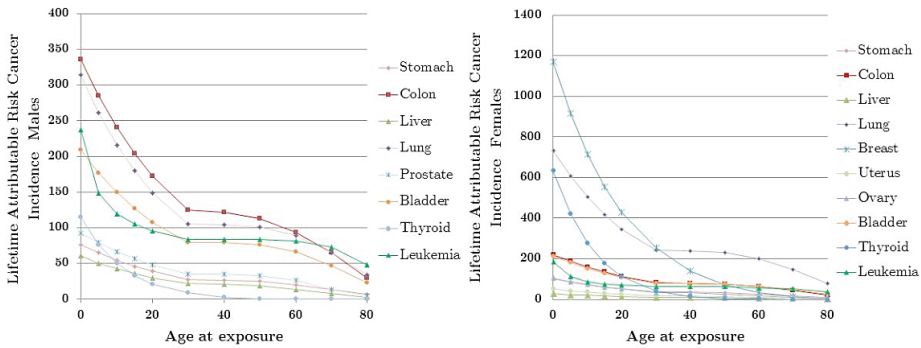


FIGURE 9.5

BEIR VII LAR models of cancer incidence for males and females, presenting the incidence per 100,000 persons exposed to a single dose of 0.1 Gy. Figure based on Table 12D-1 of (20).

Another source for LAR risk estimates taking into account sex and age at exposure, comparable with the BEIR VII report, was more recently published by the US Environmental Protection Agency, under the EPA Radiogenic Cancer Risk Models and Projections for the US Population (64). The report is generally based on the models recommended by the BEIR VII, but a number of extensions and modification have been implemented. For some sites such as stomach, liver and prostate, EPA's LAR projections are larger, but comparison of the EPA and BEIR VII LAR projections of cancer incidence per 10 000 persons/Gy provides very similar results: total cancer incidence for males is 955 compared to 900, and 1350 compared to 1382 for females, in EPA and BEIR VII respectively.

Recent reports of ICRP (65) and UNSCEAR (66) provide also information on risk models, in terms of ERR and EAR values. ICRP and BEIR VII based their models largely on 1958-1998 LSS incidence data, whereas the UNSCEAR models are based on 1950-2000 mortality data (64). The ICRP risk projections assume a LNT dose-response and the approach is very similar to that used by both EPA and BEIR VII. However, one of the main differences is the fact that ICRP uses a DDREF of 2 instead of 1.5. In ICRP, the ERR and EAR for most solid cancer sites decrease with age-at-exposure by about 17% (ERR) or 24% (EAR) per decade (even beyond age 30). In BEIR VII, the decrease per decade for exposures before age 30 was somewhat steeper, typically 26% (ERR) or 34% (EAR), but there is no decrease in risk with age-at exposure after age 30. A comparison with the UNSCEAR 2008 models is more complicated, since the form of the UNSCEAR ERR and EAR models depend on cancer site. In contrast to the BEIR VII models, age-at-exposure is seldom used as a dose effect modifier, but exceptions are the EAR and ERR models for thyroid cancer and the ERR model for brain/CNS cancers.

The 'residual site' cancers in the risk model of BEIR VII and EPA deserve special attention. The residual category generally includes cancers for which there were insufficient data from the LSS cohort or other epidemiological studies to quantify reliably radiogenic site-specific risks. For example cancer of oesophagus, bone, kidney, skin, brain and CNS are included in BEIR VII's 'remainder'; while the more recent EPA report provides additional lifetime risk models for kidney and skin cancer. Although the UNSCEAR 2013 report claims that children are at higher risk to develop brain and CNS tumours after IR exposure, neither BEIR VII nor EPA have developed separate lifetime risk models for brain and CNS cancers. These cancers are also included as part of the 'remainder'. No conclusive evidence is available on which model one should use to estimate brain/CNS cancer risks and how the attained age should be included (64).

As BEIR VII uses the primary LSS cohort data for the estimation of lifetime risk for the US population, several assumptions had to be made that involve large uncertainties. Therefore we should interpret specific estimates of LAR with a healthy scepticism. A confidence interval is the usual statistical way to reflect the uncertainty. However, the BEIR VII approach also has to deal with uncertainties external to the data, since the uncertainty depends not only on direct numerical observations, but also

on opinions. Three major sources of uncertainty in the quantitative analysis are mentioned by the committee:

- Sampling variability in risk model parameter estimates from the LSS data
- The uncertainty about the use of risk estimates based on Japanese atomic bomb survivors to estimate risk for the US population
- The appropriate value of DDREF to adjust the low dose risks based on LNT models

An additional important remark by EPA on the BEIR VII risk estimates is about the lack of uncertainty on the form of the dose-response relationship, which is a more 'subjective' uncertainty. Underlying mechanisms of the biological effects of low dose IR are extensively investigated, which could eventually mandate a different dose-response model. The latter could result in large changes in low dose risk estimates. Based on the dose-response curve of our *in vivo* γ -H2AX foci data, application of the LNT model in the diagnostic dose range could result in an underestimate of the radiation risks. Based on the γ -H2AX foci data, the LAR would be approximately 10 times higher when using the foci-LAR conversion factor obtained after an *in vitro* dose of 0.5 Gy x-rays. EPA does not propose to quantify the uncertainty on the dose-response, but it is important that all predictions of the effects of low doses of ionizing radiation should disclose all of the limitations in the current state of knowledge about low dose radiation effects. Because of these limitations and uncertainties in the data used to develop risk models, risk estimates can be a factor of 2 or 3 larger or smaller.

9.3**In vivo biomarker data illustrate the necessity of CT dose reduction: the “Image Gently” message**

Our *in vivo* biomarker study on direct DNA damage induced by CT x-rays, clearly demonstrates that lower patient doses result in less DNA damage (see Figure 4 in paper 2). The DLP and CTDI values of the Belgian multi-centre study indicate that most of the participating hospitals applied good clinical practice for paediatric CT imaging compared to national DRLs. However, substantial differences in dose-sparing CT equipment and protocols, resulted in differences in blood doses and corresponding DNA damage. These results should encourage justification of the indications for which CT imaging is used in children and optimization of the scanning techniques and protocols.

CT is still extensively used in paediatric radiology and will not be abandoned any time in the near future. MSCT has revolutionised image quality by improvement of spatial resolution and reduction of acquisition time, thereby reducing strongly the problems of movement artefacts among children. From a patient’s perspective, the benefits of a medically indicated CT scan exceed by far the small radiation-induced cancer risk (LAR for cancer mortality was 0.08 and 0.13 ‰ for paediatric chest CT and abdomen CT respectively). Nevertheless MSCT allows rapid and repeated examinations of large volumes, which can lead to high individual radiation exposure. Especially for the radiosensitive paediatric population, this is a topic of high concern (see also 2.2.2). We should reduce the medical radiation exposure to children as much as possible, the “as low as reasonably achievable” (ALARA) concept (67). Several campaigns have been launched to create awareness among CT prescribers, users, vendors and patients (68, 69). The most extensive initiative came from the Alliance for Radiation Safety in Pediatric Imaging: the “Image Gently” Campaign in the USA (<http://www.imagegently.org/>) (69). This initiative presents a coalition of health care organizations dedicated to provide safe, high quality paediatric imaging worldwide. The primary objective of the Alliance is to raise awareness in the imaging community of the need to adjust radiation dose when imaging children. The ultimate goal of the Alliance is to change practice. Figure 9.6 presents the CT campaign poster used to encourage health care providers

to pledge to “Image Gently” in paediatric CT imaging. In Belgium we have a campaign intended for the whole population and not specifically for children, funded by the Belgian government: “Zuinig met straling - Medische beelden zijn geen vakantiekiekjes” (<http://www.zuinigmetstraling.be/>).

Main messages of the “Image Gently” campaign are justification of the CT scans and optimization of the CT protocols taking into account the age and biometry of the paediatric patients.

Justification of scan. Some studies suggest that a third of paediatric CT scans are unnecessary (2, 70). This means that reduction of the radiation dose and its associated risk in children starts with performing CT scans in



FIGURE 9.6

The left picture represents the Image Gently campaign poster for CT imaging (<http://www.imagegently.org/>). The right picture is the 2013-2014 campaign poster of the Belgian initiative (<http://www.zuinigmetstraling.be/>).

children only when properly indicated. The referring physician and radiologist should consider whether the exam is truly clinically indicated and was not recently performed in another hospital. Furthermore, they should check if no alternative diagnostic procedure might be available, not involving ionizing radiation such as ultrasound (US) and MRI. As published by Nievelstein *et al.*, US should be the first-line imaging modality in children

for most abdominal, neck and muscoskeletal indications, as children usually lack large amounts of fatty tissue (67). Furthermore, MRI is increasingly been used outside the central nervous system. The latter is of special interest in paediatric oncology, where diagnostic imaging is repeatedly used during follow-up.

Optimisation of paediatric CT. When CT is indicated, great care should be taken to optimize radiation exposure in order to minimize the risk for carcinogenic effects later in life. Updated strategies to optimize radiation doses in paediatric CT imaging have recently been published on the Image Gently website under “Image Gently Development of Paediatric CT Protocols 2014”. The protocols consist of two Excel worksheets, one for body and one for head protocols, to provide guidance on how to set up techniques for all size patients, newborns to adults, which provides diagnostic image quality at well-managed radiation dose levels for any department’s or practice’s CT scanner. The scan and technical parameters should be tailored to the size of the child, the body region of interest and the clinical indication. Furthermore, dose reduction techniques should be implemented taking into account the required image quality (ATCM, iterative reconstruction and/or adaptive collimation). The primary goal should be to achieve sufficient diagnostic image quality instead of optimal image quality, which means that a certain amount of image noise is acceptable as long as the clinical question can be solved (67). Excellent strategies for dose optimization in paediatric (MS)CT imaging can be found in the following publications (67, 71-73)

The observations of our paediatric CT study should encourage medical practitioners to maximize the benefit-to-risk ratio of CT imaging in paediatric radiology (7). Even more than for adults, the benefit of each imaging study using IR should be balanced against the long-term risk of cancer development for children (74). However, we should keep radiation risks in perspective. The estimated cancer risk associated with paediatric CT examinations in this PhD research were small compared to the natural cancer incidence and the uncertainties on the risks are large. Nevertheless, this small increase in radiation-associated cancer risk for an individual can become a public health concern when we multiply this risk by the 2.7 million procedures performed each year in children (75).

9.4

References

1. Brody AS, Frush DP, Huda W, Brent RL, Amer Acad P. Radiation risk to children from computed tomography. *Pediatrics*. 2007;120(3):677-82.
2. Brenner DJ, Hall EJ. Current concepts - Computed tomography - An increasing source of radiation exposure. *New England Journal of Medicine*. 2007;357(22):2277-84.
3. Pearce MS, Salotti JA, Little MP, McHugh K, Lee C, Kim KP, et al. Radiation exposure from CT scans in childhood and subsequent risk of leukaemia and brain tumours: a retrospective cohort study. *Lancet*. 2012;380(9840):499-505.
4. Morgan WF, Bair WJ. Issues in Low Dose Radiation Biology: The Controversy Continues. A Perspective. *Radiation Research*. 2013;179(5):501-10.
5. Little MP, Wakeford R, Tawn EJ, Bouffler SD, Berrington de Gonzalez A. Risks associated with low doses and low dose rates of ionizing radiation: why linearity may be (almost) the best we can do. *Radiology*. 2009;251(1):6-12.
6. Rothkamm K. Different Means to an End: DNA Double-Strand Break Repair. In: Kiefer J, editor. *Life Sciences and Radiation*: Springer Berlin Heidelberg; 2004. p. 179-86.
7. Vandevoorde C, Franck C, Bacher K, Breyssem L, Smet MH, Ernst C, et al. gamma-H2AX foci as in vivo effect biomarker in children emphasize the importance to minimize x-ray doses in paediatric CT imaging. *European Radiology*. 2015;25(3):800-11.
8. Beels L, Bacher K, De Wolf D, Werbrouck J, Thierens H. gamma-H2AX Foci as a Biomarker for Patient X-Ray Exposure in Pediatric Cardiac Catheterization Are We Underestimating Radiation Risks? *Circulation*. 2009;120(19):1903-9.
9. Lobrich M, Rief N, Kuhne M, Heckmann M, Fleckenstein J, Rube C, et al. In vivo formation and repair of DNA double-strand breaks after computed tomography examinations. *Proceedings of the National Academy of Sciences of the United States of America*. 2005;102(25):8984-9.
10. Rothkamm K, Balroop S, Shekhdar J, Fernie P, Goh V. Leukocyte DNA damage after multi-detector row CT: A quantitative biomarker of low-level radiation exposure. *Radiology*. 2007;242(1):244-51.
11. Beels L, Bacher K, Smeets P, Verstraete K, Vral A, Thierens H. Dose-length product of scanners correlates with DNA damage in patients undergoing contrast CT. *European Journal of Radiology*. 2012;81(7):1495-9.
12. Halm BM, Franke AA, Lai JF, Turner HC, Brenner DJ, Zohrabian VM, et al. gamma-H2AX foci are increased in lymphocytes in vivo in young children 1 h after very low-dose X-irradiation: a pilot study. *Pediatr Radiology*. 2014;44(10):1310-7.
13. Nordenson I, Beckman G, Beckman L, Lemperg R. Chromosomal aberrations in children exposed to diagnostic X-rays. *Hereditas*. 1980;93(1):177-9.
14. Seidenbusch MC, Schneider K. [Radiation exposure of children in pediatric radiology]. *Rofo*. 2008;180(5):410-22.
15. Gajski G, Milkovic D, Ranogajec-Komor M, Miljanic S, Garaj-Vrhovac V. Application of dosimetry systems and cytogenetic status of the child population exposed to diagnostic X-rays by use of the cytokinesis-block micronucleus cyto assay. *Journal of Applied Toxicology*. 2011;31(7):608-17.
16. Milkovic D, Garaj-Vrhovac V, Ranogajec-Komor M, Miljanic S, Gajski G, Knezevic Z, et al. Primary DNA damage assessed with the comet assay and comparison to the absorbed dose of diagnostic X-rays in children. *International Journal of Toxicology*. 2009;28(5):405-16.
17. Andreassi MG, Ait-Ali L, Botto N, Manfredi S, Mottola G, Picano E. Cardiac catheterization and long-term chromosomal damage in children with congenital heart disease. *European Heart Journal*. 2006;27(22):2703-8.
18. Ait-Ali L, Andreassi MG, Foffa I, Spadoni I, Vano E, Picano E. Cumulative patient effective dose and acute radiation-induced chromosomal DNA damage in children with congenital heart disease. *Heart*. 2010;96(4):269-74.
19. Stephan G, Schneider K, Panzer W, Walsh L, Oestreicher U. Enhanced yield of chromosome aberrations after CT examinations in paediatric patients. *International Journal of Radiation Biology*. 2007;83(5):281-7.
20. *Health Risks from Exposure to Low Levels of Ionizing Radiation: BEIR VII Phase 2: The National Academies Press*; 2006.
21. Brenner DJ, Doll R, Goodhead DT, Hall EJ, Land CE, Little JB, et al. Cancer risks attributable to low doses of ionizing radiation: Assessing what we really know. *Proceedings of the National Academy of Sciences of the United States of America*. 2003;100(24):13761-6.
22. Averbeck D. Does scientific evidence support a change from the LNT model for low-dose radiation risk extrapolation? *Health Physics*. 2009;97(5):493-504.
23. Tubiana M, Feinendegen LE, Yang CC, Kaminski JM. The Linear No-Threshold Relationship Is Inconsistent with Radiation Biologic and Experimental Data. *Radiology*. 2009;251(1):13-22.
24. Grudzinski S, Raths A, Conrad S, Ruebe CE, Loeblich M. Inducible response required for repair of low-dose radiation damage in human fibroblasts. *Proceedings of the National Academy of Sciences of the United States of America*. 2010;107(32):14205-10.

25. Beels L, Werbrout J, Thierens H. Dose response and repair kinetics of gamma-H2AX foci induced by in vitro irradiation of whole blood and T-lymphocytes with X- and gamma-radiation. *International Journal of Radiation Biology*. 2010;86(9):760-8.
26. Short SC, Bourne S, Martindale C, Woodcock M, Jackson SP. DNA damage responses at low radiation doses. *Radiat Research*. 2005;164(3):292-302.
27. Nagasawa H, Little JB. Induction of sister chromatid exchanges by extremely low doses of alpha-particles. *Cancer Research*. 1992;52(22):6394-6.
28. Morgan WF, Sowa MB. Non-targeted effects induced by ionizing radiation: Mechanisms and potential impact on radiation induced health effects. *Cancer Letters*. 2015;356(1):17-21.
29. Seymour CB, Mothersill C. Relative contribution of bystander and targeted cell killing to the low-dose region of the radiation dose-response curve. *Radiation Research*. 2000;153(5 Pt 1):508-11.
30. Belyakov OV, Malcolmsom AM, Folkard M, Prise KM, Michael BD. Direct evidence for a bystander effect of ionizing radiation in primary human fibroblasts. *British Journal of Cancer*. 2001;84(5):674-9.
31. Schettino G, Folkard M, Prise KM, Vojnovic B, Held KD, Michael BD. Low-dose studies of bystander cell killing with targeted soft X rays. *Radiation Research*. 2003;160(5):505-11.
32. Azzam EI, de Toledo SM, Gooding T, Little JB. Intercellular communication is involved in the bystander regulation of gene expression in human cells exposed to very low fluences of alpha particles. *Radiation Research*. 1998;150(5):497-504.
33. Azzam EI, de Toledo SM, Little JB. Direct evidence for the participation of gap junction-mediated intercellular communication in the transmission of damage signals from alpha-particle irradiated to nonirradiated cells. *Proceedings of the National Academy of Sciences of the United States of America*. 2001;98(2):473-8.
34. Mothersill C, Seymour C. Medium from irradiated human epithelial cells but not human fibroblasts reduces the clonogenic survival of unirradiated cells. *International Journal of Radiation Biology*. 1997;71(4):421-7.
35. Zhao Y, de Toledo SM, Hu G, Hei TK, Azzam EI. Connexins and cyclooxygenase-2 crosstalk in the expression of radiation-induced bystander effects. *British Journal of Cancer*. 2014;111(1):125-31.
36. Azzam E, de Toledo S, Harris A, Ivanov V, Zhou H, Amundson S, et al. The Ionizing Radiation-Induced Bystander Effect: Evidence, Mechanism, and Significance. In: Sonis ST, Keefe DM, editors. *Pathobiology of Cancer Regimen-Related Toxicities*: Springer New York; 2013. p. 35-61.
37. Oyamada M, Oyamada Y, Takamatsu T. Regulation of connexin expression. *Biochimica et Biophysica Acta*. 2005;1719(1-2):6-23.
38. Shareef MM, Cui N, Burikhanov R, Gupta S, Satishkumar S, Shajahan S, et al. Role of tumor necrosis factor-alpha and TRAIL in high-dose radiation-induced bystander signaling in lung adenocarcinoma. *Cancer Research*. 2007;67(24):11811-20.
39. Chou CH, Chen P-J, Lee P-H, Cheng A-L, Hsu H-C, Cheng AC-H. Radiation-induced hepatitis B virus reactivation in liver mediated by the bystander effect from irradiated endothelial cells. *Clinical Cancer Research*. 2007;13(3):851-7.
40. Faocetti A, Ballarini F, Cherubini R, Gerardi S, Nano R, Ottolenghi A, et al. Gamma ray-induced bystander effect in tumour glioblastoma cells: A specific study on cell survival, cytokine release and cytokine receptors. *Radiation Protection Dosimetry*. 2006;122(1-4):271-4.
41. Iyer R, Lehnert BE. Factors underlying the cell growth-related bystander responses to alpha particles. *Cancer Research*. 2000;60(5):1290-8.
42. Prise KM, O'Sullivan JM. Radiation-induced bystander signalling in cancer therapy. *Nature Reviews Cancer*. 2009;9(5):351-60.
43. Coates PJ, Robinson JI, Lorimore SA, Wright EG. Ongoing activation of p53 pathway responses is a long-term consequence of radiation exposure in vivo and associates with altered macrophage activities. *Journal of Pathology*. 2008;214(5):610-6.
44. El-Saghire H, Thierens H, Monsieure P, Michaux A, Vandevoorde C, Baatout S. Gene set enrichment analysis highlights different gene expression profiles in whole blood samples X-irradiated with low and high doses. *International Journal of Radiation Biology*. 2013;89(8):628-38.
45. Al-Mayah AH, Irons SL, Pink RC, Carter DR, Kadhim MA. Possible role of exosomes containing RNA in mediating nontargeted effect of ionizing radiation. *Radiation Research*. 2012;177(5):539-45.
46. Nagasawa H, Huo L, Little JB. Increased bystander mutagenic effect in DNA double-strand break repair-deficient mammalian cells. *International Journal of Radiation Biology*. 2003;79(1):35-41.
47. Kim GJ, Chandrasekaran K, Morgan WF. Mitochondrial dysfunction, persistently elevated levels of reactive oxygen species and radiation-induced genomic instability: a review. *Mutagenesis*. 2006;21(6):361-7.
48. Zhou H, Suzuki M, Geard CR, Hei TK. Effects of irradiated medium with or without cells on bystander cell responses. *Mutation research*. 2002;499(2):135-41.
49. Kaminski JM, Shinohara E, Summers JB, Niermann KJ, Morimoto A, Brousal J. The controversial abscopal effect. *Cancer Treatment Reviews*. 2005;31(3):159-72.

50. Prise KM, O'Sullivan JM. Radiation-induced bystander signalling in cancer therapy. *Nature reviews Cancer*. 2009;9(5):351-60.
51. Mancuso M, Pasquali E, Leonardi S, Tanori M, Rebessi S, Di Majo V, et al. Oncogenic bystander radiation effects in Patched heterozygous mouse cerebellum. *Proceedings of the National Academy of Sciences of the United States of America*. 2008;105(34):12445-50.
52. Mancuso M, Pasquali E, Giardullo P, Leonardi S, Tanori M, Di Majo V, et al. The Radiation Bystander Effect and its Potential Implications for Human Health. *Current Molecular Medicine*. 2012;12(5):613-24.
53. Schmidt B, Kalender WA. A fast voxel-based Monte Carlo method for scanner- and patient-specific dose calculations in computed tomography. *Physica Medica*. 2002;18(2):43-53.
54. Frank C, Vandevoorde C, Goethals I, Smeets P, Achten E, Verstraete K, Thierens H, Bacher K. The role of size-specific dose estimate (SSDE) in patient-specific organ dose and cancer risk estimation in paediatric chest and abdominopelvic CT examinations. Submitted to *European Radiology* with major revisions 2015.
55. Valentin J. Basic anatomical and physiological data for use in radiological protection: reference values: ICRP Publication 89. *Annals of the ICRP*. 2002;32(3-4):1-277.
56. Sak A, Grehl S, Erichsen P, Engelhard M, Granmass A, Levegruen S, et al. gamma-H2AX foci formation in peripheral blood lymphocytes of tumor patients after local radiotherapy to different sites of the body: Dependence on the dose-distribution, irradiated site and time from start of treatment. *International Journal of Radiation Biology*. 2007;83(10):639-52.
57. Redon CE, Weyemi U, Parekh PR, Huang D, Burrell AS, Bonner WM. gamma-H2AX and other histone post-translational modifications in the clinic. *Biochimica Et Biophysica Acta- Gene Regulatory Mechanisms*. 2012;1819(7):743-56.
58. Zwicker F, Swartman B, Sterzing F, Major G, Weber KJ, Huber PE, et al. Biological in-vivo measurement of dose distribution in patients' lymphocytes by gamma-H2AX immunofluorescence staining: 3D conformal- vs. step-and-shoot IMRT of the prostate gland. *Radiation Oncology*. 2011;6:62.
59. Lee C, Lodwick D, Williams JL, Bolch WE. Hybrid computational phantoms of the 15-year male and female adolescent: Applications to CT organ dosimetry for patients of variable morphometry. *Medical Physics*. 2008;35(6):2366-82.
60. Bakhmutsky MV, Joiner MC, Jones TB, Tucker JD. Differences in Cytogenetic Sensitivity to Ionizing Radiation in Newborns and Adults. *Radiation Research*. 2014;181(6):605-16.
61. Health effects of exposure to low levels of ionizing radiation: BEIR VII: The National Academies Press; 1990.
62. Royal HD. Effects of low level radiation-what's new? *Seminars in Nuclear Medicine*. 38. 2008;38(5):392-402.
63. Preston DL, Mattsson A, Holmberg E, Shore R, Hildreth NG, Boice JD. Radiation effects on breast cancer risk: A pooled analysis of eight cohorts. *Radiation Research*. 2002;158(2):220-35.
64. Air USEPAORaI. EPA Radiogenic Cancer Risk Models and Projections for the U.S. Population 2011.
65. The 2007 Recommendations of the International Commission on Radiological Protection. ICRP publication 103. *Ann ICRP*. 2007 (37). p. 1-332.
66. UNSCEAR. Sources and effects of ionizing radiation. New York: 2008.
67. Nievelstein RAJ, van Dam IM, van der Molen AJ. Multidetector CT in children: current concepts and dose reduction strategies. *Pediatric Radiology*. 2010;40(8):1324-44.
68. Goske MJ, Applegate KE, Boylan J, Butler PF, Callahan MJ, Coley BD, et al. The Image Gently campaign: Working together to change practice. *American Journal of Roentgenology*. 2008;190(2):273-4.
69. Strauss KJ, Goske MJ, Kaste SC, Bulas D, Frush DP, Butler P, et al. Image Gently: Ten Steps You Can Take to Optimize Image Quality and Lower CT Dose for Pediatric Patients. *American Journal of Roentgenology*. 2010;194(4):868-73.
70. Donnelly LF. Reducing Radiation Dose Associated with Pediatric CT by Decreasing Unnecessary Examinations. *American Journal of Roentgenology*. 2005;184(2):655-7.
71. Vock P, Wolf R. Dose Optimization and Reduction in CT of Children. In: Tack D, Gevenois P, editors. *Radiation Dose from Adult and Pediatric Multidetector Computed Tomography*. Springer Berlin Heidelberg; 2007. p. 223-36.
72. Singh S, Kalra MK, Moore MA, Shailam R, Liu B, Toth TL, et al. Dose reduction and compliance with pediatric CT protocols adapted to patient size, clinical indication, and number of prior studies. *Radiology*. 2009;252(1):200-8.
73. Verdun FR, Gutierrez D, Schnyder P, Aroua A, Bochud F, Gudinchet F. CT dose optimization when changing to CT multi-detector row technology. *Current Problems in Diagnostic Radiology*. 2007;36(4):176-84.
74. Pauwels EK, Bourguignon MH. Radiation dose features and solid cancer induction in pediatric computed tomography. *Medical Principles and Practice*. 2012;21(6):508-15.
75. Hall EJ. Lessons we have learned from our children: cancer risks from diagnostic radiology. *Pediatric Radiology*. 2002;32(10):700-6.

10

Radiation-induced leukaemia and radiosensitivity of haematopoietic stem- and progenitor cells

While the primary function of stem and progenitor cells during embryonic development and early post-natal life is one of “tissue building”, their role in adults turns more into one of “tissue maintenance” (1). As described in part 1 of the thesis, this is achieved by the ability of stem cells to both differentiate to give rise to specialized cell types, and to self-renew so that stem cell reserves are maintained over lifetime. However, these unique characteristics of stem cells makes them also a logical origin for carcinogenesis. Stem cells are long-lived, which increases the odds that a single cell could accumulate multiple mutations necessary for transformation (2). Furthermore, the quiescent nature of stem cells is frequently described as a “double-edged sword”, that allows the cells to survive IR exposure but renders them intrinsically vulnerable to mutagenesis (3).

The low number of residual DNA DSBs at 24h after radiation exposure and the high number of radiation-induced MN yields observed in HSPCs (see paper 3), indicate fast error-prone DNA repair and mutagenesis after IR exposure, which could trigger leukaemia development. Although it is clear from literature that DNA damage repair is crucial for maintaining homeostasis and prevent malignant transformation, the radiation re-

sponse of human HSPCs is not yet fully explored. In the following sections, we will give an overview of current literature on DDR of HSPCs and the potential link to radiation-induced leukaemia.

10.1

A distinctive DNA damage response in HSPCs

After IR exposure, an appropriate DNA damage response is the initial attempt of the cell to repair the radiation-induced lesions, but if damage is too extensive, a signalling cascade will trigger cell death. When we see this in the context of stem cell biology, genomic damage which drives HSCs to apoptosis may lead to depletion of the stem cell pool. Whereas DNA damage accrual in HSCs may propagate the impact of genomic damage, since lesions arising in the stem cell compartment can be horizontally propagated through self-renewing progeny, and vertically passed on to downstream progenitors (1). Several publications suggest that stem cells have specific mechanisms to protect their genomes, such as the ATP-binding cassette (ABC) transporter (1, 4, 5) and the immortal strand hypothesis described for stem cells of crypts of the small intestinal mucosa and neural stem cells (6, 7). The basic assumption of this immortal strand hypothesis is that by selective conservation of template DNA, adult stem cells avoid acquiring mutations arising from errors in DNA replication that could lead to cancer (8). However, the latter theory is challenged by an alternative hypothesis that states that asymmetric cell divisions and cell fate are codirected by epigenetic differences between sister chromatids, proposed as the silent sister hypothesis (9).

In our study presented as paper 3 in this thesis, the number of direct γ -H2AX/53BP1 foci did not differ between CD34+ cells and T-lymphocytes of newborns after low dose x-ray exposure. However, the number of residual γ -H2AX/53BP1 foci after high dose x-ray exposure, was significantly lower in CD34+ cells compared to newborn T-lymphocytes. It is generally accepted that the disappearance of γ -H2AX foci is representative for the repair of DNA DSBs after IR exposure (10, 11). The kinetics of formation or loss of γ -H2AX foci may reflect the rate or efficiency of DSB repair (12, 13). The scoring of radiation-induced γ -H2AX foci after 24h *in vivo* irradiated lymphocytes of RT patients, is used to assess their radiosensitivity and to predict patients responses to radiotherapy. It remains

questionable if residual γ -H2AX foci mark misrepaired or unrepaired sites (14, 15). Studies suggest that residual γ -H2AX foci 24h after irradiation were correlated with the percentage of cells that lost clonogenicity, indicating that residual foci represent incomplete repair and may result in cell death (16, 17). However, these studies used cancer cell lines and not lymphocytes.

DNA DSB repair shows a biphasic behaviour with a fast (initial hours) and a slow (hours to days) component, with the fast component responsible for the majority of DSB repair (18). Studies indicate that the rejoining by the slow component increases with increasing LET, which could reflect the higher complexity of the breaks repaired by the slow component (19, 20). As described by Rothkamm *et al.* the number of radiation-induced γ -H2AX foci at 24h are distinctly higher than background levels, at least for doses of several hundred mGy or more (10). A remarkable finding was provided by the analysis of human fibroblasts exposed to different doses, which showed a similarity in the rate of γ -H2AX foci loss irrespective of the initial number of DNA DSBs induced (11). This finding is consistent with the rationale that DNA repair enzymes are in abundant supply such that the rejoining process can start simultaneously at all damaged sites. The number of residual foci will depend on the radiation quality, since high LET irradiation induces more complex breaks resulting in slower DNA repair. Additionally, our results in paper 3 together with other studies on DNA repair in HSPCs suggest that speed of DNA repair can also be cell type dependent. This could be explained by cell intrinsic differences in DNA repair mechanisms or conformational inaccessibility of DNA lesions due to location within highly condensed chromatin. The latter results in less accessibility for repair proteins to start DDR signalling and results in retention of unrepaired foci. A recent study of Brenner and co-workers, showed that the residual foci levels for donors were largely influenced by age (21), however, no children were included in this study (19 – 50 years).

Human HSPCs are usually considered CD34⁺. However, this population represents a heterogeneous mixture of cells at various stages of differentiation. The maturation of all blood cells from HSCs involves developmental progression through a series of downstream progenitor cells with increasingly restricted lineage potential (see chapter 1). The human haematopoietic stem cell population is divided into primitive HSCs (Lin⁻CD34⁺CD38⁻CD90⁺CD45RA⁻), MPPs (Lin⁻CD34⁺CD38⁻CD90⁻CD45RA⁻) and oligopotent progenitors (CD34⁺CD38⁺) (see Table 2 and Figure 12 in

chapter 1). There is intriguing evidence to accept that there is a difference in radiosensitivity between these hierarchically organised subsets (22). Recently, two research groups investigated independently the maintenance of genomic integrity in the face of radiation-induced DNA damage in human and murine HSPCs, although the underlying mechanisms may differ in the two species (3, 23).

The first study of Milyavsky *et al.* compared the DDR in human haematopoietic stem cells, more specifically in primitive HSCs, MPPs and oligopotent progenitors (23). The different cell types were purified from cord blood and irradiated *ex vivo*. DNA DSB repair after 15 Gy was assessed by using the neutral comet assay. Remarkably, the initial response of HSCs and MPPs was slow and no detectable rejoining was seen in the first 30 min. At 1h post irradiation significantly less repair was seen compared to the progenitor population. In order to confirm the finding that the DDR response of HSCs and MPPs would differ from more differentiated progenitors, the formation of γ -H2AX foci was scored at different time points after irradiation. One hour after 3 Gy IR, no detectable differences in the induction of γ -H2AX foci was observed in the three populations (26 γ -H2AX foci/cell). However, 12h after IR, significantly more γ -H2AX foci remained in HSCs and MPPs compared to the progenitor fraction (7.1 versus 2.7 foci/cell respectively). The low number of γ -H2AX foci scored after IR exposure in progenitors is in line with our results of paper 3. The majority of the observed DNA damage is attributable to the CD34⁺CD38⁺ progenitor fraction in our study, since only a very small fraction, as low as 3% of the enriched cells were CD34⁺CD38⁻ (based on literature, (24-26)). Milyavsky *et al.* could also demonstrate that HSCs and MPPs underwent significantly more late apoptosis (Annexin⁺, 7AAD⁺) and showed reduced clonogenic survival compared to their oligopotent progenitors following IR exposure. These results confirm the 7-AAD apoptosis results of a previous study of Hayashi *et al.*, who reported the highest number of apoptotic cells in CD34⁺/CD38⁻ (HSCs and MPPs) compared to more differentiated CD34⁺/CD38⁺ and CD34⁻/CD38⁺ cells, all isolated from UCB (27). Furthermore, Milyavsky *et al.* could demonstrate that the p53 plays a major role in the maintenance of HSC function. The human HSCs exhibited enhance p53-dependent apoptosis after IR exposure. Inactivation of p53 reduced apoptosis significantly and rescued the repopulating ability of the irradiated HSCs in primary recipient mice. The delay in DSB rejoining and persistent γ -H2AX foci may be part of a HSC strategy to emphasize ac-

curacy of DNA repair over efficiency, but not in CD34⁺CD38⁺ progenitors. Although the biological relevance of the different sensitivities of the CD34⁺ stem cell subpopulations remain elusive, these first data reveal that differences in radiosensitivity exist in human HSPC populations (22).

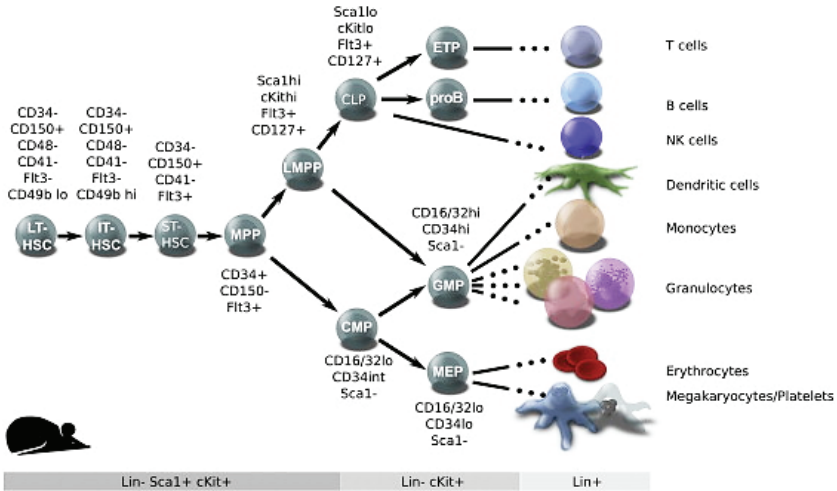


FIGURE 10.1

The murine counterpart of Figure 12 in chapter 1. In mice, HSCs can be separated into long-term (LT), intermediate-term (IT), and short-term (ST) classes based on the duration of repopulation (29).

In contrast to human HSCs, Mohrin *et al.* reported that murine HSCs have cell-intrinsic mechanisms ensuring their survival in response to IR (3). In contrast to human HSCs, murine HSCs are enriched in the CD34⁻ negative fraction. Interestingly, scientific evidence suggests that human HSCs have little correspondence with murine HSCs in terms of surface marker expression (28). In the study of Mohrin *et al.* HSPCs (Lin⁻c-Kit⁺Sca-1⁺Flk2⁻), CMPs (Lin⁻c-Kit⁺Sca-1⁻CD34⁺FcγR⁻) and GMPs (Lin⁻c-Kit⁺Sca-1⁻CD34⁺FcγR⁺) were isolated from the pooled bone marrow of mice. Clonogenic survival assays showed an enhanced radioresistance of HSPCs compared to the more differentiated progenitors after 2 Gy irradiation. The scoring of γ-H2AX foci at 4h and 24h post irradiation showed a relatively faster decline in HSCs and MPPs compared to the more differ-

entiated CMPs and GMPs, which is in contrast to their human analogues. A comet assay demonstrated less damaged tail DNA content in HSPCs without overall loss of cells, which represents active ongoing DNA repair. Thus, the murine HSPCs (HSCs and MPPs) generally undergo growth arrest but survive, whereas the more differentiated progenitor cells undergo apoptosis after IR exposure. Although the survival of murine HSCs may prevent acute defects in haematopoiesis, it may also result in error-prone repair of radiation-induced DNA DSBs, since the quiescent HSPCs use the NHEJ pathway.

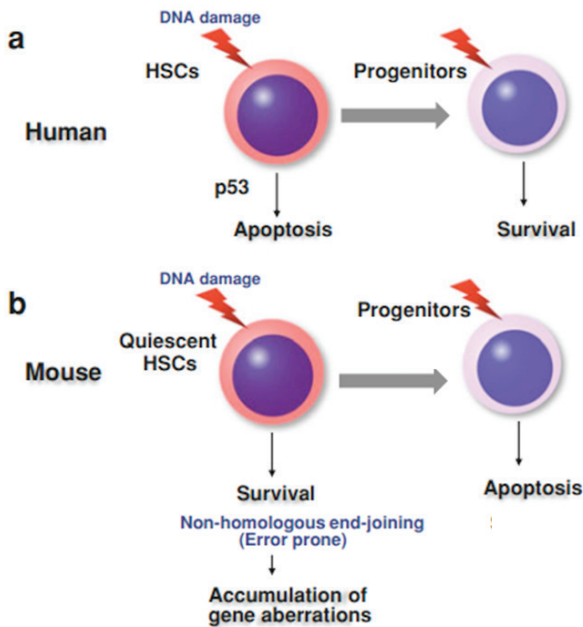


FIGURE 10.2

Specific DNA damage response of HSCs and progenitors in human and mouse. **a.** Human HSCs and MPPs tend to undergo p53-dependent apoptosis, whereas committed progenitors tend to survive in response to IR exposure. **b.** Murine HSPCs are more resistant to apoptosis after IR exposure compared to their committed myeloid progenitors. As a result, surviving murine HSPCs that used NHEJ to repair their radiation-induced DNA damage can accumulate genomic alterations. Figure adapted from (30).

The differences in results between human and mouse studies may be due to species-specificity in DDR or experimental conditions. However, caution is urged when data obtained in mice are extrapolated to humans (see Figure 10.2). Current literature suggests that human primitive HSCs and MPPs (CD34⁺CD38⁻) turn out to be more sensitive to apoptosis after IR exposure than mature oligopotent progenitors (CD34⁺CD38⁺). Furthermore, the data of Milyavsky *et al.* suggest that there is a faster DNA damage signalling in oligopotent progenitors compared to HSCs and MPPs (23). This is in line with our findings in paper 3, in which the majority of HSPC population was CD34⁺CD38⁺, showing a low number residual γ -H2AX foci 24h post irradiation. However, the apoptosis studies of Hayashi *et al.* (27) and Milyavsky *et al.* (23) are based on only three donors and more studies are required to confirm these findings and to take into account inter-individual differences.

Our study is the first in which the CBMN assay was used to evaluate the mutagenic effects of IR exposure on CD34⁺ cells, which makes it impossible to compare our results with current literature. When we compare the chromosomal radiosensitivity of CD34⁺ cells with newborn T-lymphocytes, no significant difference was observed. In a recent study of Becker *et al.*, chromosomal aberrations were scored in CD34⁺ cells isolated from peripheral blood of healthy donors in order to characterise the radiation response of adult human HSPCs with respect to x-ray and carbon ion irradiation (31). For each experiment, the CD34⁺ enriched HSPCs from 2 to 6 donors were pooled. The authors compared the cytogenetic response of HSPCs to x-rays and carbon ions with the response of PHA stimulated peripheral blood lymphocytes (32) and concluded that the cytogenetic response of HSPC was comparable with previously published studies on mature lymphocytes. When the CBMN results of HSPCs are compared with peripheral T-lymphocytes of donors at the same age, no difference in mutagenic effects are observed.

The determination of the response of HSCs to genotoxic stress (e.g. IR exposure) is not only critical for understanding of the fundamental mechanisms of cancer, but also of aging. DNA damage accrual in HSCs was comprehensively described by Rossi *et al.* in the context of aging (1). This review states that HSC quiescence attenuates checkpoint control and DDR for repair and apoptosis, however this is again mostly based on murine data. Consequently, these murine data indicate that the quiescent state would permit DNA damage accumulation during aging, which may result

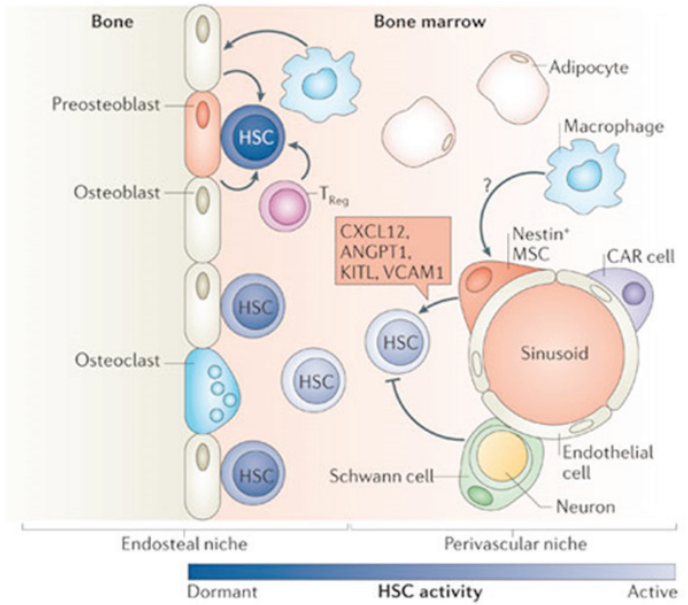
in a diminished capacity of aged stem cells to mediate a return to homeostasis after acute stress or injury. Moreover, this could be a mechanism through which potentially dangerous lesions can accumulate in the stem cell pool with age. Several publications on HSC aging showed that endogenous DNA damage accumulates in repair-competent HSCs with age. In particular, Rube *et al.* studied the formation and loss of γ -H2AX foci in different human stem and progenitor populations exposed to ionizing radiation to gain insight into age dependent changes in DSB repair capacity (33). In CD34⁺ cells obtained from UCB, the number of endogenous γ -H2AX foci was low, which is in line with low background levels of co-localizing γ -H2AX/53BP1 foci obtained in our study.

10.2

Extrapolation of “*in vitro*” results to the “*in vivo*” situation: protective role of the bone marrow niche

Schofield was the first to introduce the concept of a stem cell niche as a stem cell-specific microenvironment (34). He suggested that such a niche 1) would provide an anatomic space that determines the number of stem cells that can be supported, 2) would be responsible for the maintenance of the stem cell phenotype, and 3) would affect the mobility of stem cells. In case of the bone marrow niche, there reside two major types of multipotent stem cells: HSCs and mesenchymal stem cells (MSCs). Unlike most other stem cells, which reside either within their niche or within a relatively limited range of travelling distance surrounding the niche, HSCs are extraordinarily mobile. During homeostasis, HSCs often travel from one bone marrow compartment to another. Under stress conditions when the bone marrow cannot sustain sufficient haematopoiesis, HSCs can even travel to the spleen or liver (35). It seems that HSCs undergo regular trafficking in and out the bone marrow, spending brief intervals in the circulation (36).

The hierarchical structure of haematopoiesis puts minimal proliferative pressure on the HSCs. This results in the hallmark of HSCs, namely their ability to adopt a quiescent state and remain in the non-dividing G₀ phase of the cell cycle. It has been described that an appropriate association between HSCs and the bone marrow niche, may influence the fate of HSCs and modulate haematopoiesis (37). This concept is referred to as the

**FIGURE 10.3**

Most haematopoietic stem cells (HSCs) reside in the bone marrow, which can be subdivided into endosteal and perivascular niches. HSCs located on the endosteal side tend to be more quiescent, whereas HSCs located at the perivascular side are more active. The most dormant HSCs have been reported to locate near osteoblast progenitors (pre-osteoblasts). With the exception of osteoclasts, all of the cellular components in the diagram have been reported to modulate HSC behaviour. Figure from (35).

“niche hypothesis”, in which the niche forms a regulatory unit that limits the entry of HSCs into the cell cycle, thereby protecting them from exhaustion or from errors in DNA replication. Interaction with the niche is also critical for the maintenance of stem cell properties, including self-renewal and differentiation potential (38). It has been suggested that low oxygen tension is a critical feature of the metabolic environment of the bone marrow niche. Bone marrow is considered a tissue with limited oxygen supply and therefore often referred to as the “hypoxic niche”. Several studies have demonstrated that hypoxic culture conditions efficiently maintain HSCs in an undifferentiated state, supporting that the niche is naturally hypoxic (19). While not all components of the HSC niche have been defined, growing evidence suggests that the bone marrow contains at least two different types of niches (39). The first endosteal niche is located in the endosteum

close to the bone surface and provides a hypoxic environment, while a second perivascular niche is located in the central marrow, both shown in Figure 10.3. It has been postulated that the location of HSCs directly affects their activity, presumably because of the different environmental stimuli they encounter at each location. HSCs are more quiescent when they are closer to the hypoxic niche, which is enriched for osteoblasts, osteoclasts and stromal fibroblasts. By contrast, HSCs migrating to the perivascular niches tend to be more active. The perivascular niche is marked by perivas-

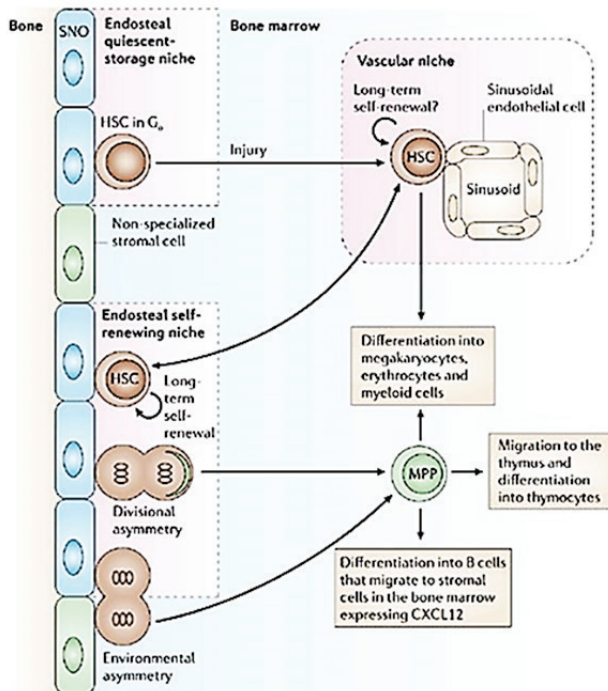


FIGURE 10.4

The quiescent endosteal niche would maintain dormant HSCs long-term. In response to injury, quiescent HSCs might be activated and recruited to the vascular niche. Self-renewing LT HSCs produce MPPs either by divisional (cell-fate determinants are asymmetrically localized to only one of the daughter cells, while the second daughter differentiates) or environmental asymmetry (two identical daughters are produced of which one relocates outside the niche to differentiate). Figure from (46).

cular MSCs, sinusoid endothelial cells and neural cells (35). The view that the endosteal niche serves more as a compound niche, while the mobilization of HSC occurs more through the vascular niche was recently confirmed by Miharada *et al.* (40).

Nevertheless, it still a question where the physical location of the hypoxic niche is and it is possible that the bone marrow sinusoidal endothelium is hypoxic. In this way, HSCs localize close to the endosteal niche in trabecular regions of long bones, whereas more differentiated progenitors were found mainly in the central bone-marrow region (41). However, large discrepancies exist in literature on the percentage and the anatomical localization of HSCs and progenitor cells, but several levels of evidence suggest that HSCs prefer the hypoxic environment to more oxygen-rich locations (42-44). Figure 10.4 suggests and illustrates a model of the bone marrow niches.

The hypoxia levels in the endosteal niche raise the question if there is a differential sensitivity of HSCs to IR depending on their location in the bone marrow (39). However, most of the niche experiments are performed on *in vivo* mouse models, and it remains to be clarified if the same mechanisms are maintained in humans. According to Richardson, the hypoxic conditions of the periosteal niche provide a radioprotective microenvironment that is 2 to 3 times less radiosensitive than vascular niches (45). The results of Mohrin *et al.* (see section 10.1 in this chapter) indicate that the quiescence makes (murine) HSCs more radioresistant to apoptosis compared to their lineage-committed progenitors, and rely on error-prone NHEJ, what makes the cells susceptible to leukaemogenesis (3).

In a hypoxic environment, HSCs have a low metabolism and a long lifespan, whereas HSCs and their progenitors proliferate under higher oxygen pressure (46). It has been demonstrated that hypoxia-inducible factor-1 α (Hif-1 α), the oxygen sensor, is highly expressed in LT-HSCs (47). Hif-1 is a master regulator of cellular metabolism and drives hypoxic gene expression changes that adapt HSCs to survive the exposure to a reduced-oxygen environment (41, 42). Hif-1 stimulates glycolysis in hypoxic regions, in order to produce energy, it represses mitochondrial oxidative phosphorylation and oxygen consumption (41). The glycolytic metabolism in the hypoxic niche protects HSCs from ROS and reduces thereby the consequential oxidant DNA damage.

In conclusion, hypoxia appears to regulate haematopoiesis in the bone marrow by maintaining important HSC functions, such as cell cycle con-

trol, survival, metabolism, and protection against oxidative stress. DDR and ROS play an important role in the maintenance of the genomic integrity of HSCs in the bone marrow niche. The endosteal niche and its components protect stem cells from stress, such as accumulation of ROS and DNA damage. Therefore it is very difficult to compare *in vivo* and *in vitro* radiosensitivity of HSCs, since it is very difficult to mimic the hypoxic endosteal niche *in vitro*. Humanized xenograft mouse models look promising to study radiosensitivity of human HSCs in an *in vivo* model, however, several studies reported limitations to this set-up. Human HSPCs may lack quiescence after engraftment and they remain in active cycle (48). This results in unusual high frequencies of human CD34⁺ cells in the BM of xenografted mice (10-20%) compared to a normal BM (1-2% CD34⁺ cells). It is likely that multiple signals are aberrant in the murine microenvironment, and a complex array of genetic changes will be needed to mimic the human BM niche (28).

10.3

The leukemic stem cell: Are HSPCs the target cells for radiation-induced leukaemia?

As already described in the Introduction of this PhD thesis (see section 1.3.2), leukaemia is hierarchically organized in subpopulations of leukemic cells, similar to normal haematopoiesis. Leukaemia represents a dysregulation of the homeostatic mechanisms of the bone marrow. Certain types of leukaemia have been described as newly formed, abnormal haematopoietic tissue generated from transformed cells that have either retained or reacquired the capacity of self-renewal, proliferation and resistance to apoptosis through accumulated mutations. These cells can be described as leukaemic stem cells (LSCs) (43). The LSC is responsible for disease initiation and maintenance, and gives rise to more differentiated malignant blasts (49). The leukemic state is very efficient in cell mass production, but is compromised by the functionality of the produced cells. Given the shared properties between LSCs and normal HSCs, it has been proposed that leukaemia's may be initiated by transforming events taking place in HSCs as the result of accumulated mutations. Since HSCs have the machinery for self-renewal, it may require fewer mutations to become leukemic than more differentiated cells. HSCs also persist throughout life,

therefore they have a higher chance to accumulate mutations. Alternatively, leukaemia may also arise from more committed progenitors, caused by mutations that enhance their normally limited self-renewal capacities (50) (see Figure 10.5).

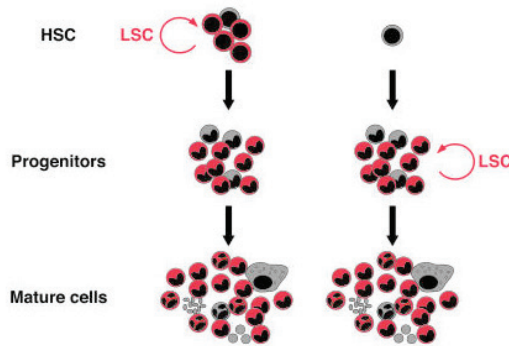


FIGURE 10.5

The origin of LSCs can be either HSCs, which have become leukemic as the result of accumulated mutations, or more committed progenitors, which have reacquired the stem cell capacity of self-renewal. Regardless of their origin, both types of LSCs give rise to similar end-stage leukaemia's. Figure from (50).

Most studies on the determination of cancer stem cells (CSCs) (e.g. LSCs) follow a common scenario: a cell surface marker or marker combination is found to be expressed heterogeneously in a certain tumour type. On the basis of this marker heterogeneity, subpopulations of cells are sorted from primary tumours and can be transplanted into immunodeficient mice, after which tumour growth is scored some weeks or months later. Different capacities for tumour initiation between tumour cell subsets can be interpreted as evidence for the presence of CSCs in the primary tumour (51). This technique was also used by John Dick and his co-workers, who first identified the presence of cancer stem cells in acute lymphoid leukaemia through extensive cell cloning and demonstration of their self-renewing capacity (52). Since then, the isolation and identifica-

tion of the rare cancer stem cells population (about 1% of the tumour) became a challenging issue in cancer biology (43). This research has traditionally focused on the haematopoietic system, since detailed lineages and CD cell surface markers could be used in the attempt to identify leukemic stem cells. Bonnet *et al.* showed that the malignant leukemic stem blasts in AML were exclusively CD34⁺CD38⁻, suggesting that the primitive HSCs, rather than committed progenitor cells, are the target for AML transformation (53). However, later studies could identify LSCs in CD34⁺CD38⁺ and even in CD34⁻ fractions (54, 55). More recently, surface markers have been identified being present only in leukemic samples and not in normal bone marrow, such as CD96⁺/CD90⁻ for AML (56). More than 90% of the CML patients express the Philadelphia chromosome translocation which serves as a cytogenetic hallmark of the disease, and contains the BCR-ABL fusion gene (57, 58). This fusion protein was found in myeloid, erythroid, B lymphoid and occasionally T lymphoid cells, suggesting that the original translocation takes place in primitive HSCs (or MPPs). In contrast, a study on patients with the M3 subtype of AML, acute promyeloid leukaemia (APML), showed that the APML-associated fusion gene PML/RAR α was present in CD34⁺CD38⁺ cell populations, but not in CD34⁺CD38⁻ HSC populations (59). These observations suggest that the transformation process in APML may involve a more differentiated cell type than HSCs and/or MPPs. Furthermore, several studies suggested that the LSC hierarchy could also be applied to childhood ALL. One of the studies could identify CD34⁺CD19⁺CD38⁻ cells as candidate pre-leukemic stem cells for TEL/AML-1 positive ALL (60). Another study of Cox *et al.* showed that for a variety of ALL blasts expressed CD34, but not CD10 and CD19, suggesting that cells with a more immature phenotype, rather than committed B-lymphoid cells, may be the targets for transformation in B-ALL (61). Emerging evidence indicates that leukaemia's are initiated by a few LSCs that can be heterogeneous in terms of their origin, both HSCs and more differentiated progenitors could be the initiating cell, illustrated in Figure 10.6.

Chromosomal alterations induced by external factors, such as IR, can be an underlying feature in the emergence of a LSC. The genetic lesions in LSCs result in a block of differentiation (maturation arrest) that allow cells belonging to a certain clone not only to continue proliferation and to resist apoptosis, but also to accumulate in large numbers (43). The development of cancer is a multistage process and for most individuals a combination of factors appears to be necessary to initiate cancer. In many cases of leukaemia-

mia, the events leading to cell transformation can be traced back to specific chromosomal aberrations and a concomitant deletion of genes or altered signal transduction. It is most likely that the development of leukaemia occurs as a result of a combination of the constitutional genome plus the exposure to genotoxic agents (such as IR) and the ability to repair DNA damage appropriately (62).

Several recent publications demonstrate the effect of individual leukaemia-associated oncogenes on human HSPCs, actually building human

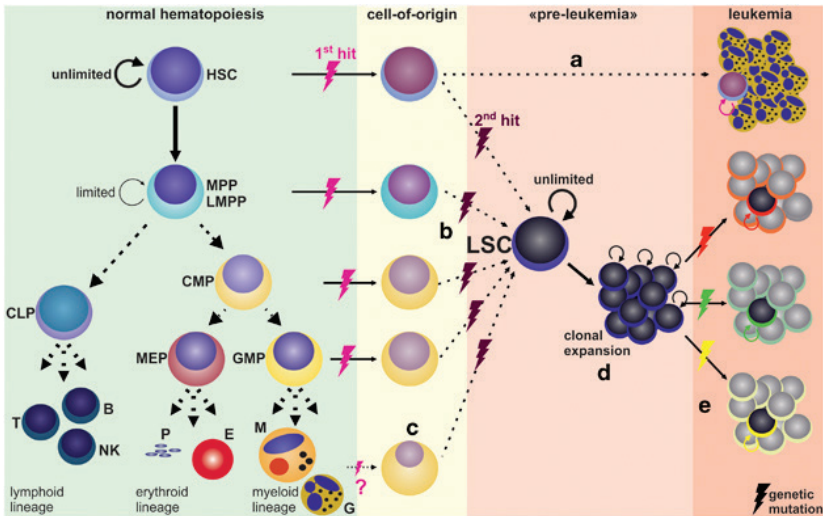


FIGURE 10.6

The left part of the figure illustrates the normal haematopoietic hierarchy, in which long-term HSCs have self-renewal capacity, while short-term (HSCs and) MPPs have limited self-renewal capacity. (a) The LSC is derived from an HSC. (b) LSCs exhibit immunophenotypes of MPPs or GMPs, supporting the concept that more differentiated cells can give rise to LSCs after re-acquisition of self-renewal. (c) Recent studies suggest that some AML LSC express low amount of lineage markers, suggesting that differentiated haematopoietic cells may serve as cell-of-origin for LSCs. (d) Illustration of the pre-leukemic disease phase, genetically unstable, in which self-renewing LSCs expand. (e) The development of different leukemic clones. Figure from (49).

leukaemia using primary human HSPCs. Up to now, most of these studies suggest only partial phenotypes, but they are consistent with a model of stepwise progression to transformation (28, 63). Already in the 1990s, studies suggested that high dose IR could induce leukaemia-associated fusion genes (64, 65). An important remark in light of these studies, is the finding that human cells are more refractory to transformation than murine cells (66). Furthermore, it is also likely that the BM microenvironment plays a critical role for pre-leukaemic HSPC initiation and leukaemia progression.

Our study (paper 3) demonstrates that CD34⁺ HSPCs of UCB are sensitive to the mutagenic effect of radiation. These results support the strong epidemiological evidence on radiation-induced leukaemia and make IR a potential causative factor to initiate a LSC. Nevertheless, from the general knowledge about leukaemogenesis, it is very likely that the initiation and progression of leukaemia would require the combination of a number of causative factors (61). Furthermore, the potential radioprotective role of the hypoxic BM niche has to be further explored.

10.4

References

1. Rossi DJ, Seita J, Czechowicz A, Bhattacharya D, Bryder D, Weissman IL. Hematopoietic stem cell quiescence attenuates DNA damage response and permits DNA damage accumulation during aging. *Cell Cycle*. 2007;6(19):2371-6.
2. Niedernhofer LJ. DNA repair is crucial for maintaining hematopoietic stem cell function. *DNA Repair*. 2008;7(3):523-9.
3. Mohrin M, Bourke E, Alexander D, Warr MR, Barry-Holson K, Le Beau MM, et al. Hematopoietic Stem Cell Quiescence Promotes Error-Prone DNA Repair and Mutagenesis. *Cell Stem Cell*. 2010;7(2):174-85.
4. de Jonge-Peeters SDPWM, Kuipers F, de Vries EGE, Vellenga E. ABC transporter expression in hematopoietic stem cells and the role in AML drug resistance. *Critical Reviews in Oncology/Hematology*. 2007;62(3):214-26.
5. Zhou S, Schuetz JD, Bunting KD, Colapietro AM, Sampath J, Morris JJ, et al. The ABC transporter *Bcrp1/ABCG2* is expressed in a wide variety of stem cells and is a molecular determinant of the side-population phenotype. *Nature Medicine*. 2001;7(9):1028-34.
6. Potten CS, Owen G, Booth D. Intestinal stem cells protect their genome by selective segregation of template DNA strands. *Journal of Cell Science*. 2002;115(Pt 11):2381-8.
7. Karpowicz P, Morshhead C, Kam A, Jervis E, Ramunas J, Cheng V, et al. Support for the immortal strand hypothesis: neural stem cells partition DNA asymmetrically in vitro. *Journal of Cell Biology*. 2005;170(5):721-32.
8. Cairns J. Mutation selection and the natural history of cancer. *Nature*. 1975;255(5505):197-200.
9. Lansdorp PM. Immortal strands? Give me a break. *Cell*. 2007;129(7):1244-7.
10. Rothkamm K, Horn S. gamma-H2AX as protein biomarker for radiation exposure. *Annali Dell Istituto Superiore Di Sanita*. 2009;45(3):265-71.
11. Loblrich M, Kiefer J. Assessing the likelihood of severe side effects in radiotherapy. *International Journal of Cancer*. 2006;118(11):2652-6.
12. Loblrich M, Kuhne M, Wetzel J, Rothkamm K. Joining of correct and incorrect DNA double-strand break ends in normal human and ataxia telangiectasia fibroblasts. *Genes Chromosomes Cancer*. 2000;27(1):59-68.
13. Olive PL, Banath JP. Phosphorylation of histone H2AX as a measure of radiosensitivity. *International Journal of Radiation Oncology, Biology, Physics*. 2004;58(2):331-5.
14. Olive PL, Banath JP, Keyes M. Residual gammaH2AX after irradiation of human lymphocytes and monocytes in vitro and its relation to late effects after prostate brachytherapy. *Radiation Oncology*. 2008;86(3):336-46.
15. Bourton EC, Plowman PN, Smith D, Arlett CF, Parris CN. Prolonged expression of the gamma-H2AX DNA repair biomarker correlates with excess acute and chronic toxicity from radiotherapy treatment. *International Journal of Cancer Journal International du Cancer*. 2011;129(12):2928-34.
16. Chua MLK, Horn S, Somaiah N, Davies S, Gothard L, A'Hern R, et al. DNA double-strand break repair and induction of apoptosis in ex vivo irradiated blood lymphocytes in relation to late normal tissue reactions following breast radiotherapy. *Radiation and Environmental Biophysics*. 2014;53(2):355-64.
17. Suzuki M, Suzuki K, Kodama S, Watanabe M. Phosphorylated Histone H2AX Foci Persist on Rejoined Mitotic Chromosomes in Normal Human Diploid Cells Exposed to Ionizing Radiation. *Radiation Research*. 2006;165(3):269-76.
18. Paull TT, Rogakou EP, Yamazaki V, Kirchgessner CU, Gellert M, Bonner WM. A critical role for histone H2AX in recruitment of repair factors to nuclear foci after DNA damage. *Curr Biol*. 10. England2000. p. 886-95.
19. Banáth J, Klovov D, MacPhail S, Banuelos C, Olive P. Residual gammaH2AX foci as an indication of lethal DNA lesions. *BMC Cancer*. 2010;10(1):1-12.
20. Banath JP, Macphail SH, Olive PL. Radiation sensitivity, H2AX phosphorylation, and kinetics of repair of DNA strand breaks in irradiated cervical cancer cell lines. *Cancer Research*. 2004;64(19):7144-9.
21. Sharma PM, Ponnaiya B, Taveras M, Shuryak I, Turner H, Brenner DJ. High Throughput Measurement of gammaH2AX DSB Repair Kinetics in a Healthy Human Population. *PLoS ONE*. 2015;10(3):e0121083.
22. Heylmann D, Roedel F, Kindler T, Kaina B. Radiation sensitivity of human and murine peripheral blood lymphocytes, stem and progenitor cells. *Biochimica Et Biophysica Acta-Reviews on Cancer*. 2014;1846(1):121-9.
23. Milyavsky M, Gan OI, Trotter M, Komosa M, Tabach O, Notta F, et al. A Distinctive DNA Damage Response in Human Hematopoietic Stem Cells Reveals an Apoptosis-Independent Role for p53 in Self-Renewal. *Cell Stem Cell*. 2010;7(2):186-97.
24. Hao QL, Shah AJ, Thiemann FT, Smogorzewska EM, Crooks GM. A Functional comparison of CD34(+)CD38(-) cells in cord-blood and bone-marrow. *Blood*. 1995;86(10):3745-53.
25. Darena G, Musto P, Cascavilla N, DiGiorgio G, Zendoli F, Carotenuto M. Human umbilical cord blood: Immunophenotypic heterogeneity of CD34(+) hematopoietic progenitor cells. *Haematologica*. 1996;81(5):404-9.

26. Kato K, Takahashi K, Monzen S, Yamamoto H, Maruyama A, Itoh K, et al. Relationship between Radiosensitivity and Nrf2 Target Gene Expression in Human Hematopoietic Stem Cells. *Radiation Research*. 2010;174(2):177-84.
27. Hayashi T, Hayashi I, Shinohara T, Morishita Y, Nagamura H, Kusunoki Y, et al. Radiation-induced apoptosis of stem/progenitor cells in human umbilical cord blood is associated with alterations in reactive oxygen and intracellular pH. *Mutation Research*. 2004;556(1-2):83-91.
28. Goyama S, Wunderlich M, Mulloy JC. Xenograft models for normal and malignant stem cells. *Blood*. 2015;125(17):2630-40.
29. Doulatov S, Notta F, Laurenti E, Dick JE. Hematopoiesis: a human perspective. *Cell Stem Cell*. 2012;10(2):120-36.
30. Naka K, Hirao A. Maintenance of genomic integrity in hematopoietic stem cells. *International Journal of Hematology*. 2011;93(4):434-9.
31. Becker D, Elsasser T, Tomm T, Seifried E, Durante M, Ritter S, et al. Response of human hematopoietic stem and progenitor cells to energetic carbon ions. *International Journal of Radiation Biology*. 2009;85(11):1051-9.
32. Lee R, Nasonova E, Ritter S. Chromosome aberration yields and apoptosis in human lymphocytes irradiated with Fe-ions of differing LET. *Advances in Space Research*. 2005;35(2):268-75.
33. Rube CE, Fricke A, Widmann TA, Furst T, Madry H, Pfreundschuh M, et al. Accumulation of DNA Damage in Hematopoietic Stem and Progenitor Cells during Human Aging. *Plos One*. 2011;6(3):9.
34. Schofield R. The relationship between the spleen colony-forming cell and the haemopoietic stem cell. *Blood Cells*. 1978;4(1-2):7-25.
35. Hsu YC, Fuchs E. A family business: stem cell progeny join the niche to regulate homeostasis. *Nat Rev Mol Cell Biol*. 13. England 2012. p. 103-14.
36. Adams GB, Scadden DT. The hematopoietic stem cell in its place. *Nature Immunology*. 2006;7(4):333-7.
37. Arai F, Suda T. Maintenance of quiescent hematopoietic stem cells in the osteoblastic niche. *Annals of the New York Academy of Sciences*. 2007;1106:41-53.
38. Arai F, Hirao A, Suda T. Regulation of hematopoiesis and its interaction with stem cell niches. *Int Journal of Hematology*. 2005;82(5):371-6.
39. Pajonk F, Vlashi E. Characterization of The Stem Cell Niche and Importance in Radiobiologic Response. *Seminars in radiation oncology*. 2013;23(4):237-41.
40. Miharada K, Karlsson G, Rehn M, Rorby E, Siva K, Cammenga J, Karlsson S. Cripto regulates hematopoietic stem cells as a hypoxic-niche-related factor through cell surface receptor GRP78. *Cell Stem Cell*. 2011;9(4):330-44.
41. Papandreou I, Cairns RA, Fontana L, Lim AL, Denko NC. HIF-1 mediates adaptation to hypoxia by actively down-regulating mitochondrial oxygen consumption. *Cell Metabolism*. 2006;3(3):187-97.
42. Eliasson P, Jonsson JL. The hematopoietic stem cell niche: low in oxygen but a nice place to be. *Journal of Cellular Physiology*. 2010;222(1):17-22.
43. Bapat S. *Cancer Stem Cells: Identification and Targets*. New Jersey: John Wiley and Sons; 2009.
44. Zhang CC, Sadek HA. Hypoxia and metabolic properties of hematopoietic stem cells. *Antioxidants and Redox Signalling*. 2014;20(12):1891-1901.
45. Richardson RB. Stem cell niches and other factors that influence the sensitivity of bone marrow to radiation-induced bone cancer and leukaemia in children and adults. *International Journal of Radiation Biology*. 2011;87(4):343-59.
46. Wilson A, Trumpp A. Bone-marrow haematopoietic-stem-cell niches. *Nature Reviews. Immunology*. 2006;6(2):93-106.
47. Simsek T, Kocbas F, Zhen J, Deberardinis RJ, Mahmoud AI, Olson EN, et al. The distinct metabolic profile of hematopoietic stem cells reflects their location in a hypoxic niche. *Cell Stem Cell*. 2010;7(3):380-90.
47. Shima H, Takubo K, Tago N, Iwasaki H, Arai F, Takahashi T, et al. Acquisition of G(0) state by CD34-positive cord blood cells after bone marrow transplantation. *Experimental Hematology*. 2010;38(12):1231-40.
48. Riether C, Schurch CM, Ochsenein AF. Regulation of hematopoietic and leukemic stem cells by the immune system. *Cell Death and Differentiation*. 2015;22(2):187-98.
49. Passegue E, Jamieson CH, Ailles LE, Weissman IL. Normal and leukemic hematopoiesis: are leukemias a stem cell disorder or a reacquisition of stem cell characteristics? *Proceedings of the National Academy of Science USA*. 2003;100(Suppl 1):11842-9.
50. Clevers H. The cancer stem cell: premises, promises and challenges. *Nature Medicine*. 2011;17(3):313-9.
51. Lapidot T, Sirard C, Vormoor J, Murdoch B, Hoang T, Caceres-Cortes J, et al. A cell initiating human acute myeloid leukaemia after transplantation into SCID mice. *Nature*. 1994;367(6464):645-8.
52. Bonnet D, Dick JE. Human acute myeloid leukemia is organized as a hierarchy that originates from a primitive hematopoietic cell. *Nature Medicine*. 1997;3(7):730-7.
53. Klcio JM, Spencer DH, Miller CA, Griffith M, Lamprecht TL, O'Laughlin M, et al. Functional heterogeneity of genetically defined subclones in acute myeloid leukemia. *Cancer Cell*. 2014;25(3):379-92.

54. Taussig DC, Vargaftig J, Miraki-Moud F, Griessinger E, Sharrock K, Luke T, et al. Leukemia-initiating cells from some acute myeloid leukemia patients with mutated nucleophosmin reside in the CD34(-) fraction. *Blood*. 2010;115(10):1976-84.
55. Hosen N, Park CY, Tatsumi N, Oji Y, Sugiyama H, Gramatzki M, et al. CD96 is a leukemic stem cell-specific marker in human acute myeloid leukemia. *Proceedings of the National Academy of Science USA*. 2007;104(26): 11008-13.
56. Groffen J, Stephenson JR, Heisterkamp N, de Klein A, Bartram CR, Grosveld G. Philadelphia chromosomal break-points are clustered within a limited region, bcr, on chromosome 22. *Cell*. 1984;36(1):93-9.
57. Kurzrock R, Kantarjian HM, Druker BJ, Talpaz M. Philadelphia Chromosome-Positive Leukemias: From Basic Mechanisms to Molecular Therapeutics. *Annals of Internal Medicine*. 2003;138(10):819-30.
58. Turhan AG, Lemoine FM, Debert C, Bonnet ML, Baillou C, Picard F, et al. Highly purified primitive hematopoietic stem cells are PML-RARA negative and generate nonclonal progenitors in acute promyelocytic leukemia. *Blood*. 1995;85(8):2154-61.
59. Hong D, Gupta R, Ancliff P, Atzberger A, Brown J, Soneji S, et al. Initiating and cancer-propagating cells in TEL-AML1-associated childhood leukemia. *Science*. 2008;319(5861):336-9.
60. Cox CV, Evely RS, Oakhill A, Pamphilon DH, Goulden NJ, Blair A. Characterization of acute lymphoblastic leukemia progenitor cells. *Blood*. 2004;104(9):2919-25.
61. Eden T. Aetiology of childhood leukaemia. *Cancer Treatment Reviews*. 2010;36(4):286-97.
62. Rizo A, Horton SJ, Olthof S, Dontje B, Ausema A, van Os R, et al. Bmi1 collaborates with BCR-ABL in leukemic transformation of human CD34+ cells. *Blood*. 116. United States 2010. p. 4621-30.
63. Deininger MW, Bose S, Gora-Tybor J, Yan XH, Goldman JM, Melo JV. Selective induction of leukemia-associated fusion genes by high-dose ionizing radiation. *Cancer Res*. 1998;58(3):421-5.
64. Spencer A, Granter N. Leukemia patient-derived lymphoblastoid cell lines exhibit increased induction of leukemia-associated transcripts following high-dose irradiation. *Exp Hematol*. 27. Netherlands 1999. p. 1397-401.
65. Rangarajan A, Hong SJ, Gifford A, Weinberg RA. Species- and cell type-specific requirements for cellular transformation. *Cancer Cell*. 6. United States 2004. p. 171-83.

1

1

Age dependence in radiation sensitivity

In contrast to the well-documented epidemiological evidence for the higher radiosensitivity of children (see chapter 1) for specific malignancies, there is only limited ‘biological evidence’ available on the differences in cellular or tissue response to radiation exposure between children and adults. Radiation-induced elevations in cancer risk can be a consequence of corresponding DNA damage and repair. However, there is a serious lack on studies that examined the age dependency of radiation-induced DNA damage and the outcome of repair. The limited number of biomarker studies on changes in radiation sensitivity from birth to adulthood is probably due to the fact that such studies require blood samples from children of all ages, which is very problematic for ethical reasons. Therefore, UCB is frequently used as an alternative for blood of a newborn, since it is physiologically and genetically part of the foetus, it can be considered as blood of a newborn (1).

One of the major findings of this PhD research, was the difference in cellular chromosomal sensitivity and residual DNA damage between newborn and adult T-lymphocytes (presented in paper 3). In the following sections we will present the results of a limited number of *in vitro* biomarker and *in vivo* animal studies supporting the observed age-dependency. Furthermore, a possible underlying mechanism for the observed difference in sensitivity between newborns and adult T-lymphocytes will be introduced.

11.1**Biological evidence regarding age-dependent radiosensitivity**

In the third paper of this PhD thesis, statistically significant differences were observed between newborn and adult T-lymphocytes in residual γ -H2AX/53BP1 foci levels and radiation-induced MN yields. At 24h after 4 Gy x-ray irradiation, 7.13 (± 0.25) foci/cell were observed in newborns compared to 5.77 (± 0.26) foci/cell in adults ($p < 0.05$). Furthermore, a high radiation-induced MN yield of 351 (± 23) MN/1000 BN cells was observed in newborns compared to a significantly lower yield of 275 (± 18) MN/1000 BN cells in adults ($p < 0.05$). Already in 1994, Floyd *et al.* determined the intrinsic radiosensitivity of adult and cord blood lymphocytes by using the MN assay (2). They analysed the radiation-induced micronuclei for 10 different samples of adult peripheral blood lymphocytes (ABL) and 5 UCB lymphocytes (CBL). Comparison of the level of MN induced after 2 Gy x-rays (dose rate of 2.35 Gy/min) revealed that only two CBL samples were more radiosensitive than the mean of the ABLs. However at 4 Gy, four out of five CBLs were clearly more radiosensitive than the mean radiosensitivity of the ABLs. It is important to note that the percentage of micronucleated cells was scored in this study and not the more commonly used micronucleus frequency. When the slope of the dose-response curves of the 5 CBL donors were compared to the mean dose response of the adult group, a significant difference was observed ($p < 0.02$). The higher radiosensitivity of newborns was also reported in a study of Bakhmutsky *et al.*, where the authors determined the age influence on the frequency and types of chromosome damage in response to IR, by irradiating peripheral blood samples of 20 adults (range 22 - 78 years) and 10 UCB samples with 60-Co γ -rays (3). Peripheral blood lymphocytes from newborns showed a statistically significantly higher number of induced frequencies of translocated chromosomes, dicentrics, acentric fragments, colour junctions and abnormal cells at several radiation doses when compared to adults. However, when adults were evaluated separately, no significant changes with age were observed. The increased sensitivity of newborns relative to adults was 37 (± 9)%, 18 (± 4)%, 12 (± 2)% and 4 (± 5)% based on the scoring of chromosomal aberrations at doses of 1, 2, 3 and 4 Gy, respectively. Even though age was a statistically significant factor when the baseline data were not subtracted, the effect of age was even stronger when induced values were evaluated (Figure 11.1). The lack of an age effect in response to IR ex-

posure in the adult population, was already observed by others (4). These results suggest that the change in sensitivity appears to occur between birth and adulthood, rather than gradually over the years from birth to senescence. The lack of an age effect among adult humans is perhaps the result of the completion of growth and development. The statistically significant increase in all aberrations types with age observed by Bakhmutsky *et al.* in the non-irradiated samples reflects the increase of accumulated mutagenic burden with age (Figure 11.1 – a) (3).

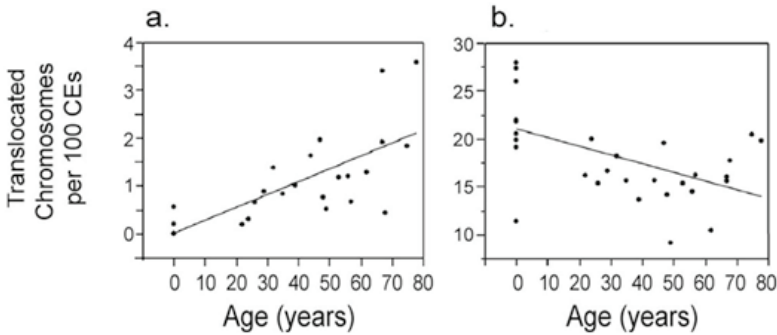


FIGURE 11.1

a. Translocated chromosomes frequency per 100 CE (1 cell equivalent = 0.56 metaphase cells) by age in non-irradiated samples. Each point represents one subject; **b.** Radiation-induced translocated chromosome frequencies per 100 CE by age. The graph for 1 Gy is shown here as an example. In both graphs, the lines are least squares linear regressions, which are statistically significant ($p < 0.012$). Figures from (3).

Also *in vivo* rodent studies indicate that the rate of cancer induction after IR exposure decreases with age. Hattis *et al.* evaluated age-related differences in susceptibility to carcinogenesis by analysing the U.S. Environmental Protection Agency (EPA) animal cancer bioassay data over different periods of life (5). The relative sensitivity for radiation-related carcinogenesis decreased tremendously with age. The maximum likelihood estimates relative to young adults (90-105 days) for radiation carcinogenesis per Gy in mice and rats were 3.1 in the birth-to-weaning period, 1.5 between weaning and 60 days of age, 0.32 between 6 and 12 months of age and 0.36 in elderly animals (19-21 months) The data were based on obser-

vations for four radiation types: ^{137}Cs γ -rays, x-rays, neutrons and internal β -rays resulting from the injection of tritiated water. The neonatal period is suggested to be the most sensitive period, which is consistent with our results of paper 3 and the findings of Bakhmutsky *et al.* (3). Another *in vivo* study on female mice investigated the influence of age at the time of irradiation on the lifetime risk for excess mortality from solid tumours (6). Mice were irradiated with 1.9 Gy γ -rays at day 0, 7, 35, 105 or 365 of postnatal age. Again, the lifetime excess mortality from solid tumours was apparently higher in mice irradiated during the neonatal to puberty period than in the mice irradiated in adult period, as illustrated in Figure 11.2. Sasaki *et al.* proposed already in 1991 that age-dependence of susceptibility for induction of specific type of neoplasms is common among animal species of mammals. However, it is important to mention that the developmental stage at the time of birth in mice is not the same as that in humans. The status of development of the early postnatal period in mice corresponds to the third trimester of gestation in humans. A next step towards applying these data for quantitative human risk assessment is to develop time/age mapping between rodents and humans, to define what ages in human

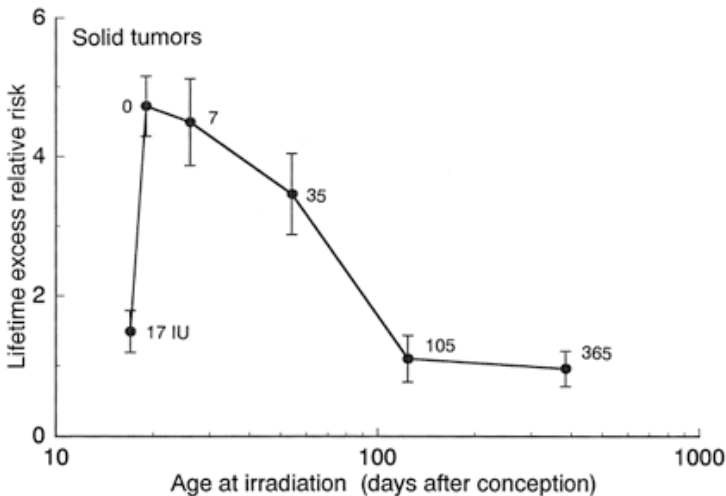


FIGURE 11.2

Influence of age at irradiation on the lifetime excess relative risk for mortality from solid tumours as investigated by Sasaki *et al.* (6).

development approximately correspond to the postnatal and adult stages in rodents. Furthermore, extensive studies are indicated to investigate the organ tissue dependence in radiation-induced carcinogenesis.

Similar to the increase in CA with age in the study of Bakhmutsky *et al.* (3), we observed also a statistically significant higher number of DNA DSBs and spontaneous MN in non-irradiated T-lymphocyte samples of adults compared to newborns. Moreover, similar results were obtained for CD34⁺ cells of newborns in paper 3. The accumulation of DNA damage with age was also examined in CD34⁺/CD34⁻ stem/progenitor cells by using the γ -H2AX foci assay in a study on human aging (7). An increase of endogenous γ -H2AX foci levels with advancing donor age was reported, associated with an age-related decline in telomere length. However, combined immunofluorescence and telomere in situ hybridisation could demonstrate a telomere-independent origin for the majority of foci. Schuler *et al.* reported similar findings for an *in vivo* model by analysing molecular events of the DDR in hair follicle stem cells and epidermal cells of aging mouse (8). An increase in 53BP1 foci was observed during the natural aging process, suggesting substantial accumulation of DSBs in hair follicle stem cells. The 53BP1 accumulation in long-living follicle stem cells during aging, likely represents DSBs arising from endogenously induced ROS damage. Oxidative DNA damage is one of the major contributors to the accumulation of DSBs in heterochromatin DNA regions and the aging process (9). Furthermore, several other publications confirm the low number of spontaneous MN expression in cord blood and children's lymphocytes, as observed in paper 3 (10-14).

11.2

Differences in immunophenotypic profile of newborn and adult T-lymphocytes

The major difference between UCB T-lymphocytes and adult peripheral blood T-lymphocytes, is their immunophenotypic profile. The majority of UCB or newborn T-lymphocytes are phenotypically immature or naive, expressing the RA isoform of the CD45 cell surface marker. This is a likely consequence of poor antigenic experience during pregnancy (15). Our immunophenotypic study to determine the percentage of T-lymphocyte subsets in the UCB samples and adult PB samples by using flow cytometry

are in line with the results of D'Arena *et al.* (15). A comparison of the mean values of both studies is presented in Table 11.1.

Subpopulation	Umbilical cord blood		Adult peripheral blood	
	Our study	D'Arena (15)	Our study	D'arena (15)
CD4+CD45RA+ (%)	97.3 ± 2.3	87.6 ± 5.2	38.2 ± 19.0	44.8 ± 9.6
CD4+CD45RO+ (%)	2.5 ± 2	12.3 ± 5.2	58.6 ± 17.3	55.2 ± 9.6
CD8+CD45RA+ (%)	99.7 ± 0.3	93.5 ± 7.8	61.9 ± 18.6	71.5 ± 8.1
CD8+CD45RO+ (%)	0.3 ± 0.3	6.4 ± 7.8	35.6 ± 13.8	28.5 ± 8.1

TABLE 11.1

The percentage of naive and memory CD4⁺ and CD8⁺ T-lymphocytes determined in umbilical cord blood and adult peripheral blood in our study, compared to a previous publication of D'Arena *et al.* (15). Values are expressed as mean percentage (± standard deviation).

The human immune system maintains both naive and memory T-lymphocytes, which can most simply be characterised by the reciprocal expression of the CD45RA or CD45RO isoforms (16). In general, naive (CD45RA⁺/CD45RO⁻) T-lymphocytes represent the most homogeneous pool of T cells as they lack most effector functions. After a combined process of positive and negative selection in the thymus, immature thymocytes differentiate into mature T cells that exit the thymus to form the long-lived pool of naive T lymphocytes, recirculating within the confines of the peripheral lymphoid tissue (17). Naive T-cells are maintained by IL-7 and T cell receptor (TCR) signalling from contact with major histocompatibility complex (MHC). The cells migrate through secondary lymphoid organs seeking antigens presented by dendritic cells. Once they encounter antigens and become activated through the TCR, naive T cells undergo massive expansion for several days and generate effector T cells that are CD45RO⁺ with a variety of functions, able to eliminate the pathogens (18, 19). Most of these effector cells die within the next few weeks, but a small proportion of these effector cells persist as memory cells which give an accelerated response upon a future encounter with the specific antigen (20). The latter memory T cells can be further subdivided into central memory

and effector memory T-lymphocytes with distinct functions and homing capabilities.

The shift in a population of predominantly naive T-lymphocytes to memory T-lymphocytes during aging, reflects the cumulative exposure to foreign pathogens over time (21). Several large population studies could also demonstrate that the degree of environmental antigen exposure in early life leads to differences in immune status in individuals (e.g. more frequent exposure to various infections in the African environment) (21, 22). A comparative study of Tsegaye *et al.* showed a remarkable reduction in naive CD4⁺ T-lymphocytes during childhood (23). The median percentage values were: 97% at birth, 32.6% in children aged 5–16, and 14.2% during adulthood. In the CD8⁺ T-lymphocyte compartment, the percentage of naive cells also significantly declined from birth to childhood but the decline was less pronounced compared to the change seen in the CD4⁺ T-lymphocyte compartment. The percentages reported in this study are not directly comparable to our own flow cytometry results, since a combination of CD45RO and CD27 antigens was used to quantify the naive and memory subsets. Another study by Shearer *et al.* determined the distribution of lymphocyte subsets in a large set-up with 807 children from birth through 18 years of age in the United States, to serve as a suitable control group for the interpretation of disease conditions in children, notably paediatric HIV-1 infection (24) (see Figure 11.3).

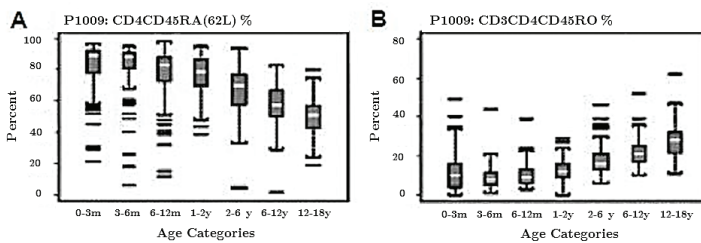


FIGURE 11.3

Change in distribution of CD4⁺CD45RO⁺ and CD4⁺CD45RA⁺ peripheral blood lymphocytes percentages with age in healthy children (m = months; y = years). Box plots indicate data from birth through 18 years of age, the middle line of each box is the median, the edges are the 25th and 75th percentiles. The brackets represent observations closest to 1.5 times the interquartile range away from the quartile, and the horizontal lines represent outlier points. Figure from (24).

In our third paper we investigated whether the immunophenotypic differences between T-lymphocytes of newborns and adults could explain the observed cellular differences in radiosensitivity by scoring residual DNA DSBs and MN after IR exposure. In a first pilot study, we selected the CD4⁺ subpopulation, since the shift in CD45RA⁺ and CD45RO⁺ expression is most pronounced for CD4⁺ lymphocytes and we determined a higher prevalence of CD4⁺ lymphocytes in both UCB ($74.2 \pm 5.2\%$ of CD3⁺ cells) and adult PB ($61.7 \pm 6.4\%$ of CD3⁺ cells) samples.

11.3

Chromatin condensation plays a critical role in radiosensitivity of naive and memory T-lymphocytes

In paper 3 of this PhD dissertation, we were able to present for the first time a difference in radiation sensitivity between human CD4⁺CD45RA⁺ and CD4⁺CD45RO⁺ cells. A statistically significant higher number of radiation-induced MN and residual γ H2AX/53BP1 foci were observed in naive CD4⁺ cells after IR exposure compared to memory CD4⁺ cells. In parallel, we also scored the number of radiation-induced MN and residual DNA DSBs in purified CD4⁺ lymphocytes from the same donors. The small volume culture method as designed for the CBMN assay on HSPCs was used for the purified peripheral T-lymphocyte subsets. When we apply the percentage distribution of the CD4⁺ subsets determined by flow cytometry on the MN and foci results we were able to estimate the expected value of radiation-induced MN and residual foci for the CD4⁺ population of the different donors: “estimated” CD4⁺ value = (CD4⁺CD45RA⁺ % * CD4⁺CD45RA⁺ scoring) + (CD4⁺CD45RO⁺ % * CD4⁺CD45RO⁺ scoring). The difference between the calculated value and the actual observed MN and residual foci yields was less than 10% for every donor. In order to confirm these findings, the same methodology was applied on naive and memory CD8⁺ cells (see Table 11.2). A paired analysis showed a statistically significant difference in radiation-induced MN between the naive and memory subsets of the different donors (Wilcoxon $p = 0.012$).

The underlying mechanisms of the observed difference in radiation sensitivity of human naive and memory T-lymphocyte subsets remains incompletely understood and future research is warranted. The observed

difference in radiosensitivity between naive and memory T-lymphocytes could be attributable to the chromatin structure of the cells. The presence of an open genome-wide chromatin state is a key determinant of efficient repair of DNA damage in T-lymphocytes and an explanation for the observed differences in naive and memory T-lymphocyte radiosensitivity.

In line with our findings, studies in murine models found that naive T cells were more sensitive to radiation than their memory counterparts (25, 26). In a first study, Grayson *et al.* demonstrated that memory CD8⁺ T-lymphocytes are more resistant to apoptosis than their naive counter-

		Subpopulations					
		CD4 ⁺ CD45RO ⁺	CD4 ⁺ CD45RA ⁺	CD4 ⁺	CD8 ⁺ CD45RO ⁺	CD8 ⁺ CD45RA ⁺	CD8 ⁺
Donor 1	RI MN/1000 BN	213	346	259	274	379	360
	Flow cytometry	48.2%	51.3%		21.0%	79.0%	
	"Estimated value"			280			357
Donor 2	RI MN/1000 BN	229	335	263	214	271	225
	Flow cytometry	75.8%	25.2%		35.0%	65.0%	
	"Estimated value"			258			251
Donor 3	RI MN/1000 BN	322	395	334	392	412	393
	Flow cytometry	66.7%	35.6%		22.0%	79.0%	
	"Estimated value"			355			412
Donor 4	RI MN/1000 BN	259	334	312	309	361	337
	Flow cytometry	66.8%	36.4%		28.0%	70.0%	
	"Estimated value"			295			339
Group Mean	RI MN/1000 BN	256	353	292	297	356	329
	Flow cytometry	64.4%	37.1%		26.5%	73.3%	
	"Estimated value"			296			339

PART III

TABLE 11.2

Radiation-induced number of MN per 1000 BN cells CD4⁺ and CD8⁺ subpopulations after 2 Gy x-ray irradiation. Based on the percentage distribution determined by flow cytometry, an estimate of the expected radiation-induced MN yield was made (indicated in gray).

parts after whole body irradiation of mice (25). Both naive and memory CD8⁺ T cells decreased in number, but the reduction in the number of naive cells was 8-fold larger than that in memory CD8⁺ T cells. Previously, the same research group already documented that Ag-specific memory CD8⁺ T-lymphocytes contain increased levels of Bcl-2 compared with either naive or effector CD8⁺ cells (27). These results are in agreement with a former *in vitro* study of our research group, which showed that memory (CD45RA⁻) T-lymphocytes were more prone to Annexine V apoptosis than naive (CD45RA⁺) cells 24h after 2 Gy ⁶⁰Co γ -rays (28). Since apoptosis has a critical role during development and regulation of homeostasis in the immune system, most of the immunological studies on T-lymphocyte subset radiosensitivity use apoptosis as an endpoint to evaluate radiation sensitivity.

Dispirito *et al.* described that memory T-lymphocytes rapidly express effector functions, a hallmark feature that allows them to provide protective immunity (29). Several previous studies suggested that genes involved in this rapid recall may maintain an open chromatin structure in resting memory T-lymphocytes via epigenetic modifications (30, 31). Dispirito *et al.* developed a novel flow cytometric assay, to detect diacetylated histone H3 (diAcH3), a marker of open chromatin. The authors measured histone modification on a per-cell basis in murine T-lymphocytes in combination with lineage-specific markers. The results showed that murine memory CD8⁺ T-lymphocytes have approximately 2 times more diAcH3 than their naive counterparts. Since diAcH3 is a mark of open loci (accessible to the transcriptional machinery), the elevated level in memory CD8⁺ T cells may represent their ability to rapidly and robustly accumulate cytokine and chemokine transcripts to ensure their protective capacity. However, heterochromatic DSB repair also depends on chromatin relaxation, and closed chromatin formations impair DSB repair (32, 33). Relaxation of the chromatin might facilitate genomic surveillance by enabling faster access of DDR factors to the DSB sites. The activation of the DDR (by phosphorylation of H2AX) was evaluated in human MCF7 cells by Murga *et al.* in control cells and cells treated with the histone deacetylase (HDAC) inhibitor Trichostatin A (TSA) to investigate the influence of decondensed chromatin on DDR dynamics at DSB sites (33). The treatment with TSA led to a more robust phosphorylation of H2AX (and Chk1) in response to IR. Furthermore, Falk *et al.* demonstrated that TSA treatment of human skin fibroblasts slowed down the efficiency of DSB repair post-irradiation

(34). In the last years, several small modulators of the chromatin structure known as inhibitors of HDAC have been identified and tested, such as valproate, TSA and vorinostat. On the other hand there are also compounds that modulate chromatin compaction in the opposite direction by decreasing the accessibility of the DNA, such as resveratrol (35).

We can consider that more open and accessible chromatin should facilitate DNA repair. Rawlings *et al.* demonstrated that during thymocyte development, a condensation of the chromatin occurs which is required for proper T cell development and maintenance of the quiescent state (36). This mechanism ensures that cytokine driven proliferation can only occur when quiescent naive T cells encounter their TCR-specific antigen. Rawlings *et al.* demonstrated that TCR activation results in a decondensation of the chromatin in naive T lymphocytes, which permits the engagement of Stat5, an essential component for proliferation. Finally, Pugh *et al.* investigated T-lymphocyte subset radiosensitivity in mice and highlighted also the critical role of an open chromatin state on radiosensitivity (26). It should be noted that the authors examine also the difference in radiosensitivity between effector memory (EM) and central memory (CM) T cell subsets in this paper. However, this comparison is beyond the scope of this PhD dissertation. Survival trends between T cell subsets were tested *in vivo* in mice 72h after exposure to 1, 2 and 4 Gy. In agreement with previously mentioned studies, memory T cells were more resistant and naive T cells more sensitive following *in vivo* irradiation. Maximal upregulation of γ -H2AX following irradiation over time was the highest in naive T cells, which correlates with the observed survival trends in radiosensitivity. By incubating irradiated cells with or without valproic acid (VPA), an HDAC inhibitor that opens chromatin, for 12 and 72h, the authors could prove that naive T-lymphocyte survival improved, whereas memory T-lymphocyte survival remained unchanged.

The relationship between DNA repair and apoptosis is a complex process, which makes it difficult to project the apoptosis results obtained in the murine studies on our results of *in vitro* radiosensitivity differences within human T-lymphocytes subsets. However, the murine studies illustrate clearly that the chromatin state has a major influence on radiosensitivity. Further research is needed to determine the differences in chromatin state of the human T-lymphocyte subsets and the possible link with the higher number of residual DNA DSBs scored after 24h and radiation-

induced mutagenic effects observed in naive compared to memory human T-lymphocytes.

Besides the murine studies on the influence of the chromatin compaction on the radiosensitivity of naive and memory T-lymphocytes, it was already clear from earlier studies that the compaction/dispersion status of DNA throughout the cell cycle appears to be an important factor for determining intrinsic cell radiosensitivity (37). The influence of chromatin structure on the susceptibility of DNA damage, and the efficiency of DNA repair in human lymphocytes is also reflected in the different yields of chromosomal aberrations observed in the different stages of the cell cycle (38). The latter is well established and proven by studies with synchronized mammalian cells, which were clearly more sensitive to IR during the G2/M phase of the cell cycle when their chromatin is highly condensed (39-41). These findings, together our results (in paper 3) of the difference in radiation-induced mutagenic effects and residual DNA DSBs in human naive and memory T-lymphocytes, indicate that radiation sensitivity is strongly influenced by the chromatin structure. Further research is needed to investigate if chromatin condensation can be considered as a general phenomenon related to explain the observed age dependency of radiation effects.

11.4

References

1. Carroll PD, Nankervis CA, Iams J, Kelleher K. Umbilical cord blood as a replacement source for admission complete blood count in premature infants. *Journal of Perinatology*. 2012;32(2):97-102.
2. Floyd DN, Cassoni AM. Intrinsic radiosensitivity of adult and cord blood lymphocytes as determined by the micronucleus assay. *European Journal of Cancer*. 1994;30A(5):615-20.
3. Bakhmutsky MV, Joiner MC, Jones TB, Tucker JD. Differences in Cytogenetic Sensitivity to Ionizing Radiation in Newborns and Adults. *Radiation Research*. 2014;181(6):605-16.
4. Mei N, Imada H, Nomoto S, Kunugita N, Norimura T. Individual variation and age dependency in the radiosensitivity of peripheral blood T-lymphocytes from normal donors. *Journal of Radiation Research*. 1996;37(4):235-45.
5. Hattis D, Goble R, Russ A, Chu M, Ericson J. Age-related differences in susceptibility to carcinogenesis: A quantitative analysis of empirical animal bioassay data. *Environmental Health Perspectives*. 2004;112(11):1152-8.
6. Sasaki S, Fukuda N. Temporal variation of excess mortality rate from solid tumors in mice irradiated at various ages with gamma rays. *Journal of Radiation Research*. 2005;46(1):1-19.
7. Rube CE, Fricke A, Widmann TA, Furst T, Madry H, Pfreundschuh M, et al. Accumulation of DNA Damage in Hematopoietic Stem and Progenitor Cells during Human Aging. *Plos One*. 2011;6(3):9.
8. Schuler N, Ruebe CE. Accumulation of DNA Damage-Induced Chromatin Alterations in Tissue-Specific Stem Cells: The Driving Force of Aging? *Plos One*. 2013;8(5).
9. Woodbine L, Brunton H, Goodarzi AA, Shibata A, Jeggo PA. Endogenously induced DNA double strand breaks arise in heterochromatic DNA regions and require ataxia telangiectasia mutated and Artemis for their repair. *Nucleic Acids Research*. 2011;39(16):6986-97.
10. Barale R, Chelotti L, Davini T, Del Ry S, Andreassi MG, Ballardini M, et al. Sister chromatid exchange and micronucleus frequency in human lymphocytes of 1,650 subjects in an Italian population: II. Contribution of sex, age, and lifestyle. *Environmental and Molecular Mutagenesis*. 1998;31(3):228-42.
11. Bolognesi C, Abbondandolo A, Barale R, Casalone R, Dalpra L, De Ferrari M, et al. Age-related increase of baseline frequencies of sister chromatid exchanges, chromosome aberrations, and micronuclei in human lymphocytes. *Cancer Epidemiology, Biomarkers and Prevention*. 1997;6(4):249-56.
12. Levario-Carrillo M, Sordo M, Rocha F, Gonzalez-Horta C, Amato D, Ostrosky-Wegman P. Micronucleus frequency in human umbilical cord lymphocytes. *Mutation Research*. 2005;586(1):68-75.
13. Cakmak Demircigil G, Aykanat B, Fidan K, Gulleroglu K, Bayrakci US, Sepici A, et al. Micronucleus frequencies in peripheral blood lymphocytes of children with chronic kidney disease. *Mutagenesis*. 2011;26(5):643-50.
14. Gajski G, Gerić M, Oreščanin V, Garaj-Vrhovac V. Cytogenetic status of healthy children assessed with the alkaline comet assay and the cytokinesis-block micronucleus cytome assay. *Mutation Research/Genetic Toxicology and Environmental Mutagenesis*. 2013;750(1-2):55-62.
15. D'Arena G, Musto P, Cascavilla N, Di Giorgio G, Fusilli S, Zendoli F, et al. Flow cytometric characterization of human umbilical cord blood lymphocytes: immunophenotypic features. *Haematologica*. 1998;83(3):197-203.
16. Merkenschlager M, Beverley PC. Evidence for differential expression of CD45 isoforms by precursors for memory-dependent and independent cytotoxic responses: human CD8 memory CTLp selectively express CD45RO (UCHL1). *International Immunology*. 1989;1(4):450-9.
17. Surh CD, Sprent J. Homeostasis of naive and memory T cells. *Immunity*. 29. United States 2008. p. 848-62.
18. Mackay CR. Homing of naive, memory and effector lymphocytes. *Current Opinion in Immunology*. 1993;5(3):423-7.
19. Sprent J, Surh CD. Normal T cell homeostasis: the conversion of naive cells into memory-phenotype cells. *Nature Immunology*. 2011;12(6):478-84.
20. Dutton RW, Bradley LM, Swain SL. T cell memory. *Annual Review Immunology*. 1998;16:201-23.
21. Ben-Smith A, Gorak-Stolinska P, Floyd S, Weir RE, Lalor MK, Mvula H, et al. Differences between naive and memory T cell phenotype in Malawian and UK adolescents: a role for Cytomegalovirus? *Bmc Infectious Diseases*. 2008;8.
22. Messele T, Abdulkadir M, Fontanet AL, Petros B, Hamann D, Koot M, et al. Reduced naive and increased activated CD4 and CD8 cells in healthy adult Ethiopians compared with their Dutch counterparts. *Clinical and Experimental Immunology*. 1999;115(3):443-50.
23. Tsegaye A, Wolday D, Otto S, Petros B, Assefa T, Alebachew T, et al. Immunophenotyping of blood lymphocytes at birth, during childhood, and during adulthood in HIV-1-uninfected Ethiopians. *Clinical Immunology*. 2003;109(3):338-46.
24. Shearer WT, Rosenblatt HM, Gelman RS, Oymopito R, Plaeger S, Stiehm ER, et al. Lymphocyte subsets in healthy children from birth through 18 years of age: The pediatric AIDS clinical trials group P1009 study. *Journal of Allergy and Clinical Immunology*. 2003;112(5):973-80.

25. Grayson JM, Harrington LE, Lanier JG, Wherry EJ, Ahmed R. Differential sensitivity of naive and memory CD8(+) T cells to apoptosis in vivo. *Journal of Immunology*. 2002;169(7):3760-70.
26. Pugh JL, Sukhina AS, Seed TM, Manley NR, Sempowski GD, van den Brink MRM, et al. Histone Deacetylation Critically Determines T Cell Subset Radiosensitivity. *Journal of Immunology*. 2014;193(3):1451-8.
27. Grayson JM, Zajac AJ, Altman JD, Ahmed R. Cutting edge: increased expression of Bcl-2 in antigen-specific memory CD8+ T cells. *Journal of Immunology*. 2000;164(8):3950-4.
28. Philippe J, Louagie H, Thierens H, Vral A, Cornelissen M, De Ridder L. Quantification of apoptosis in lymphocyte subsets and effect of apoptosis on apparent expression of membrane antigens. *Cytometry*. 1997;29(3):242-9.
29. DiSpirito JR, Shen H. Histone Acetylation at the Single-Cell Level: A Marker of Memory CD8(+) T Cell Differentiation and Functionality. *Journal of Immunology*. 2010;184(9):4631-6.
30. Araki Y, Fann M, Wersto R, Weng N-p. Histone Acetylation Facilitates Rapid and Robust Memory CD8 T Cell Response through Differential Expression of Effector Molecules (Eomesodermin and Its Targets: Perforin and Granzyme B). *Journal of immunology*. 2008;180(12):8102-8.
31. Kersh EN, Fitzpatrick DR, Murali-Krishna K, Shires J, Speck SH, Boss JM, et al. Rapid demethylation of the IFN-gamma gene occurs in memory but not naive CD8 T cells. *Journal of Immunology*. 2006;176(7):4083-93.
32. Price BD, D'Andrea AD. Chromatin Remodeling at DNA Double-Strand Breaks. *Cell*. 2013;152(6):1344-54.
33. Murga M, Jaco I, Fan Y, Soria R, Martinez-Pastor B, Cuadrado M, et al. Global chromatin compaction limits the strength of the DNA damage response. *Journal of Cell Biology*. 2007;178(7):1101-8.
34. Falk M, Lukasova E, Kozubek S. Chromatin structure influences the sensitivity of DNA to gamma-radiation. *Biochimica Et Biophysica Acta-Molecular Cell Research*. 2008;1783(12):2398-414.
35. Keuser B, Khobta A, Galle K, Anderhub S, Schulz I, Pauly K, et al. Influences of histone deacetylase inhibitors and resveratrol on DNA repair and chromatin compaction. *Mutagenesis*. 2013;28(5):569-76.
36. Rawlings JS, Gatzka M, Thomas PG, Ihle JN. Chromatin condensation via the condensin II complex is required for peripheral T-cell quiescence. *Embo Journal*. 2011;30(2):263-76.
37. Stobbe CC, Park SJ, Chapman JD. The radiation hypersensitivity of cells at mitosis. *International Journal of Radiation Biology*. 2002;78(12):1149-57.
38. Darroudi F, Fomina J, Meijers M, Natarajan AT. Kinetics of the formation of chromosome aberrations in X-irradiated human lymphocytes, using PCC and FISH. *Mutation Research*. 1998;404(1-2):55-65.
39. Carrier F. Chromatin Modulation by Histone Deacetylase Inhibitors: Impact on Cellular Sensitivity to Ionizing Radiation. *Molecular Cell Pharmacology*. 2013;5(1):51-9.
40. Terasima T, Tolmach LJ. Variations in Several Responses of HeLa Cells to X-Irradiation during the Division Cycle. *Biophysical Journal*. 1963;3(1):11-33.
41. Sinclair WK, Morton RA. X-ray sensitivity during the cell generation cycle of cultured Chinese hamster cells. *Radiation Research*. 1966;29(3):450-74.

12

Final Conclusions

In this PhD dissertation, we investigated the health effects of CT x-rays in children by using biomarkers of exposure. A first purpose was the *in vivo* assessment of the direct DNA damage induced by CT x-ray exposure in children using the γ -H2AX foci assay. In order to start this *in vivo* biomarker study on a vulnerable population of paediatric patients in a multi-centre setting, we had to optimise successfully the sensitive γ -H2AX foci assay while taking into account a number of logistic and ethical constraints related to paediatric patients and a multicentre set-up. The *in vitro* experiments comprised two low dose intercomparison studies within the EU FP7 project EPI-CT and demonstrated that it is feasible to apply the γ -H2AX foci assay as a potential cellular biomarker of exposure in a large scale multicentre prospective study of the effects of paediatric CT imaging.

The *in vivo* paediatric patient study in Belgium of patients undergoing a chest or abdomen CT shows that even at low doses, CT x-rays induce a small, but significant number of DNA DSBs in children's lymphocytes. The observed low dose hypersensitivity challenges the LNT hypothesis and may indicate the presence of a bystander effect. The steep increase in the low dose range was confirmed by an *in vitro* dose response study on umbilical cord blood. However, our study also demonstrated that the use

of optimised paediatric CT protocols and CT dose reduction techniques results in less DNA damage for the patient. Furthermore, the data of the paediatric CT study indicate an intrinsic radiosensitivity decreasing with age, but regression analysis was not statistically significant. These conclusions should encourage medical practitioners to minimize radiation doses in paediatric radiology and to apply the “Image Gently” philosophy. Although our results suggest that the widely accepted LNT model may underestimate low dose radiation risks, we have to put the estimated risks in perspective. First of all, one should be aware of the large uncertainties on current low dose risk estimations and not forget that the calculated risks are small compared to the overall cancer incidence.

The age dependency of the health effects of CT x-rays was further investigated in a comparative *in vitro* study of lymphocytes of cord blood and adult volunteers. In this study we used the γ -H2AX/53BP1 foci assay in T-lymphocytes to assess the number of DNA DSBs induced by x-rays and the residual number of DSBs 24h post-irradiation, which is representative for DNA damage repair. Furthermore the CBMN assay was used to assess the mutagenic effects induced by x-rays. We could demonstrate that the T-lymphocytes of newborns were more sensitive to IR compared to adults for the residual DNA damage and the mutagenic effects. The main difference between newborn and adult T-lymphocytes in these *in vitro* experiments, was their immunophenotypic profile. This brings us to one of the major findings of this PhD dissertation, which is the observed higher radiation sensitivity of the phenotypically immature naive T-lymphocytes compared to memory T-lymphocytes. For these studies the radiosensitivity of isolated subpopulations of lymphocytes was investigated. A possible underlying mechanism of this difference in sensitivity is the more condensed chromatin structure of naive T-lymphocytes.

Since radiation-induced leukaemia is an endpoint of great concern at young ages, we investigated the radiosensitivity of HSPCs (CD34⁺ cells) of newborns, defined as target cells for radiation-induced leukaemogenesis. In this study we used the same biomarkers of x-ray effects as in the comparative study of lymphocytes of newborns and adults. The low number of residual DNA DSBs in CD34⁺ cells suggest fast error prone DNA repair and the CBMN results confirm that the quiescence of HSPCs promotes mutagenesis after IR exposure, which may trigger leukaemia development.

13

Future Perspectives

Currently, we are forced to rely on the LNT hypothesis for the extrapolation of radiation risks to low doses (< 20 mGy). The growing number of epidemiological studies on radiation-induced cancer following CT scans in childhood (1-5) and the large scale EU-FP7 funded epidemiologic EPI-CT project will provide great potential to substantiate the epidemiological evidence for radiation effects at low doses as used in paediatric radiology in children. Furthermore, it is anticipated that significant insights will emerge from the integration of epidemiological and biological research, made possible by molecular epidemiology studies incorporating biomarkers and bioassays (6). After the *in vitro* feasibility studies, low dose inter-comparison studies and the Belgian *in vivo* paediatric CT study, presented in this PhD dissertation, the next step would be an international European multicentre CT study in which the γ -H2AX foci assay is used as a molecular epidemiology biomarker in a large scale paediatric patient population. Besides patients undergoing a CT chest or CT abdomen scan, also head CT scans should be included as an extension of the study performed in Belgium, since this is the most frequently performed CT procedure in children. Due to the ethical constraints regarding the collection of blood samples from children, it would be interesting to develop a non-invasive

method to assess direct low-dose effects in children. Detection of γ -H2AX foci can be done with non-invasive methods as collecting exfoliated buccal cells, to assess DNA damage in buccal mucosa after CT head in children (7, 8). In this framework, pilot studies are warranted to test the low dose sensitivity of the γ -H2AX foci assay on buccal cells.

The low dose hypersensitivity observed in the paediatric CT study can be attributed to the bystander effect. This implies that in the low dose range a tissue radiation response is observed rather than a cellular DNA damage response. The bystander phenomenon is subject to active debate in the scientific community (9). However at present, there is evidence that at least two independent and probably non-exclusive mechanisms of communication are involved in bystander effects, namely gap junction-mediated communication (GJIC) and secreted soluble factor dependent signalling (10). Further studies on the underlying non-targeted effects of the hypersensitive response induced by low-doses of x-rays could imply the inhibition of GJIC by using carbenoxolone (CBX), a widely used gap-junction inhibitor (11). However, this PhD research was focused on peripheral blood T-lymphocytes and in these suspension cultures, direct intercellular interaction between irradiated and bystander cells is less obvious. In this way, it seems more appropriate that soluble factors released from irradiated cells into the culture medium would initiate the bystander response. The influence of soluble factors can be studied by performing medium-transfer experiments. The medium harvested from irradiated T-lymphocyte cultures could be transferred to recipient bystander cells cultured in separate plates. Furthermore, it is also possible to co-culture irradiated and non-irradiated T-lymphocytes, by mixing cultures in which one population of cells is labelled with a cytoplasmic dye cell tracker (CellTracker™ Red CMTPX, Life Technologies) in order to score the bystander-induced γ -H2AX foci in non-irradiated cells. The role of free radicals in the bystander response such as reactive oxygen species (ROS) released into the cell-culture medium has been shown by applying antioxidants such as superoxide dismutase or inhibitors of superoxide and NO generators. Zhou *et al.* showed that the COX-2-related pathway, which is essential in mediating cellular inflammatory response, is a critical signalling link for the bystander phenomenon (11). Treatment of bystander cells with a COX-2 inhibitor (NS-398) could reduce the bystander effect. Another approach is the use of radiation microbeams that can be delivered in a highly temporal and spatially constrained manner. The combination of microbeams with multiphoton

fluorescence microscopy, which allows to study living tissue samples in 3D, could be used to map post-irradiation cellular dynamics (13).

For the evaluation of the radiation sensitivity of haematopoietic stem cells, we used a heterogeneous population of CD34⁺ cells. In a next phase of this research, the radiation sensitivity of the different primitive and more lineage-committed subsets should be investigated. As described in the discussion of this PhD dissertation, caution is urged when data on the radiosensitivity of HSPCs in mice are extrapolated to humans. However, more evidence is needed to elucidate the differences in radiation sensitivity of HSPCs in mice and human (14, 15). The latter is of utmost importance in studies on the radioprotective characteristics of the bone marrow niche, since *in vivo* murine models are required to study this phenomenon.

Based on the observed difference in radiosensitivity between newborn and adult T-lymphocytes and the link with the immunophenotypic profile of the cells, it would be appropriate to study the chromatin state of naive and memory T-cell subsets. Epigenetic hallmarks of silenced heterochromatic DNA include histone 3 lysine 9 and lysine 27 trimethylation (H3K9me3, H3K27me3), and histone 4 lysine 20 di-/trimethylation (H4K12me2/3). Histone modifications specific for active euchromatin are acetylation of histone 3 lysine 9 (H3K9ac), histone 4 lysine 16 (H4K16ac) and methylation of histone 3 at lysine 4 (H3K4me) (an overview can be found in (16)). Schuler *et al.* have established a transmission electron microscopy (TEM) method to detect gold-labelled repair components in different chromatin environments (17). The ultra-high resolution of TEM allows to detect core components of the DNA repair machinery (e.g. ATM, γ -H2AX...) at the single-molecule level and visualizes their molecular interactions with specific histone modifications for hetero- or euchromatic DNA. Another approach to determine the differences in chromatin state between human CD45RA⁺ and CD45RO⁺ T-lymphocyte subsets, is the use of flow cytometry to measure histone modification (e.g. diAcH3 as a marker of open chromatin) in combination with lineage-specific cell surface markers (18). In a last step, it is also possible to study the influence of the condensed chromatin structure of naive CD45RA⁺ CD4⁺ and CD8⁺ T-lymphocytes on their radiation sensitivity by using inhibitors of chromatin compaction (19). In our set-up, the incubation of naive T cells with a HDAC inhibitor such as TSA (20), should reduce the number of residual DNA DSBs in naive T-lymphocytes to the level observed for memory T-lymphocytes. In previous studies, it was already demonstrated that the compaction/disper-

sion status of DNA throughout the cell cycle appeared to be an important factor for determining intrinsic cell radiosensitivity (21). Studies with synchronized cells have shown that mammalian cells are most sensitive to IR at mitosis, the time at which their chromatin is maximally condensed (22, 23). This scientific literature together with the results obtained in present PhD thesis indicate that the radiation sensitivity is strongly influenced by the chromatin structure. Further research is needed to investigate if chromatin condensation can be interpreted as a general phenomenon to explain the observed age dependency in radiation effects.

13.1

References

1. Pearce MS, Salotti JA, Little MP, McHugh K, Lee C, Kim KP, et al. Radiation exposure from CT scans in childhood and subsequent risk of leukaemia and brain tumours: a retrospective cohort study. *Lancet*. 2012;380(9840):499-505.
2. Huang WY, Muo CH, Lin CY, Jen YM, Yang MH, Lin JC, et al. Paediatric head CT scan and subsequent risk of malignancy and benign brain tumour: a nation-wide population-based cohort study. *British Journal of Cancer*. 2014;110(9):2354-60.
3. Mathews JD, Forsythe AV, Brady Z, Butler MW, Goergen SK, Byrnes GB, et al. Cancer risk in 680 000 people exposed to computed tomography scans in childhood or adolescence: data linkage study of 11 million Australians. *Bmj-British Medical Journal*. 2013;346.
4. Journy N, Rehel JL, Ducou Le Pointe H, Lee C, Brisse H, Chateil JF, et al. Are the studies on cancer risk from CT scans biased by indication? Elements of answer from a large-scale cohort study in France. *British Journal of Cancer*. 112. England2015. p. 185-93.
5. Krille L, Dreger S, Schindler R, Albrecht T, Asmussen M, Barkhausen J, et al. Risk of cancer incidence before the age of 15 years after exposure to ionising radiation from computed tomography: results from a German cohort study. *Radiation and Environmental Biophysics*. 2015;54(1):1-12.
6. Pernet E, Hall J, Baatout S, Benotmane MA, Blanchardon E, Bouffler S, et al. Ionizing radiation biomarkers for potential use in epidemiological studies. *Mutation Research-Reviews in Mutation Research*. 2012;751(2):258-86.
7. Yoon AJ, Shen J, Wu HC, Angelopoulos C, Singer SR, Chen R, et al. Expression of activated checkpoint kinase 2 and histone 2AX in exfoliated oral cells after exposure to ionizing radiation. *Radiation Research*. 2009;171(6):771-5.
8. Gonzalez JE, Roch-Lefevre SH, Mandina T, Garcia O, Roy L. Induction of gamma-H2AX foci in human exfoliated buccal cells after in vitro exposure to ionising radiation. *International Journal of Radiation Biology*. 2010;86(9):752-9.
9. Kadhim M, Salomaa S, Wright E, Hildebrandt G, Belyakov OV, Prise KM, et al. Non-targeted effects of ionising radiation--implications for low dose risk. *Mutation Research*. 2013;752(2):84-98.
10. Little JB. Genomic instability and bystander effects: a historical perspective. *Oncogene*. 2003;22(45):6978-87.
11. Rozental R, Srinivas M, Spray DC. How to close a gap junction channel. Efficacies and potencies of uncoupling agents. *Methods in Molecular Biology*. 2001;154:447-76.
12. Zhou HN, Ivanov VN, Gillespie J, et al. Mechanism of radiation-induced bystander effect: Role of the cyclooxygenase-2 signaling pathway. *Proceedings of the National Academy of Sciences of the United States of America*. 2005;102(41):14641-6.
13. Schettino G, Al Rashid ST, Prise KM. Radiation microbeams as spatial and temporal probes of subcellular and tissue response. *Mutation Research*. 2010;704(1-3):68-77.
14. Milyavsky M, Gan OI, Trottier M, Komosa M, Tabach O, Notta F, et al. A Distinctive DNA Damage Response in Human Hematopoietic Stem Cells Reveals an Apoptosis-Independent Role for p53 in Self-Renewal. *Cell Stem Cell*. 2010;7(2):186-97.
15. Mohrin M, Bourke E, Alexander D, Warr MR, Barry-Holson K, Le Beau MM, et al. Hematopoietic Stem Cell Quiescence Promotes Error-Prone DNA Repair and Mutagenesis. *Cell Stem Cell*. 2010;7(2):174-85.
16. Tamaru H. Confining euchromatin/heterochromatin territory: jumonji crosses the line. *Genes & Development*. 2010;24(14):1465-78.
17. Schuler N, Ruebe CE. Accumulation of DNA Damage-Induced Chromatin Alterations in Tissue-Specific Stem Cells: The Driving Force of Aging? *Plos One*. 2013;8(5).
18. DiSpirito JR, Shen H. Histone Acetylation at the Single-Cell Level: A Marker of Memory CD8(+) T Cell Differentiation and Functionality. *Journal of Immunology*. 2010;184(9):4631-6.
19. Pugh JL, Sukhina AS, Seed TM, Manley NR, Sempowski GD, van den Brink MRM, et al. Histone Deacetylation Critically Determines T Cell Subset Radiosensitivity. *Journal of Immunology*. 2014;193(3):1451-8.
20. Keuser B, Khobta A, Galle K, Anderhub S, Schulz I, Pauly K, et al. Influences of histone deacetylase inhibitors and resveratrol on DNA repair and chromatin compaction. *Mutagenesis*. 2013;28(5):569-76.
21. Stobbe CC, Park SJ, Chapman JD. The radiation hypersensitivity of cells at mitosis. *International Journal of Radiation Biology*. 2002;78(12):1149-57.
22. Terasima T, Tolmach LJ. Variations in Several Responses of HeLa Cells to X-Irradiation during the Division Cycle. *Biophysical Journal*. 1963;3(1):11-33.
23. Sinclair WK, Morton RA. X-ray sensitivity during the cell generation cycle of cultured Chinese hamster cells. *Radiation Research*. 1966;29(3):450-74.

PAR

T W V

Curriculum Vitae

14

Curriculum Vitae

Personal Information

Name, First Name	Vandevoorde, Charlot
Adress	Limbastraat 49 9000 Ghent Belgium
Email	vandevoordecharlot@gmail.com
Mobile	+32 485458335
Date of birth	15-10-1987
Place of birth	Ghent
Nationality	Belgian
Civil status	Cohabitated

Education

2010 - 2015	PhD student in Biomedical Sciences PhD thesis: Biomarker investigation of the health effects of CT x-ray exposure in children: A plea to "Image Gently" Supervisors: Prof. Dr. H. Thierens and Prof. Dr. Ir. K. Bacher Ghent University
2005 - 2010	Master in Biomedical Sciences – Medical Radiation Sciences Master thesis: Patient dosimetry in the application of cone-beam CT for uterine artery embolization Supervisors: Prof. Dr. H. Thierens and Prof. Dr. Ir. K. Bacher Ghent University
1999 - 2005	Latin-Mathematics Emmaus Institute Aalter

A1 Publications

1. Vandevoorde C, Vral A, Vandekerckhove B, Philippé J, Thierens H. Radiation sensitivity of human CD34+ cells versus peripheral blood T-lymphocytes of newborns and adults: DNA repair and mutagenic effects. *Radiation Research*. Submitted. 2011;38(12):2269-81.
2. Vandevoorde C, Gomolka M, Roessler U, Samaga D, Lindholm C, Fernet M, Hall J, Pernot E, El-Saghire H, Baatout S, Kesminiene A, Thierens H. EPI-CT: in vitro assessment of the applicability of the γ -H2AX-foci assay as cellular biomarker for exposure in a multicentre study of children in diagnostic radiology. *International Journal of Radiation Biology*. Accepted (DOI: 10.3109/09553002.2015.1047987)
3. Vandevoorde C, Franck C, Bacher K, Breysen L, Smet MH, Ernst C, De Backer A, Van De Moortele K, Smeets P, Thierens H. γ -H2AX foci as in vivo effect biomarker in children emphasize the importance to minimize x-ray doses in paediatric CT imaging. *European Radiology*. 2015;25(3):800-11.
4. Kulka U, Ainsbury L, Atkinson M, Barnard S, Smith R, Barquinero JF, Barrios L, Bassinet C, Beinke C, Cucu A, Darroudi F, Fattibene P, Bortolin E, Monaca SD, Gil O, Gregoire E, Hadjidekova V, Haghdoost S, Hatzi V, Hempel W, Herranz R, Jaworska A, Lindholm C, Lumniczky K, M'kacher R, Mörtl S, Montoro A, Moquet J, Moreno M, Noditi M, Ogbazghi A, Oestreicher U, Palitti F, Pantelias G, Popescu I, Prieto MJ, Roch-Lefevre S, Roessler U, Romm H, Rothkamm K, Sabatier L, Sebastià N, Sommer S, Terzoudi G, Testa A, Thierens H, Trompier F, Turai I, Vandevoorde C, Vaz P, Voisin P, Vral A, Ugletveit F, Wieser A, Woda C, Wojcik A. Realising the European Network of Biodosimetry: RENE status quo. *Radiation Protection Dosimetry*. 2014;164(1-2):42-5.
5. Barnard S, Ainsbury EA, Al-Hafidh J, Hadjidekove V, Hristova R, Lindholm C, Monteiro Gil O, Moquet J, Moreno M, Rößler U, Thierens H, Vandevoorde C, Vral A, Wojewódzka M, Rothkamm K. The first gamma-H2AX biodosimetry intercomparison exercise of the developing European Biodosimetry network RENE. *Radiation Protection Dosimetry*. 2015;164(3):265-70.
6. Thierens H, Vral A, Vandevoorde C, Vandersickel V, de Gelder V, Romm H, Oestreicher U, Rothkamm K, Barnard S, Ainsbury E, Sommer S, Beinke C, Wojcik A. Is a semi-automated approach indicated in the application of the automated micronucleus assay for triage purposes? *Radiation Protection Dosimetry*. 2014;159(1-4):87-94.

7. Ainsbury EA, Al-Hafidh J, Bajinskis A, Barnard S, Barquinero JF, Beinke C, de Gelder V, Gregoire E, Jaworska A, Lindholm C, Lloyd D, Moquet J, Nylund R, Oestreicher U, Roch-Lefèvre S, Rothkamm K, Romm H, Scherthan H, Sommer S, Thierens H, Vandevoorde C, Vral A, Wojcik A. Inter- and intra-laboratory comparison of a multibiodosimetric approach to triage in a simulated, large scale radiation emergency. *International Journal of Radiation Biology* 2014;90(2):193-202.
8. El-Saghire H, Vandevoorde C, Ost P, Monsieurs P, Michaux A, De Meerleer G, Baatout S, Thierens H. Intensity modulated radiotherapy induces pro-inflammatory and pro-survival responses in prostate cancer patients. *International Journal of Oncology*. 2014;44(4):1073-83.
9. Ainsbury EA, Barnard S, Barrios L, Fattibene P, de Gelder V, Gregoire E, Lindholm C, Lloyd D, Nergaard I, Kai Rothkamm, Romm H, Scherthan H, Thierens H, Vandevoorde C, Woda C, Wojcik A. Multibiodose radiation emergency triage categorization software. *Health Physics*. 2014;107(1):83-9.
10. El-Saghire H, Thierens H, Monsieurs P, Michaux A, Vandevoorde C, Baatout S. Gene set enrichment analysis highlights different gene expression profiles in whole blood samples X-irradiated with low and high doses. *International Journal of Radiation Biology*. 2013;89(8):628-38.
11. Eberlein U, Broer, JH, Vandevoorde C, Santos P, Bardies M, Bacher K, Nosske D, Lassmann M. Biokinetics and dosimetry of commonly used radiopharmaceuticals in diagnostic nuclear medicine - a review. *European Journal of Nuclear Medicine and Molecular Imaging*. 2011;38(12):2269-81.

Conferences

1. 23th Annual Congress of the European Association of Nuclear Medicine
Vienna, 09 – 13/10/2010
Attendance
2. 29th Annual Meeting of the Belgian Environmental Mutagen Society
Etterbeek, 05/11/2010
Attendance
3. 26th Annual Meeting of the Belgian Hospital Physicists Association
(BHPA)
Charleroi, 04 – 05/02/2011
Attendance

4. 17th European Congress of Radiology (ECR)
Vienna, 03 – 07/03/2011
Oral presentation (Peddose.net session): CT-Protocols and Radiation Exposure in multimodality imaging
5. Nuklear Medizin Congress (not attended)
Bregenz, 13 – 16/04/2011
Poster presentation: Multimodality imaging in nuclear medicine: a strong need for optimization of CT protocols
6. 24th Annual Congress of the European Association of Nuclear Medicine
Birmingham, 15 – 19/10/2011
Oral presentation (Pre-congress symposium 3): Development in nuclear medicine imaging – Impact on patient radiation dose
7. 2nd International conference on Clinical PET and Molecular Nuclear Medicine (iPET 2011)
Vienna, 08 - 11/11/2011
Oral Presentation (Panel Discussion - Practical aspects of CT): CT protocols and CT dose contribution in PET/CT
8. 2nd periodic DoReMi meeting – Student and post-doc session
Paris, 21 – 25/01/2012
Oral presentation: Direct assessment of low dose effects in children undergoing a computed tomography examination
9. 18th European Congress of Radiology (ECR) (not attended)
Vienna, 01-05/03/2012
Electronic poster presentation: Results of the EU project PEDDOSE. NET: Impact of technological development on patient dose in nuclear medicine imaging
10. MELODI Workshop 2013
Brussels, 08-10/10/2013
Poster presentation: Direct assessment of low dose effects in children undergoing a computed tomography examination
11. 26th Annual Congress of the European Association of Nuclear Medicine (not attended – presentation was presented by Prof. Dr. K. Bacher)
Lyon, 19 – 23/10/2013
Oral Presentation: Patient dose and image quality of a cone-beam CT system for SPECT/CT: comparison with 16 slice CT

12. 7th PhD Day of the Department of Basic Medical Sciences
Ghent, 05/02/2014
Oral Presentation: γ -H2AX-foci after CT X-ray exposure in children: evidence of the bystander effect

13. 20th European Congress of Radiology (ECR)
Vienna, 06 - 10/03/2014
Oral Presentation: γ -H2AX foci as effect biomarker for CT radiation exposure in paediatric patients: an individualised approach to estimate radiation risks
Award: Best Scientific Presentation - Paediatric

14. 15th International Congress of Radiation Research
Kyoto, 25 – 29/05/2015
Poster presentation: Differences in radiosensitivity between CD34+ hematopoietic stem cells and T-lymphocytes
FWO grant for participation in an international conference